Terms and Conditions of Use of Digitised Theses from Trinity College Library Dublin

Copyright statement

All material supplied by Trinity College Library is protected by copyright (under the Copyright and Related Rights Act, 2000 as amended) and other relevant Intellectual Property Rights. By accessing and using a Digitised Thesis from Trinity College Library you acknowledge that all Intellectual Property Rights in any Works supplied are the sole and exclusive property of the copyright and/or other IPR holder. Specific copyright holders may not be explicitly identified. Use of materials from other sources within a thesis should not be construed as a claim over them.

A non-exclusive, non-transferable licence is hereby granted to those using or reproducing, in whole or in part, the material for valid purposes, providing the copyright owners are acknowledged using the normal conventions. Where specific permission to use material is required, this is identified and such permission must be sought from the copyright holder or agency cited.

Liability statement

By using a Digitised Thesis, I accept that Trinity College Dublin bears no legal responsibility for the accuracy, legality or comprehensiveness of materials contained within the thesis, and that Trinity College Dublin accepts no liability for indirect, consequential, or incidental, damages or losses arising from use of the thesis for whatever reason. Information located in a thesis may be subject to specific use constraints, details of which may not be explicitly described. It is the responsibility of potential and actual users to be aware of such constraints and to abide by them. By making use of material from a digitised thesis, you accept these copyright and disclaimer provisions. Where it is brought to the attention of Trinity College Library that there may be a breach of copyright or other restraint, it is the policy to withdraw or take down access to a thesis while the issue is being resolved.

Access Agreement

By using a Digitised Thesis from Trinity College Library you are bound by the following Terms & Conditions. Please read them carefully.

I have read and I understand the following statement: All material supplied via a Digitised Thesis from Trinity College Library is protected by copyright and other intellectual property rights, and duplication or sale of all or part of any of a thesis is not permitted, except that material may be duplicated by you for your research use or for educational purposes in electronic or print form providing the copyright owners are acknowledged using the normal conventions. You must obtain permission for any other use. Electronic or print copies may not be offered, whether for sale or otherwise to anyone. This copy has been supplied on the understanding that it is copyright material and that no quotation from the thesis may be published without proper acknowledgement.

Role of CED-9/Bcl-2 family proteins in mitochondrial fission and fusion dynamics

Thesis submitted to Trinity College Dublin

for the degree of Doctor of Philosophy

2008

Petrina Delivani

Thesis supervisor: Prof. Seamus J. Martin

Molecular Cell Biology Laboratory,

Department of Genetics,

University of Dublin,
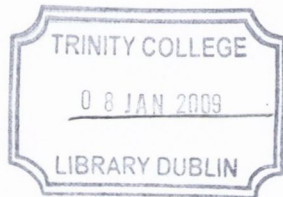
Trinity College Dublin,

Dublin 2.

Ireland

ph. D. Genetics

Declaration

I certify that this thesis, submitted to Trinity College Dublin for the degree of Doctor of Philosophy, has not been submitted as an exercise for a degree at this or any other university. I certify that the work presented here is entirely my own, except where otherwise acknowledged. This thesis may be made available for consultation within the university library and may be copied or lent to other libraries upon request.

_____

Petrina Delivani

October 2008

Acknowledgement

First of all I would like to thank Dr. Colin Adrain, Dr. Patrick Duriez, Dr. Rebecca Taylor, Dr. cand. Clare Sheridan and Dr. cand. Sean Cullen for allowing me to use some of their data in this thesis and their invaluable help for finishing our publications.

I would also like to thank my supervisor Prof. Seamus Martin for providing the exciting topic for this thesis. Your help, time and patience for explaining all details of apoptosis and cell biology was and will be of great value to me. I am also grateful having been able to visit conferences and meet interesting and important people of the field. Also, work was pepped up by lab retreats for everybody and time to get to know each other better. Thanks for all that.

My days in the lab were made good and funny even in tough times, by past and present members: Emma, Brona, Colin, Patrick, Gustavo, Alex, Rebecca, Sean, Clare, Gabi, Susan, Jon, Inna, Claudia, Jill and Declan. Thanks to everybody for listening to my stories and sometimes to my outbursts about chaos and untidiness. You were all great friends and support, which I needed loads of for this period!

My biggest thank you from my heart goes to my husband Markus, who was there with me for such a difficult time in my life, listened to all my worries and always knew how to built me up again. You have no idea how much help you are to me and without you, I would not have come so far! Thank you so much. I also stick my family, Markus family and all our friends in Germany, UK or wherever they are, in this line of thanks, who supported me all the time from the distance with their love and encouragement. And finally thanks for the greatest gift in the world, Helen and Eva.

Publications

Petrina Delivani, Colin Adrain, Rebecca *c.* Taylor, Patrick J. Duriez, Seamus J. Martin (2006). Role for CED-9 and EGL-1 as regulators of mitochondrial fission and fusion dynamics. Molecular Cell, 21, 761-773.

Petrina Delivani and Seamus J. Martin (2006). Mitochondrial membrane remodeling in apoptosis: an inside story. Cell Death and Differentiation, 13, 2007-2010.

Colin Adrain, Patrick J. Duriez, Gabriela Brumatti, **Petrina Delivani**, Seamus J. Martin (2006). The cytotoxic lymphocyte protease, granzyme B, targets the cytoskeleton and perturbs microtubule polymerization dynamics. Journal of Biological Chemistry, 281, 8118-8125.

Clare Sheridan, **Petrina Delivani**, Sean P. Cullen and Seamus J. Martin (2008). Bax or Bak-Induced Mitochondrial Fission can be Uncoupled from Cytochrome *c* Release. Molecular Cell, 31, 570-585.

Table of contents

Figures

Summary

Programmed cell death in the nematode *C. elegans* is the equivalent process to human apoptosis. Studying this process in the model organism has led to a great amount of knowledge about the details of pathway steps and proteins that are involved. While the system in the worm appears trivial with only four regulating proteins, in mammalian cells at least twenty proteins are already involved in the initiation of apoptosis. In this study we set out to investigate worm cell death proteins *in vivo* and *in vitro*. Although many things are already known, it has never been shown before, where and when the only worm caspase CED-3 is expressed *in vivo*. In the first part of our study we initially wanted to analyze the localization and *in vivo* expression pattern of CED-3 in *C. elegans* worm embryos. Although we employed several commercially available and self-generated anti-CED-3 antibodies, we were not able to achieve CED-3 staining in worm cells. However, during these experiments we found reorganization of the mitochondrial network by the expression of CED-9 in HeLa cells.

Bcl-2 family proteins play central roles in apoptosis by regulating the release of mitochondrial intermembrane space proteins such as cytochrome *c*. Death promoting Bcl-2 family members, such as Bax, can promote cytochrome *c* release and fragmentation of the mitochondrial network, whereas apoptosis-inhibitory members, such as Bcl-2 and Bcl-xL, can antagonize these events. It remains unclear whether CED-9, the worm Bcl-2 relative, can regulate mitochondrial fission/fusion dynamics or the release of proteins from the mitochondrial intermembrane space. In the second part of this thesis we investigated the role of the apoptosis-inhibitor protein family. We show that CED-9 interacts with Mitofusin-2/fuzzy onions and can promote mitochondrial clustering and dramatic reorganization of mitochondrial networks. Consistent with its ability to neutralize CED-9 function, EGL-1 antagonized CED-9-dependent remodeling of the mitochondrial network. However, CED-9 failed to inhibit mitochondrial cytochrome *c* release or apoptosis induced by diverse triggers in mammalian cells. Our data suggest that the ability to regulate

mitochondrial fission/fusion dynamics is an evolutionarily conserved property of the Bcl-2 family.

Bax and Bak promote apoptosis by perturbing the permeability of the mitochondrial outer membrane and facilitating the release of cytochrome *c* by a mechanism that is still poorly defined. During apoptosis, Bax and Bak also promote fragmentation of the mitochondrial network, possibly by activating the mitochondrial fission machinery. It has been proposed that Bax/Bak-induced mitochondrial fission may be required for release of cytochrome *c* from the mitochondrial intermembrane space. The third chapter of this thesis demonstrates that Bcl-xL, as well as other members of the apoptosis-inhibitory subset of the Bcl-2 family, antagonized Bax and/or Bak-induced cytochrome *c* release but failed to block mitochondrial fragmentation associated with activation of these proteins. These data suggest that Bax/Bak-initiated remodeling of mitochondrial networks and cytochrome *c* release are separable events.

Abbreviations

A1	Bcl-2 related protein A1
Abs	Antibodies
Act D	Actinomycin D
Apaf-1	Apoptotic protease activating factor
ATP	Adenosine triphosphate
Bad	Bcl-2 antagonist of cell death
Bak	Bcl-2 antagonist/killer
Bax	Bcl-2 associated X protein
Bcl-2	B-cell lymphoma-2
Bcl-B	Bcl-2 like B protein
Bcl-w	Bcl-2 like w protein
Bcl-xL	Bcl-2 like x protein
BH	Bcl-2 homology region
Bid	BH3 interacting domain death agonist
Bik	Bcl-2 interacting killer
Bim	Bcl2 interacting mediator of cell death
Bmf	Bcl-2 modifying factor
Bok	Bcl-2 related ovarian killer
BSA	Bovine serum albumin
C. elegans	*Caenorhabditis elegans*
CARD	Caspase activation and recruitment domain
CASPASE	Cysteinyl aspartate-specific protease
CED	Cell death defective
Cyt *c*	Cytochrome *c*
D. melanogaster	Drosophila melanogaster
dATP	Deoxyadenosine triphosphate
Dauno	Daunorubicin
DCI	3,4-Dichloroisocoumarin
DD	Death domain
ddH$_2$O	Double distilled H$_2$O
DED	Death effector domain
DIABLO	Direct IAP binding protein with low pI
DIAP-1	Drosophila inhibitor of apoptosis protein-1
DISC	Death-inducing signalling complex
DMEM	Dulbecco's modified eagle medium
DMSO	Dimethyl sulphoxide
DNA	Deoxyribonucleic acid
Drp-1	Dynamin related protein-1
EDTA	Ethylenediaminetetraacetic acid
EGL	Egg-laying defective
ER	Endoplasmic reticulum
FACS	Fluorescence-activated cell sorter
FADD	Fas-associated protein with death domain
FasL	Fas ligand
FCS	Fetal calf serum
FITC	Fluorescein isothiocyanate
Fis-1	Fission protein-1
FL	Full length

FZO	Fuzzy onions-related protein
GFP	Green fluorescent protein
Gf	Gain of function
GTP	Guanine triphosphate
HA	Haemaglutinin
HBS	Hepes-buffered saline
HEK	Human embryonic kidney
Hepes	N-(2-hydroxyethyl) piperazine-N'-(2-ethanesulphonic acid)
His	Histidine
HR	Heptade repeat
Hrk	Activator of apoptosis harakiri
HRP	Horse radish peroxidase
ICE	Interleukin-1β-converting enzyme
IL-1β	Interleukin-1β
kDa	kilodalton
LB	Luria Bertani
Lf	Loss of function
Mcl-1	myeloid cell leukemia sequence-1
Mfn	Mitofusin
MOMP	Mitochondrial outer membrane permeabilization
Myc	myelocytomatosis viral oncogene
NBD	Nucleotide binding domain
NGM	Nematode growth medium
NP40	Nonidet P40
OD	Optical density
Opa-1	Optic atrophy-1
PAGE	Polyacrylamide gel electrophoresis
PARP	Poly(ADP-ribose) polymerase
PBS	Phosphate-buffered saline
PCD	Programmed cell death
PCR	Polymerase chain reaction
Puma	p53 up-regulated modulator of apoptosis
RNA	Ribonucleic acid
RPMI	Roswell Park Memorial Institute
SDS	Sodium dodecyl sulphate
siRNA	Small interfering RNA
SMAC	Second mitochondrial activator of caspases
TAE	Tris acetate EDTA
TBST	Tris buffered saline with tween
TE	Tris EDTA
TNF	Tumour necrosis factor
TM	Transmembrane domain
TPCK	N-tosyl-l-phenylalanine chloromethyl ketone
UV	Ultraviolet irradiation
YFP	Yellow fluorescence protein
zVADfmk	Benzylocarbonyl-Val-Ala-Asp-(OMe) fluoromethylketone

CHAPTER I

Introduction

1 Introduction

1.1 Cell suicide

During the lifetime of an organism, cells divide and differentiate in a regulated manner to fulfill certain tasks. In the same way that mechanisms exist to control the development of cells and organs, there must be a corresponding mechanism to allow the elimination of excess or damaged cells. The process controlling the elimination of cells is referred to as programmed cell death or, as Kerr *et al.* termed it, apoptosis (Kerr *et al.*, 1972). Apoptosis or programmed cell death is a cell fate occurring in all multicellular organisms. During embryonic development for example there is a balance between cell division and removal. In order to sculpt the hands and feet of a human embryo removal of excess cells, forming the interdigital skin, between the fingers and toes has to occur. The process underlying this removal of cells is apoptosis (Jacobson *et al.*, 1997). Figure 1.1 demonstrates how the loss of a particular protein involved in apoptosis leads to a defect in cell removal and incomplete development of a mouse embryo (Yoshida *et al.*, 1998).

Apoptosis is not only important during development or in developing tissues it is also involved in cell turnover in adult tissues. Normal homeostasis of the human body is maintained by apoptosis, i.e. senescent cells or cells that are required only transiently are removed and replaced by newly generated ones (Jacobson *et al.*, 1997). The astonishing aspect about apoptosis is that cells in the process of apoptosis can be recognized by distinct morphological changes, which is easily observed under the microscope. These elements include nuclear condensation, blebbing of the plasma membrane and break up of the cell into apoptotic bodies (Kerr *et al.*, 1972) (Figure 1.2). Another important aspect of apoptosis is the preservation of the plasma membrane integrity, which guarantees the silent removal of dying cells by other cells through phagocytosis (by macrophages) without causing damage to their neighboring cells. Phagocytosis of the apoptotic bodies of dying cells guarantees that no intracellular components escape into the environment, which would cause an unwanted inflammatory response in mammalian systems (Raff, 1998).

wildtype
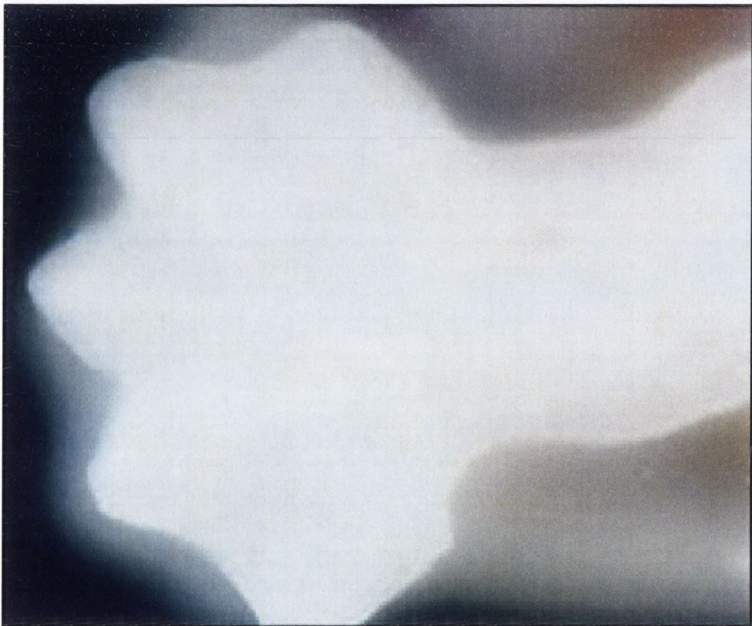
Apaf-1-knockout

Yoshida *et al.*, 1998

Figure 1.1: Knockout of apoptosis proteins *in vivo*
Hind limbs of wildtype and knockout mouse embryos.
Loss of Apaf-1 leads to the delayed removal of interdigital
webs in Apaf-1 knockout embryos.
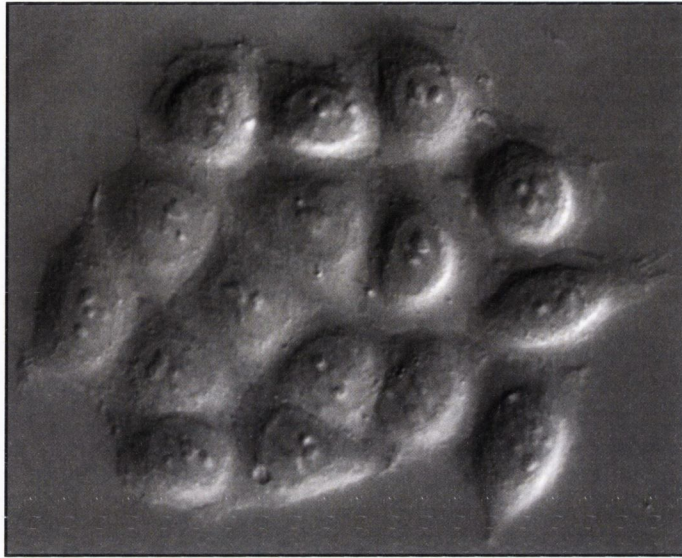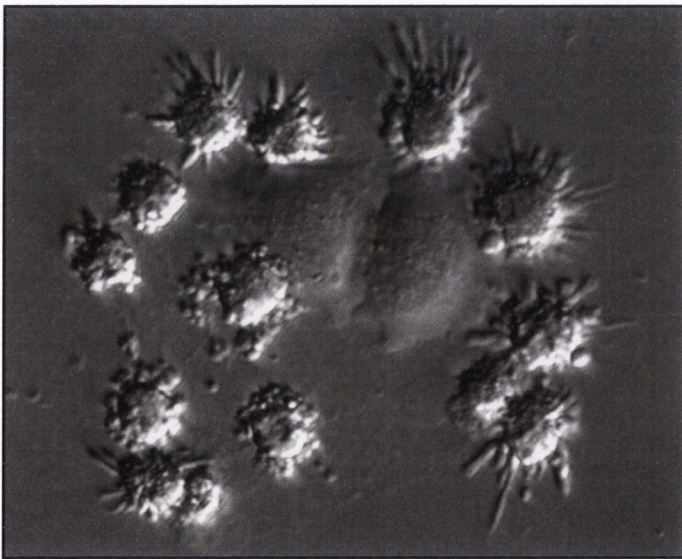
Figure 1.2: Morphology of dying cells in culture
HeLa cells were treated with actinomycin D (5µM) and observed for 10 hours. This RNA-synthesis inhibitor induces apoptosis in human cells. At the beginning of the treatment, cells are streched out and attached to the plate. After 10 hours of treatment, cells show a characteristic apoptotic morphology, including rounding up of the cell, shrinkage, plasma membrane blebbing and fragmentation into apoptotic bodies.

A very important reason for understanding apoptosis in all its molecular detail becomes evident if the cell death machinery ceases to function. Cells that have either lost the ability to initiate programmed cell death, or gained the ability to circumvent it can be the cause for diseases. Cancer development and neurodegenerative diseases can result as a consequence of disrupted apoptosis. Therefore, understanding the precise mechanisms behind this process are crucial to develop new therapies for human diseases in which apoptosis plays a role.

1.2 Apoptosis and Necrosis

Many environmental influences and agents can damage cells. For example heat, chemicals or physical injury to a tissue can lead to a deregulated, passive mode of cell death referred to as necrosis. In humans, necrosis results in the activation of an immune response. This happens because the plasma membrane of cells bursts and cytoplasmic contents are spilled into the surrounding. Cells of the immune system become deployed and infiltrate the affected tissue, thereby excreting inflammatory cytokines and amplifying the immune response (Raff, 1998).

The active form of cell death, apoptosis, is the focus of this study. Apoptosis is controlled by genetical and biochemical processes, which have been evolutionarily conserved from the nematode *Caenorhabditis elegans* (*C. elegans*) to man. For the regulation of apoptosis a battery of proteins have been identified that are involved. The execution of apoptosis relies on a family of proteases called caspases (cystein-aspartate specific proteases). While only one caspase is necessary in *C. elegans* (described in paragraph 1.6), more than 12 caspases have been identified to date in humans that are instrumental for different apoptotic pathways (Figure 1.3).

1.2.1 Caspases: the executioners of apoptosis

The human caspases can be seperated into two groups, based on the length of their N-terminal prodomains and their function. The first group are the initiator caspases, which are upstream in the apoptosis process (e.g. caspase-2, -8 and –9). They contain long prodomains, which include domains required for protein-protein interactions. Caspase-9 for example contains a CARD domain
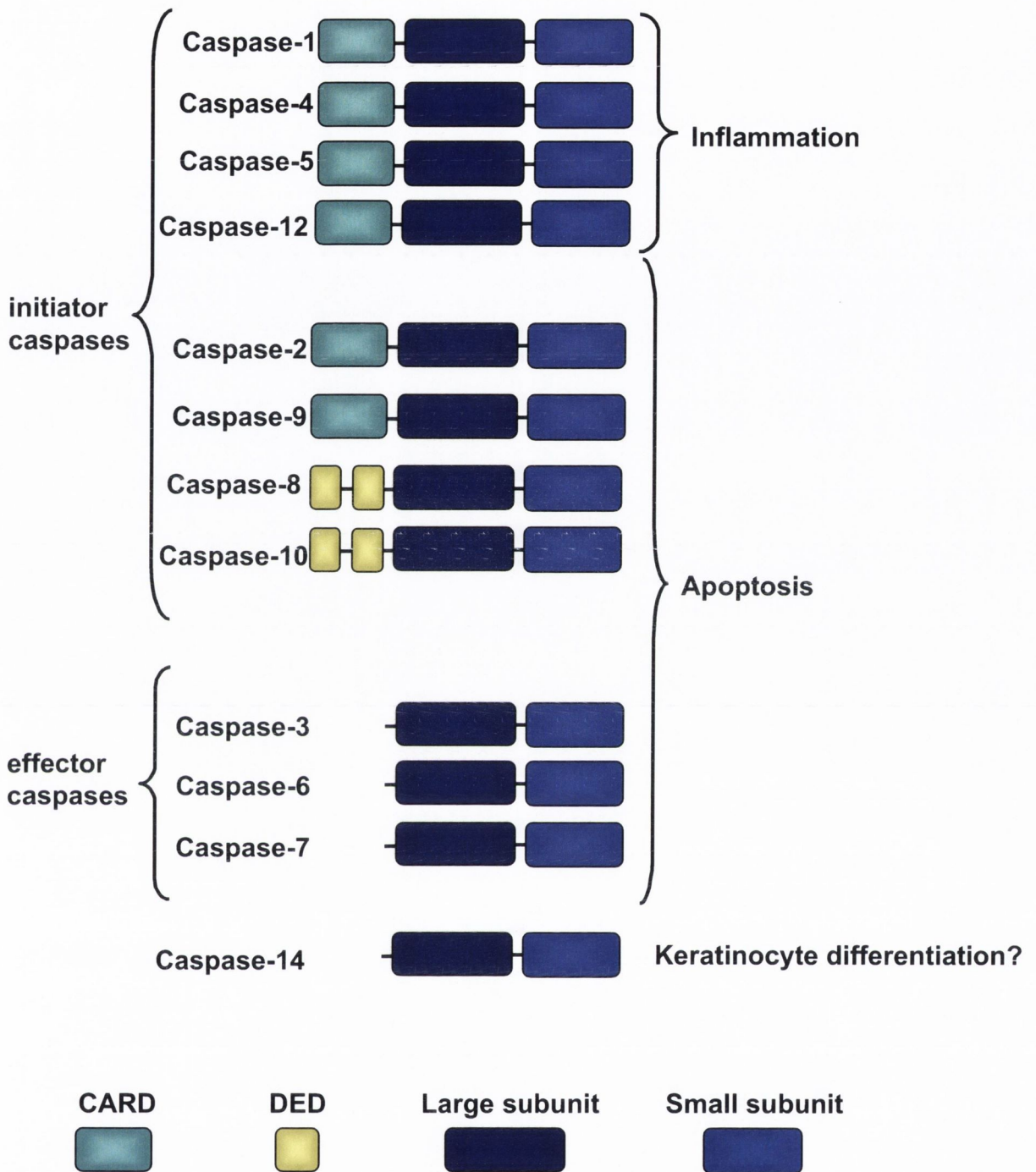
Figure 1.3: Schematic representation of caspases
Human caspases consist of a prodomain, which can include a CARD
(caspase recruitment domain), or a DED (death effector domain). The
prodomain is followed by a large and a small subunit. Caspases-1, -4, -5
and -12 have been implicated in inflammatory responses,
caspases-2, -3, -6, -7, -8, -9 and -10 are mediators of apoptosis.

(caspase recruitment domain), while caspase-8 and −10 contain a DED (death effector domain) (Nicholson, 1999) (Figure 1.3). Examples of activation mechanisms are described in detail below for caspase-8 and caspase-9, which are acting in two distinct apoptotic pathways. The main function of initiator caspases is to activate downstream effector caspases, which occurs through proteolytic cleavage of the latter. Effector caspases are seen as the main substrates for initiator caspases, and they contain conserved caspase cleavage sites (between their large and small subunit) for the proteolytic processing by initiator caspases. This region was found to be important for their activation, but also for a positive feedback loop to accelerate apoptosis (Earnshaw et al., 1999). The effector caspases (caspases -3, -6 and −7) contain short prodomains and exhibit the second group of caspases. They are the executioners of the cell death process and cleave downstream target proteins. The destruction of cellular substrate proteins then leads to the dismantling and death of the cell (Fischer et al., 2003). Such substrates include structural proteins of the cytoskeleton like actin and tubulin, which lead to the reorganization and break down of the cell once they are cleaved. More examples for substrates are the nuclear protein responsible for DNA repair PARP (poly ADP-ribose polymerase), as well as signaling kinases like Raf-1 that are cleaved by caspases. Another context in which caspases play a role is inflammation. This process employs the caspases-1, -4, -5 and -12, which are also long, CARD-containing proteases (Earnshaw et al., 1999; Creagh and Martin, 2003) (Figure 1.3).

1.2.2 Activation of caspases

Caspases are synthesized and exist in the cell as inactive zymogens, which require proteolytic processing in order to be activated (Martin and Green, 1995; Earnshaw et al., 1999). The general structure of a caspase is comprised of the prodomain followed by a large subunit and a small subunit. In order to become activated, caspases are first proteolytically processed between their large and small subunit, followed by a further step in which the prodomain is removed (Earnshaw et al., 1999). The processed enzyme then undergoes a conformational change and hetero-dimerizes its large and small subunit to reveal the active site pocket. In a final step, hetero-dimerization of two

processed caspase-chains occurs and reveals the tetrameric active caspase (Shi, 2002) (Figure 1.4). The active site of the protease is located on the C-terminus of the large subunit. This active site consists of a penta-peptide and contains the catalytic cysteine residue (QA**C**RG), which is conserved throughout the caspase family (Cohen *et al.*, 1997). Both subunits of a caspase contribute residues for the formation of the substrate-binding pocket comprised of four loops (S4-S3-S2-S1). This cleft binds precisely to four specific residues on a substrate molecule (target tetra-peptide: P4-P3-P2-P1). All known caspases possess an absolute specificity for cleavage after an aspartic acid residue at position P1 of the substrate target sequence (Thornberry *et al.*, 1997). As well as this absolute requirement for aspartic acid on P1, caspases show lose specificity for P2, prefer glutamic acid at P3 and have variable preferences for P4 (Thornberry *et al.*, 1997; Nicholson, 1999). Caspase activation occurs in different pathways, which are described below.

1.3 Apoptotic pathways

There are two main ways for a cell to die by apoptosis, which are referred to as the extrinsic pathway, dependent on signals from outside the cell, and the intrinsic pathway, dependent on signals from within the cell.

1.3.1 The extrinsic pathway: Death receptor mediated caspase activation

The extrinsic pathway involves receptors that are anchored into the plasma membrane with domains facing the extra-cellular matrix and domains reaching into the cytoplasm (Figure 1.5). These receptors, namely Fas- (fibroblast associated), or TNF- (tumor necrosis factor) receptor, belong to the TNF-receptor super-family (Schmitz *et al.*, 2000). They are characterized by the presence of cystein rich domains in the extra-cellular matrix part of the receptor (Ashkenazi and Dixit, 1998).

Activation of the receptor-mediated apoptotic pathway occurs via binding of their respective ligand (FasL=Fas ligand, or TNFα=tumor necrosis factor α) onto the extra-cellular matrix receptor domain. When for example FasL binds its receptor, the receptor trimerizes and the intracellular part of the receptor,
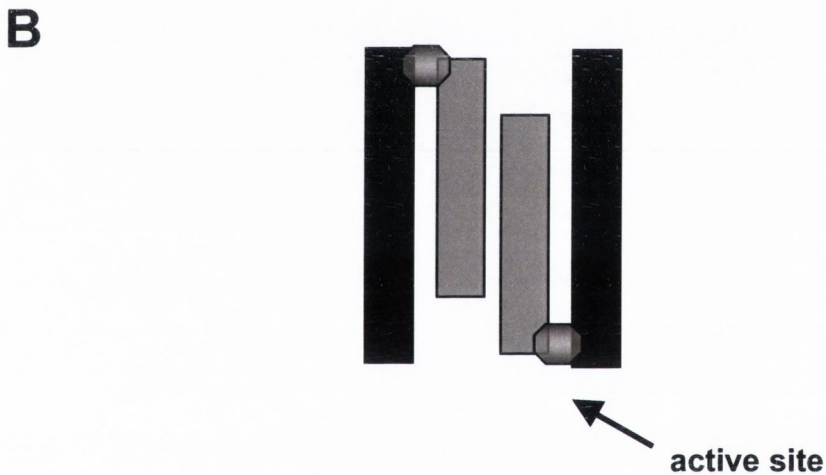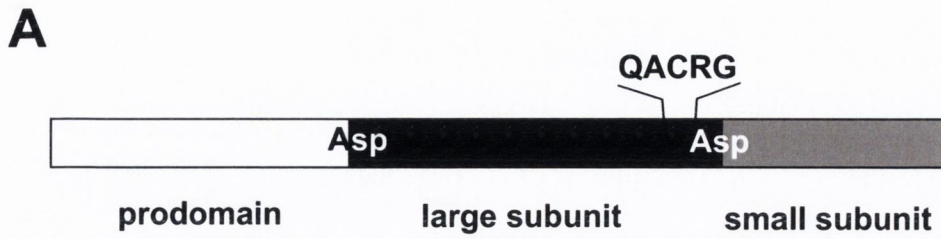
Figure 1.4: General structure of caspases
A) Domain structure of a pro-caspase: indicated are the prodomain and the large and small subunit. Caspases are synthesized as inactive zymogens and processed for activation. The processing sites (Asp= aspartic acid) are indicated where cleavage occurs for caspase maturation.

B) Structure of an active caspase: The active caspase is a heterodimer consisting of two large and two small subunits, the prodomain is removed. After processing, the caspase single chain precursor changes its conformation to expose the active site for substrate binding and cleavage.

containing death domains (DD), clusters to recruit the adaptor protein FADD (Fas-associated protein with death domain) with which it builds the so-called DISC (death inducing signaling complex) (Kischkel *et al.*, 1995). This leads to the further recruitment and binding of multiple caspase-8 molecules to FADD, resulting in caspase-8 activation via auto-processing between several caspase-8 molecules (Muzio *et al.*, 1996; Medema *et al.*, 1997). The mode of action downstream of caspase-8 activation depends on the cell type. In so-called type I cells, active caspase-8 directly targets the effector caspase pro-caspase-3 in order to activate it by proteolytical processing (Peter and Krammer, 2003). In contrast, in type II cells, caspase-8 first targets the pro-apoptotic molecule Bid and cleaves it. Truncated Bid (tBid) translocates to mitochondria and stimulates cytochrome *c* release via activation of Bax/Bak oligomerization. Cytochrome *c* release results in the formation of the apoptosome where caspase-9 is activated and only then leads to downstream activation of the effector caspase-3 (Kuwana *et al.*, 2002). The release of cytochrome *c* and downstream caspase activation is described below.

1.3.2 The intrinsic pathway: Caspase activation via mitochondria

Stimuli that trigger the intrinsic apoptosis pathway are factors like UV-light or drugs, which can cause cell stress. This in turn can lead to DNA damage, which induces the up-regulation of the molecule p53 in the cytoplasm of the cell and activates Bax (Chipuk *et al.*, 2004). Molecules acting as cell damage sensors, including p53 and the BH3-only proteins, transmit signals to mitochondria, which act as a platform for the integration of the intrinsic death pathway. In response to these damage signals, the molecules Bax and Bak are activated and result in the permeability of the mitochondrial outer membrane to cause cytochrome *c* release (Figure 1.5). Once released into the cytoplasm, cytochrome *c* together with dATP, binds to Apaf-1 (apoptosis protease-activating factor-1) a protein required for the activation of caspase-9. Apaf-1 is comprised of three domains, the CARD for interaction with the CARD of caspase-9, the nucleotide-binding domain (NBD) for oligomerization and the WD40 repeat region (Adrain *et al.*, 1999). Cytochrome *c* binds to the WD40 repeat region, thereby inducing a conformational change and unmasking the CARD of Apaf-1. The reorganized activating protein oligomerizes and binds to
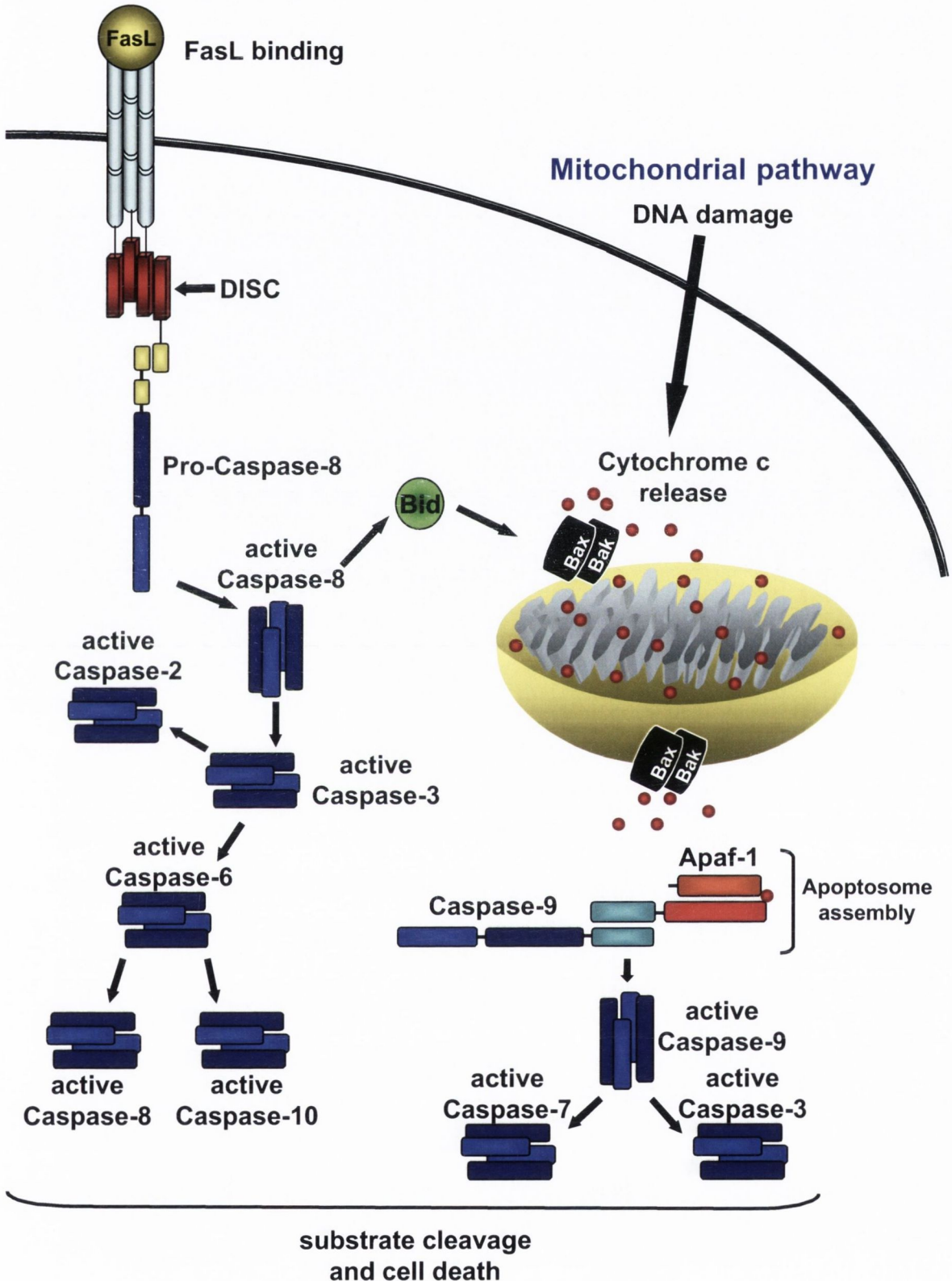
Figure 1.5: Activation of caspases in apoptotic pathways
The left hand side represents the receptor mediated pathway for caspase activation. On the right hand side the intrinsic pathway that acts through mitochondria to activate caspases is displayed. Both pathways result in activation of a caspase cascade, substrate proteolysis and cellular collapse. For details see text.

caspase-9. It was found that seven molecules of Apaf-1 oligomerize and recruit caspase-9 (Acehan *et al.*, 2002). The resulting complex forms a structure that resembles a wheel and is referred to as the apoptosome (Yu *et al.*, 2006, Adrain *et al.*, 2006). In this high molecular weight protein complex multiple caspase-9 molecules come into close proximity and auto-activate each other by proteolytical processing (Salvesen and Dixit, 1999). Once the initiator caspase (caspase-9) is active, a well-defined caspase cascade occurs to induce downstream effector caspase activation of caspase-3 and caspase-7, which cause the dismantling of the cell (Slee *et al.*, 1999) (Figure 1.5).

The focus of this study belonged to the mitochondrial apoptosis pathway, which is explained in the next section.

1.4 The role of mitochondria in apoptosis

1.4.1 Mitochondria in healthy cells

As described above, mitochondria play a central role in apoptotic processes in mammalian cells in both the extrinsic and the intrinsic apoptotic pathway. In healthy cells, these organelles guarantee the supply of energy through the production of ATP. Structurally, mitochondria are special organelles, because they are comprised of two membranes, an outer and an inner membrane. Both membranes harbor important proteins for the formation of channels, components of the electron transport chain and for oxidative phosphorylation (Figure 1.6). Over ninety percent of mitochondrial proteins are encoded in the nucleus and synthesized in the cytoplasm. Therefore, transport proteins are required to import proteins into the mitochondrion. TOM (transporter of the outer membrane) and TIM (transporter of the inner membrane) molecules, located in the respective membrane, can interact and form a channel when a protein has to be transported into the organelle (Bauer *et al.*, 2000).

The inner mitochondrial membrane is constructed in large invaginations reaching into the matrix of the organelle, which are called the cristae. Components of the electron transport chain, which is crucial for ATP production, are localized to the inner-mitochondrial membrane. This electron transport chain functions by transferring electrons in a step-by-step manner from complex I (*NADH dehydrogenase*) to complex II (*succinate dehydrogenase*) to complex
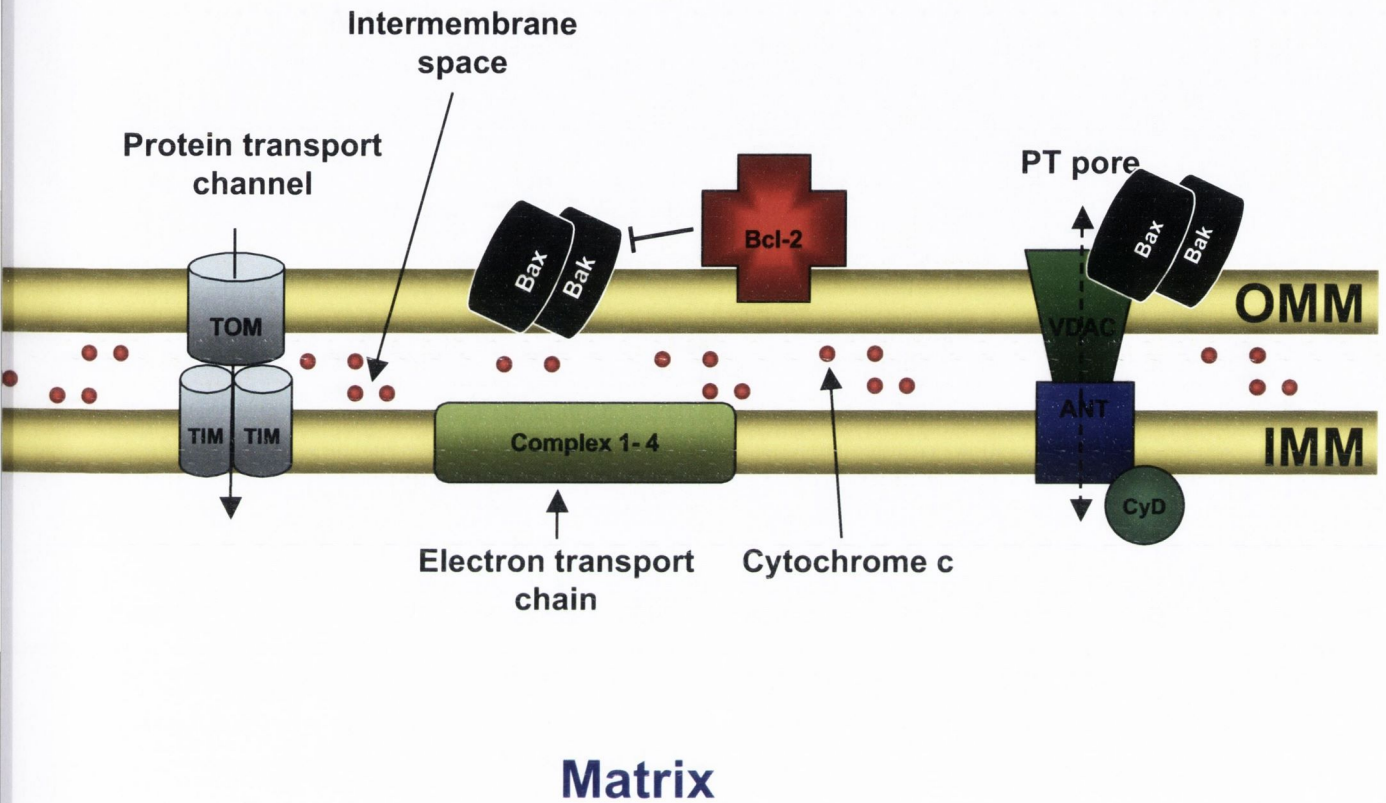
Figure 1. 6: Composition of the mitochondrial membrane
The double membrane of the mitochondria contains many proteins with various
functions for their physiological role. The translocator of the outer and inner
membrane (TOM and TIM, light blue) import proteins into the mitochondria.
Components of the electron transport chain (Complex 1-4, in yellow) transport
electrons from one to another and supply the energy potential to produce ATP.
VDAC (voltage dependent anion channel) and ANT (adenin nucleotide translocator)
are yet another transport channel for small molecules and nucleotides, which might
play a role in cell death by forming the PT (permeability transition) pore. OMM
(outer mitochondrial membrane), IMM (inner mitochondrial membrane).

III (*ubiquinol-cytochrome c- reductase*) to complex IV (*cytochrome c-oxidoreductase*). The molecule that delivers electrons from complex III to complex IV is cytochrome *c*, a small and mobile intermembrane space protein, which also plays a crucial role during the initiation phase of the mitochondrial apoptosis pathway. Complex IV uses the received electrons to generate water from oxygen and protons. During this electron transport the substrates of each of the complexes (I-IV) export protons from the matrix into the intermembrane space, thereby fueling a charge gradient across the inner membrane. This charge gradient was dubbed the mitochondrial transmembrane potential ($\Delta\psi$m) and is a hallmark for the function of mitochondria (Newmeyer and Ferguson-Miller, 2003). The membrane potential is used by complex V for production of energy. Complex V (or ATP synthase) is a multisubunit protein, which drives ATP synthesis via oxidative phosphorylation of ADP. ATP is exported from the mitochondrial matrix, and again, the potential is used to import ADP. Exchange of ADP/ATP is secured through the integral membrane molecules VDAC (voltage dependent anion channel) on the outer mitochondrial membrane and ANT (adenine nucleotide transporter) on the inner mitochondrial membrane (Zamzami and Kroemer, 2001). VDAC normally allows the passage of molecules of around 5 kDa across the outer membrane, supporting the exchange of respiratory chain substrates. In contrast, ANT only permits molecules smaller than 1.5 kDa (like ADP/ATP) to pass through the inner membrane, securing the maintenance of the inner membrane potential which is crucial for oxidative phosphorylation (Zamzami and Kroemer, 2001) (Figure 1.6).

1.4.2 Mitochondria in dying cells

As described in 1.3.2, release of cytochrome *c* is a crucial step leading to caspase activation. In fact it is the point of no return, after which cells will surely die. Other mitochondrial intermembrane space proteins are co-released in this process, for example Smac (second mitochondrial derived activator of caspases) and Omi/HtrA2, which also have roles in cell death, but are not described here. Permeabilization of the mitochondrial membrane must precede the release of cytochrome *c*, but the precise mechanism mediating this permeabilization has not been fully understood so far. Indeed, over the past

decades a huge controversy has built up in the literature and several hypotheses as to how mitochondrial membrane permeabilization occurs, have emerged.

One model of permeabilization of the outer membrane is its rupture through expansion of the inner membrane, by diffusion of water and solutes smaller than 1,5 kDa in size into the matrix. As a consequence of the physical rupture of the outer membrane, proteins harbored in the inter-membrane space, including pro-apoptotic proteins, are released (Martinou and Green, 2001). Oxidative stress or low ATP concentration have been proposed to cause this effect.

Another mechanism was postulated in studies investigating the formation of a pore for release of mitochondrial components. Interaction of VDAC with ANT and Cyclophilin D in the matrix of mitochondria was suggested as the components of the so-called permeability transition (PT) pore. Formation of this pore was thought to lead to the loss of mitochondrial membrane potential, which is seen during apoptosis. Once again this was thought to result in the release of cytochrome *c* and other inter-mitochondrial membrane space proteins, and subsequently in cell death (Zamzami *et al.*, 1995). However, Goldstein *et al.* observed the release of cytochrome *c* from the mitochondrial inter-membrane space despite the preservation of a mitochondrial membrane potential, indicating that it was independent of its loss (Goldstein *et al.*, 2000). In addition, it was found that caspase activation was required to cleave complexes of the electron transport chain in order to lose membrane potential, indicating a downstream effect of apoptosis (Ricci *et al.*, 2003). These observations were finally confirmed when animals were used that lacked either the inner membrane protein ANT (Kokoszka *et al.*, 2004) or the matrix protein cyclophilin D (Nakagawa *et al.*, 2005; Baines *et al.*, 2005). It was reported that apoptosis and cytochrome *c* release occurs normally and cells die without delay in such knockout cells, suggesting that those proteins are not important for the death of a cell, and contradicting the theory that the PT pore was responsible for the permeabilization of mitochondria.

So how is mitochondrial permeabilization initiated? A group of proteins, the pro-apoptotic Bcl-2 family members, are now known to be essential and can carry

out channel formation and permeabilization of the mitochondrial membrane. These proteins and their function are described in the next paragraph.

1.5 Bcl-2 family proteins: control of the mitochondrial apoptosis pathway

More than twenty Bcl-2 family members have been found in mammals to date (Figure 1.7). They are divided into two groups, according to their function and structural composition. The first group contains the multi-domain anti-apoptotic proteins, which contain four BH (Bcl-2 homology) domains and in some cases also a hydrophobic transmembrane domain. The most studied anti-apoptotic molecules are Bcl-2, Bcl-xL, Mcl-1 and A1. The second group of Bcl-2 family proteins is the group of the pro-apoptotic molecules, which is further divided into two sub-groups. Bax, Bak and Bok belong to the multi-domain pro-apoptotic proteins and the last group is defined by only containing one BH domain, the pro-apoptotic BH3-only sub-group (Puthalakath and Strasser, 2002; Danial and Korsmeyer, 2004) (Figure 1.7). Functions of the Bcl-2 family proteins are described below.

1.5.1 Apoptosis activation by Bcl-2 family members

The pro-apoptotic members of the Bcl-2 family Bax and Bak, are involved in mitochondrial outer membrane permeabilization (MOMP). The group of Stan Korsmeyer showed that knockout mice, lacking Bax and Bak proteins, are resistant to basically the majority of all apoptotic stimuli (Lindsten *et al.*, 2000, Wei *et al.*, 2001). However, the precise mechanism of mitochondrial permeabilization through Bax and Bak has remained obscure and has been the focus of much research to date. Different models have been suggested, by which for example Bax can induce mitochondrial outer membrane permeabilization.

Firstly, it was hypothesized that Bax interacts with the mitochondrial channel proteins ANT and VDAC to promote opening of the PT pore and allow water to diffuse into the mitochondrial matrix (Figure 1.6). Subsequent swelling and rupture of the outer membrane was thought to lead to the release of cytochrome *c*, similar to the model described above (Marzo *et al.*, 1998;
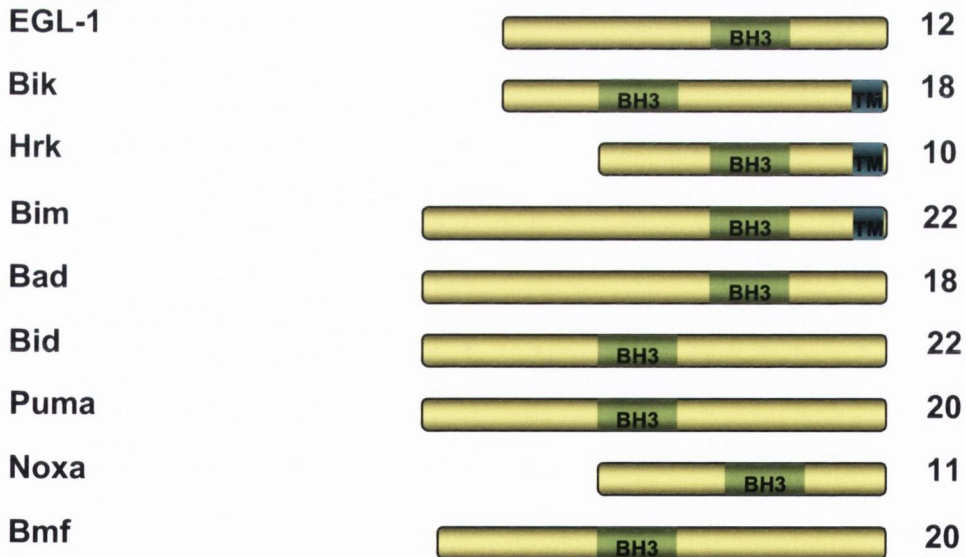
Figure 1.7: Classification of the family of Bcl-2 proteins
The Bcl-2 family of proteins contains pro- and anti- apoptotic members. As shown, all proteins contain at least one BH-domain (Bcl-2 homology). The anti-apoptotic proteins possess all four BH-domains, whereas multi-domain pro-apoptotic proteins lack he BH4 domain. The C-terminal membrane anchor of some members is hydrophobic and tethers them to the mitochondria. The molecular weight of the proteins is given on the right, as in www.uniprot.org.

Shimizu *et al.*, 1999). However, this was contradicted by showing that Bax-induced apoptosis could not be blocked by substances inhibiting the PT pore like cyclosporine A (Eskes *et al.*, 1998). In addition, physical interaction of Bax with PT pore forming proteins could not be demonstrated (Martinou and Green, 2001). Eskes *et al.* tested further PT pore inhibiting substances like bongkrekic acid and ADP. These compounds also failed to inhibit Bax-induced release of cytochrome *c* from isolated mitochondria and were only capable of inhibiting release of cytochrome *c* induced by the known PT pore opener Ca^{2+} (Eskes *et al.*, 1998).

A second model for channel formation in the mitochondrial outer membrane derived from studies based on structural analysis. It was revealed that Bax shows striking structural homology to bacterial toxins that form pores in their target cells, suggesting that Bax could be capable of forming similar pores into the mitochondrial membrane (Muchmore *et al.*, 1996; Antonsson *et al.*, 1997; Schlesinger *et al.*, 1997). Furthermore, it was observed that the inactive form of Bax is localized to the cytosol and has its C-terminal tail hemmed in a hydrophobic cleft, which is formed by its BH-domains. After activation, Bax releases its C-terminal transmembrane domain, translocates to mitochondria and inserts into the outer membrane (Nechushtan *et al.*, 1999; Suzuki *et al.*, 2000). However, insertion of monomeric Bax in the outer membrane of mitochondria was insufficient for cytochrome *c* release, therefore, it was suggested that Bax must oligomerize to form channels (Antonsson *et al.*, 2000 and 2001). Evidence for this hypothesis came from *in vitro* assays, where artificial liposome membranes were generated and oligomeric Bax indeed formed channels to release fluorescent-labeled cytochrome *c* after inserting into the artificial membrane (Saito *et al.*, 2000; Epand *et al.*, 2002). In addition, a recent *in vitro* study, using an artificial Bax/Bak channel blocker, supported the idea that the channel is required during apoptosis for the release of cytochrome *c* (Hetz *et al.*, 2005). As mentioned above, in order for Bax to induce cytochrome *c* release it must be activated. One way in which Bax can be activated is through interaction with the BH3-only proteins. Studies on those small pro-apoptotic members of the Bcl-2 family revealed interactions between multi-domain proteins Bax and Bak, and BH3-only domain molecules, leading to

activation of the Bax/Bak channel and are described in more detail in the next paragraph (Desagher *et al.*, 1999; Wei *et al.*, 2000).

The BH3-only proteins have been categorized into direct (Bid and Bim) and indirect (Puma, Noxa, Bmf, Bad, Hrk and Bik) activators of Bax and Bak (Kuwana *et al.*, 2005). These small pro-apoptotic molecules are regulated by a variety of mechanisms and factors that cause cell stress, thereby BH3-only proteins act as sensors for apoptotic stimuli. For example Puma and Noxa are under controlled by p53, which transcriptionally up-regulates these proteins after DNA damage (Oda *et al.*, 2000; Nakano *et al.*, 2001). Bad is regulated by the status of its phosphorylation in response to growth or survival factors (Zha *et al.*, 1996). Bim is kept in check by its sequestration to cytoskeletal structures and released to induce apoptosis in response to many stimuli (Puthalakath *et al.*, 1999). Another member, Bid, must be proteolytically processed by caspase-8 for its activation as described in 1.3.1 (Desagher *et al.*, 1999; Wei *et al.*, 2000).

Thus, in response to an apoptotic stimulus, the direct activators Bid and Bim shuttle to Bax and/or Bak and induce the necessary conformational change for their activation and translocation to the mitochondrion. All other BH3-only proteins were classified as indirect or de-repressor proteins, releasing Bax or Bak from the inhibitory effect of anti-apoptotic Bcl-2 family members (Kuwana *et al.*, 2005). Since it has proven difficult to directly show multimeric Bax-channel formation *in vivo* and *in vitro*, it is still unclear how exactly Bax and other multidomain pro-apoptotic proteins induce cytochrome *c* release; further studies are required to elucidate this.

1.5.2 Inhibition of apoptosis by Bcl-2 family members

The first protein found to be an inhibitor of apoptosis was Bcl-2, which was discovered in a B-cell lymphoma. This type of cancer is characterized by a chromosome translocation [t(14;18)] resulting in a fusion of the Bcl-2 gene with an immunoglobulin heavy chain promoter (Tsujimoto *et al.*, 1984).

The localization of Bcl-2 to the mitochondrial membrane through its C-terminal transmembrane domain gave one clou that fueled the idea that the Bcl-2 family might control the mitochondrial apoptosis pathway (Hockenbery *et al.*,

1990). Additionally, the BH1-BH4 domain containing anti-apoptotic members (Bcl-2, Bcl-xL, Bcl-w, Mcl-1, A1 and Bcl-B) (Figure 1.7), have a secondary structure akin to viral survival factors (v-Bcl-2). Using the alpha helices of BH domain 1-3 a hydrophobic pocket is formed, which can accommodate a BH3 domain of a pro-apoptotic member and thereby sequester and inactivate it (Muchmore *et al.*, 1996). This suggested that Bcl-2 directly prevents the action of the Bax/Bak channel by sequestering them through their BH3 domains. Furthermore, studies searching for interactions of pro- and anti-apoptotic proteins were undertaken and revealed direct interaction of Bax and Bcl-2 (Oltvai *et al.*, 1993) or Bax and Bcl-xL (Sedlak *et al.*, 1995).

To date the exact mechanism of apoptosis inhibition by the anti-apoptotic proteins remains elusive. For example it was shown that the pan-caspase inhibitor zVADfmk blocked Bax-induced cell death but not cytochrome *c* release. In contrast, over-expression of Bcl-xL blocked both cell death and cytochrome *c* release (Finucane *et al.*, 1999). Experiments in cell-free systems where Bcl-2 was over-expressed, showed similar results. Caspase inhibition and Bcl-2 over-expression could block apoptosis, but cytochrome *c* release was only blocked by Bcl-2 (Kluck *et al.*, 1997). These findings confirmed an upstream role for Bcl-2 family members and their function in regulating cytochrome *c* release in the mitochondrial pathway of apoptosis.

Theories on the action of the Bcl-2 family members have been reviewed in many places (Borner, 2003; Newmeyer and Ferguson-Miller, 2003; Danial and Korsmeyer, 2004; Green and Kroemer, 2004). On the one hand it is speculated, that simply the ratio of pro-apoptotic Bax and Bak versus anti-apoptotic molecules on mitochondrial membranes might set the threshold for apoptosis. On the other hand, Chen *et al.* described recently how certain anti-apoptotic proteins exhibit high affinities to specific BH3-only proteins (Chen *et al.*, 2005). This suggests that anti-apoptotic proteins control the activation of Bax and Bak by fishing out their activating molecules, the BH3-only proteins. In fact, both functions of the anti-apoptotic proteins seem to be required for the inhibition of apoptosis. However, regulation might lie on the side of the BH3-only molecules, which could act via inactivation of anti-apoptotic Bcl-2 family members, and the activation of the oligomerization of Bax and/or Bak to form a

cytochrome *c* releasing channel (Green, 2006). The exact hierarchy remains to be examined.

All these studies showed that control of apoptosis is a complex venture and requires activation of pro-apoptotic proteins as well as inhibition of anti-apoptotic proteins. The key components seem to be the Bcl-2 family proteins, but their precise interactions for regulation are complex, and to date not fully understood. Therefore, they need to be defined in more detail.

1.6 Cell death in the worm *Caenorhabditis elegans*

In 1974 Sydney Brenner and colleagues described programmed cell death during development in the model organism *C. elegans*. The group discovered that all cell death in *C. elegans* appeared to be invariant and developmentally programmed. Therefore, this model system was used to dissect the genetic control underlying the process of programmed cell death.

One nematode normally consists of 1090 somatic cells of which 131 cells undergo cell death during the embryonic development of the animal. This happens in a reproducible pattern in each *C. elegans* embryo with the same 131 cells dying (Sulston and Horvitz, 1977). The short generation time (3 days at 20°C) and a large brood size of around 300 progeny facilitated the genetic analysis of the worm. Genes encoding proteins involved in the regulation of cell death were found by genetic screening of mutants with defects in cell death. Four key players (CED-3, CED-4, CED-9 and EGL-1) were discovered to be essential for the regulation of the cell death program (Figure 1.8).

The worm caspase CED-3 (CED for <u>ce</u>ll <u>d</u>eath defective) is the effector protein and the most downstream component of the genetic pathway. Ellis and Horvitz isolated mutants of CED-3 together with CED-4 mutants (Ellis and Horvitz, 1986). *Ced*-3 and *ced*-4 mutant embryos contained extra cells that were normally destined to die. Cloning of the *ced*-3 gene revealed that it was similar to the mammalian Interleukin-1-beta (IL-1β) -converting enzyme (ICE), responsible for the proteolytic maturation of IL-1β (Yuan *et al.*, 1993). These two enzymes (CED-3 and ICE) became the founding members of the family of
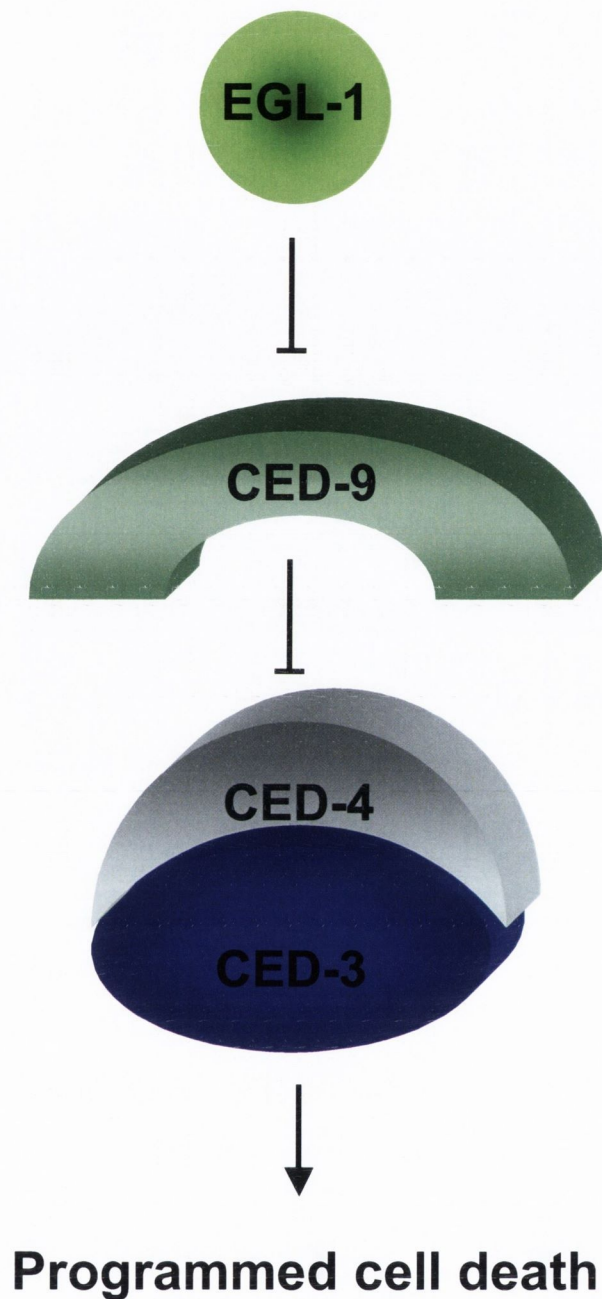
Figure 1.8: Programmed cell death in *C. elegans*
Genetic screens and subsequent analysis have established the regulatory pathway of cell death in the worm. The most upstream component is the BH3-only molecule EGL-1, which is transcriptionally upregulated. EGL-1 binds to CED-9, thereby inactivating its inhibitory function, resulting in the release of CED-4. Activation of the CED-3 caspase occurs due to the interaction of CED-4 with this protease.

caspases at the time. Like the mammalian cell death proteases, CED-3 contains a N-terminal CARD domain for interaction with other CARD containing molecules and an active site cystein in the penta-peptide region QA**C**RG (Figure 1.4). Although CED-3 resembles caspase-1 structurally, it is functionally more similar to human caspase-3, because it shares more substrate specificity with this protease (Xue *et al.*, 1996). Like the human caspases, CED-3 is thought to be synthesized by the cell as an inactive zymogen and requires activation to unleash its protease activity. Once activated, CED-3 (like caspase-3) targets downstream substrates and leads to the dismantling of the cell through substrate cleavage (Taylor *et al.*, 2007).

Activation of CED-3 occurs in a similar manner as activation of human caspases. Binding of CED-3 to the protein CED-4 is required for its activation. CED-4 is also essential for programmed cell death in the worm and is a homolog of the human protein Apaf-1 (Yuan *et al.*, 1992). Like Apaf-1, CED-4, contains a CARD on its N-terminus, which is necessary for binding to the caspase CED-3. In fact, direct physical interaction was found to occur and to be required for the activation of CED-3 caspase (Chinnaiyan *et al.*, 1997a; Irmler *et al.*, 1997). As mentioned above, the model of CED-3 activation resembles the activation of caspase-9 by Apaf-1 through the apoptosome and is therefore also referred to as the worm-apoptosome. In contrast to the human apoptosome only four CED-4 molecules (compared to seven Apaf-1 molecules) form the platform for CED-3 binding and activation (Shi, 2002; Adrain *et al.*, 2006). A CED-4 hetero-tetramer interacts with pro-CED-3. Precursor CED-3 proteins come into close proximity and activate each other through auto-processing (Seshagiri and Miller, 1997; Chinnaiyan *et al.*, 1997b; Yan *et al.*, 2005). Despite its significant similarity to Apaf-1, CED-4 activation of CED-3 does not require the binding of cytochrome *c* (Seshagiri and Miller, 1997; Chinnaiyan *et al.*, 1997b). Therefore, involvement of cytochrome *c* in the nematode death pathway has not been demonstrated so far and may not be important.

The only antagonist of programmed cell death in the worm is the Bcl-2 homologous protein CED-9. The first CED-9 mutant identified (*ced-9* (n1950)) revealed an identical phenotype to CED-3 or CED-4 mutants with 13 extra cells

present in the anterior pharynx, indicating that cell death was abolished (Hengartner *et al.*, 1992). Examinations of additional organs in this strain revealed surviving cells that were normally destined to die. Thus this mutant was determined to be a gain-of-function (*gf*) allele of CED-9 (Hengartner *et al.*, 1992). Further studies led to the mapping and cloning of the *ced-9* gene, and mutants were discovered that failed to block cell death. A loss-of-function (*lf*) mutant, (*ced-9* (n1653ts)) displayed multiple defects. First generation heterozygote *lf* mutant animals were missing neuronal cells, necessary for movement or egg laying. Additionally, embryos from loss-of-function animals died during embryogenesis, which underpinned an important role for CED-9 in the development and survival of *C. elegans* (Hengartner and Horvitz, 1994). Mechanistically, CED-9 functions through sequestration of CED-4 and thus prevents CED-4 from forming the CED-3 activating apoptosome. Analysis of the interaction of the two proteins by structure crystallizations showed that CED-9 binds to an asymmetric dimer of CED-4, but is only in direct contact with one of the two CED-4 molecules (Yan *et al.*, 2005). This mechanism is described in more detail in the next paragraph.

The fourth protein to be discovered with a pivotal role in worm cell death was EGL-1 (EGL=egg laying defective). This small (106 amino acids) protein contains a BH3-only domain and belongs to the pro-apoptotic family of proteins (Conradt and Horvitz, 1998). EGL-1 is a transcriptionally up-regulated protein, which binds to CED-9 (Jagasia *et al.*, 2005). Structural studies revealed the binding pocket for EGL-1 on CED-9, which was distinct from the binding site of CED-4 (Yan *et al.*, 2004). This study revealed that the two proteins (CED-4 and EGL-1) were not competing for the same binding site on the inhibitor protein CED-9. When EGL-1 binds to CED-9, the latter protein changes its conformation drastically rendering it incapable of binding to CED-4. By this EGL-1 leads to the release of CED-4 from CED-9 and triggers CED-3 dependent cell death (del Peso *et al.*, 1998; Yan *et al.*, 2004). Recently a further BH3-only protein was discovered in the worm, CED-13. This protein has been proposed to be important for damage-induced death in the germline of the worm. However, no mutant phenotypes have been found to play a role in the developing *C. elegans* embryo (Schumacher *et al.*, 2005).

1.7 Mechanism of death inhibition by CED-9

Bcl-2 is the human homolog of CED-9 and inhibits apoptosis in mammalian cells. To determine the inhibitory mechanism, studies were undertaken to examine whether Bcl-2 could block cell death in *C. elegans*. The generation of transgenic worms expressing heat shock inducible Bcl-2 (hs-Bcl-2) revealed that over-expression of Bcl-2 could in fact inhibit the death of cells normally destined to die (Vaux *et al.*, 1992). Furthermore, despite a relatively low sequence similarity of less than 30 percent, Bcl-2 was able to substitute for CED-9 and rescue loss-of-function *ced*-9 mutant animals (Hengartner and Horvitz, 1994). However, the putative model of programmed cell death inhibition is different from worm to man. Although both proteins are localized to mitochondria by a C-terminal transmembrane domain, the mode of cell death inhibition in the worm is through sequestration of the caspase activating protein CED-4, and not, as in mammalian cells, through inhibition of the release of pro-apoptotic molecules from mitochondria such as cytochrome *c* (Figure 1.9).

Another approach to elucidate CED-9 protein function and the pathway of cell death, involved the controlled expression of the genes *ced*-3, *ced*-4 and *ced*-9 under a promoter specific to touch sensory neurons (Shaham and Horvitz, 1996). In a CED-4 deficient strain the over-expression of CED-3 was sufficient to kill cells. In contrast, the inverse experiment of CED-4 over-expression in a *ced*-3 *lf* strain did not kill. These findings demonstrated the requirement of CED-3 for all cell death. Interestingly, prevention of the CED-3 killing activity by CED-9 (in the CED-4 deficient animals) was dependent on CED-4. CED-9 could not block CED-3 over-expression in the absence of functional CED-4 protein (Shaham and Horvitz, 1996). These *in vitro* studies indicated a pathway, in which CED-9 acts upstream of CED-4 to inhibit it from binding to, and thereby activating CED-3.

Following these *in vivo* investigations, the molecular mechanism mediating *C. elegans* programmed cell death was revealed by biochemical assays. CED-9 interacted strongly with CED-4 in a yeast-two-hybrid assay (Spector *et al.*, 1997). To perform co-immunoprecipitation experiments, CED-9 was heterologously expressed in human cells and interactions were found between CED-9 and CED-4, but not CED-3 (Chinnaiyan *et al.*, 1997a; Wu *et al.*, 1997b). Finally, mimicking the cell death pathway in human cells by co-
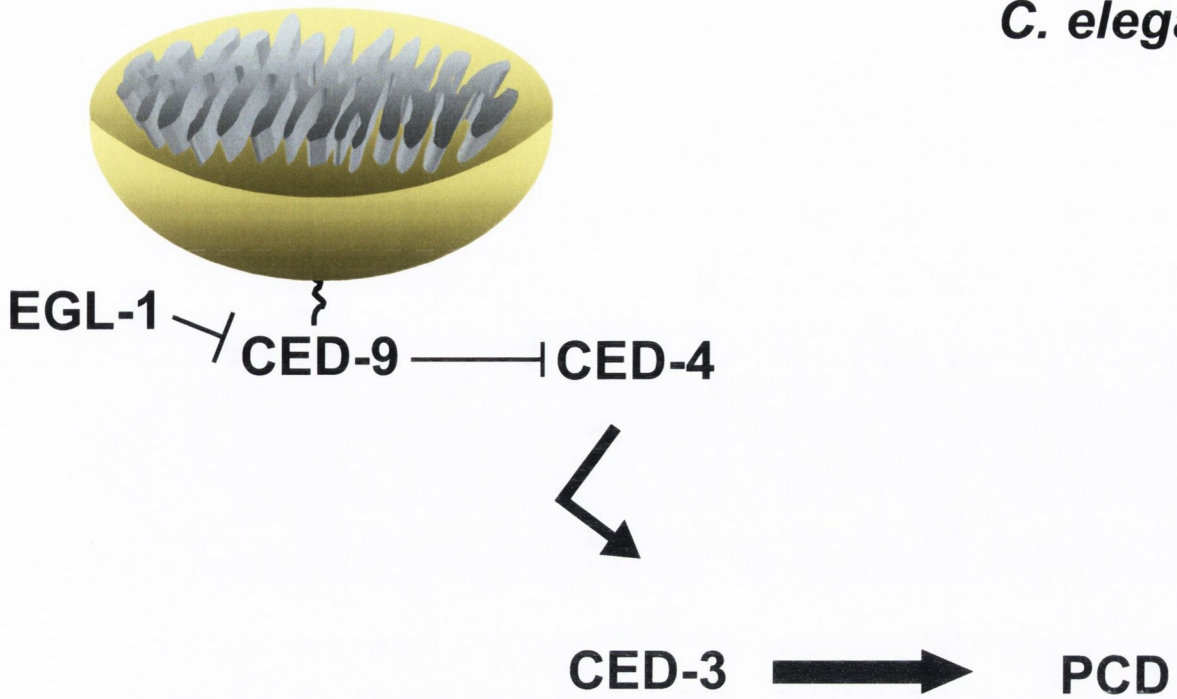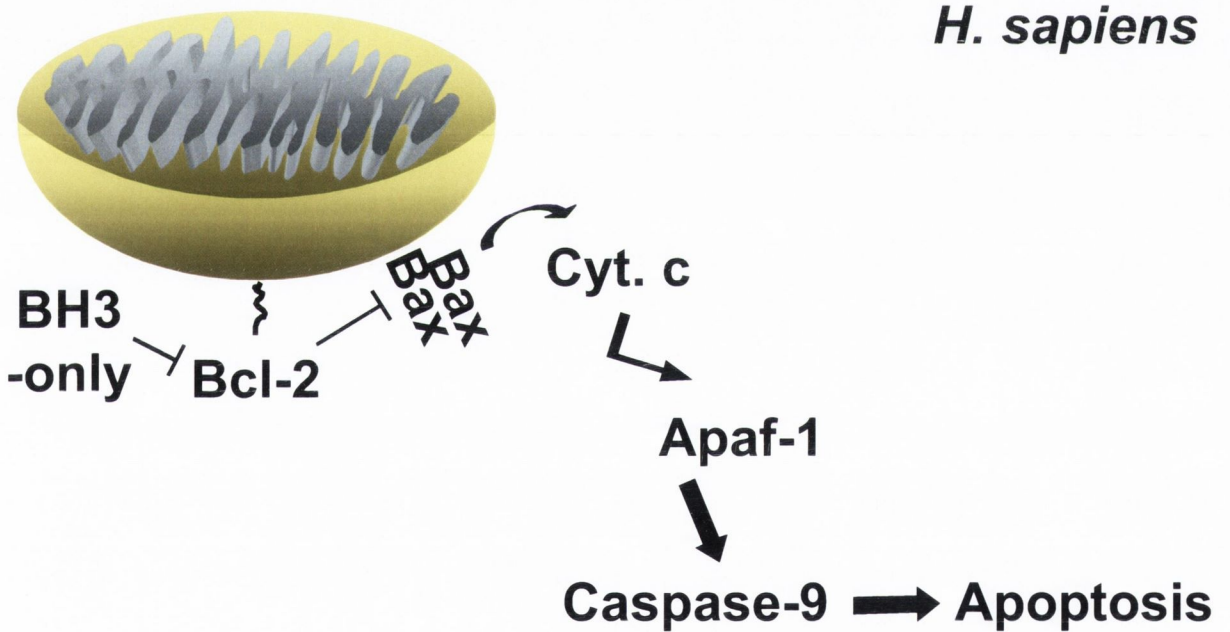
Figure 1.9: Cell death regulation by the Bcl-2 family of proteins
In *C. elegans* the mitochondrial pathway of programmed cell death is regulated by the sequestration of CED-4 by CED-9 on the mitochondrial outer membrane. This prevents CED-4 from binding and activating CED-3. EGL-1 can bind to CED-9 and displace CED-4, which leads to the activation of the cell death machinery.

In human cells, cytochrome c release from mitochondria is required for cell death activation. Bcl-2 family members block the oligomerization of Bax and Bak, thereby blocking cytochorome c release. BH3-only proteins can overrule the blocking and induce apoptosis by binding to Bcl-2 or Bcl-xL.

expression of the core proteins confirmed the proposed model of inhibition of death. While CED-3 and CED-4 induced apoptosis in different cell lines, addition of CED-9 was able to block this (Wu *et al.*, 1997b; Yang *et al.*, 1998; Hisahara *et al.*, 1998).

Recently, an explanation for the gain-of-function mechanism of the CED-9 (G169E) mutant protein was found, when structural analysis showed the physical alterations in the protein. The EGL-1 binding groove of CED-9, consisting of the BH1, BH2 and BH3 domain, is altered in this mutant. The amino acid glycin 169, a residue within the BH1-domain, is substituted with glutamic acid, which results in the protrusion of the side chain of this amino acid. This bulky extension inhibits the integration of EGL-1 into the groove of CED-9 (Yan *et al.*, 2004).

Attempts to immunolocalize the cell death machinery in worm embryos have proven to be problematic. However, one study from Chen *et al.* suggests that CED-9 localizes to mitochondria of *C. elegans* embryos, which is supported by the presence of a transmembrane domain on the C- terminus of the protein (Chen *et al.*, 2000). In addition CED-4 was sequestered by CED-9 to mitochondria and translocated to the nuclear periphery after cell death induction (Chen *et al.*, 2000). Despite these pieces of evidence it remains a puzzle why CED-9 and many Bcl-2 family proteins are localized to the mitochondrion, and whether mitochondria play a role in the nematode cell death pathway. There is evidence to suggest that, in human cells Bcl-2 and other anti-apoptotic proteins protect cells from dying by regulating the release of cytochrome *c* from the mitochondrial intermembrane space. However, this has not been shown to be the case for CED-9. So the question is, whether CED-9 plays another role in the cell due to its anchorage in the mitochondrial membrane.

1.8 Mitochondrial fusion and fission

Mitochondria are dynamic organelles that form an interconnected network throughout the mammalian cell. In contrast to textbook illustrations of small round shaped structures, mitochondria in live cells usually exist as a tubular, dynamic network. Movement of mitochondria from one end of the cell to the other is important for several reasons. For example, in order to secure the

energy supply of the whole cell, mitochondria move along the cytoskeletal scaffold and deliver ATP. Another very important reason for the dynamic nature of mitochondria comes into focus during cell division. In order to furnish the future daughter cell with an equal amount of mitochondria they are required to divide and disperse into the two halves of a dividing cell (Yaffe 1999).

The dynamics of mitochondria are orchestrated by two groups of proteins, one that controls fusion, and another that controls division (or fission) of mitochondrial membranes (Figure 1.10). Proteins inducing fusion of the organelles are the mitofusins-1 and -2 (Mfn-1 and Mfn-2), which are located on the outer mitochondrial membrane. A third fusiogenic protein is Opa-1, which spans the inner mitochondrial membrane (Figure 1.11). The group responsible for mitochondrial fission is comprised of the protein Drp-1 (dynamin related protein-1) and Fis-1 (human Fis-1). With the exception of Fis-1, these fission or fusion proteins belong to a family of large GTPases with diverse physiological functions. Mutations in the protein Mfn-2, for example, cause Charcot-Marie-Tooth type 2A, a neuropathy that is characterized by the loss of myelinated axons of the peripheral nervous system (Zuechner et al., 2004). Mutations in the Opa-1 gene are the prevalent causes for the atrophy of the optic nerve and can lead to childhood blindness (autosomal dominant optic atrophy) (Delettre et al., 2000). The fusion protein Opa-1 was named after the phenotype of the disease it is causing.

1.8.1 Mitochondrial fusion

Mitochondrial fusion is required to balance fission events and thereby maintain mitochondrial function. The first protein identified, which is responsible for fusion of mitochondrial structures, was found in sterile *Drosophila melanogastor* mutant males (Hales and Fuller, 1997). It was called *fuzzy onions* (fzo) according to the mitochondrial phenotype it caused in the sperm of male flies that resembled sliced onions. Mutations in *fzo* led to a failure of mitochondria to fuse to a "Nebenkern" and they aggregated beside the nucleus in the early sperm. Homologous proteins in Yeast (*FZO*), *C. elegans* (Fzo related protein-1) and mammals (Mfn-1 and –2) have been identified, which revealed evolutionary conserved domains also indicating a functional conservation of the protein (Mozdy and Shaw, 2003). Sequence analysis showed that the Fzo protein and
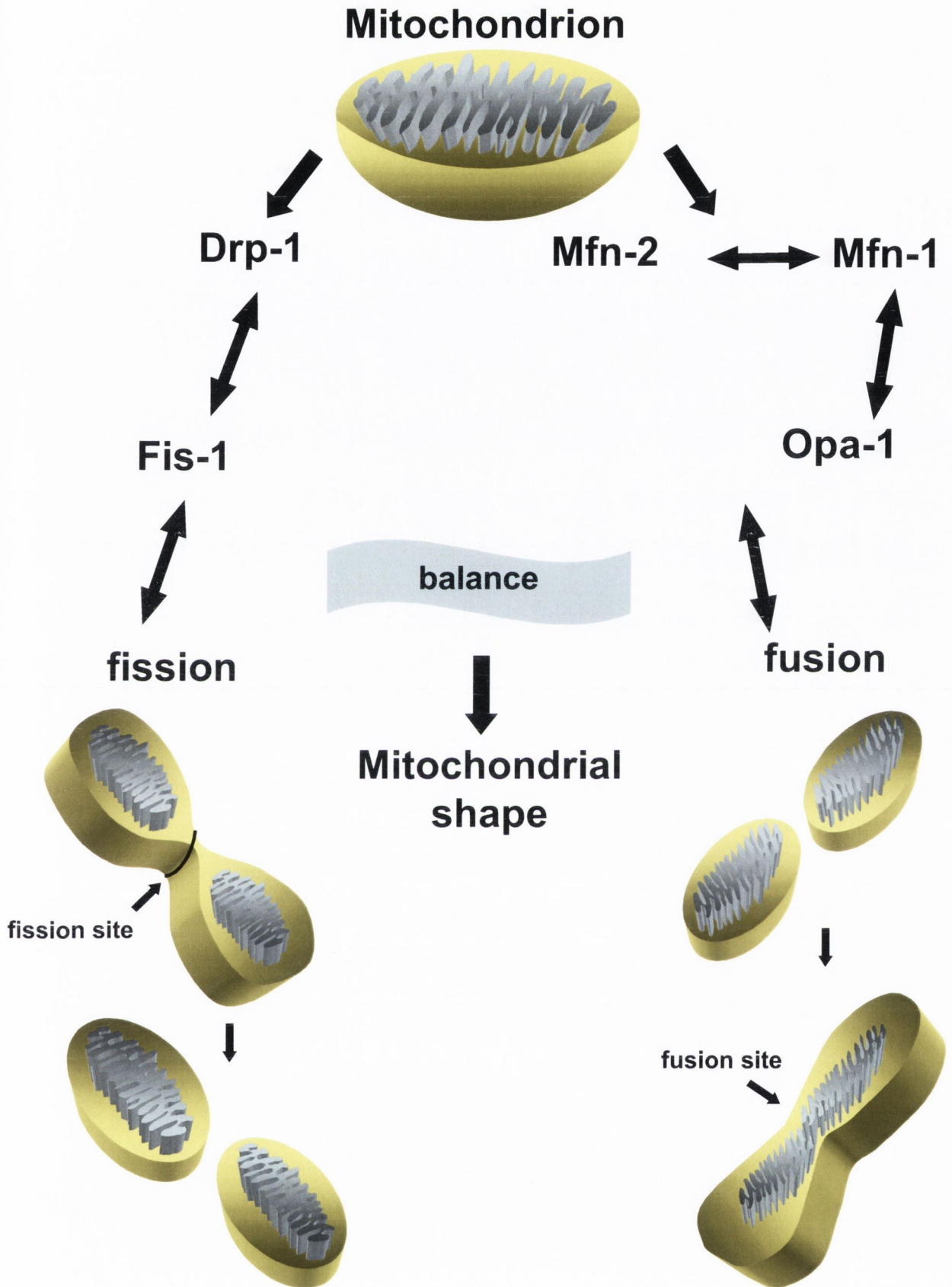
Figure 1.10: Mitochondrial fission and fusion
Fission and fusion events of mitochondria must be balanced. This role is taken on by Drp-1 and Fis-1, which control the scission of the organelle and Mfn-1, Mfn-2 and Opa-1, which control the fusion. If fission is blocked in cells, mitochondria elongate into long tubules doubling the size of normal mitochondria. If fusion is blocked, mitochondria disintegrate into small fragment. arrow indicates interaction ⟷

its homologues are large GTPases, belonging to the same super-family of dynamin related GTPases as Drp-1 (Praefcke and McMahon, 2004). The difference to Drp-1 lies in the protein structure, which in contrast to the mitofusins does not contain a hydrophobic transmembrane domain in the C-terminus. Structural analysis of the proteins showed that Mfn-1 and Mfn-2 span the outer mitochondrial membrane twice, with the N- and C-terminal part exposed to the cytoplasm (Santel and Fuller, 2001). A small, 2-3 amino acid linker region separates the C-terminal bipartite transmembrane domain and two conserved heptad repeat (HR) regions flank the transmembrane domain (Figure 1.11). Those HR domains form anti-parallel coiled coils, which mediate fusion of mitochondria by tethering opposing mitofusins on two adjacent organelles (Koshiba *et al.*, 2004).

Interestingly, transient over-expression of Mfn-1 and Mfn-2 in mammalian cells resulted in a phenotype strongly differing from the normal tubular mitochondrial network. Mitochondria in those cells showed a collapsed network with organelles clustering around the nucleus in a bulky, bony appearance. Although the N-terminal GTPase domain of mitofusins was required for proper mitochondrial fusion events, the clustered phenotype was achieved even when the GTPase domain was mutated. Point mutations or deletions in the GTP binding region still showed collapsed mitochondria (Santel and Fuller, 2001). In contrast, truncations of the C-terminus and mutations in the loop linking the transmembrane domains, abolished mitochondrial localization and stopped the formation of mitochondrial clusters of Mfn-1 and Mfn-2 mutants (Rojo *et al.*, 2002; Santel *et al.*, 2003). In addition the HR domains revealed to be necessary for mitochondrial tethering and clustering, because fusion was abolished after disrupting the helical structure of the coils with an amino acid substitution to proline (Koshiba *et al.*, 2004).

Light was shed on the essential role of mitofusins for steady state mitochondrial dynamics, when the proteins were deleted in mice. Knockout of either Mfn-1 or Mfn-2 led to embryonic lethality, and demonstrated the importance of mitochondrial fusion during development. In addition, MEFs (mouse embryonic fibroblasts), derived from knockout embryos contained fragmented mitochondria. After reintroduction of either Mfn-1 or Mfn-2 into
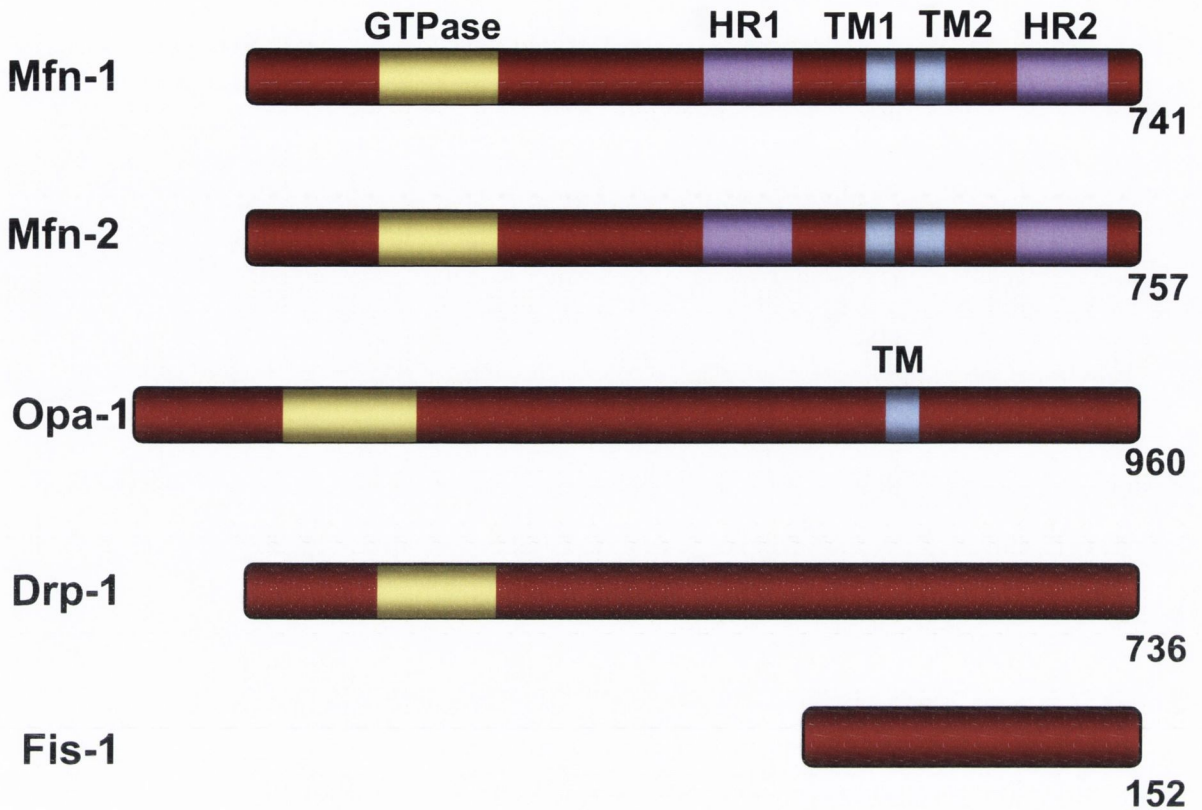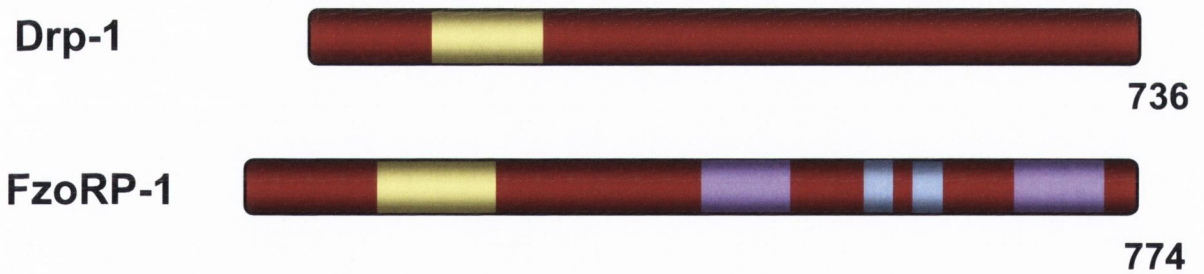
Figure 1.11: Overview of fission and fusion proteins
Most proteins required for mitochondrial dynamics are dynamin-related large GTPases except for Fis-1. They are separated into two groups that are promoting fission or fusion. The fission proteins are Drp-1 and Fis-1, and the fusion proteins are Mfn-1, Mfn-2 and Opa-1. The latter ones contain a transmembrane domain (TM) for anchoring into the mitochondrial membrane. Fission and fusion proteins are evolutionarily conserved and can also be found in *C. elegans* (Drp-1 and FzoRP-1 [fuzzy onion related protein-1]). GTPase (GTP hydrolysis domain), HR (heptad repeat region), TM (transmembrane domain).

knockout MEFs restored fusion and mitochondrial function, again underscoring the importance of these proteins (Chen *et al.*, 2003) (Figure 1.12).

Recently a role for mitochondrial fusion proteins in the mechanism of apoptosis has been suggested. For example, Sugioka *et al.* over-expressed the rat homolog of mitofusins (Fzo-1) in HeLa cells, and observed that the fusion protein reduced apoptosis induced by etoposide most likely through the inhibition of the oligomerization of Bax (Sugioka *et al.*, 2004). In addition, a dominant active form of Mfn-2 (which showed increased GTP binding) could block Bax activation and its translocation to regions of fusion clusters. This suggested that the dominant active form of Mfn-2 is acting as a direct inhibitor of Bax oligomerization and subsequent cytochrome *c* release (Neuspiel *et al.*, 2005). Furthermore silencing of endogenous mitofusins and Opa-1 in rat and human cells resulted in a sensitization of those cells to drug induced cell death and cytochrome *c* release (Lee *et al.*, 2004; Sugioka *et al.*, 2004).

The third member of the large GTPase super-family Opa-1 was suggested to be responsible for the fusion events of the inner mitochondrial membrane (Olichon *et al.*, 2003). Cipolat and co-workers reported that Opa-1 requires Mfn-1 to mediate fusion of the inner mitochondrial membrane, because when it was over-expressed in Mfn-1 knockout MEFs it failed to restore tubular shaped, elongated mitochondria. This was not observed in Mfn-2 knockout cells, where endogenous Mfn-1 was still present and interacted with Opa-1 to fuse mitochondria (Cipolat *et al.*, 2004). Further studies in cultured cells gave clues about the mechanism of Opa-1 action in the pathology of optic atrophy. By silencing Opa-1 in HeLa cells with siRNA, a dramatic fragmentation of mitochondria was observed. This fragmentation was proposed to lead to subsequent loss of cytochrome *c* and apoptosis of the affected cell. A similar mechanism was therefore suggested for the loss of the neurons in the phenotype of childhood blindness (Olichon *et al.*, 2003; Griparic *et al.*, 2004). Further underscoring a role of Opa-1 in apoptosis was the finding by Frezza *et al.* (2006) where it was claimed that over-expression of Opa-1 protects cells from undergoing apoptosis by preventing cytochrome *c* release (Frezza *et al.*, 2006). In this study Opa-1 was shown to control the tightness of the cristae
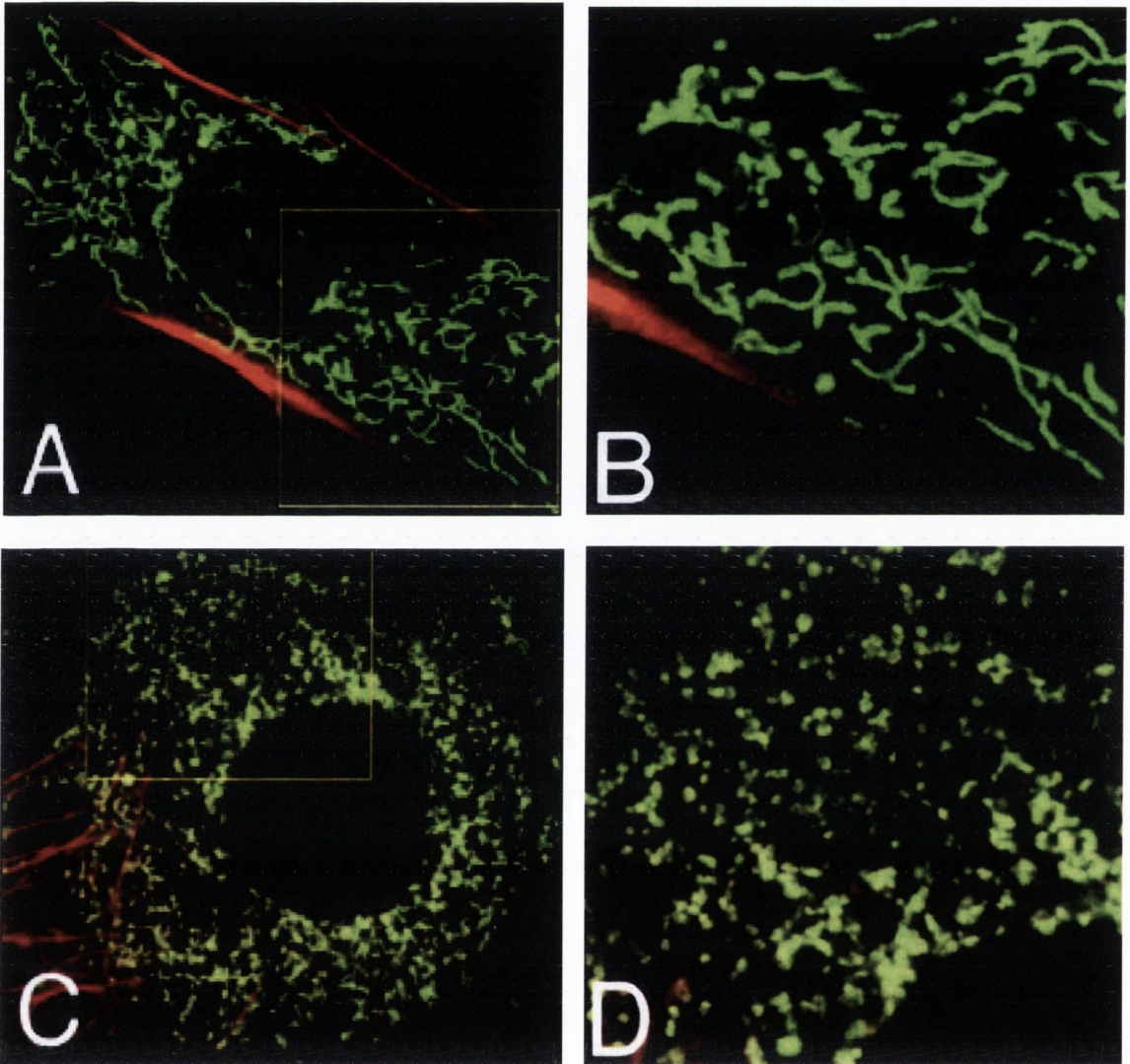
Figure 1.12: Mitochondrial phenotype in healthy and Mfn-1 mutant cells
A) Mouse embryonic fibroblasts (MEF) of wild type animals are shown. In healthy cells mitochondria build a tubular network throughout the cell. MEFs were transfected with a YFP protein targeted to the mitochondria. B) is an enlargement of A).

C) MEFs from Mfn-1 knockout animals were observed for mitochondrial morphology by transfection with mitoYFP. Mutant mitochondria lack the ability to fuse and therefore display a fragmented mitochondrial phenotype. D) is an enlargement of C).

junctions of the mitochondrial inner membrane. Since the bulk concentration of cytochrome *c* is stored in the cristae structure, by controlling their gate, Opa-1 could suppress its release when over-expressed. However, the group could not find evidence of Opa-1 interfering with Bax and Bak to block apoptosis like the anti-apoptotic proteins do.

Taken together, the above observations have been instrumental for the suggestion that mitochondrial fusion proteins are involved and necessary in the regulation of apoptosis. This adds another level of the regulation of the intrinsic mitochondrial pathway and the control of cytochrome *c* release that is fundamental for the initiation of apoptosis.

1.8.2 Mitochondrial fission

First clues about the role of Drp-1 in mitochondrial fission came from the over-expression of a dominant negative mutant of Drp-1 (Drp-1K38A) in COS-7 cells. Drp-1 is related to dynamin a membrane trafficking protein that assembles a spiral constriction site to cut off vesicles from the plasma membrane during endocytosis. The mutation in Drp-1K38A mapped to the conserved GTP binding domain and caused a dramatic redistribution of the mitochondrial network into large perinuclear aggregates (Smirnova *et al.*, 1998).

A Drp-1 homolog was found in *C. elegans* with more than sixty percent homology to human Drp-1. Labrousse *et al.* (1999) showed that silencing of DRP-1 in the nematode with siRNA led to embryonic lethality (Labrousse *et al.*, 1999). This death was suggested to be due to the missorting of mitochondria in the maternal gonads when DRP-1 was absent. Furthermore, over-expression of DRP-1 in transgenic animals showed enhanced function of the protein resulting in spherical shaped, fragmented mitochondria. In addition, localization studies found DRP-1 on constriction sites of mitochondrial division in muscle cells. This led to the suggestion that DRP-1 functions as a scission protein (Labrousse *et al.*, 1999).

In order to recruit Drp-1 to fission sites on mitochondria, Fis-1 was suggested to act as receptor. Clues for this interaction emerged from studies undertaken in yeast cells where Dlp-1 (the yeast homolog of Drp-1) recruitment to the

mitochondria depended on yeast Fis-1p (Mozdy *et al.*, 2000). Through its transmembrane domain Fis-1 is localized to the mitochondrial outer membrane where it recruits Drp-1. Furthermore, Drp-1 and Fis-1 interacted by co-immunoprecipitation and Fis-1, which further underlined Fis-1 as a recruitment factor for Drp-1 (James *et al.*, 2003; Yoon *et al.*, 2003). A role for Fis-1 during apoptosis has been suggested and is described more detailed in the next section.

As for the mitochondrial fusion proteins, fission proteins have lately been suggested to be involved in the regulation of apoptosis. Resulting mitochondrial fragmentation is believed to be crucial during apoptosis to regulate cytochrome *c* release.

1.8.3 The role of mitochondrial fission in apoptosis

Changes of mitochondrial distribution in mammalian cells during apoptosis were described by several groups (De Vos *et al.*, 1998; Desagher and Martinou, 2000). The group around De Vos had treated L929 cells with TNFα , and Martinou and colleagues had over-expressed Bax in HeLa cells and observed that the mitochondrial network clustered at the nuclear periphery after induction of apoptosis. The group suggested a cooperative effect of mitochondrial fragmentation for the induction of cell death.

This hypothesis was further investigated to explore the potential role of mitochondrial shaping proteins during apoptosis. Over-expression studies of Drp-1 in the mammalian system sensitized cells to apoptotic stimuli like staurosporin (Frank *et al.*, 2001) or Bax and Bak (Arnoult *et al.*, 2005), which suggested that mitochondrial fragmentation, induced by the over-expression of a fission protein was sufficient to induce cell death. Strikingly, when the dominant negative form of Drp-1 (Drp-1K38A) was over-expressed in mammalian cells, it protected cells from apoptosis and cytochrome *c* release in the presence of different apoptotic stimuli. This led to the conclusion that Drp-1 must play an important role in apoptosis (Frank *et al.*, 2001; Arnoult *et al.*, 2005). However, the sensitization for death of mammalian cells through Drp-1 though seemed to be very stimulus dependent in those studies. Because when calcium was used to induce apoptosis, experiments in which Drp-1 was over-

expressed revealed that the presence of Drp-1 actually blocked cell death. In this study it was speculated, that the cells became protected by the fragmentation and distribution of small mitochondria throughout the cell, thereby diluting the deadly effect of calcium signaling (Szabadkai *et al.*, 2004).

Like Dlp-1, Fis-1p was first identified in Yeast where their deletion caused a malfunction in mitochondrial division (Mozdy *et al.*, 2000). Fis-1 (human fission protein-1) is an additional mitochondrial scission protein that resembles Drp-1 functionally. Indeed, Fis-1 revealed an even stronger function in mitochondrial fragmentation than Drp-1. Over-expression of Fis-1 alone (without addition of apoptotic stimuli) clearly led to fragmentation of mitochondria and the release of cytochrome *c*, resulting in cell death (James *et al.*, 2003; Yoon *et al.*, 2003). Moreover, silencing of Drp-1 and Fis-1 by siRNA not only enhanced fusion of mitochondria, but blocked apoptosis induced by a variety of agents. These findings again suggested a requirement for mitochondrial fission during apoptosis (Lee *et al.*, 2004).

Recently the role of DRP-1 in *C. elegans* development was investigated (Jagasia *et al.*, 2005). Jagasia and coworkers generated heat-shock inducible *drp*-1 transgenic animals and mitochondria were observed in developing embryos. Visualization of mitochondria, by rhodamine red staining, revealed that high levels of DRP-1 resulted in mitochondrial fragmentation. Furthermore, higher numbers of dying cells were observed, suggesting that DRP-1 might be sufficient to induce death in developing worm embryos. This effect was blocked when DPR-1 was over-expressed in a gain-of-function CED-9 (*ced*-9n1950) mutant background, indicating a DRP-1 function in parallel or downstream of CED-9, and introduces the possibility of a role of CED-9 protein in mitochondrial fission or fusion (Jagasia *et al.*, 2005).

1.8.4 Aims

In this study we initially explored the expression patterns of the worm cell death regulators CED-9, CED-4 and CED-3 in *C. elegans* embryos as well as upon over-expression in human HeLa cells. During these studies we noticed that worm CED-9 was localized to mitochondria when over-expressed in human cells and remodeled these organelles to produce highly fused mitochondrial

networks. Despite this, CED-9 had no effect on either apoptosis or cytochrome *c* release. These data challenge the emerging view that mitochondrial fission promotes cytochrome *c* release during apoptosis. Furthermore, our observations also suggested that worm CED-9 may have a hitherto unrecognized role as a regulator of mitochondrial fission or fusion. To explore this further, we then investigated whether members of the human Bcl-2 family might have a similar role as regulators of mitochondrial fission and fusion. Our subsequent investigations revealed that Bcl-2 family proteins can drive both, mitochondrial fusion as well as fission, but these effects could be uncoupled from their role as regulators of both, cytochrome *c* release and apoptosis. Thus, we propose that the CED-9/Bcl-2 family play a previously unappreciated role as regulators of mitochondrial morphogenesis. The latter role of the Bcl-2 family may be a primordial role as our data indicate that mitochondrial fission and fusion plays only a minor, if any, role in the regulation of apoptosis.

33

CHAPTER II

Materials and Methods

2.1 Materials

2.1.1 Reagents and chemicals

Unless otherwise stated, chemicals were purchased from SIGMA (Ireland), and enzymes from NEB (New England Biolabs, UK).

2.1.2 Antibodies

The following lists give details and sources of the antibodies used in this study.

Primary Antibodies	Source
anti-HA (12C5)	ROCHE, Ireland
anti-Myc (9E10)	ROCHE, Ireland
anti-His (BMG-His-1)	ROCHE, Ireland
anti-FLAG (M2)	SIGMA, Ireland
anti-Bcl-2 (7)	BD Bioscience, UK
anti-Bcl-xL (4)	BD Bioscience, UK
anti-Bax (3)	BD Bioscience, UK
anti-Mcl-1 (22)	BD Bioscience, UK
anti-Bid (polyclonal)	BD Bioscience, UK
anti-Cytochrome *c* (6H2.B4)	BD Bioscience, UK
anti-actin (clone4)	ICN Biomedicals, UK
anti-tubullin (DM1A)	ICN Biomedicals, UK

Secondary Antibodies	Source
anti-mouse Alexaflour°488	Molecular Probes, USA
anti-mouse Texas Red	Molecular Probes, USA
anti-rabbit Alexaflour°488	Molecular Probes, USA
anti-rabbit Texas Red	Molecular Probes, USA
Goat anti-mouse-HRP	JACKSON ImmunoResearch Laboratories Inc, USA
Goat anti-rabbit-HRP	JACKSON ImmunoResearch Laboratories Inc, USA

Further antibodies that were used are mentioned or listed in the specific section.

2.1.3 List of plasmid constructs and sources

In the course of this study various plasmids were used, as listed below.

Caenorhabditis elegans genes	
Construct	Source
pcDNA3-CED-3	generated in the Laboratory
pcDNA3-CED-3C358A	generated in the Laboratory
pcDNA3-HA-CED-9	Dr. Gabriel Nunez
pcDNA3-HA-CED-9ΔTM	Dr. Gabriel Nunez
pcDNA3-HA-CED-9G169E	generated in the Laboratory
pcDNA3-HA-CED-9Y149N	generated in the Laboratory
pcDNA3-Myc-CED-4	Dr. Gabriel Nunez
pcDNA3-FLAG-EGL-1	generated in the Laboratory
pcDNA3-FLAG-FzoRP-1	generated in the Laboratory

Homo sapiens genes	
Construct	Source
pCB6-Myc-Mfn-1	Dr. Richard Youle
pCB6-Myc-Mfn-2	Dr. Richard Youle
pCMVtag5a-Myc-Opa-1	Dr. Luca Scorrano
pcDNA3-FLAG-Drp-1	generated in the Laboratory
pcDNA3-HA-Drp-1K38A	generated in the Laboratory
pCI-His-Fis-1	Dr. Jean-Claude Martinou
pcDNA3-Bax	generated in the Laboratory
pcDNA3-Bak	generated in the Laboratory
pcDNA3-Bcl-2	Dr. Christoph Borner
pcDNA3-Bcl-x_L	Dr. Christoph Borner
pcDNA3-Mcl-1	generated in the Laboratory
pcDNA3-A1	generated in the Laboratory
pcDNA3- Bcl-w	generated in the Laboratory
pcDNA3-Bcl-B	generated in the Laboratory
pcDNA3-Bid	generated in the Laboratory
pcDNA3-Bim	generated in the Laboratory
pcDNA3-Puma	generated in the Laboratory
pcDNA3-Myc-Nac	generated in the Laboratory

2.2 Methods

2.2.1 Preparation of Competent bacteria

To obtain competent bacteria for plasmid-DNA transformation, the *Escherichia coli* (*E. coli*) strain DH5α was typically prepared by the Inoue method (Inoue *et al.*, 1990). Therefore, bacteria were streaked onto LB agar plates (Luria Bertani, 0.5 % Yeast extract, 1 % tryptone, 1 % NaCl, 1.5 % agar, pH 7.0) and grown over night at 37°C. A single well-defined colony was picked to inoculate a starter culture in 3 ml liquid LB medium (0.5 % Yeast extract, 1 % tryptone, 1 % NaCl, pH 7.0). The next day, the overnight culture was diluted into 50 ml of SOB medium (2 % tryptone (BD), 0.5 % yeast extract (BD), 10 mM NaCl, 2.5 mM KCl, 10 mM $MgCl_2$, 10 mM $MgSO_4$) to give an OD_{600} of 0.1. The Culture was grown at room temperature to an OD_{600} of 0.4 - 0.6, and cells were then harvested by centrifugation at 2,500 g for 10 minutes at 4°C. After resuspension in 20 ml of transformation buffer (10 mM Pipes, 55 mM $MnCl_2$, 15 mM $CaCl_2$, 250 mM KCl, pH 6.7), cells were incubated for 10 minutes on ice. Centrifugation was repeated and cells resuspended in a further 4 ml of transformation buffer. DMSO was added to a final concentration at 7 % and the cells incubated for 10 minutes on ice. Cells were then divided into 100 μl aliquots and frozen at –70 °C.

2.2.2 Transformation of bacteria

For the transformation of DH5α, 50 μl cells were thawed on ice and incubated with 1 μl of the desired plasmid-DNA for 30 min. Transformation occurred by heat shock treatment of the cells for 40 sec. at 42°C. Incubation on ice (2 min.) was followed by addition of 450 μl LB and cells were allowed to recover at 37°C (220 rpm) for one hour. Bacteria (50 μl) were then plated on LB agar plates with antibiotics (100 μg/ml ampicillin or 50 μg/ml kanamycin), and incubated over night at 37°C.

2.2.3 DNA purification and manipulation

2.2.3.1 Isolation of plasmid-DNA

(I) Mini- preparation

A well-defined colony of transformed bacteria with the desired plasmid was picked to inoculate a 3 ml LB starter culture, containing the necessary antibiotic (100 µg/ml ampicillin or 50 µg/ml kanamycin). After over night growth (37°C, 280 rpm), 1,5 ml culture was harvested (20000 g, 1 min.), the supernatant removed and the bacterial pellet was resuspended in 100 µl buffer P1 (10 mM EDTA, 50 mM Tris-HCl pH 8.0). For cell lysis 200 µl buffer P2 (0.2 M NaOH, 1 % SDS) was added, the tube was inverted carefully 6 times, and the pellet was incubated for 1 min. on ice. Finally 200 µl buffer P3 (3 M KAc pH 5.5) was added and the DNA precipitated. This was enhanced by thorough inversion of the sample and incubation on ice for 5 min. To separate the DNA from cell debris, the sample was spun down at 20000g for 10 min. The supernatant, containing the DNA was then transferred to a fresh tube with 0,7 volumes of isopropanol, mixed and incubated at room temperature for 20 min. The DNA was pelleted by centrifugation at 20000g for 15 min. and then washed with 1 ml of ice-cold 70 % ethanol and spun again. The DNA-pellet was air dried and dissolved in a 1:1 mixture of ddH$_2$O and TE (10 mM Tris-HCl pH8.0, 1 mM EDTA). Analysis of DNA was performed by agarose gel electrophoresis.

(I) Midi- preparation

High yield plasmid-DNA was achieved by midi-preparation. Therefore, a single colony was picked to inoculate a 3 ml starter culture. After over night growth, the culture was used to setup a main culture in LB, supplemented with the required antibiotic. 500 µl of starter culture was diluted in 50 ml LB and grown until at 37°C, 280 rpm. Cells were harvested the next day by centrifugation at 6000 g (15 min., 4°C). For the preparation of highly purified DNA for transient transfections, the QUIAGEN midi kit was used and the protocol was followed as recommended by the manufacturer.

2.2.4 Agarose gel electrophoresis

To analyse DNA yield produced in bacteria or for use in restriction reactions, agarose gel electrophoresis was performed. A 0.6 % agarose matrix was therefore dissolved in 100 ml 1X TAE (50X: 0,04 M Tris, 0,06 M EDTA, 57 ml acetic acid) and cooked in a microwave. After cooling the liquid gel was poured into a gel-casting rig (BioRad) and allowed to solidify. Typically 5 μl of DNA-sample was diluted with 5 μl ddH$_2$O and 2 μl 6X loading dye (40 % sucrose, 2 g bromphenol blue), and the mixture loaded onto the gel. Samples were run at a constant voltage (74 Volts) alongside a ladder of marker DNA fragments of known sizes, and then stained with ethidium bromide. Visualization of the obtained DNA was done by UV light on a BioRad Gel Doc 2000 system.

2.2.5 Quantification of DNA

A spectrophotometer (BioRad) was used to quantify DNA concentrations. Samples were diluted 1:50 in TE (10 mM Tris-HCl pH8.0, 1 mM EDTA) and the OD measured. A triplicate reading at OD$_{260/280}$ was measured in a quartz cuvette and the concentration calculated.

2.2.6 Polymerase chain reaction (PCR)

For the construction of plasmid clones, primers were produced by SIGMA-Genosys Ltd. UK after our instructions, and dissolved with TE (10 mM Tris-HCl pH8.0, 1 mM EDTA) to a final concentration of 100 μM. To amplify the desired gene, standard PCR procedure was performed. All reactions were assembled in a 50 μl reaction as below.

Component	Volume in μl	Final concentration
Template (ng/μl)	x	100- 200 ng
Taq buffer (Quiagen, UK)	5	1X
Forward primer (100 μM)	x	100- 200 nM
Reverse primer (100 μM)	x	100- 200 nM
dNTPs (ROCHE, Germany)	4	2.5 mM
Taq polymerase (Quiagen, UK)	0.5	2.5 units
ddH$_2$O up to 50 μl		

PCR reaction conditions were the follwing:

- 94°C for 5 min. initial DNA denaturation
- 94°C for 1 min. denaturation
- 60- 70°C for 1 min. primer annealing ⎫
- 72°C for 1 min. elongation ⎬ 30 cycles
                              ⎭
- 72°C for 10 min. final elongation

Resulting PCR products were analysed by agarose gel electrophoresis (as in 2.2.4) and stained with ethidium bromide as described above.

2.2.7 Construction and cloning of plasmid-DNA

2.2.7.1 Restriction

Appropriate restriction sites were included during the construction of primers for PCR. Resulting PCR-products therefore carried specific sites that could be used to insert the DNA into a vector. Typically a 20 µl reaction was setup, containing 4 µg of vector-DNA or 1- 2 µg PCR-product. The specific buffer for a certain enzyme was diluted 1:10 and 0,5 µl (1-2 U) enzyme was added in a final volume of 20 µl in ddH$_2$O. Reactions were left over night to allow a complete digest of DNA.

2.2.7.2 Gene clean

(I) Gene cleaning from solution

Gene cleaning was used after restriction reaction with enzymes to generate ultra-pure DNA for cloning. To purify nucleic acids from solution, 3 x volumes of 6 M NaI were added to the DNA followed by 5 µl/µg (DNA) silica (100 mg/ml suspension in 3 M NaI). The suspension was incubated under rotation at room temperature for 10 min. to allow DNA to bind to the silica. The silica-bound DNA was pelleted for 5 seconds at 20000 g and washed 3 times in 500 µl volumes of wash buffer (10 mM Tris-HCl, pH 7,5, 50 mM NaCl, 2,5 mM EDTA, 50 % ethanol). The silica pellet was air-dried for 5 minutes and DNA eluted into 0,5 X TE.

(II) Gene cleaning from gels

To purify DNA from agarose gels, DNA was stained with ethidium bromide and the DNA-band was excised on a UV-lamp. Three volumes of 5 M NaI were added and the sample was mixed and shaken until the gel was dissolved. A silica-matrix was added and the procedure followed as described above. To estimate the resulting amount of vector and PCR- product, an agarose gel electrophoresis was performed and used as a read out for the DNA-concentrations.

2.2.7.3 Ligation

For best ligation results, the linearised vector and the digested DNA-fragment were combined at a 1:3 molar ratio, analyzed by the agarose gel (see above). In a 10 µl reaction the appropriate DNA amounts were mixed with T4-DNA ligase and its recommended buffer as instructed by the manufacturer (typically 1:10). Ligation reactions were incubated for 1-4 hours at 16°C and a 3 µl sample transformed into competent bacteria (see above).

2.2.8 Mammalian cell culture methods

2.2.8.1 Cell culture

All cell cultures used in this study were kept either in RPMI (GIBCO) supplemented with 5 % FCS and 1 % L-Glutamine (HeLa, MCF-7, MEF) or in DMEM (GIBCO) with 10 % FCS and 1 % L-Glutamine (HEK293T, COS-7, CHO). Cells were grown and incubated at 37°C and 5 % CO_2. For the passaging of cells they were typically incubated at 37°C in 1,5 ml Trypsin-EDTA (0,25 % Trypsin, 1 mM EDTA in Hank's salt solution) (GIBCO) for 5 min. To inactivate the Trypsin, cells were then harvested with fresh medium and pelleted at 400 g for 10 min, before the transfer onto fresh tissue culture plates.

2.2.8.2 Transfection by Genejuice

For the uptake of plasmid-DNA by cultured cells (i.e. HeLa, plated at 2×10^5 cells per well on the day before), the DNA porter Genejuice (NOVAGEN) was used, and the instructions were followed as recommended by the manufacturer.

2.2.8.3 Calcium phosphate precipitation

Cells on 10 cm plates were transfected with plasmids according to the standard calcium phosphate precipitation method. Routinely HEK293T cells were seeded at a density of 2×10^6 cells/10cm plate 24 hours prior to transfection. Precipitates were prepared by mixing the appropriate amount of DNA made up to 200 µl with sterile 0,5 X TE (5 mM Tris-HCl pH 8.0, 0.5 mM EDTA) and 50 µl sterile $CaCl_2$ was added. The $DNA/CaCl_2$ mixture was added slowly and drop-wise to 250 µl 2 X HBS (280 mM NaCl, 10 mM KCl, 1.5 mM Na_2HPO_4, 12 mM dextrose, 50 mM HEPES pH 7.15). After a 30 min incubation period the DNA-complexes were added to the cells and left on over night. Following transfection, cells were typically lysed on ice for 15 min in 600 µl SDS-buffer or lysis buffer (50 mM Tris-HCl pH 8.0, 150 mM NaCl, 1 % Nonidet P-40, 0.1 % SDS, 0.5 % sodium deoxycholate.

2.2.9 Immunostaining

Cells grown on a coverslip at a density of 1×10^5 cells per well were used for immunostaining. Typically 24 hours after plating, cells were transiently transfected for a further 24 hours. After sufficient protein-expression time, cells were fixed by incubation for 10 min. in 3 % paraformaldehyde in PBS (8 g NaCl, 14,4 g Na_2HPO_4, 2 g KCl, 2,4 g KH_2PO_4, pH 7,2). The fixed cells were washed three times in 1 X PBS, pH 7.2 and permeabilized for 15 min. in 0.15 % Triton X-100 in PBS. Cells were blocked for 30 min. in 2 % BSA in PBS and probed with a 1:100- 1:500 dilution of primary antibody for 1 h at room temperature. The cells were once again washed three times 10 min. in 2 % BSA in PBS, followed by probing for 45 min with a 1:1000- 1:1500 dilution of fluorescence conjugated secondary antibody. Cells were then washed three times in 1 X PBS, pH 7.2 and stained for further 10 min. with 20 µM Hoechst33358 in PBS. For microscope analysis, the coverslips with stained cells were mounted in Slowfade Light Antifade mounting medium (Molecular Probes) before visualization.

2.2.10 Apoptosis induction

Different cell lines were plated and transfected with various plasmids along with a GFP reporter (pAAV-EGFP) as described above. To induce apoptosis, 24 hours after transfection, cells were treated with varying amounts of Actinomycin D, Daunorubicin, TPCK, DCI and TNFα/CHX for 6-18 hours. GFP-expressing cells were scored for apoptotic morphology at different time points and at least 300 cells counted in each treatment.

2.2.11 Co-immunoprecipitation

Usually 24 hours after transfection, cell lysates were prepared by resuspending the cells in 600 µl IP lysis buffer (50 mM Tris-HCl pH 8.0, 150 mM NaCl, 1 % NP-40) containing 100 µM PMSF, 10 µg/ml leupeptin, 2 µg/ml aprotinin. Lysates were cleared by centrifugation at 20000g at 4°C for 15 min. Lysates were transferred to new eppendorf tubes and incubated with 1 µg of monoclonal antibody and 30 µl of a 50 % slurry of protein A/G agarose beads (Santa Cruz Biotechnology, Inc). The tubes were rotated continuously at 4°C for 4- 6 hours. The resulting IP complexes were washed three times in IP lysis buffer (50 mM Tris-HCl pH 8.0, 150 mM NaCl, 0.1 % NP-40), and Immunoprecipitates were then analysed by immunoblotting as described below.

2.2.12 FRAP analysis of mitochondrial fusion

Flourescence recovery after photobleaching (FRAP) was utilized to investigate the mitochondrial fusion activity. HeLa cells (2 X 10^5 cells/well) growing on coverslips were transfected and subsequently stained with 50 nM MitoTrackerCMXRos® for 30 min. at 37°C. Analysis took place on an Olympus confocal microscope. Cells displaying different phenotypes (checked by co-expression of 100ng of the reporter pEFMitoGFP) were chosen for FRAP. The cell of question was then prescanned five times on a region of interest (ROI) at a low laser power (3%) with the 543nm HeNe- laser. The ROI of each cell, covering approximately 2 µM, was then photobleached for a millisecond with 3 lasers at 100% laser power and observed over time. The recovery of the bleached area in the ROI was observed over a period of 140 seconds for each

cell with the same 543nm HeNe-laser from the pre-scan, and pictures taken every five seconds.

2.2.12 Analysis of proteins

2.2.12.1 SDS- PAGE

Standard SDS-polyacrylamide gel electrophoresis (SDS-PAGE) was carried out as described by Sambrook and Maniatis (1989). 8- 15 % polyacrylamide gels were prepared as described. The most common gel cast was 12 %, with 15 % gels used for the electrophoresis of smaller sized proteins (<20 kDa) and 8 % gels used for the electrophoresis of larger proteins (>50 kDa). Protein samples were prepared for electrophoresis by denaturing at 90°C for 7 min, typically in the presence of 2 X SDS loading buffer (100 mM Tris-HCl pH 6.8, 4 % SDS, 0.2 % bromophenol blue, 20 % glycerol). The initial voltage applied to the gel was 55 V to drive the protein samples through the stacking gel and then this was increased to 75 V to drive the samples through the resolving gel. The running buffer composition was 25 mM Tris-HCl pH 8.3, 250 mM glycine and 0.1 % SDS.

2.2.11.2 Western Blot

(I) Protein transfer onto membranes

Following SDS-PAGE, proteins were transferred onto a 0.2 µm nitrocellulose membrane (Schleicher and Schuell, Germany). Four sheets of 3MM blotting paper (Whatman, UK) were cut to the same size as the scotch-brite pads used in the transfer cassette. The cassette was assembled with four pieces of Whatman paper placed inside two scotch-brite pads and this cassette was then immersed in Transblot Buffer (39 mM glycine, 48 mM Tris-HCl pH 8.3, 0.037 % SDS, 20 % methanol). The membrane was then soaked for 5 min. in Transblot buffer. The cassette was opened and the membrane was placed onto one side of the cassette, stacked with two pieces of Whatman paper on top of one scotch-brite pad. The gel was then carefully placed on top of the membrane, ensuring no air bubbles were trapped in the process. The remaining two pieces of Whatman paper and the final scotch-brite pad were placed on top of the gel and the cassette was reassembled and placed in a transfer cassette and

covered with Transblot buffer. The described assembled transfer sandwich was left for the proteins to transfer onto the membrane overnight at a constant current of 35 mA.

(II) Immunoblotting of proteins

The next day, the nitrocellulose membrane was initially blocked in blocking solution (1 mM Tris-HCl pH 8.0, 15 mM NaCl, 0.005% Tween, 5 % non- fat dried milk) for 30 min. The primary antibody was added to the blot, and then incubated for 2 hours under constant rotation in a heat-sealed bag at room temperature. The primary antibody was typically diluted 1:1000 in 5 ml blocking solution. The membranes were then washed at least three times in TBST (1 mM Tris-HCl pH 8.0, 15 mM NaCl, 0.005 % Tween) for 10 min. each time. The secondary antibody was also diluted 1:1000 in blocking solution. The membranes were washed once more in TBST three times for 10 min before protein detection.

(III) Immunodetection of proteins

Proteins were detected by briefly pipetting both sides of the membrane with equal volumes of Supersignal West Pico Stable Peroxide and Luminol/Enhancer solutions (Pierce, UK) to provide chemiluminescent substrate. The membrane was then transferred to an exposure cassette, covered in saran wrap, and images obtained by exposing the membrane to autoradiography film (Hyperfilm, Amersham Biosciences, UK). On occasions where it was difficult to obtain a signal using these conditions, the Supersignal West Dura reagent (Pierce, UK) was used to improve the signal.

2.2.12 *C. elegans* based methods

2.2.12.1 Cultivation of worms

Different worm strains (see list below) were obtained from the *C. elegans* Genetics Centre (CGC, USA). Worms were cultured at 20°C in NGM (3 g/l NaCl, 16g/l Bacto-agar, 2,5 g/l Bacto-peptone, 5 µg/ml cholesterol, 1 mM $MgSO_4$, 1 mM $CaCl_2$, 25 mM KPO_4, pH6,0). To supply a food source for the animals, NGM-plates were priory seeded and incubated with the *E. coli* strain

OP50. To seed the NGM- plates with OP50, bacteria were streaked onto a LB-plate and grown over night at 37°C. A starter culture of 3 ml LB-medium was inoculated the next day and 24 hours later bacteria had grown to a confluent culture. 100 µl were dispersed on a NGM plate, and again the bacteria were allowed to grow to a lawn overnight.

Worms were cultured by transferring (with a spatula) chunks containing worms from saturated plates onto a freshly seeded NGM-plate with OP50. This procedure was repeated every time worms had cleared the bacterial-lawn on the plate and therefore populations kept at a exponential growth rate.

2.2.12.2 Isolation of worm embryos; hypochlorite treatment

For the isolation of C. elegans embryos, worms of mixed stages from 2- 3 NGM plates were collected with M9 buffer (3 g/l KH_2PO_4, 6 g/l Na_2HPO_4, 5 g/l NaCl, 1 mM $MgSO_4$) in a red cap tube and spun down at 200 g for 5 min. The supernatant was aspirated to a small volume to transfer the worms into smaller, fresh tubes. Another spin at 200 g for 5 min. condensed the worm pellet and the supernatant was taken off to leave a 50- 100 µl pellet. A hypochlorite buffer (750 µl ddH_2O, 500 µl 5 M NaOH, 250 µl 10 % NaOCl) was always freshly mixed and seven times of the sample volume added to the worms. During a period of 10 min. the worm pellet was frequently mixed on a vortex. Every time a sample (2 µl) was taken and observed under the microscope. The reaction was stopped immediately in 20 ml ddH_2O, when the bodies of the adult worms started to dissolve and released the embryonic eggs. The isolated embryos were spun down at 1000 g for 5 min., and the supernatant with the corpses was aspirated to leave a small volume. This was then transferred to a fresh tube and spun down again to obtain a 100 µl embryo pellet, which was washed in M9 buffer. A sample of 2 µl was used to count the number of isolated embryos per micro-liter on the microscope.

2.2.12.3 Immunostaining of nematode embryos

To obtain a mixed stage sample of embryos, consisting of 1 cell to almost a L1 larval stage embryos, freshly isolated eggs (as described above) were immediately fixed in 3 % paraformaldehyde (in M9) for at least 10 min.

Samples were then washed 3 times for 10 min. in M9 in order to avoid interference of the fixative with the staining. The *C. elegans* embryo is covered in a chitinous eggshell. These structures must be broken open to ensure penetration of antibody during the staining. Thus, the "batch method" or the "freeze crack method" were engaged for staining cytoskeleton components or intracellular structures, respectively. Both methods are described in detail below.

(I) Batch method

Permeabilization of the embryos by the batch method was done by taking the whole embryonic preparation (see above) and adding 1 ml of M9+T (3 g/l KH$_2$PO$_4$, 6 g/l Na$_2$HPO$_4$, 5 g/l NaCl, 1 mM MgSO$_4$, 0.5 % TX-100). The sample was quickly frozen in liquid nitrogen (30 sec.) and immediately thawed under running water. To secure cracking of the eggshell, this step was repeated three times. Finally the embryos were vortexed 30 sec., spun down (200 g, 1 min.) and the broken shells removed with the supernatant. A further incubation step in M9+T was undertaken for 15 min. at room temperature on a tabletop rotator. A drop of water was placed onto a glass slide and a sample of 10- 50 µl of embryos was added. Eggs were allowed to settle onto the slide for a few minutes, which was observed under a microscope.

(II) Freeze crack

Another method to open the embryonic eggshell is to physically crack it open. This method is only useful if no cytoskeletal components of the worm are stained. Embryos isolated from the worms as above were spotted on a glass slide covered with poly-L-lysin. The excess liquid was wicked off with whatman paper and the sample left to settle down for a few minutes. A coverslip was placed over the sample as shown in the picture below and again excess liquid was wicked off until the embryos got slightly squeezed, which was observed on a microscope at 4 X magnification.

glass slide
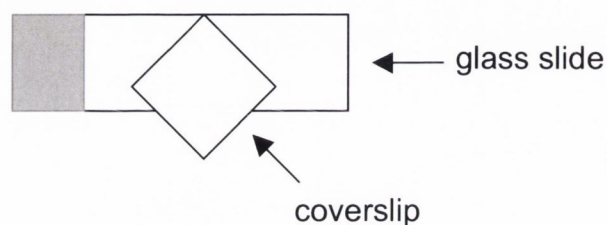
coverslip

Glass slides were then placed carefully in a Styrofoam box filled with liquid nitrogen and frozen for 5- 20 seconds. Then the glass slide was taken out and the coverslip was quickly knocked off with tweezers so that a crack was audible. The sample was immediately transferred to -20°C methanol for a postfix and left for 10 minutes before proceeding with the immunostaining protocol.

(III) Immunostaining of embryos

After permeabilization of the embryos, either by 'batch' or 'freeze crack' method, they were stained with various antibodies. Firstly, embryos were permeabilized with 015 % Triton X-100 for 15 min in M9. Then, samples were blocked in M9+BSA (3 g/l KH_2PO_4, 6 g/l Na_2HPO_4, 5 g/l NaCl, 1 mM $MgSO_4$, 0.5 % TX-100, 2 % BSA) for 30 minutes in a coplin jar. To avoid dehydration, the embryo samples on the glass slides were placed in a humidy chamber. Then the primary antibody was added in a 1:500- 1:2000 dilution for 2- 4 hours at room temperature. This was followed by three wash steps for 10 min. in M9+T buffer. A fluorescence-conjugated secondary antibody was added at a 1:2000 dilution and the embryos incubated for a further 45 min. at room temperature. Finally the embryos were washed again to wash out any unbound antibody. The second wash step included HOECHST (20 µM) to stain the nucleus. After mounting the sample it was observed on a microscope.

CHAPTER III

Subcellular Localization of *C. elegans* CED-3, CED-4 and CED-9

3.1 Introduction

CED-3 is the founder member of the *C. elegans* cell death machinery and was the first of the four cell death proteins to be identified. It was found in a screen searching for genes that are involved in cell death defects of the nematode. After identifying *ced*-1 and *ced*-2, which are genes encoding proteins important for engulfment of dead cells in the worm, *ced-3* was the third gene identified in this screen, hence its name (Ellis and Horvitz, 1986). It acts together with CED-4 and CED-9 to regulate worm cell death. Defects in the *ced-3*-gene permit cells that normally die to survive. The majority of cell deaths occur during the embryonic development of the worm, where 113 cells die. Therefore, in this phase it would be most likely that expression of CED-3 protein is highest throughout *C. elegans* life span. An increase of CED-3 concentration in cells of early and late embryos should become apparent and traceable. However, this has not been proven *in vivo* or biochemically to date. While expression and subcellular localization of the other PCD components could be shown in the past, the spatial and temporal expression of CED-3 in the worm cell remains an open question. For example, interaction of CED-4 with CED-9 was not only shown by *in vitro* assays using co-immunoprecipitations and Yeast-two-hybrid assays (Chinnaiyan *et al.*, 1997a; Spector *et al.*, 1997; Wu *et al.*, 1997a), but also by immunostaining with specific antibodies in cells of early *C. elegans* embryos (Chen *et al.*, 2000). In the latter study even the co-localization of CED-4 with CED-9 on mitochondria, and its dependency on the CED-9 protein could be analyzed, which indicates the potency of this tool.

Recombinant CED-3 protein has been analyzed in many *in vitro* studies. After recognizing its homology to the first identified human caspase ICE (interleukin-1beta-converting enzyme) (Yuan and Horvitz, 1993), its functional characterization took its course. CED-3 was heterologously over-expressed in human cells and displayed apoptotic function (Miura *et al.*, 1993). Following the characterization of CED-3 as a caspase, proteolytic function was established and substrates identified (Xue *et al.*, 1996; Taylor *et al.*, 2007).

Despite all the *in vitro* assays that have been undertaken to examine the function of CED-3 protein, *in vivo* studies are lacking to show its localization in worm embryonic cells.

3.2 Aims and Summary

In this initial phase of the study we aimed to fill the gap of when and where the *C. elegans* caspase CED-3 is expressed in the worm. Assuming our assay would result in identification of CED-3 protein in the worm, we also aimed to analyze CED-3 behavior in the presence and absence of functional CED-9 protein, using suitable worm strain. As there is no sustainable worm-embryonic cell line available, the only way of examining nematode cells is *in vivo*. We decided to do this in embryos after isolating them from whole worms. To achieve this, we chose to use immunostaining technique and thereby label endogenous CED-3 protein in developing embryos. First the worm eggs needed to be permeabilized to allow the diffusion of antibody through the tough embryonic eggshell. Therefore, we established common permeabilization techniques, the so-called batch method and the freeze-crack method in our laboratory.

After setting up worm embryo isolation and staining techniques with control antibodies, we used commercially available antibodies to stain for CED-3. This first approach was unsuccessful, for which reason we tested another set of antibodies. Previously, polyclonal antibodies had been made in the laboratory, which were generated against recombinant CED-3-protein. We also failed to find CED-3-positive cells with those antibodies. Finally we decided to generate another set of polyclonal antibodies, which promised to be more specific, since each of them were targeted against a small and known peptide of the protein. Although we found positive staining with one of these antibodies, the result appeared not to be reproducible, even when antibodies were tested in several different *C. elegans* worm strains.

For further verification of the used antibodies and to identify subcellular localization we went on to analyze *C. elegans* CED-3, CED-4 and CED-9 in human HeLa cells. Heterologously expressed proteins were detected by anti-epitope tag antibodies and their influence on each other was observed.

3.3 Results

3.3.1 Isolation of *C. elegans* embryos

Immunostaining is a very useful tool for characterizing the behavior and subcellular localization of proteins. To explore the developmental expression pattern of the *C. elegans* caspase CED-3 we wanted to immunostain worm embryos. While other components of the *C. elegans* cell death machinery have been successfully detected by immunoflourescence, CED-3 protein has never been visualized in intact cells (Chen *et al.*, 2000). For the extraction of embryos from adult nematode animals, we established a new protocol by adopting a common and widely applied protocol to our requirements (Hope *et al.*, 2000). Mixed stage worms were collected from several culture dishes after a three-day growth. The worms were dissolved in Sodium-hypochlorite by which not only the cuticle, but the whole worm is solubilized (Figure 3.1). Since the embryonic eggshell is also susceptible to total degradation by this treatment we went through a series of tests to find the appropriate concentration of Sodium-hypochlorite. Different concentrations of Sodium-hypochlorite and various incubation times were used to establish optimal conditions (as described in chapter 2.2.12.2 and Figure 3.1). After concentration of the egg samples, embryos could be mounted on glass slides and the stages of development determined, using Hoffman optics on an inverted microscope. Figure 3.2 depicts *C. elegans* embryos from cell stage one (a), two cell stage (b), 20 cell stage (e), comma stage (g), two-fold (h) and prezel (i) stage larva.

3.3.2 Staining of embryos

The chitinous eggshell of *C. elegans* embryos represents a difficult barrier that has to be conquered for staining endogenous proteins. In order for the antibodies to diffuse into the worm embryo and to stain for CED-3 protein, the eggshell had to be broken open. To achieve this, we used two different approaches by which the chitinous wall would be physically fractured (Figure 3.3). As mentioned in the above paragraph, by isolating the worm embryos with the Sodium-hypochlorite treatment, the eggshell was already weakened slightly but not sufficiently.
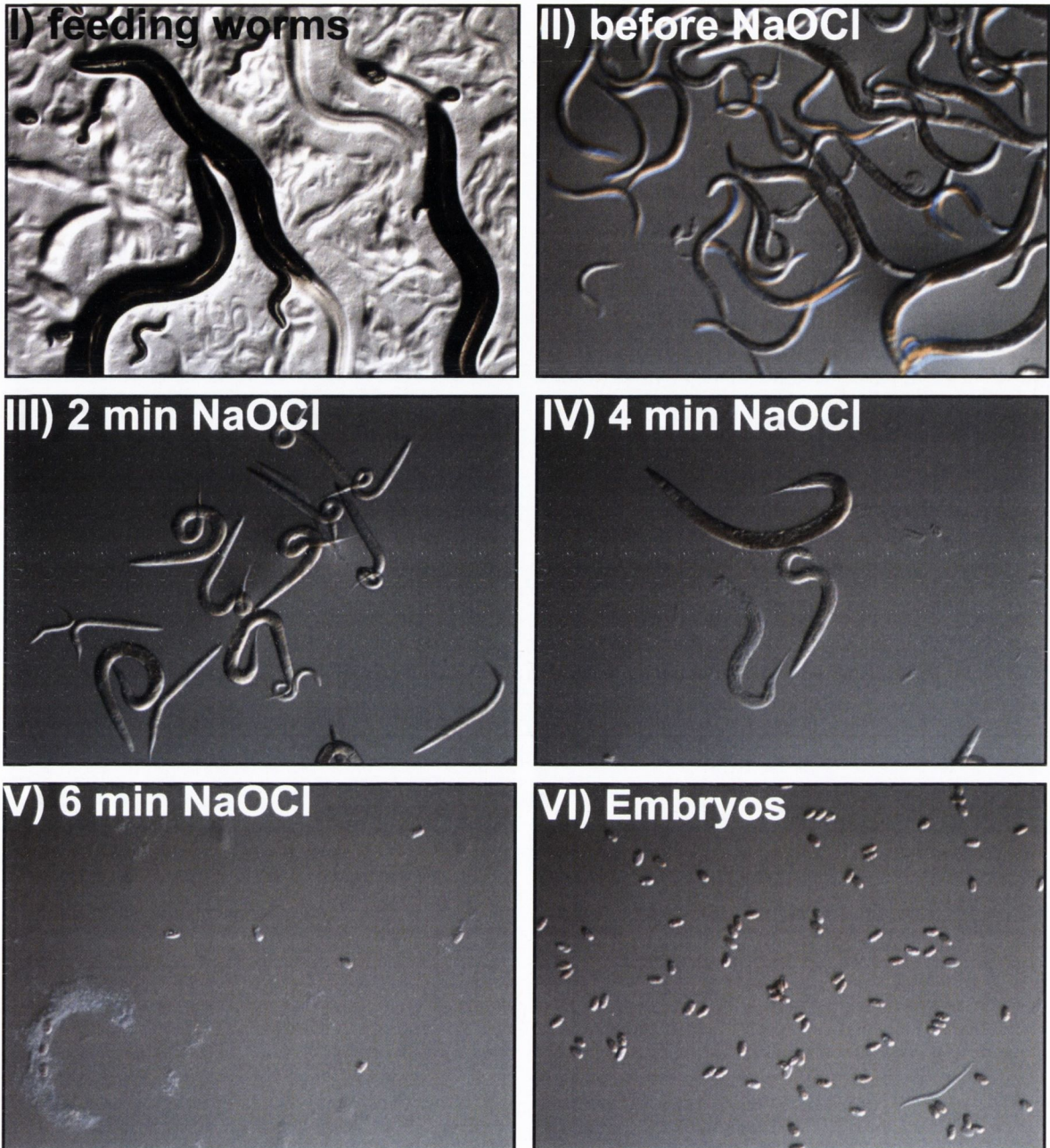
Figure 3.1: Isolation of *C. elegans* embryos

Pictures depict (I) adult and larval *C. elegans* worms, feeding on a NGM plate seeded with a lawn of OP50. (II) Mixture of living worms of different developmental stages, collected with M9 buffer. (III) After addition and a 2 minutes incubation in NaOCl, worms are dead. (IV) Quick solubilization of worms is visibile after 4 minutes incubation in NaOCl. (V) Almost no worm corpses are left after 6 minute incubation. (VI) Culture is cleared of worm material and only embryonic eggs are left. For more details, see Chapter 2.2.12.2.

Stages of *C. elegans* development
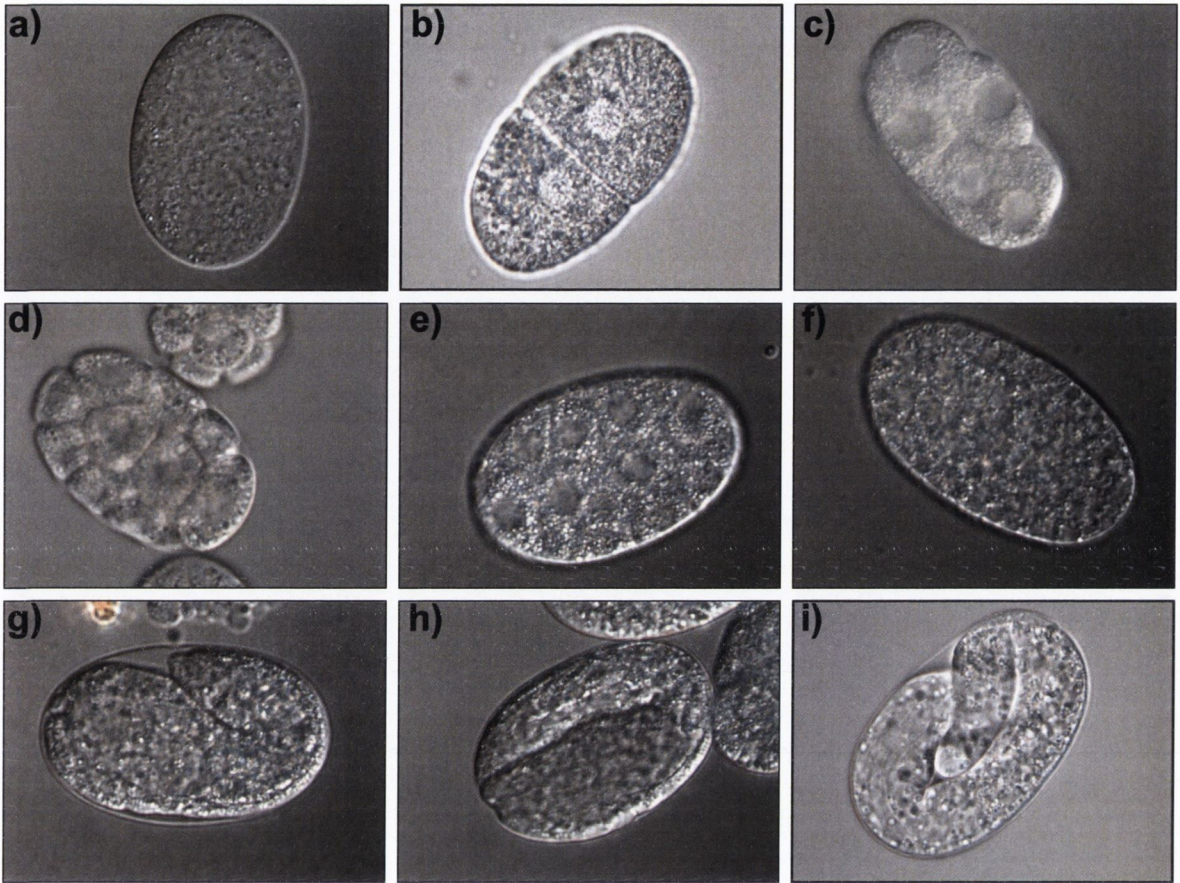
Figure 3.2: Stages of embryonic development in *C. elegans*
Isolated embryos were observed with Hoffman optics and representative pictures taken at 60 X magnification. Embryogenesis takes about 14 hours and starts with a) fertilized egg, b) 2 cell stage, c) 5 cells, d) 10 cells, e) 20 cells to f) about 200 cells. Cell size and nucleus do visibly shrink during this time to fit into the confines of the egg. At the comma stage (g) the larvae starts elongating over the 2 fold stage (h) to the 3 fold or pretzel stage (i) and remains in this for a couple of hours before hatching.

In the freeze-crack method we took isolated embryos, which were mounted on a glass slide and covered these with a coverslip. Subsequent freezing of the slide in liquid nitrogen and a quick removal of the coverslip resulted in an audible crack, which indicated the breaking of the eggshells. The immunostaining protocol was undertaken in a humidity chamber to avoid drying out of the sample and was standardized as described in 2.2.12.3.

The second approach we used was the batch method, which is recommended if cytoskeletal structures are stained, since it is less destructive to such components. Whole embryo preparations were taken and frozen three times in liquid nitrogen. In between freezing steps the sample was quickly thawed under running tab-water. These quick changes of temperature produced cracked eggshells that were now permeable to antibodies. The antibody staining procedure was carried out as above, but with the whole sample in the batch.

All antibodies that were used to stain *C. elegans* embryos, are listed in figure 3.4 and those labeled with "+" were able to stain their specific antigen in the worm using the given method.

3.3.3 Actin and Tubulin staining as controls

We first evaluated the efficiency of our techniques by using antibodies against proteins that are known to appear in high abundance in *C. elegans* embryos. As in human cells, the cytoskeletal proteins actin and tubulin are highly expressed in the worm. Worm embryos isolated by the batch method were prepared for immunostaining. We used antibodies raised against human antigens, which cross-react with *C. elegans* proteins to stain for actin-filaments. Mouse anti-actin antibody detected actin protein in different stages of *C. elegans* embryos (Figure 3.5). A secondary, FITC-conjugated anti-mouse antibody detected the primary mouse antibody and animals were analyzed on a fluorescence microscope. Actin staining appeared circular, surrounding each cell, from a 2 cell stage embryo to a 60 cell embryo.

A second control antibody we employed was as well raised against a human protein, anti-tubulin antibody. This mouse monoclonal antibody also cross-reacts with the *C. elegans* microtubule component (Figure 3.6). Tubulin

Staining procedures

Freeze-crack method

mount embryos on subbed
slides

↓

add coverslip
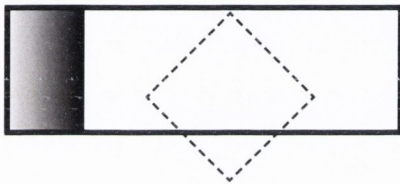
freeze in liquid N2

↓

knock off coverslip

↓

fix in methanol

↓

stain

Batch method

Use whole embryo
preperation in tube

↓

Freeze in liquid N2

↓

Thaw under running water
and repeat 3x

↓

fix in methanol

↓

stain

Figure 3.3: Procedures for staining *C. elegans* embryos
Schematic for two different methods that were used in this study to permebealize *C. elegans* embryonic eggs. The very robust egg-shell required a manual crack as described above on the left hand side. A second method was tested, in which the eggs were physically cracked by freezing and thawing them several times, as described above on the right hand side.

Antibodies

Name	Source	state	in *C.elegans*	in HeLa
α-Actin(C4)	MP Biomedical, monoclonal		+	+
α-Tubulin(DM1A)	MP Biomedical, monoclonal		+	+
α-SC-CED4-N	Santa Cruz, polyclonal	affinity purified	+	+
α-SC-CED9-N	Santa Cruz, polyclonal	affinity purified	-	+
α-SC-CED9-C	Santa Cruz, polyclonal	affinity purified	-	+
CED3 antibodies				
α-SC-CED3-N	Santa Cruz, polyclonal	affinity purified	-	-
α-SC-CED3-C	Santa Cruz, polyclonal	affinity purified	-	-
α-CED3-A1	Lab generated with HARLAN, polyclonal	not purified	-	-
α-CED3-A2	Lab generated with HARLAN, polyclonal	not purified	-	-
α-CED3-B1	Lab generated with HARLAN, polyclonal	not purified	-	-
α-CED3-B2	Lab generated with HARLAN, polyclonal	not purified	-	-
α-CED3pro-1877	Lab generated with SIGMA-Genosys, polyclonal	not purified	-	-
α-CED3pro-1878	Lab generated with SIGMA-Genosys, polyclonal	not purified	-	-
α-CED3p20-1873	Lab generated with SIGMA-Genosys, polyclonal	not purified	+	+
α-CED3p20-1874	Lab generated with SIGMA-Genosys, polyclonal	not purified	-	-
α-CED3p10-1875	Lab generated with SIGMA-Genosys, polyclonal	not purified	-	-
α-CED3p10-1876	Lab generated with SIGMA-Genosys, polyclonal	not purified	-	-

Figure 3.4: List of antibodies used in this chapter
The above list displays all antibodies used in this chapter for *C. elegans* immunostaing. On the right it is notified with + or - if antibodies detected the target antigen in the two different species tested.

staining was nicely visible in the 2 cell stage embryo along the centromeric structures connecting to the nuclei of the cells (Figure 3.6, top panel). In addition, staining of microtubules appeared in all cells at all stages in the analyzed embryos.

3.3.4 Staining for CED-4 and CED-9

The key players of the cell death machinery in *C. elegans* are the proteins CED-3, CED-4 and CED-9. These proteins act mostly during worm embryonic development where the majority of all cell deaths take place (Sulston and Horvitz 1977). Subcellular localization of those proteins has been mainly studied in human cells (Wu *et al.*, 1997a; del Peso *et al.*, 1998). Only two studies showed CED-4 and CED-9 localization in *C. elegans* embryos (Chen *et al.*, 2000; Tzur *et al.*, 2006).

We immunostained CED-4 with antibodies that were commercially available. Firstly, embryos were obtained by the Sodium-hypochlorite treatment and prepared for staining with the freeze-crack method. Secondly, we subjected the embryos to staining with CED-4 antibody (α-SC-CED-4N, Santa Cruz) as shown in figure 3.7. Embryos of two or more cells always revealed the same reproducible pattern of perinuclear staining, which was in contrast to the pattern observed in another study (Chen *et al.*, 2000). This group had observed perinuclear CED-4 staining only in CED-9 loss of function mutants, but not in the wild type strain N2. This might be due to the different antibody that was used in their study, which they had generated in their laboratory. Since it was not the primary goal of our study to clarify this we carried on with immunostaining for the other components of the PCD machinery.

CED-9 protein contains a transmembrane domain and is suggested to concentrate on intra-cellular membranes. To stain for CED-9 protein, *C. elegans* embryos were again isolated as described above. Two commercially available antibodies were used to stain for CED-9 (α-SC-CED-9N, α-SC-CED-9C, Santa Cruz). Although antibodies were titrated and conditions varied to accommodate them, we could not achieve a positive result with either of the two antibodies (Figure 3.8, and data not shown).
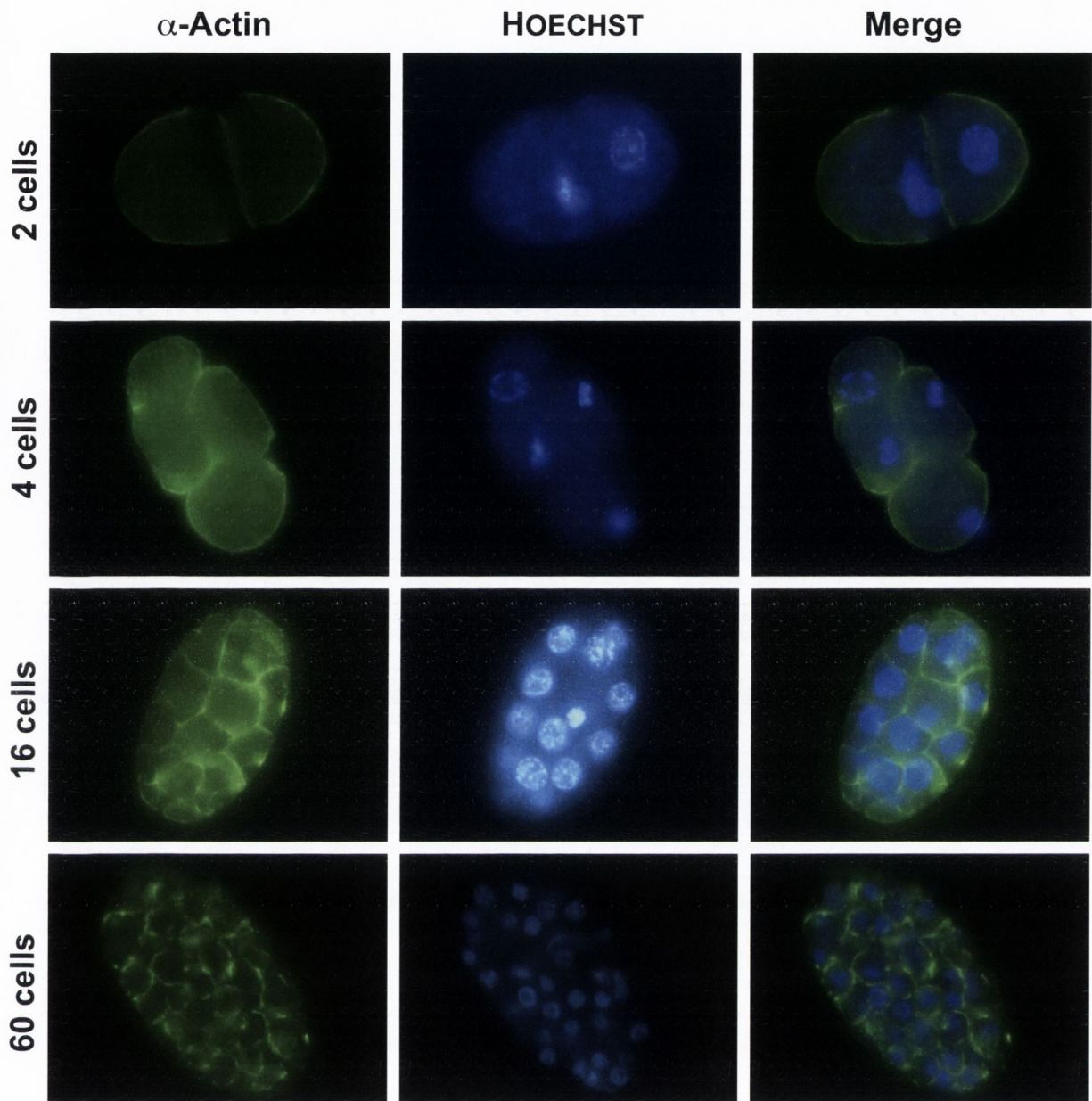
Figure 3.5: Actin-staining of *C. elegans* embryos
Isolated embryos of wild type worms (N2), permeabilized by the batch method, were used to test the efficency of the immunostaining technique with control antibodies for high abundance proteins. The left hand panels show embryos of different stages (as indicated) with positive actin filaments stained at the cell surfaces. Nuclei were stained with HOECHST (middle panels) and the two pictures merged on the right hand side. Representative pictures were taken at 60 X magnification on an Olympus fluorescence microscope. Results represent at least three independent experiments.
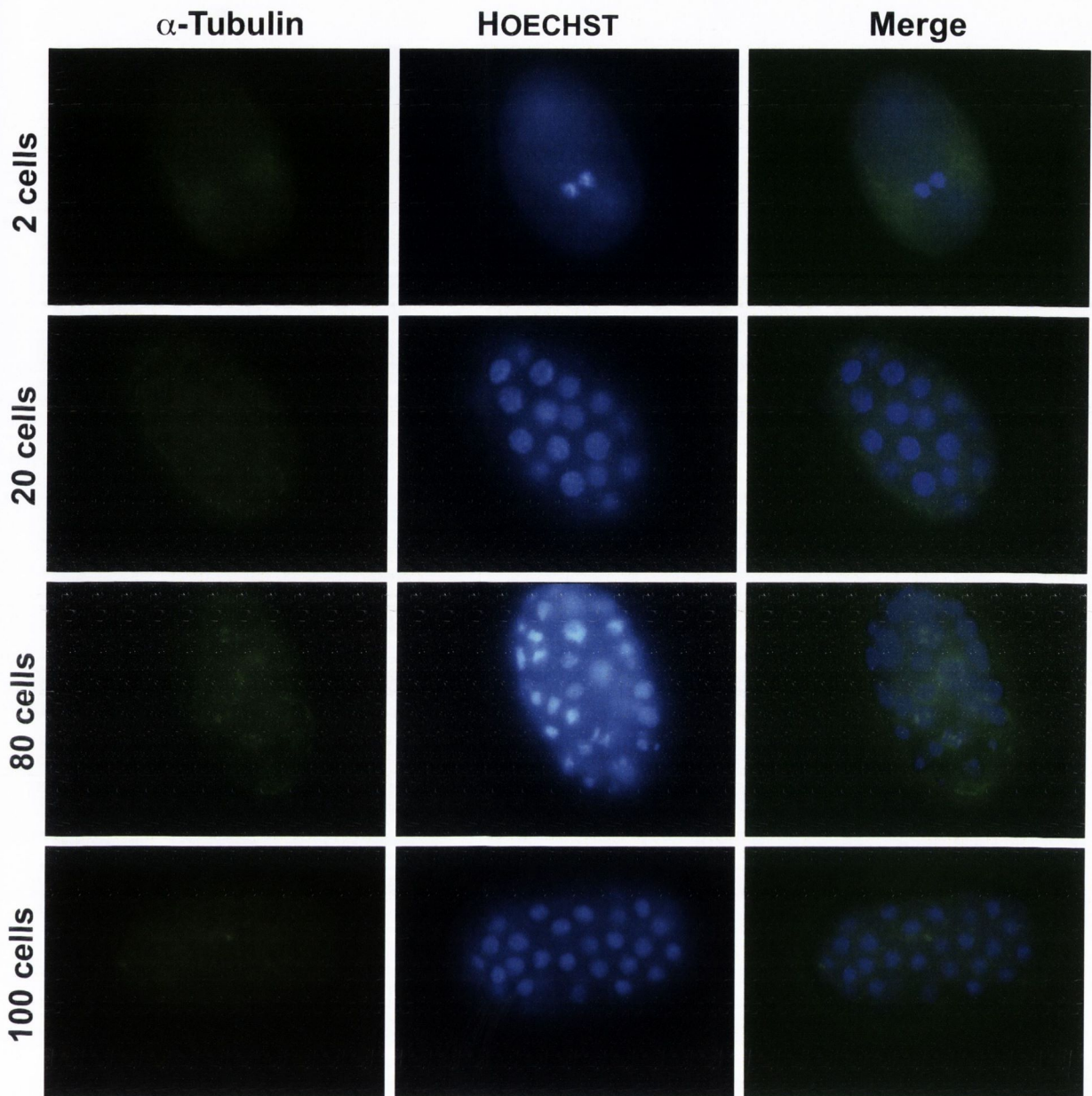
Figure 3.6: Tubulin-staining of *C. elegans* embryos
Embryos of wild type worms (N2), isolated by the batch method, were stained with
the control antibody against alpha-tubulin. The left hand panels show embryos of
different stages (as indicated) with positive staining for microtubules. Nuclei were
stained with HOECHST (middle panels) and the two pictures merged on the right hand
side. Representative pictures were taken at 60 X magnification on an Olympus fluo-
rescence microscope. Results represent at least three independent experiments.

3.3.5 CED-3 immunostaining

The worm caspase, CED-3, has been extensively investigated. Functional characterization and studies of the CED-3 domain structure has revealed similarities to human caspases (Yuan *et al.*, 1993). However, CED-3 has not been previously immunolocalized in the worm or even upon over-expression in heterologous systems, thus little is known concerning the behavior of this protease in vivo.

As for CED-4 and CED-9, we initially obtained commercially available CED-3 antibodies (Santa Cruz). Isolated embryos, obtained by Sodium-hypochlorite treatment, were permeabilized by the freeze-crack method or by the batch method (data not shown), and were stained using two different CED-3 antibodies α-SC-CED-3N and α-SC-CED-3C (Figure 3.9, and data not shown). However, in all developmental stages examined (from 2 cell to 500 cell embryos) we were not able to find cells that showed positive staining for CED-3 with either of the two commercial antibodies. A range of different conditions were tested, but CED-3 positive cells were never observed.

3.3.6 CED-3 immunostaining with antibodies generated in our laboratory

We then tried anit-CED-3 antibodies that had recently been generated in our laboratory by cloning CED-3ΔCARD into a bacterial expression plasmid expressing protein in *E. coli* (Taylor *et al.*, 2007). This CED-3 protein was used to generate polyclonal antibodies by immunizing rabbits.

However, once again, we failed to detect positive staining for CED-3 using four different polyclonal antibodies (α-CED-3-A1, α-CED-3-A2, α-CED-3-B1 and α-CED-3-B2) (Figure 3.10, and data not shown). All cells in each observed embryo appeared rather pale and with no specific staining evident. Again, various staining conditions were tried, but without success. Despite this, the used antibodies worked well to detect CED-3 recombinant protein when used by Western blot experiments down to a concentration of 10 ng of protein (R. C. Taylor, unpublished observations).

Figure 3.7: Staining of *C. elegans* embryos against CED-4
Isolated embryos of wild type worms (N2), permmeabilized by the freeze crack method, were used for staining with the *C. elegans* specific α-SC-CED4-N antibody from Santa Cruz. The left hand panels show embryos of different stages (as indicated) with positive peri-nuclear CED4 staining. Nuclei were stained with HOECHST (middle panels) and the two pictures merged on the right hand side. Representative pictures were taken at 60 X magnification on an Olympus fluorescence microscope. Results represent at least three independent experiments.

Figure 3.8: Staining of *C. elegans* embryos against CED-9
Isolated embryos of wild type worms (N2), permeabilized by the freeze crack method, were used for staining with the *C. elegans* specific α-SC-CED9-C antibody from Santa Cruz. The left hand panels show embryos of different stages (as indicated). Nuclei were stained with HOECHST (right panels). Note that no positive CED9 staining could be obtained with this antibody. Representative pictures were taken at 60 X magnification on an Olympus fluorescence microscope. Results represent at least three independent experiments.

3.3.7 Generating peptide antibodies

The surface of a native protein generally offers multiple different epitopes to raise antibodies against. By analysis of the protein sequence, peptides that cover the protein surface in its final conformation can be loosely predicted using computer algorithms.

Since the set of antibodies against CED-3 that were used thus far did not achieve a positive signal, we attempted another strategy to generate antibodies. Because there were no other commercial antibodies against CED-3 available, we decided to generate polyclonal anti-peptide antibodies. To find suitable peptides, some important details had to be considered. First, the ideal peptide length was approximately 15-20 amino acids to make sure an epitope was properly covered but did not lead to sterical and conformational problems. Second, unstable amino acids were avoided to ensure peptide stability during the process of antibody production. Last, the predicted antigenicity of the peptide was evaluated, i.e. whether the epitope was likely to be on the protein exterior. Therefore, the protein sequence of CED-3 (Figure 3.11, A) was evaluated with a Kyte-Doolittle hydrophobicity plot (Figure 3.11, B). With this, the degree of hydrophobicity of a protein can be analyzed and epitopes can be found that are likely to be surface exposed (Kyte and Doolittle, 1982).

We chose three epitopes within the CED-3 protein sequence. As shown in figure 3.11, A the first peptide was in the prodomain (pro), the second in the large subunit (p20) and the third peptide in the small subunit (p10). These peptides were then used to immunize two rabbits per peptide. Antibodies were labeled as follows: α-CED-3pro-1877 and α-CED-3pro-1878 for the peptides from the prodomain, α-CED-3p20-1873 and α-CED-3p20-1874 for antibodies raised against the large subunit and α-CED-3p10-1875 and α-CED-3p10-1876 for the small subunit. The resulting sera were then tested on worm embryos.

3.3.8 CED-3 immunostaining with peptide antibodies

Immunostaining of CED-3 with peptide antibodies (generated as described above) was performed on isolated *C. elegans* embryos. Those were collected by the Sodium-hypochlorite treatment and permeabilized with the freeze-crack
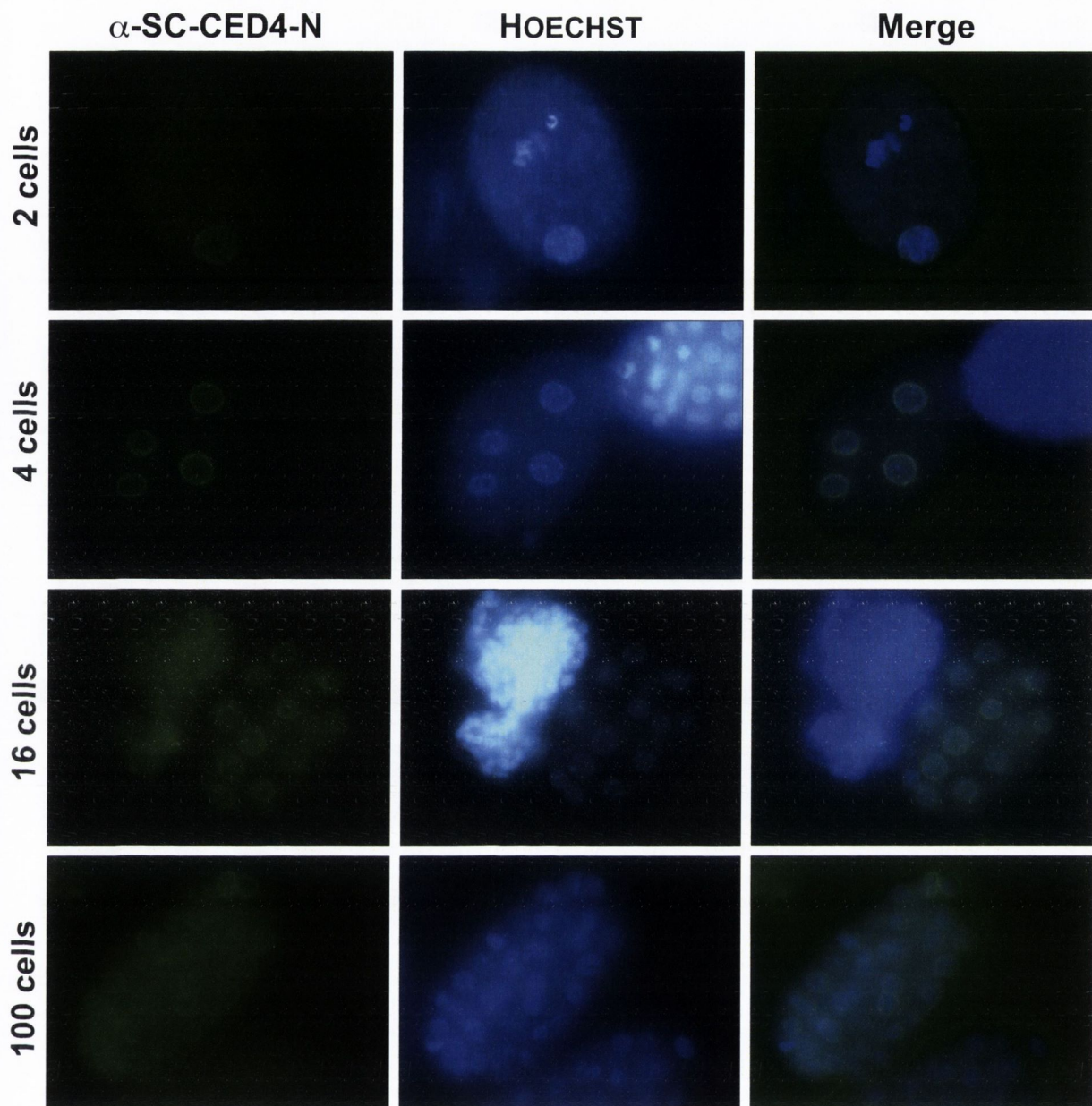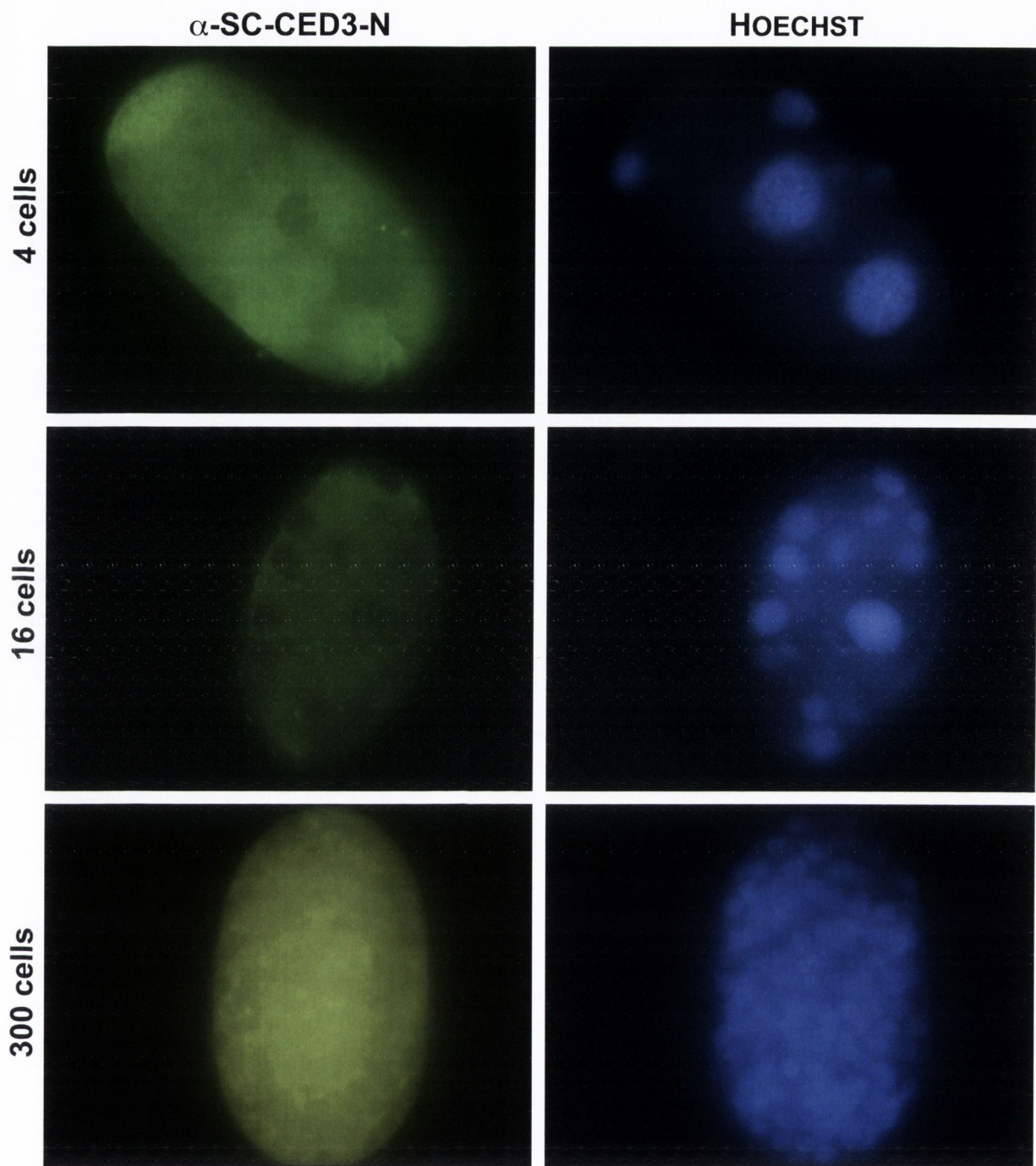
Figure 3.9: Staining of *C. elegans* embryos against CED-3 with α-SC-CED3-N
Isolated embryos of wild type worms (N2), permebealized by the freeze crack method, were used for staining with the *C. elegans* specific α-SC-CED3-N antibody from Santa Cruz. The left hand panels show embryos of different stages (as indicated). Nuclei were stained with HOECHST (right panels). Note that no positive CED-3 staining could be obtained with this antibody. Representative pictures were taken at 60 X magnification on an Olympus fluorescence microscope. Results represent at least three independent experiments.
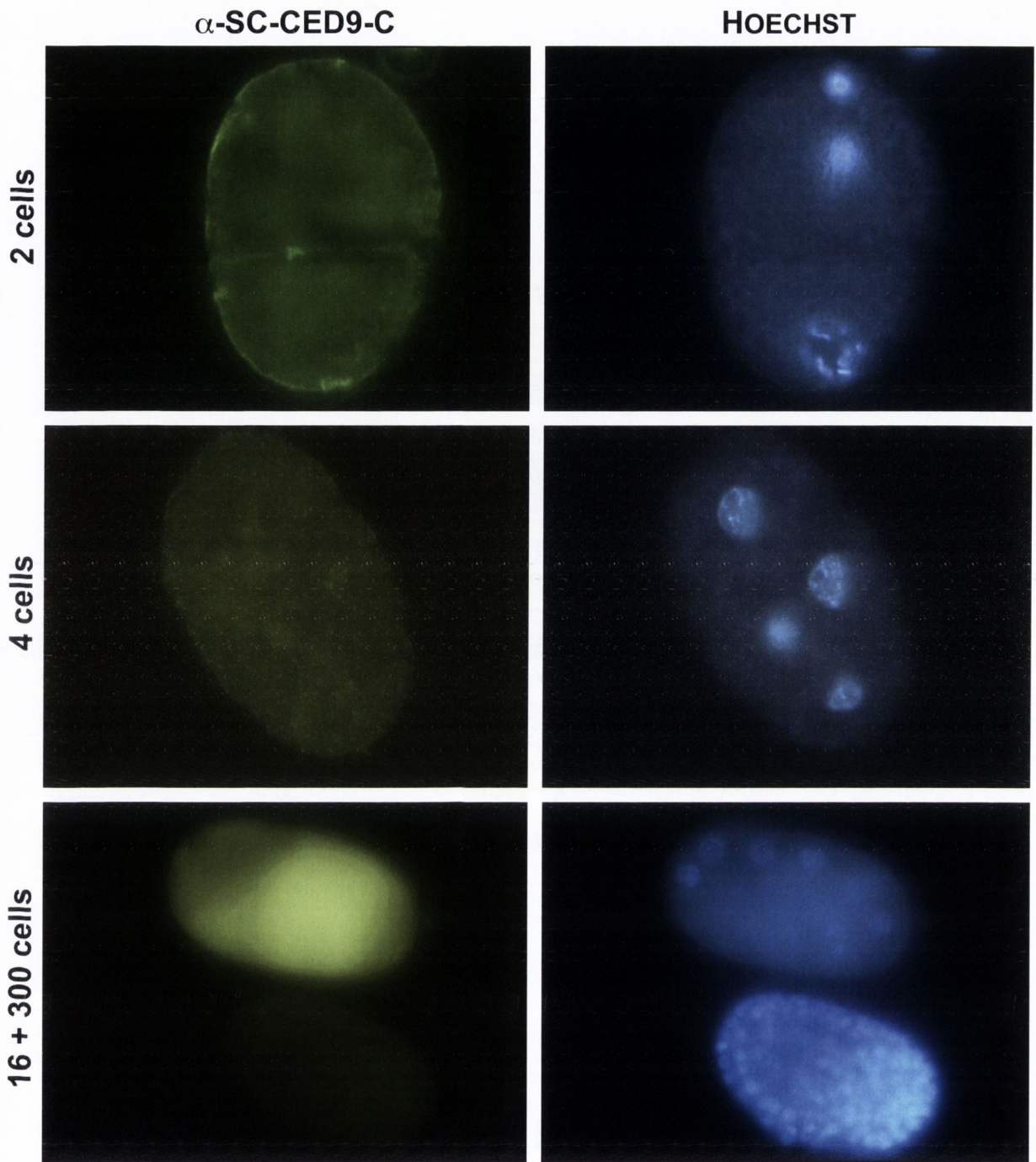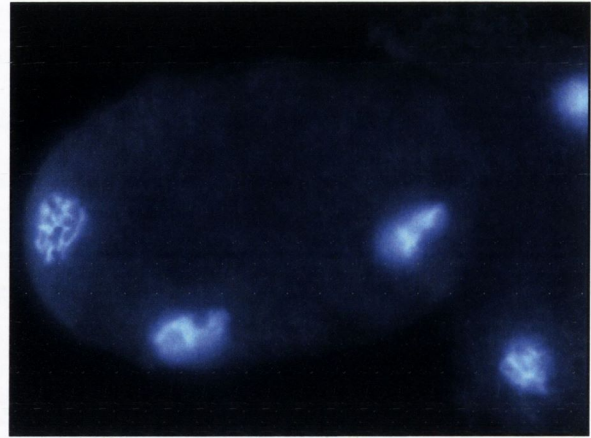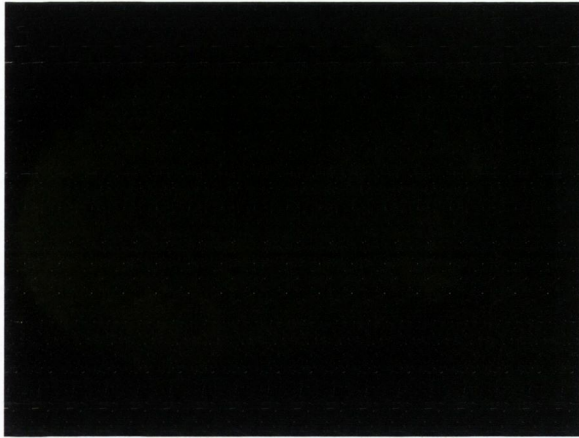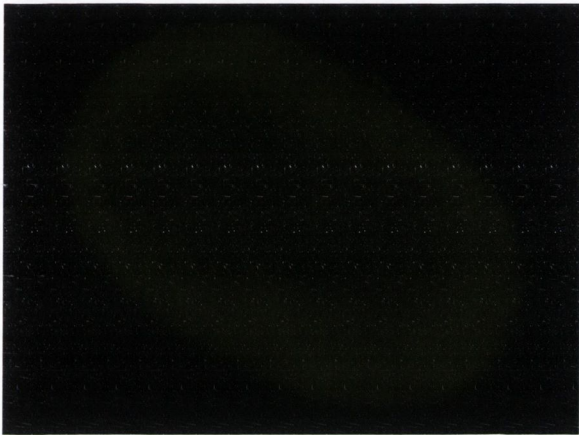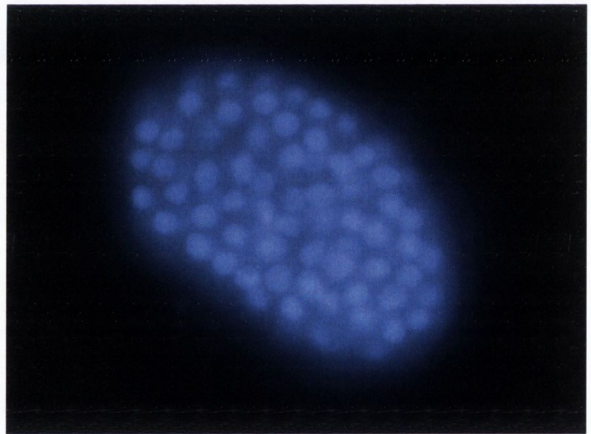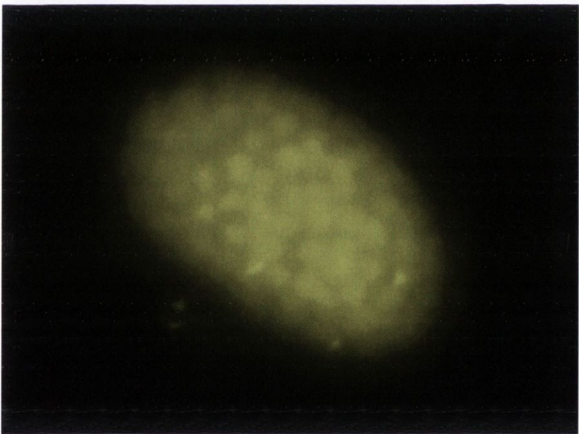
Figure 3.10: Staining of *C. elegans* embryos against CED-3 with α-CED3-A1
Isolated embryos of wild type worms (N2), permeabilized by the freeze crack method, were used for staining with the *C. elegans* specific α-CED3-A1 antibody, which was generated by the laboratory's instructions from HARLAN. CED3ΔCARD(aa 221-503) purified protein was used for antibody production. The left hand panels show embryos of different stages (as indicated). Nuclei were stained with HOECHST (right panels). Note that no positive CED-3 staining could be obtained with this antibody. Similarly negative results were found with three additional anti-CED-3 antibodies (α-CED3-A2, α-CED3-B1, α-CED3-B2; data not shown). Representative pictures were taken at 60 X magnification on an Olympus fluorescence microscope. Results represent at least three independent experiments.

A

MMRQDRRSLLERNIMMFSSHLKVDEILEVLIAKQVLNSDNGDMINSCGTVREKR

REIVKAVQRRGDVAFDAFYDALRSTGHEGLAEVLEPLARSVDSNAVEFECPM

CED3pro

SPASHRRSRALSPAGYTSPTRVHRDSVSSVSSFTSYQ**DIYSRARSRSRSRAL**
143   158

HSSDRHNYSSPPVNAFPSQPSSANSSFTGCSSLGYSSSRNRSFSKASGPTQY

HEEDMNFVDAPTISRVFDEKTMYRNFSSPRGMCLIINNEHFEQM

CED3p20

PTRNGTKADKDNLTNLFRCMGYTVICKDNLTGRGMLLTIRDFAKHESHGDSAILVI
256   271

LSHGEENVIIGVDDIPIS THEIYDLLNAANAPRLANKPKIVFVQACRGERRDNGFP

CED3p10

VLDSVDGVPAFLRRGWDNRDGPLFNFLGCVRPQVQQVW**RKKPSQADILIAYA**T
406   420

TAQYVSWRNSARGSWFIQAVCEVFSTHAKDMDVVELLTEVNKKVACGFQTSQG

SNILKQMPEMTSRLLKKFYFWPEARNSAV

B
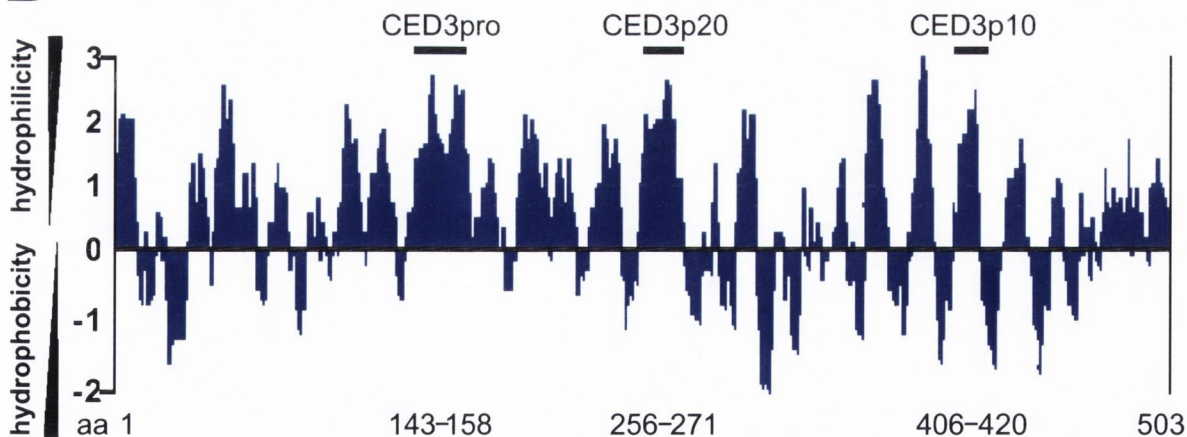
Figure 3.11: CED-3 sequence analysis for selection of immunogenic peptides
A) Protein sequence of the 503 aa *C. elegans* caspase CED-3 as by Genebank accession number AAG42045. The three peptide sequences that were chosen for antibody production for CED-3pro, CED-3p20 and CED-3p10 are highlighted by boxes and numeration. B) Hydrophilicity plot by Kite-Doolittle (Lasergene, DNASTAR inc. Madison USA). This algorithm analyzes a protein sequence for regions most likely to be hodrophilic or hydrophob. The three peptide regions that were chosen for antibody production are highlighted.

method. Unfortunately, the majority of these antibodies also failed to give positive signals (data not shown).

However, using the antibody raised against a peptide within the CED-3 large subunit α-CED-3p20-1873, we could detect occasional positive cells as displayed in Figure 3.12.

In summary, of the twelve CED-3 antibodies tested, only one antibody α-CED-3p20-1873 obtained a positive signal that might represent CED-3. Therefore, we decided to further explore this result as described below.

3.3.9 *C. elegans* wild type and mutant embryos, permeabilized with two methods and stained with α-CED-3p20-1873

In addition to *C. elegans* wild type N2, numerous mutant worm strains have been generated with mutations in cell death related genes. For example, the mutant strain MT8347 (CED-3(n2452) is a CED-3 mutant, which contains a truncated CED-3 protein that ends after amino acid 178. Cell death is repressed in these animals and 10 extra cells are found in the anterior pharynx (Shaham *et al.*, 1999). Another strain is the CED-9 mutant MT3970 (CED-9(n1653)), in which a point mutation leads to a substitution of amino acid 149 from Y (Tyrosine) to N (Asparagine). This mutant is characterized by a loss of function of the inhibitor of programmed cell death CED-9, which results in massive cell death in these worms (Hengartner *et al.*, 1992).

To further analyze the specificity of the α-CED-3p20-1873 antibody staining that was described in the previous section, we first looked at wild type (N2) worm embryos. Isolated embryos were either permeabilized by the freeze-crack or by the batch method. As shown in figure 3.12, A and B, both methods resulted in positive signals of putative CED-3 perinuclear staining. In 50 or 300 cell stage embryos, either one or two positive cells could be found. However, both methods showed the same specific staining. There was no detectable difference in the staining effect by either freeze-crack or the batch method.

Next we analyzed the antibody α-CED-3p20-1873 in *C. elegans* mutants carrying a defect in the *ced-9* gene (MT3970). This mutant phenotype would be

A <u>Freeze-crack method</u>

α-CED3p20-1873	HOECHST	Merge

50 cells

300 cells

B <u>Batch method</u>

α-CED3p20-1873	HOECHST	Merge

50 cells

300 cells
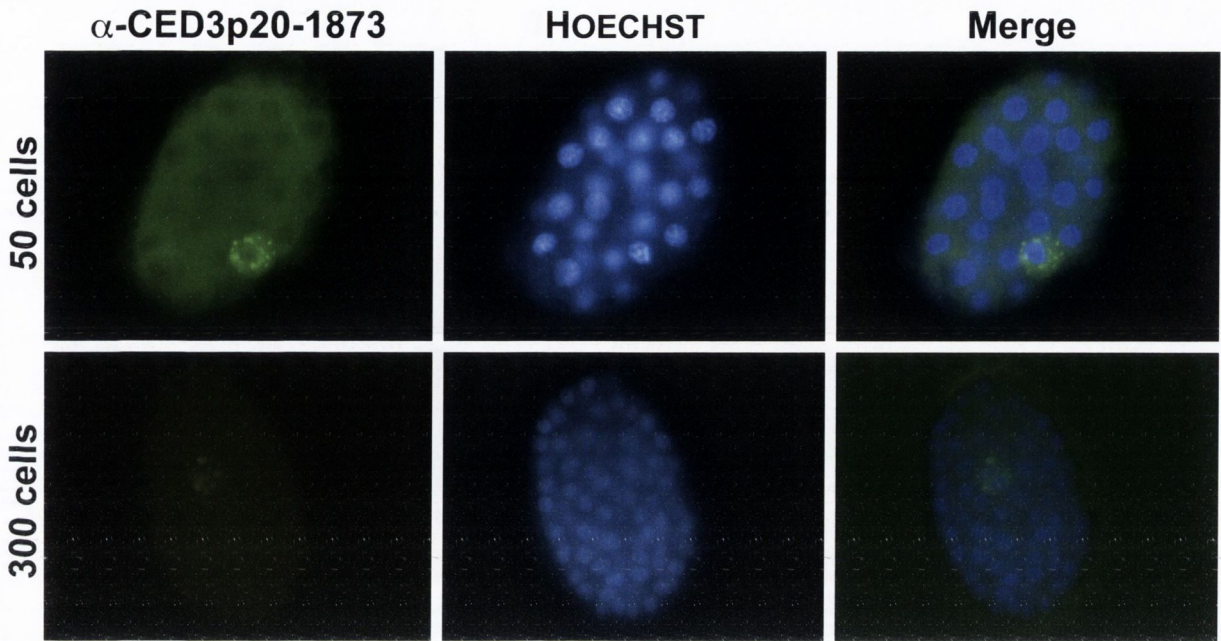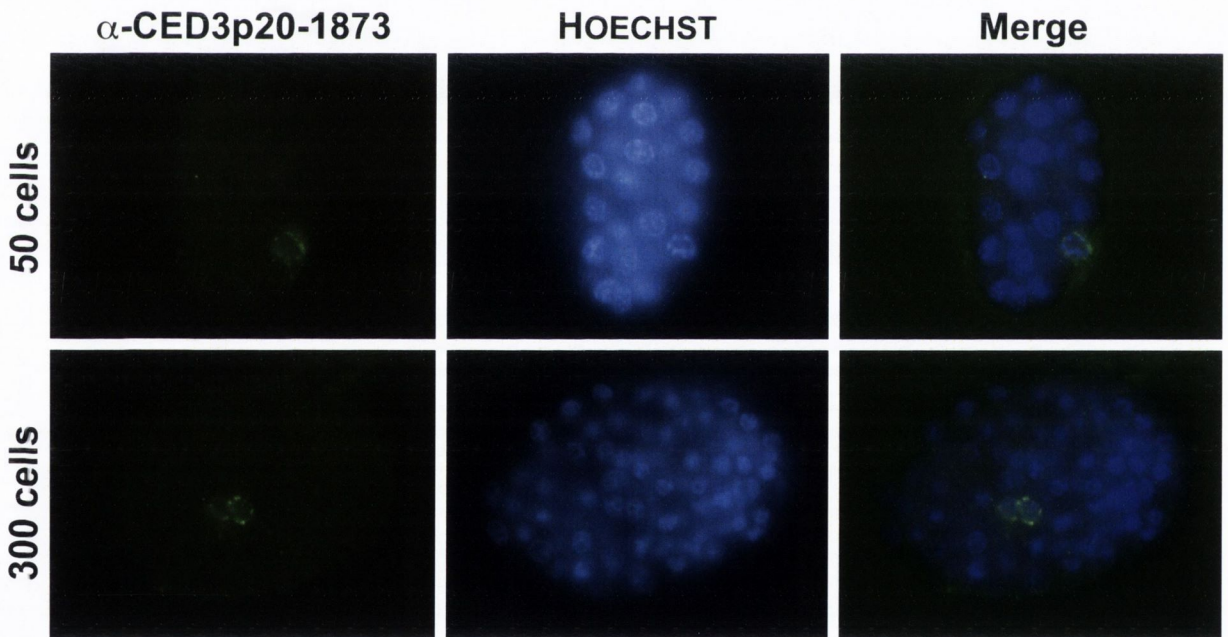
Figure 3.12: Comparison of permeabilization methods in wild type worms
Embryos from wild type worms (N2) were isolated either by the freeze crack method
(A), or by the batch method (B). Subsequently they were used for staining with the *C.
elegans* specific α-CED3p20-1873 antibody. The left hand panels show embryos of
different stages (as indicated). Nuclei were stained with HOECHST (middle panels),
and pictures were merged as on the right hand side. Note that the two methods
made no difference in the staining pattern. Representative pictures were taken at
60 X magnification on an Olympus fluorescence microscope. Results represent at
least three independent experiments.

MT3970

A Freeze-crack method

α-CED3p20-1873	HOECHST	Merge

20 cells

100 cells

B Batch method

α-CED3p20-1873	HOECHST	Merge

16 cells

50 cells
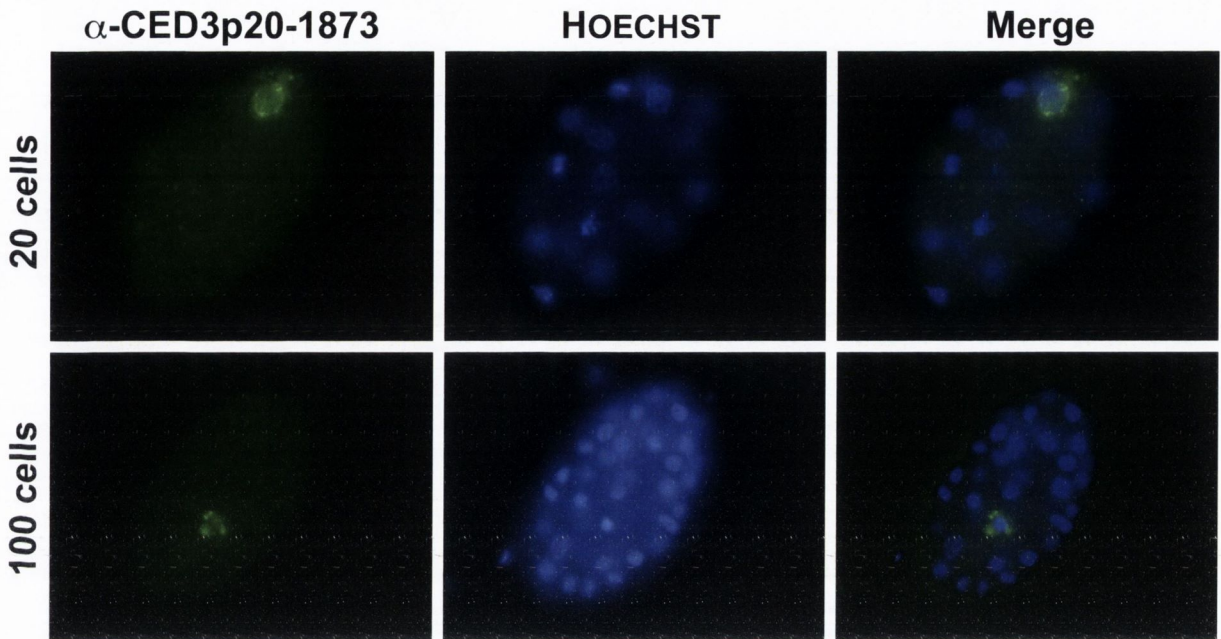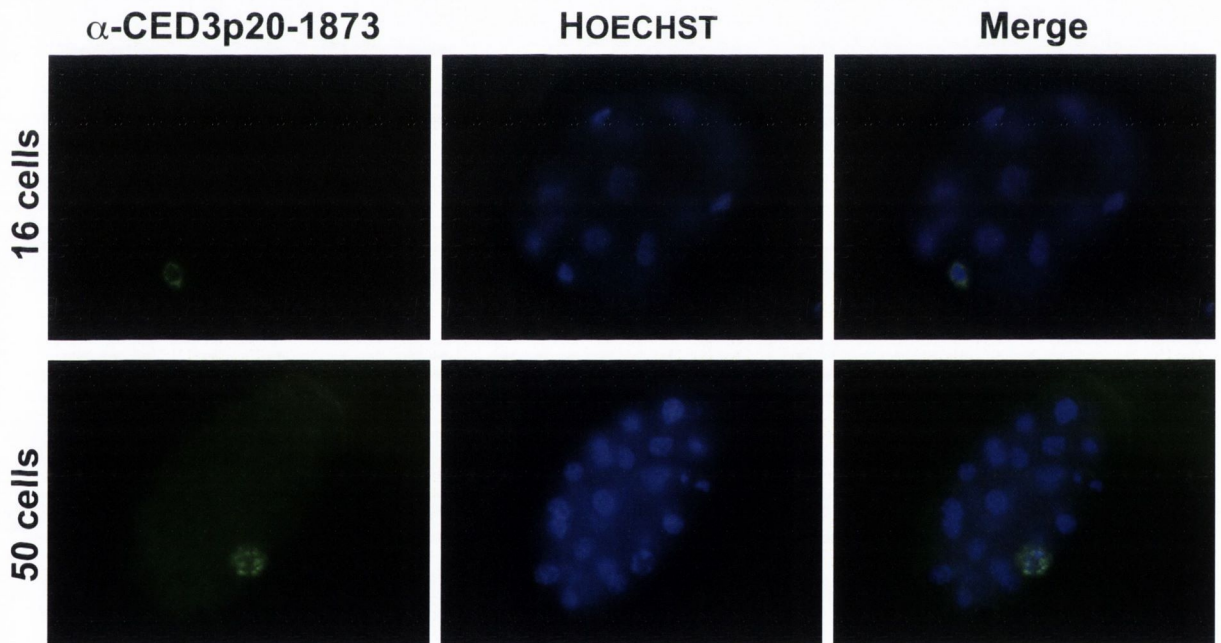
Figure 3.13: Comparison of permeabilization methods in CED-9 mutants
Embryos from CED-9 loss of function mutant worms (MT3970) were isolated either by the freeze crack method (A), or by the batch method (B). Then they were used for staining with the *C. elegans* specific α-CED3p20-1873 antibody. The left hand panels show embryos of different stages (as indicated). Nuclei were stained with HOECHST (middle panels), and pictures were merged as on the right hand side. Note that the two methods made no difference in the staining pattern even in the CED-9 mutant strain. Representative pictures were taken at 60 X magnification on an Olympus fluorescence microscope. Results represent at least three independent experiments.

MT8347

A Freeze-crack method

α-CED3p20-1873	HOECHST	Merge

50 cells

300 cells

B Batch method

α-CED3p20-1873	HOECHST	Merge

50 cells

300 cells
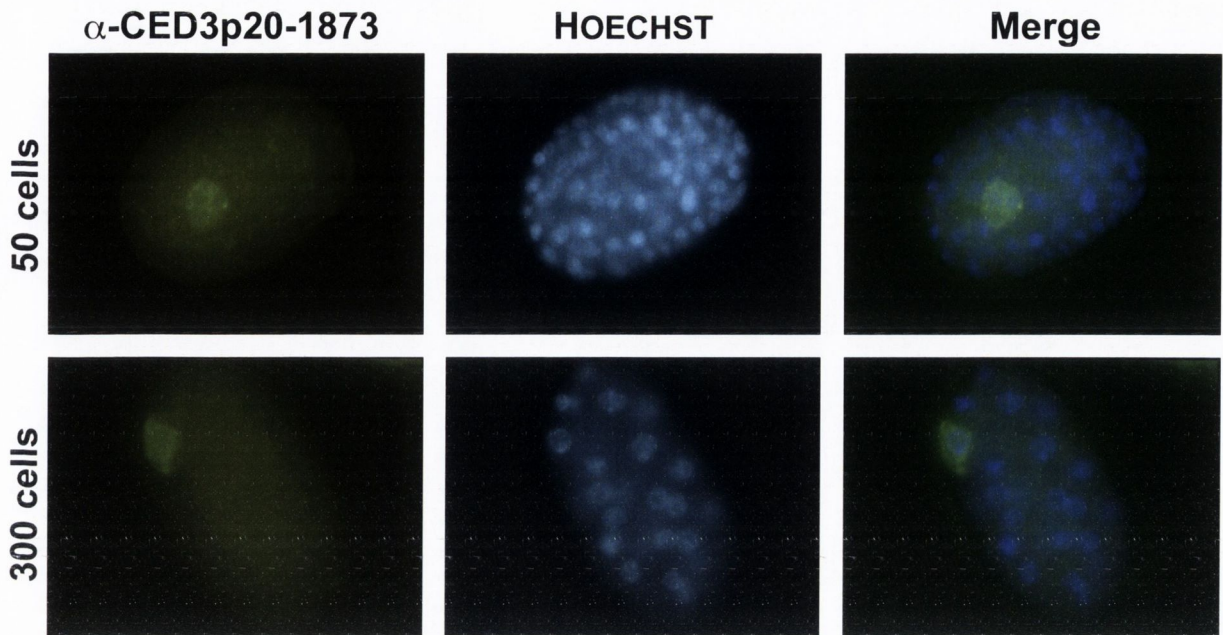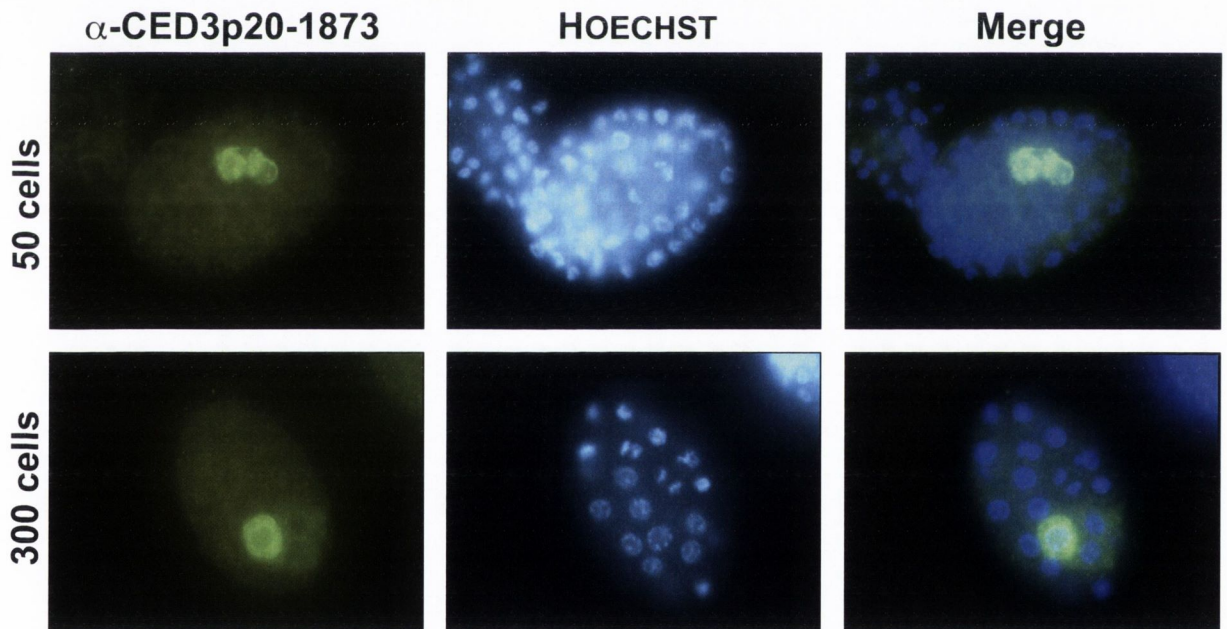
Figure 3.14: Comparison of permeabilization methods in CED-3 mutants
Embryos from CED-3 loss of function mutant worms (MT8347, truncation after aa 178) were isolated either by the freeze crack method (A), or by the batch method (B). They were used for staining with the *C. elegans* specific α-CED3p20-1873 antibody. The left hand panels show embryos of different stages (as indicated). Nuclei were stained with HOECHST (middle panels), and pictures were merged as on the right hand side. Note that the two methods made no difference in the staining pattern even in the CED-3 mutant strain. Representative pictures were taken at 60 X magnification on an Olympus fluorescence microscope. Pictures are representative for at least three independent experiments.

expected to exhibit a higher number of CED-3 positive cells, because more cells die in these mutant worms than in the wild type strain. Again, embryos collected with hypochlorite, were permeabilized with the batch method or the freeze-crack method and subsequently stained. Neither the freeze-crack method (Figure 3.13, A), nor the batch method (Figure 3.13, B) yielded a high number of positive CED-3 stained cells. In both cases, early embryos (16 – 20 cells) and late embryos (50 – 100 cells) displayed only one cell with perinuclear staining. This was repeated a number of times with different staining conditions.

Finally, α-CED-3p20-1873 immunostaining was examined in worm mutants that presumably carry a short version of CED-3 protein (aa 1-178). Our antibody was raised against an epitope beyond aa 178 (from aa 256 onwards, see Figure 3.11, B), therefore it should not recognize CED-3 protein in the mutant MT8347. Despite this, with both methods for permeabilization (freeze-crack and batch), we could detect a positive CED-3 signal in this mutant strain. As illustrated in figure 3.14, A and B, 50 and 300 cell stage embryos contained one or more positive cells. There was no significant difference detectable between the two permeabilization methods. Although we changed conditions of antibody incubation and buffer treatment, we always obtained similar results as demonstrated. Therefore, we decided to evaluate our antibodies in another system as is described below.

3.3.10 Evaluation of antibodies in HeLa cells

Because it proved very difficult to immunolocalize CED-3 in worm embryos, a different strategy was used to scrutinize the specificity of the antibodies against *C. elegans* cell death proteins that were available to us. We chose to analyze them in a human cell line. In order to do this, we cloned the respective *C. elegans* protein coding sequences into a mammalian expression vector (pcDNA3, Invitrogen). Figure 3.15 shows schematics of the proteins that were used in our studies. Constructs for CED-4, CED-9 and CED-9ΔTM were a kind gift from Dr. G. Nunez (University of Michigan, Ann Arbor, USA). All further constructs for these experiments were generated in our laboratory. Wild type CED-3, the CED-9 gain of function and the CED-9 loss of function mutants
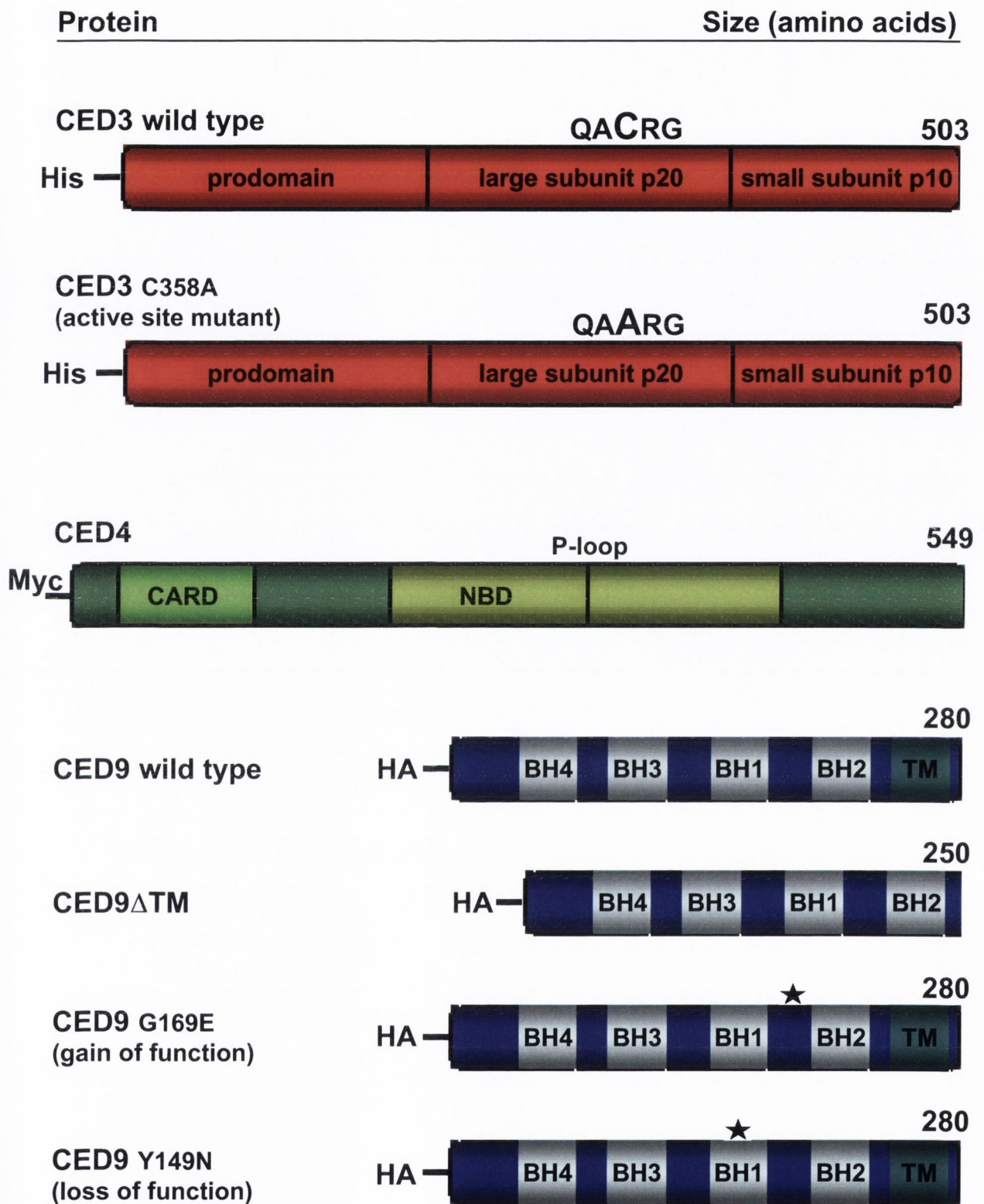
Figure 3.15: Constructs of *C. elegans* proteins
Schematic representation of *C. elegans* proteins. Constructs were generated for use in mammalian cell lines by cloning DNA sequences into pcDNA3 plasmid. CED-3 wild type was cloned by Dr. R. C. Taylor as well as the site directed mutagenesis of the CED-9 constructs (CED9G169E and Y149N). The active site mutant of CED-3 was made by Dr. P. J. Duriez in our laboratory. CED-4 wild type, CED-9 wild type and CED-9ΔTM were generous gifts from Dr. G. Nunez. Indicated are protein domains, active sites, aa and N-terminal epitope tags. The star indicates the site of the point mutation in the CED-9 protein.

(which were also used in chapter 4) were cloned by Dr. R. C. Taylor a member of the laboratory, into pcDNA3. Another member of the laboratory, Dr. P. J. Duriez, performed site directed mutagenesis on CED-3 to obtain the active site mutant protein (CED-3C358A).

3.3.11 Staining of HeLa cells with *C. elegans* specific antibodies

Transient transfection of HeLa cells with pcDNA3-CED-3 wild type generally led to apoptosis of transfected cells as expected (data not shown). Therefore, for immunostaining experiments, we routinely used the caspase active site mutant pcDNA3-CED-3C358A.

Cells transiently transfected with pcDNA3 (empty vector), pcDNA3-CED-3C358A, pcDNA3-CED-4 or pcDNA3-CED-9, were fixed and then stained with commercially available antibodies (Santa Cruz). As a positive control, endogenous cytochrome *c* was immunostained in control cells. As shown in figure 3.16, cells transfected with empty vector alone or with pcDNA3-CED-3C358A, displayed typical cytochrome *c* staining representing mitochondria (Figure 3.16, A, top panels). When cells were stained with the antibodies against CED-3 (α-SC-CED-3N, α-SC-CED-3C) from Santa Cruz, CED-3 specific staining could not be found (Figure 3.16, A, middle and bottom panels). Only an unspecific weak background staining, covering the whole of the cells was visible.

In contrast to the above, HeLa cells, transiently transfected with pcDNA3-CED-4 and stained with the Santa Cruz α-SC-CED-4N antibody, showed positive cells. CED-4 displayed a mixture of perinuclear, partially nuclear membrane bound and cytoplasmic staining in these cells, compared to cells transfected with empty vector (Figure 3.16, B). The background staining was negligible.

Like CED-4, CED-9 protein could be detected in HeLa cells transfected with pcDNA3-CED-9 construct. When cells were stained with α-SC-CED-9C (Figure 3.16, C) or α-SC-CED-9N (data not shown), a specific staining pattern was observed. Unlike CED-4, CED-9 seemed to be completely membrane
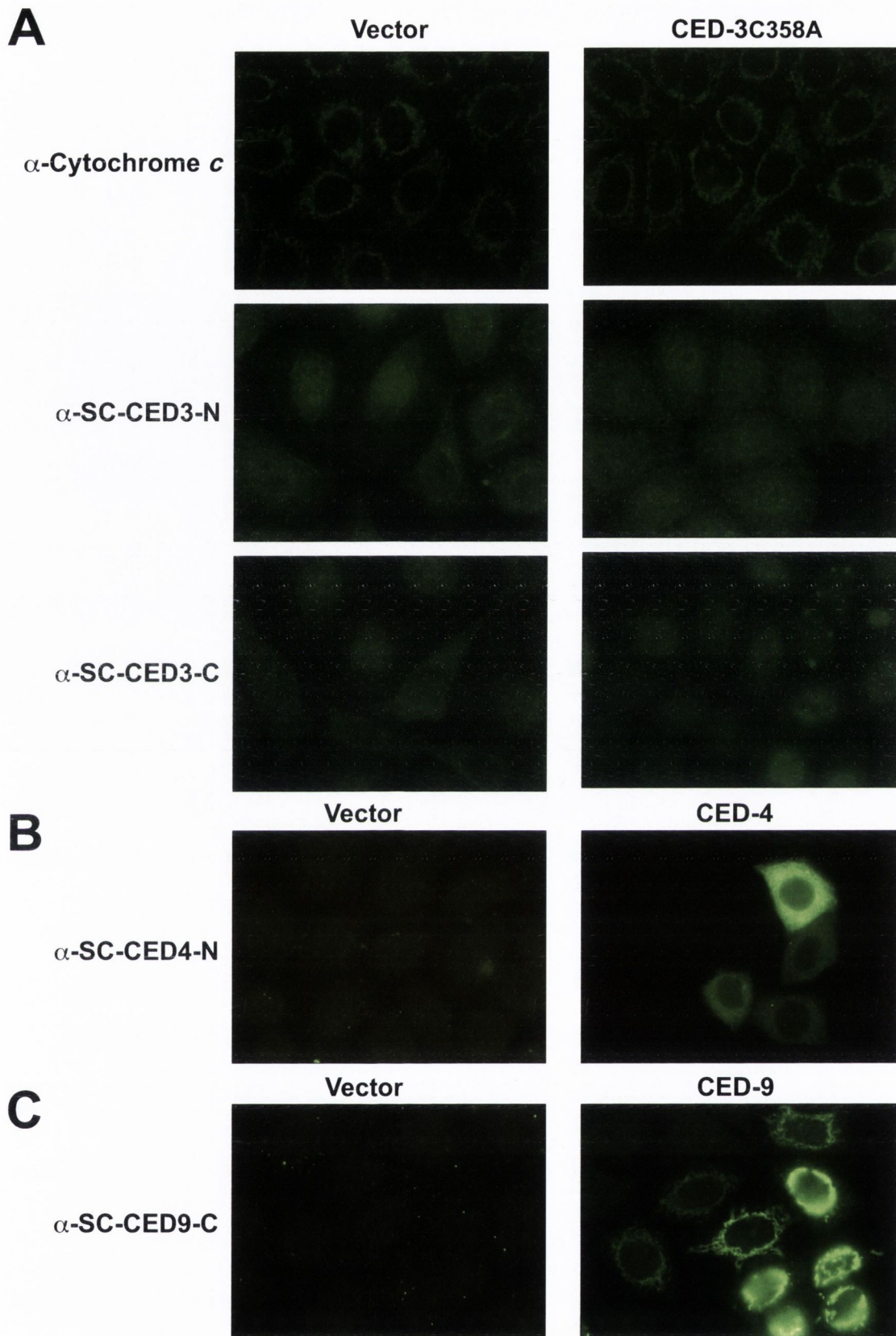
Figure 3.16: Immunostaining of *C. elegans* proteins in HeLa cells

Plasmids expressing *C. elegans* proteins were transfected into human HeLa cells, growing on coverslips, by lipofection. After 24 hours, cells were fixed and stained. A) Staining for endogenous cytochrome *c* with α-Cytochrome *c* antibody (BD) as control (upper panel). The CED-3 active site mutant was used for transfection to avoid killing of the cells. CED-3-specific staining with Santa Cruz antibodies achieved no positive staining (middle and lower panel). B) CED-4 expression could be detected by the indicated antibody in the cytoplasm and the perinuclear region. C) Expression of CED-9 was dectected by the indicated antibody in specific cell compartments. Pictures were taken on an Olympus laser-scanning microscope FV1000 at 60 X magnification. Pictures depict representative areas of three independent experiments.

bound in subcellular compartments. Only weak background staining was seen in cells expressing empty vector.

Next we examined polyclonal CED-3 antibodies generated in our laboratory. HeLa cells expressing either empty vector or pcDNA3-CED-3C358A were stained with the set of antibodies α-CED-3-A1, α-CED-3-A2, α-CED-3-B1 and α-CED-3-B2. However, no positive staining was detected with any of these antibodies (data not shown).

We also tested the anti-peptide CED-3 antibodies that were generated during this study. HeLa cells, transiently transfected with the empty vector or the active site mutant of CED-3, were stained with α-CED-3-pro-1877, α-CED-3-pro-1878, α-CED-3-p20-1873, α-CED-3-p20-1874, α-CED-3-p10-1875, α-CED-3-p10-1876. However, positive CED-3 staining of cells was only detected with α-CED-3-p20-1873 - which agreed with its potency for detecting recombinant CED-3 protein on cell lysates by Western blot (Taylor *et al.*, 2007). The staining of HeLa cells appeared as a perinuclear, speck-like pattern (data not shown).

3.3.12 Staining of HeLa cells expressing *C. elegans* proteins with anti-tag antibodies

The above results obtained for CED-3 staining were not convincing, therefore a further approach was tested. Because all the above cloned constructs of *C. elegans* genes contained N-terminal epitope-tags (Figure 3.15) we utilized commercially available anti-tag antibodies for immunostaining.

HeLa cells transiently transfected with pcDNA3-CED-3C358A (Figure 3.17, top panel) were fixed and stained with α-His antibody. Cells over-expressing CED-3 were revealed by clear nuclear staining pattern of the target protein. This was in stark contrast to what we had seen with α-CED-3-p20-1873 antibody as described above. The same pattern was observed when wild type CED-3 construct was used to transfect cells, and the caspase inhibitor (zVADfmk) was added to stop cells from dying and lifting off the plate (data not shown).
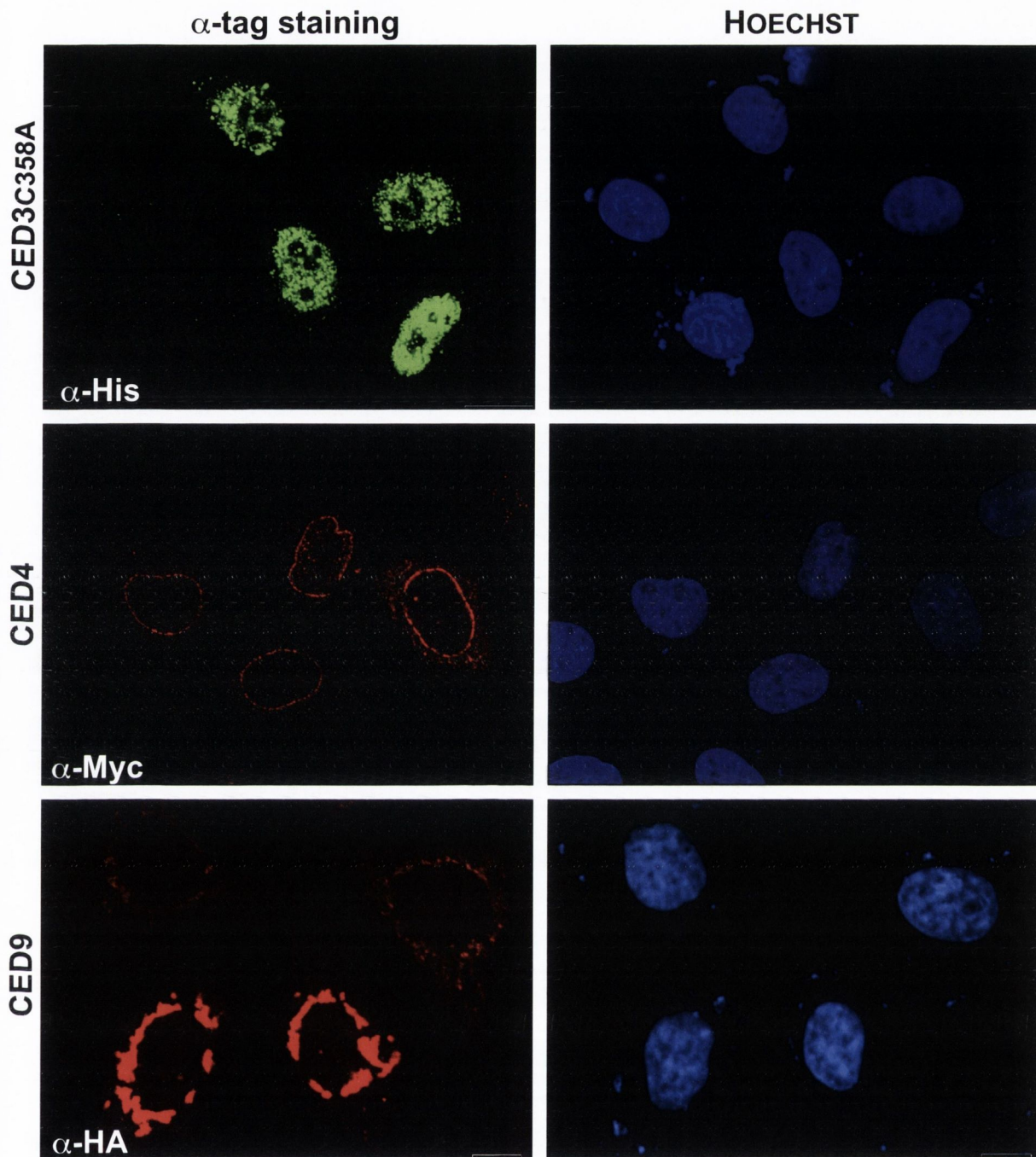
Figure 3.17: Immunostaining of C. elegans proteins with anti-epitope tag antibodies

HeLa cells, transfected with CED-3C358A, CED-4 and CED-9 encoding plasmids, were fixed and stained after 24 hours expression. Epitope-tag antibodies were used to localize the proteins and used as indicated. Nuclei were counter-stained with HOECHST (right panels). Pictures were taken on an Olympus laser-scanning microscope FV1000 at 60 X magnification. Pictures depict representative areas of at least three independent experiments.

To explore the subcellular localization pattern of CED-4 in HeLa cells, these cells were transfected with pcDNA3-CED-4 construct. After 24 hours cells were stained with α-Myc antibody and CED-4 staining was seen in the nuclear envelope and partially in the cytoplasm (Figure 3.17, middle panel). These results were in agreement with observations we consistently made in HeLa cells and *C. elegans* embryos that were each stained with α-SC-CED-4N antibody from Santa Cruz (Figures 3.7 and 3.16 B).

We also confirmed our previous observations on CED-9 staining. When HeLa cells expressing pcDNA3-CED-9 construct were stained with the epitope specific antibody α-HA, we found CED-9 staining on subcellular structures (Figure 3.17, bottom panel). This pattern overlapped with what we saw earlier when HeLa cells expressing CED-9 protein were stained with α-SC-CED-9C antibody from Santa Cruz (Figure 3.16, C).

Protein-protein interactions can be revealed by co-expressing constructs in model cells and staining for each target protein with specific antibodies. To see if co-expression of the worm cell death proteins could impact on each other and to confirm previously described interactions, we analyzed the above constructs in human cells (Wu *et al.*, 1997a and b; del Peso *et al.*, 1998, Chen *et al.*, 2000). We transfected HeLa cells transiently with pcDNA3-CED-3C358A and pcDNA3-CED-4 and co-stained these cells with antibodies against their respective epitope-tags. The top panels in figure 3.18 show typical cells that co-expressed CED-3 and CED-4. α-His staining revealed CED-3 nuclear staining and CED-4 could be seen with α-Myc staining in its perinuclear pattern (Figure 3.18, top panels). In contrast to our expectations, there were no visible changes of either CED-3 or CED-4 localization in the double transfected cells, when compared to the single transfected cells, indicating that the CED-3/CED-4 interaction might only occur in a transient manner that was not captured in our context.

HeLa cells transfected with pcDNA3-CED-3C358A and pcDNA3-CED-9 were stained with α-His and α-HA respectively to reveal target protein expression. No changes of the subcellular distribution could be observed when
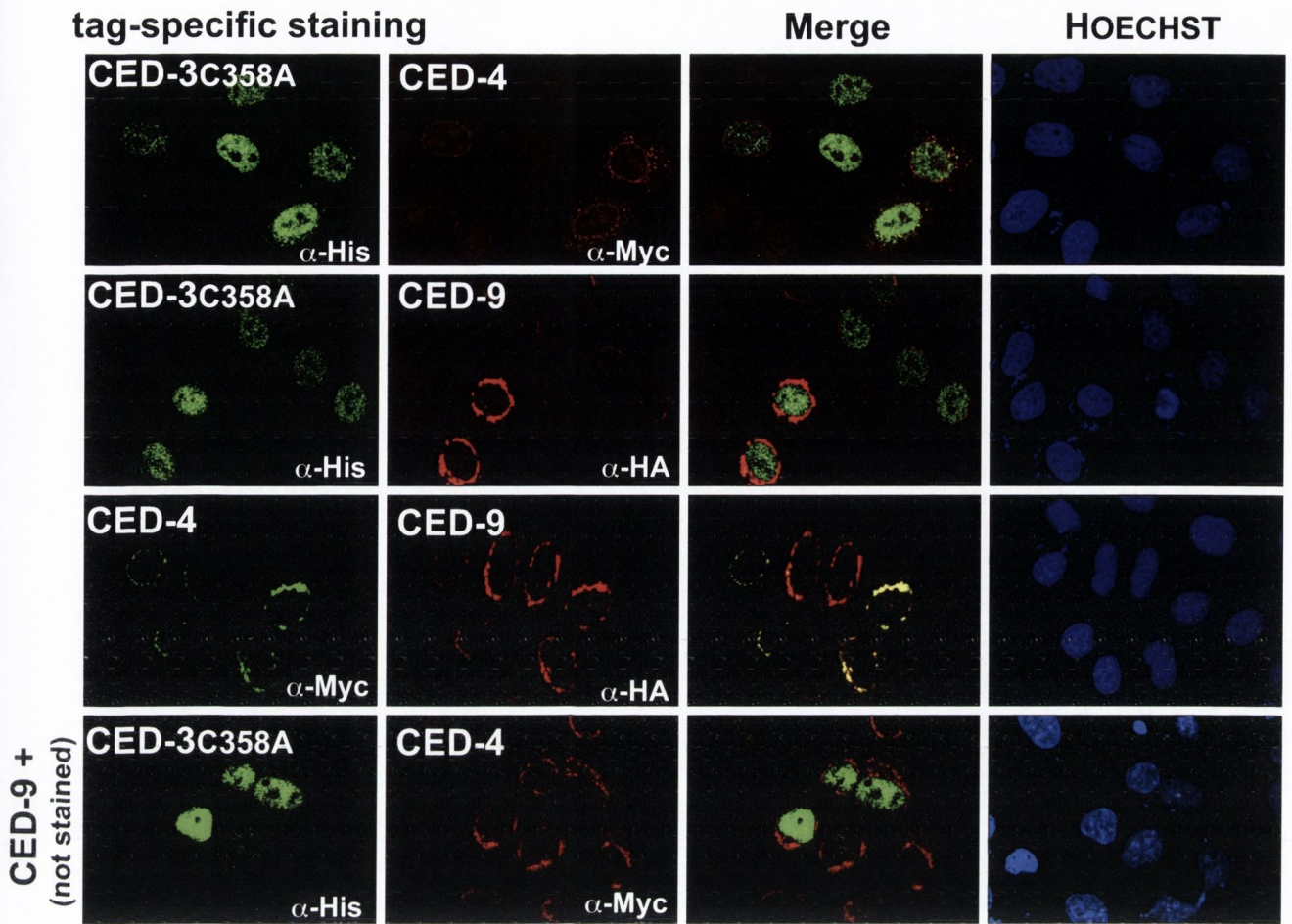
Figure 3.18: Immunostaining of combinations of *C. elegans* proteins with anti-epitope tag antibodies

HeLa cells, co-transfected with CED-3C358A, CED-4 and CED-9 encoding plasmids, were fixed and stained after 24 hours expression. Epitope-tag antibodies were used to localize the proteins and used as indicated. Co-localization appeared when CED-4 and CED-9 were co-expressed (third panel). Nuclei were counter-stained with HOECHST (right panels). Pictures were taken on an Olympus laser-scanning microscope FV1000 at 60 X magnification. Pictures depict representative areas of at least three independent experiments.

CED-3 was co-expressed with CED-9, indicating that those proteins do not interact (Figure 3.18, second row panels).

When CED-4 was expressed together with CED-9 we found dramatic changes of the CED-4 staining pattern. Instead of the typical CED-4 nuclear envelope staining pattern, we found CED-4 staining completely overlapping with the CED-9 staining on intracellular structures (Figure 3.18, third row panels). This finding confirmed the results of other groups that had shown CED-4/CED-9 interactions by other approaches (Wu *et al.*, 1997a and b; del Peso *et al.*, 1998, Chen *et al.*, 2000).

Finally we triple transfected HeLa cells with pcDNA3-CED-3C358A, pcDNA3-CED-4 and pcDNA3-CED-9. Because of technical difficulties, concerning the species specificity of our antibodies, we could not perform a triple stain for all transfected proteins. The fourth panel of figure 3.18 shows typical cells that expressed CED-3, CED-4 and CED-9. CED-3 is visualized through α-His staining (green) and CED-4 by the α-Myc staining (red). Co-expression of CED-9 becomes apparent through the atypical CED-4 staining, which is due to its sequestration by CED-9. CED-4 was translocated to subcellular organelles as in the previous experiments. CED-3 staining pattern was unchanged and localized to the nucleus.

These results confirmed early observations of interactions between *C. elegans* proteins that regulate the cell death machinery in developing worm embryos. CED-4 and CED-9 were co-localized, however, we saw no obvious interaction between CED-3 and CED-4 protein, or an influence on CED-3 by the presence of CED-9.

3.4 Discussion

3.4.1 Summary

Using indirect immunoflourescence, we wanted to explore the temporal and spatial expression pattern of *C. elegans* caspase CED-3 *in vivo*, which has not been demonstrated before. We used a large set of antibodies aimed against CED-3 protein. However, despite all our efforts to detect CED-3 in worm embryos, none of the twelve antibodies offered a satisfactory staining pattern. The only consistent CED-3 positive staining we detected was as a result of over-expression of this gene in HeLa cells.

Despite our failure to detect CED-3 in the worm, we observed an interesting staining pattern of CED-9 in HeLa cells and decided to explore this result further as described in the next results chapter.

3.4.2 Expression of CED-3 during worm development

Dying cells in the nematode *C. elegans* were observed in mutant animals that lost their ability to engulf and discard such cells. The responsible protein for this death was found to be CED-3, the only caspase of the worm (Ellis and Horvitz, 1986). Loss of CED-3 function has no apparent effect on worms and results in healthy animals with no developmental abnormality (Ellis and Horvitz, 1986).

In this study we wanted to tackle the question of where CED-3 caspase is expressed in worm embryonic cells and when its expression can first be seen. This has been demonstrated for the CED-3 cell death partners CED-4 and CED-9 by immunostaining (Chen *et al.*, 2000). CED-9 for example, was found to be expressed from the 2 cell stage on until the time of hatching of the worm (585 cell stage) with a peak of expression at the 200 cell stage, indicating the importance of CED-9 for the development of worms. In addition, CED-4 expression appeared at around the 100 cell stage, just before the appearance of the first dead cells, and was also diminished after embryonic development (Chen *et al.*, 2000). However, CED-3 expression pattern *in vivo* is still unclear. We do not know for example whether CED-3 is constitutively expressed in all embryonic cells throughout embryonic development. This can be suggested by the constant expression of CED-9, which could act as an indirect blocker for

CED-3. On the other hand, the time of onset for CED-3 expression could be after the appearance of CED-4 expression at around the 100 cell stage as the presence of CED-4 is necessary for CED-3 activation. Or, CED-3 expression could depend on transcriptional up-regulation as recently suggested for specific worm cells (Maurer *et al.*, 2007).

These observations underline that it is still unclear, and important to elucidate CED-3 expression. While human caspases are synthesized as inactive zymogens and remain inactive in cells until their arousal, the following questions can be asked about CED-3. Is it produced like its human counterparts as an inactive zymogen that is always available until CED-4 is released from CED-9 and can activate it? Is CED-3, as mentioned above, expressed constitutively in all *C. elegans* cells during the complete animal development? Is it constitutively expressed only after a certain time of development, or at a specific number of cells? Or is CED-3 expression dependent on regulation by certain transcription factors, at least in some cells? To answer these questions we attempted to immunostain CED-3 protein in *C. elegans* cells.

3.4.3 Immunostaining of *C. elegans* embryos

Investigations on *C. elegans* cells can only be undertaken by using the whole animal or embryos. Until today, no sustainable *C. elegans* cell line has been established that can be used for analysis of endogenous proteins. In addition, *C. elegans* cells are very small in size, which makes it difficult to recognize details. Staining *C. elegans* cells with antibodies had never been done in our laboratory before. Therefore, the technique needed to be established and filed. Although the method worked for some standard antibodies, we failed to detect CED-3 protein in worm embryonic cells. The reasons for this are discussed below.

First, immediately after isolating worm embryos we fixed the worm proteins to stop cell division and to be able to continue with the immunostaining protocol. We found that paraformaldehyde was best to be used. This small molecule diffuses into the embryos and cross-links proteins. We also tested other methods of fixation, such as methanol and ethanol, but the results were not feasible. Although we always undertook vigorous washings to remove the

fixative in our samples, it cannot be excluded that minor amounts of fixative were still present, which might have interfered with the antibodies, resulting in a negative outcome. In general, some antibodies are not compatible with paraformaldehyde fixation.

Second, to conquer the embryonic cells, the chitinous eggshell needs to be broken. Although we used two different methods, as described in the results section, not all embryos in a given preparation might have been permeabilized or cracked sufficiently to allow the penetration of the antibody. And the quality of cracking the eggshell was not determinable. However, in each experiment we used our control antibodies against either actin or tubulin, which was working and specific. But, in this context, it has to be considered that actin and tubulin appear in abundance in this organism. Therefore, presumably already very little antibody could have stained the embryo. In contrast CED-3 protein might be expressed only at low concentrations, sufficient to kill the cells, but insufficient to be immunostained.

Third, after entering the eggshell, the membrane of the cells posed the next barrier. After testing several different permeabilization reagents, Triton-X100 became our reagent of choice. Various concentrations and timepoints were tested and resulted in positive staining with our control antibodies. However, the permeabilization method and reagent might have interfered with the specific anti-CED-3 antibodies and inhibited a positive outcome.

All these technical difficulties might have led to the negative results we obtained when staining for the worm caspase CED-3. Fixation and permeabilzation reagents might have either interfered with the endogenous protein, i.e. changed it in a way that it was not accessible for the antibody anymore. Alternatively, the reagents might have interfered with the antibody, which is also a protein susceptible, to those reagents.

3.4.4 *C. elegans* specific antibodies used in this study

For verification of the immunostaining technique, and as possible comparison to CED-3 staining, we used some commercially available antibodies obtained from Santa Cruz. When we stained for control proteins CED-4 and CED-9 we obtained odd results. CED-4 had been described to be bound to CED-9 and

thereby to intracellular membrane structures. Only after the release of CED-4 during cell death activation, involving the up-regulation of EGL-1 and its binding to CED-9, CED-4 appears to translocate to the nuclear envelope (Chen *et al.*, 2000; Tzur *et al.*, 2002). In addition, CED-4 expression was only seen at a later developmental stage of worm embryos, after around the 100 cell stage (Chen *et al.*, 2000). In stark contrast to these observations, when we stained CED-4 using the Santa Cruz antibody, it was localized around the nuclei of each cell from a two-cell stage embryo to a late embryo. This was rather surprising, because we used embryos from untreated wild type N2 worms. The reason for these results could be either that the used *C. elegans* strain was not the one we expected it to be, or that the CED-4 antibody cross-reacted with another protein in *C. elegans* and gave us a false positive staining. We favor the latter explanation, since all worm strains used in this study, and from many worm-studying groups, were obtained from the reliable CGC (Caenorhabditis Genetics Centre). Plus, the CED-4 nuclear localization would indicate a translocation of the protein away from CED-9, which should lead to the activation of CED-3. Therefore, the embryos with such staining would be expected to die.

However, generation of the antibodies used in the above experiments were from different sources, Chen and colleagues had produced antibodies against bacterially purified full-length CED-4 protein, while the Santa Cruz antibodies were made against a CED-4 peptide of the N-terminus region. Therefore, the un-specificity of the antibodies can be different. In general, antibodies generated against peptides might bear a higher risk for cross-reactivity, which would explain the early appearance of CED-4 in a 2 cell embryo.

Unfortunately, using two Santa Cruz antibodies against CED-9 peptides of the N- and C- terminus, which were, like all their antibodies affinity purified, we failed to detect any positive staining. The reason for this could either lie in our technique, or in the un-specificity of antibodies that were used, as discussed above.

3.4.5 Staining *C. elegans* embryos against CED-3

Twelve different antibodies were tested during the course of this study in an effort to analyze the CED-3 caspase *in vivo*. However, we failed to find any CED-3 positive staining. As in the previous section, antibodies from Santa Cruz could not detect any CED-3 protein, probably due to their lack of specificity. Although the manufacturer recommended the antibodies for Western Blot and immunoflouresence, we could not confirm this.

The set of antibodies that were generated in our laboratory against CED-3 lacking the CARD-domain, were tested for their recognition of recombinant protein (Rebecca Taylor, unpublished observations). In those experiments the antibodies α-CED-3-A1, α-CED-3-A2, α-CED-3-B1 and α-CED-3-B2 detected protein down to a concentration of 10 ng by Western blot. The set of antibodies raised against peptides of the large and the small subunit of CED-3, α-CED-3p20(1874 and 1874) and α-CED-3p10(1875 and 1876) respectively, were also tested by Western blot. They readily recognized the CED-3 subunits of recombinant protein to a concentration of 500 ng (Taylor *et al.*, 2007 and data not shown). Despite this, in immunoflourescence experiments, as shown in this thesis, the antibodies failed to detect CED-3. However, detection of proteins by Western blot indeed is not an indication for the specificity of an antibody when it is used for immunostaining. In fact, protein epitopes are presented very differentially in those two techniques. During SDS-PAGE and subsequent Western transfer onto membranes, the proteins are denatured and completely lose their natural structure. In contrast, proteins that are fixed for immunostaining are expected to remain in their natural conformation. For this reason, the peptides chosen by us to generate antibodies were surface exposed protein regions. Despite taking all this into consideration, we could not detect CED-3 endogenous protein in *C. elegans* embryos.

A simple reason for the failure of detecting CED-3 could be that the concentration of this protein is very low in worm cells. Very little CED-3 could indeed be sufficient to initiate programmed cell death in the worm. In a feed forward manner more CED-3 protein could be synthesized to ensure the dismantling of cells. Another explanation for not being able to detect CED-3 could be the half life of the protein. It might be that expressed CED-3 is broken

down very quickly after its activation and function in cell death. This would need further biochemical investigations.

Of the six peptide antibodies tested, one antibody α-CED-3p20-1873 resulted in a certain staining pattern in embryonic cells. Embryos with positive cells were always of later stages with more then 20 cells. This was rather surprising, because the first round of cell death occurs only after the embryo consists of more then 100 cells. Nevertheless, we repeatedly found one or more cells with a perinuclear or cytoplasmic staining that was outstanding. Since CED-3 localization has not been described to date, this was a reasonable site for it. In addition, human caspases are harbored in the cytoplasm, where they await their activation. A functional rational would therefore be underlined by this observation.

To further evaluate our findings, we used different *C. elegans* mutants. We isolated embryos of the CED-9 loss of function mutant strain MT3970, in which we expected more CED-3 expression and a higher number of CED-3 expressing cells. As demonstrated in the next chapter (Figure 4.26) mutant worms, which lack CED-9 function, undergo a vast amount of extra cell death (Hengartner *et al.*, 1992). However, we did not observe an increase of CED-3 positive cells with our antibody. Finally, when we used a worm strain that carries a deletion of CED-3 we still obtained the same staining pattern with this antibody, which led to suspicion of this result. In MT8347 embryos CED-3 is truncated after amino acid 178. As the antibody we used here was raised against a region beyond amino acid 256, it should not detect CED-3. Therefore, the staining pattern observed must have been a false positive result, i.e. indicating unspecific staining of this antibody.

Taken together, our results of staining for the caspase CED-3 were all negative or false positive, which most likely was due to the insufficient quality of the antibodies used and probably their low titer of antibody. Therefore, more CED-3 antibodies should be tested with higher quality, such as monoclonal antibodies. Those antibodies are less likely to cross-react with other proteins.

3.4.6 Heterologous expression of *C. elegans* cell death proteins in HeLa cells

To finally assess the quality of all the antibodies used in this first chapter, we went to over-expression experiments in human cells. Recombinant *C. elegans* cell death proteins were expressed and stained in HeLa cells. Again we found CED-4 positive cells with the Santa Cruz antibody, but it rather displayed a cytoplasmic and only a partial nuclear envelope staining pattern, as we saw in the nematode. By staining for CED-9, we now could easily detect cells expressing the protein with the Santa Cruz antibody and found it bound to subcellular membranes. This is in contrast to the staining of worm embryos where we failed to achieve any CED-9 positive staining with this antibody.

CED-3 staining in HeLa cells, with the twelve CED-3 antibodies, was also unsuccessful. However, when we used epitope-specific antibodies, CED-3 was reproducibly and persuasively expressed in the nucleus of HeLa cells. Seeing that CED-4 localized to the nuclear envelope in human cells, this experiment might demonstrate a possible mechanism of CED-3/CED-4 interaction for activation by the close proximity of the two proteins in human cells. In addition, a human caspase, caspase-2 has been described to be localized to the nucleas, indicating an evolutionary conservation for the caspase localization (Colussi *et al.*, 1998; Paroni *et al.*, 2002). However, this localization could have been specific for the expression of CED-3 in human cells and might not be transferable to worm cells.

During the course of these experiments we repeatedly found dramatic changes of mitochondrial networks when CED-9 was heterologous expressed in HeLa cells. Because this appeared very interesting and unexpected, we decided to investigate this observation in more detail, which is described in the next chapter.

CHAPTER IV

Role for CED-9 and EGL-1 as Regulators of Mitochondrial Fission and Fusion dynamics

4.1 Introduction

The Bcl-2 family of proteins regulates the mitochondrial apoptotic pathway in mammals (Youle and Strasser, 2008). Mitochondrial outer membrane permeabilization (MOMP) is the crucial point in this process at which apoptosis is initiated. Bcl-2 and Bcl-xL, two anti-apoptotic proteins, function by blocking MOMP and thereby the release of cytochrome c from the mitochondrial intermembrane space (Wei *et al.*, 2001; Newmeyer and Ferguson-Miller, 2003). Downstream of this juncture they thereby indirectly inhibit the binding of cytochrome c to Apaf-1 as a cofactor, which in turn would undergo a conformational change and recruit caspase-9 to form the apoptosome for caspase activation. Once caspase-9 is activated, downstream caspases become processed in form of a cascade and the dismantling of the cell follows (Adrain *et al.*, 2006).

In the nematode *C. elegans* a homolog of Bcl-2 was found, which is the CED-9 protein (Hengartner *et al.*, 1992). In contrast to its human homologues, CED-9 suppresses cell death via direct inhibition of CED-4 (the Apaf-1 homolog in *C. elegans*) (Chinnaiyan *et al.*, 1997a). The currently accepted model suggests that through sequestration of CED-4 by CED-9, activation of the CED-3 caspase is kept in check thereby preventing cell death in the developing worm. A death stimulus can induce up-regulation of EGL-1, which binds to CED-9 (Conradt and Horvitz, 1998). As a result, CED-9 liberates CED-4, which in turn oligomerizes with other CED-4 molecules and build the worm apoptosome together with CED-3.

While Bcl-2 is functionally active in the worm and inhibits cell death effectively (Vaux *et al.*, 1992), the functionality of CED-9 in mammalian cells has not been studied. CED-9, like most anti-apoptotic members of the human Bcl-2 family is equipped with a transmembrane domain and has been found to localize to organelle membranes. Despite this, a role for mitochondria or other organelles has not been established in the worm cell death pathway to date.

The role of mitochondria during apoptosis has been under intensive investigation. The mitochondrial network becomes dramatically disrupted when a cell dies (Frank *et al.*, 2001; Karbowski *et al.*, 2002). But even in healthy

cells, mitochondria are dynamic structures that fuse and divide continuously (Hales and Fuller, 1997). Proteins that regulate mitochondrial fusion and fission events are mainly large GTPases that are, like the Bcl-2 proteins, bound to mitochondria or can translocate there and have recently been implicated in the regulation of apoptosis. For example, down-regulation of Drp-1 with RNA interference has been reported to inhibit apoptosis-associated cytochrome *c* release (Lee *et al.*, 2004). Furthermore, over-expression of mitochondrial fusion-promoting proteins, Fzo-1 and Mfn-2 has been reported to protect cells from apoptosis (Sugioka *et al.*, 2004; Jahani-Asl *et al.*, 2007; Chen *et al.*, 2007). Thus a role for mitochondrial fission and fusion proteins as regulators of apoptosis is emerging.

It remains unclear if apoptosis-related proteins, like the Bcl-2 super-family, have a role in mitochondrial dynamics in addition to their control of MOMP. Studies have shown that Bax, a pro-apoptotic member of the Bcl-2 family, not only triggers MOMP and cytochrome *c* release, but also appears to localize at foci of mitochondrial scission (Nechushtan *et al.*, 2001). Moreover, cells that are deficient in Bax and Bak appeared to have fragmented mitochondria, underlining an important role for these proteins in mitochondrial dynamics (Karbowski *et al.*, 2006). Another recent study from Jagasia and colleagues reported that the worm BH3-only protein EGL-1, which is also a pro-apoptotic protein, fragmented mitochondria in worm embryos when it was driven by an inducible promoter (Jagasia *et al.*, 2005). These observations hint at a role for the Bcl-2 family as regulators of mitochondrial fission and fusion dynamics.

4.2 Aims and Summary

During the course of our initial studies on *C. elegans* proteins expressed in HeLa cells, we observed that CED-9 induced dramatic rearrangements on mitochondrial networks. This was surprising, since no role for mitochondria in the worm cell death machinery has been reported previously. To shed light on this, and to explore whether CED-9 can substitute for Bcl-2 in mammalian cells, we decided to investigate this issue further.

The ability of CED-9 to inhibit apoptosis in HeLa cells was tested by exposing CED-9 transfected cells to a range of apoptotic stimuli. In addition, we also explored whether CED-9 could regulate apoptosis-associated cytochrome *c* release in mammalian cells. However, we could not find an inhibitory function for CED-9 in the human cell model. To analyze the function of CED-9 and its human homologues on mitochondrial fission and fusion dynamics, we chose to evaluate them in comparison with the fusion promoting proteins Mfn-1, Mfn-2, Drp1K38A and Opa-1. We found that the CED-9 mitochondrial phenotype, did not only resemble a fusion phenotype it also interacted with Mfn-2 protein by co-immunoprecipitation. Further experiments included the pro-apoptotic worm protein EGL-1 in combination with CED-9. Surprisingly, EGL-1 disrupted the fused mitochondrial phenotype of CED-9, but this had no effect on cytochrome *c*.

Our results suggest that a possible additional function of the Bcl-2 protein family might lie in the regulation of mitochondrial fission/fusion and that this function is evolutionarily conserved from CED-9 to the mammalian Bcl-2 members.

4.3 Results

4.3.1 *C. elegans* cell death proteins: functional characterization in HeLa cells

Proteins of the *C. elegans* death machinery were investigated in HeLa cells. To see if these constructs were expressed and functional in this model, we transfected HeLa cells with pcDNA3-CED-3 wild type or pcDNA3-CED-3C358A the CED-3 active site mutant. For apoptosis analysis we co-transfected the reporter plasmid pAAV-EGFP at a 1:1 to 1:100 ratio. We found that the wild type, but not the mutant form of CED-3 killed HeLa cells (Figure 4.1, A). This effect could be enhanced in our experiments by the expression of CED-4, the activator of CED-3. We chose a sub-lethal amount of CED-3 plasmid to observe its activity in combination with CED-4 plasmid. As figure 4.1, B shows, CED-3 activation, and hence the number of dying cells, increased with increasing amounts of CED-4. In contrast, when CED-9, the cell death inhibitor of the worm was co-transfected, cell death was blocked (Figure 4.1, C). A titrateable effect was apparent with increasing amounts of CED-9 plasmid. These results confirmed the established model for the *C. elegans* cell death pathway, which is under the regulation of CED-3, CED-4 and CED-9 (Yan *et al.*, 2006).

4.3.2 CED-9 failed to block Bax-induced cytochrome *c* release and apoptosis

The pro-apoptotic multi-domain Bcl-2 family member Bax is activated during apoptosis and translocates from the cytosol to the mitochondrial membrane. In its activated state Bax leads to MOMP and the release of cytochrome *c* from the intermembrane space of mitochondria. Over-expression of Bax is thought to cause oligomerization and pore formation by Bax-multimers on the mitochondrial outer membrane, and has been shown to result in cytochrome *c* release and apoptosis (Finucane *et al.*, 1999; Kluck *et al.*, 1999). Therefore, we used a Bax over-expression assay to ask whether CED-9 could inhibit apoptosis or cytochrome *c* release in this context.

HeLa cells were pre-treated with zVADfmk in the case where Bax was transfected to prevent lifting of cells from the culture dish. Cells expressing
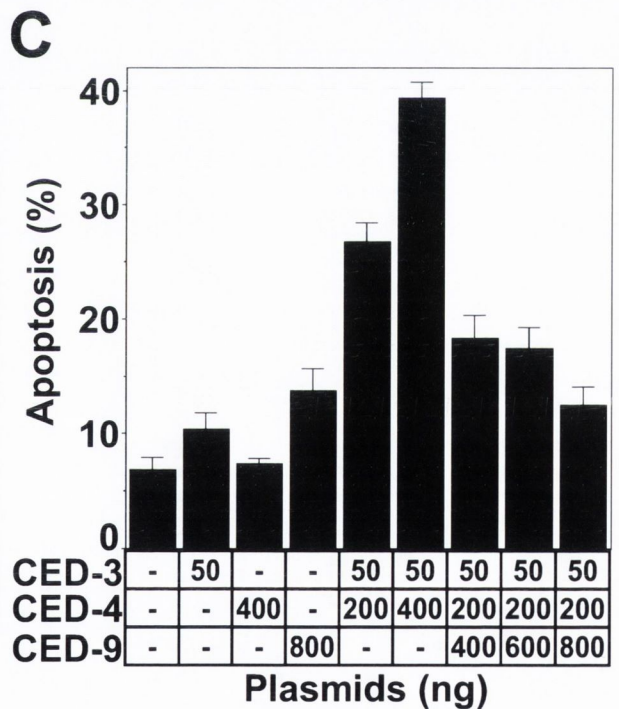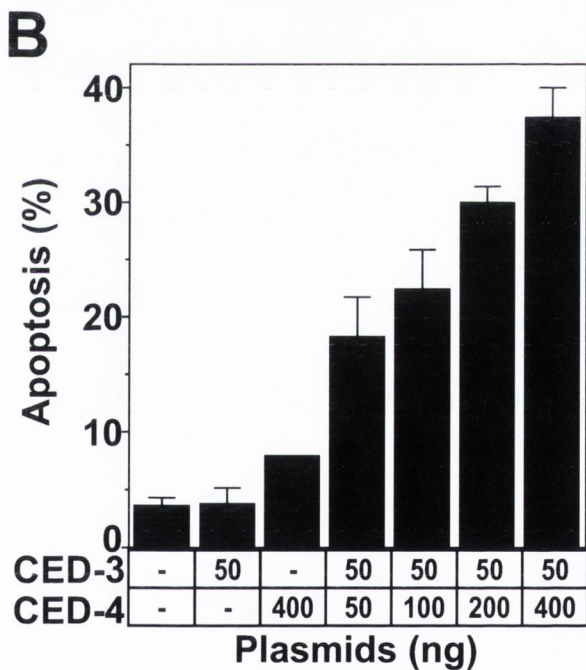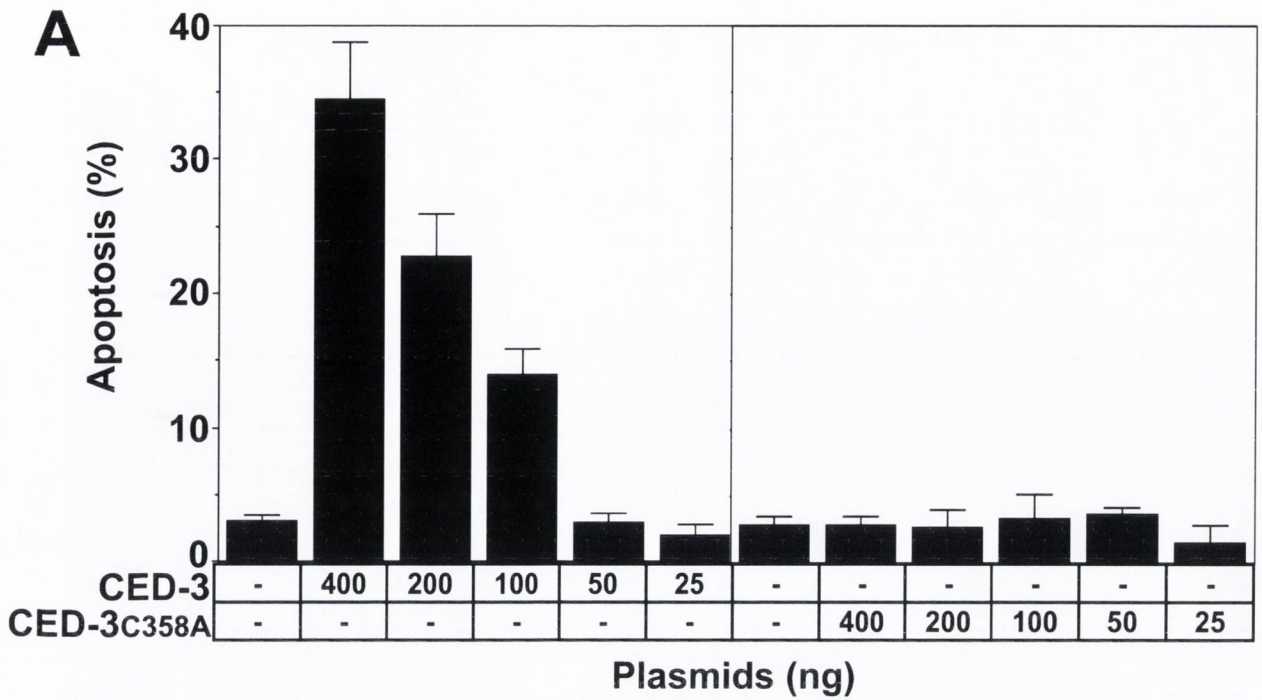
Figure 4.1: *C. elegans* proteins are functional in human cells
CED-3, CED-4 and CED-9 encoding plasmids were either single- or co-transfected into HeLa cells along with a reporter plasmid encoding GFP. Assessment of apoptosis was observed after 24 hours expression. A) CED-3 wild type, but not the catalytic inactive mutant CED3C358A lead to apoptosis. B) CED-4 co-transfection along with CED-3 enhanced the apoptotic activity of the caspase CED-3. C) Triple expression of CED-3, CED-4 and CED-9 resulted in the inhibition of the caspase apoptotic function; CED-9 blocked cell death. Plasmid amounts are indicated in the tables under the graphs. Results are representative of a triplicate of the same experiment.
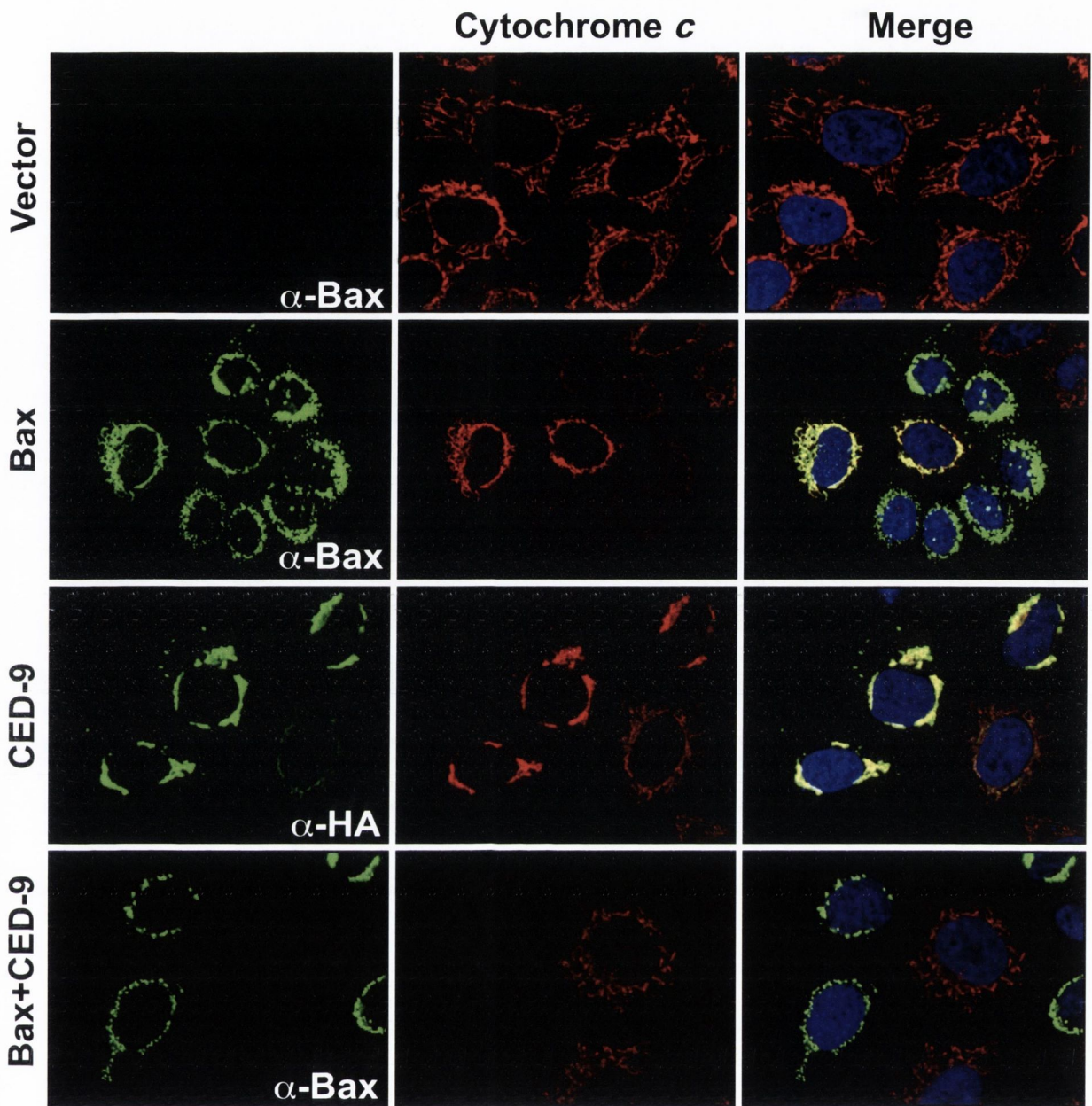
Figure 4.2: Bax induced cytochrome *c* release is not inhibited by CED-9

HeLa cells, growing on coverslips, were transfected with plasmids encoding Bax (200ng) and/or CED-9 (600ng), fixed and immunostained after 24 hours. Expressed proteins were detected by specific antibodies as indicated for Bax and CED-9 (left hand panels). Cytochrome *c* was detected by α-cytochrome *c* (BD) (middle panels). Note, where Bax and CED9 were co-expressed, cytochrome *c* release was not blocked. To prevent cell detachment caused by Bax-induced apoptosis, experiments were carried out in the presence of 50 µM zVADfmk. Representative confocal images were taken on an Olympus laser-scanning microscope FV1000 at 60 X magnification. Pictures depict representative areas of three independent experiments.
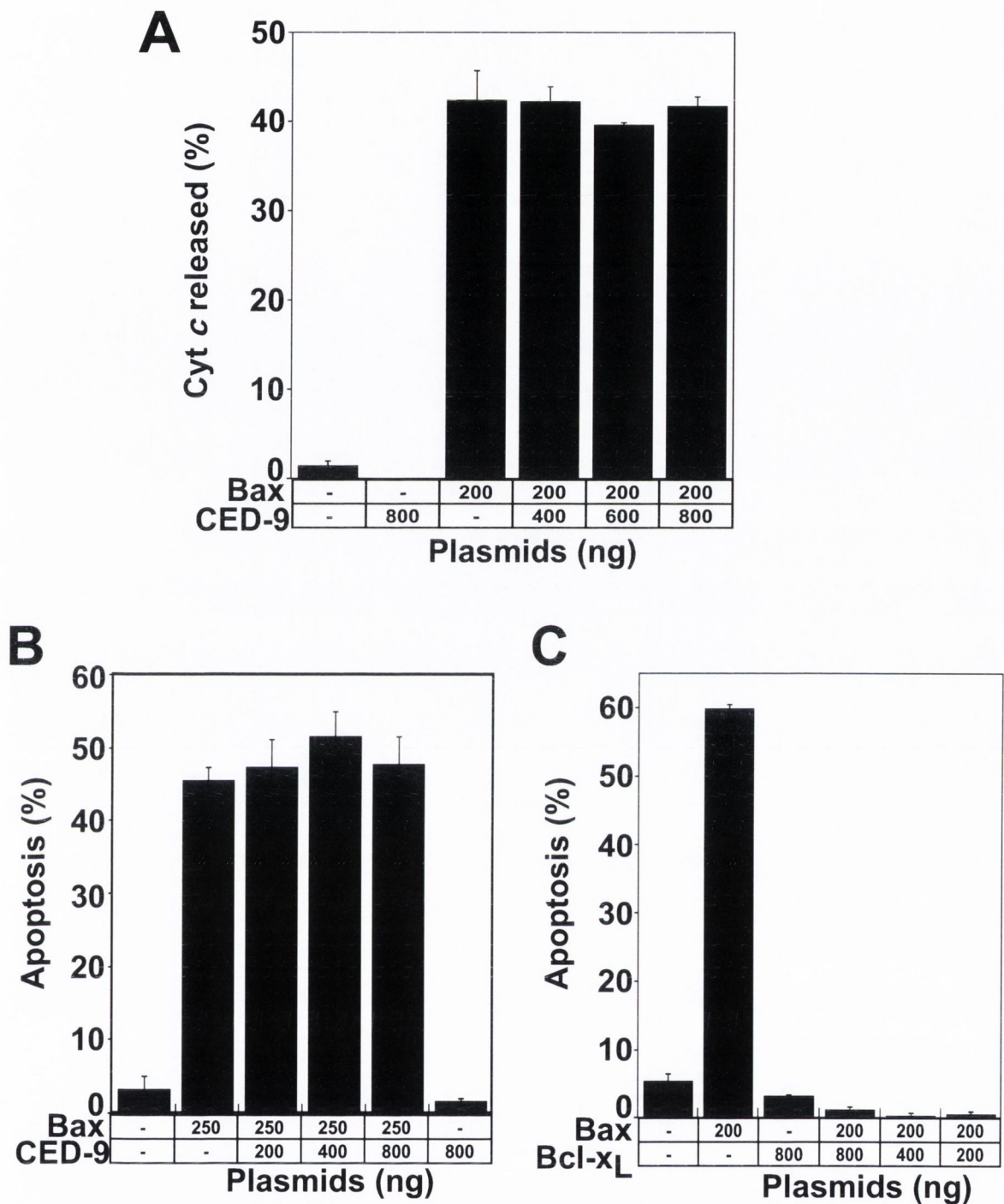
Figure 4.3: Failure of CED-9 to block Bax induced cytochrome *c* release and apoptosis

A) Cells treated as in Figure 4.2, were used to quantify cytochrome *c* release after 24 hours. B) HeLa cells were transfected with various amounts of plasmids encoding Bax and/or CED-9, as indicate in the table below the graph. Apoptosis was measured 24 hours later with GFP co-expression. C) Bcl-xL encoding plasmid was titrated along with 200 ng of Bax as indicated in the graph and apoptosis quantified by GFP co-expression. Note that Bcl-xL very potently inhibited Bax-induced apoptosis, while CED-9 had no effect on Bax. Results are representative for at least three independent experiments.

Bax, CED-9 or a combination of both proteins, were detected by immunostaining with specific antibodies. As shown in figure 4.2 (second row panels), the majority of cells over-expressing Bax protein had released cytochrome *c* at the given time-point, which was detected by co-immunostaining of Bax and cytochrome *c* with specific antibodies. When we looked at CED-9 expressing cells we could still see healthy cells that had cytochrome *c* retained in their mitochondria (Figure 4.2, third row panels). Surprisingly, mitochondria that were represented here by cytochrome *c* immunostaining, displayed a dramatically different phenotype compared to the cells expressing empty vector (Figure 4.2, top row panels). This phenomenon was already observed in chapter 3 (Figure 3.18). Bax and CED-9 co-expressing cells were negative for cytochrome *c* similar to the Bax alone-condition (Figure 4.2, bottom row panels). In this experiment we had stained for Bax in combination with cytochrome *c*, and since we transfected the cells with a 1:4 ratio of Bax to CED-9 we could assume that CED-9 would be present in the same cells as Bax. However, since we saw no retention of cytochrome *c* this meant that CED-9 could not inhibit Bax-induced MOMP.

To quantitate our observations, we examined cells that were either Bax, or CED-9 positive by immunostaining and enumerated cells that had cytochrome *c* released. While in all CED-9 positive cells cytochrome *c* was retained, Bax positive cells were negative for cytochrome *c* in about 40% of cases. Almost the same result was obtained when Bax and CED-9 were co-expressed in HeLa cells (Figure 4.3, A). We also looked at the percentage of cells that are induced to undergo apoptosis in the presence of Bax by co-transfection with a GFP-reporter plasmid. Bax alone, or in combination with CED-9 confirmed the observations already seen for the cytochrome *c* release assay. We also employed Bcl-xL, a human homolog of CED-9 and very potent inhibitor of cell death. Bcl-xL completely opposed Bax-induced apoptosis as expected (Figure 4.3, B and C). Thus, CED-9 cannot inhibit either Bax-initiated cytochrome *c* release or apoptosis.

To further test the ability of CED-9 to block apoptosis in HeLa cells, we chose to use alternative means of initiating apoptosis. Cells were treated with chemotherapeutic drugs commonly used to induce cell death. Figure 4.4
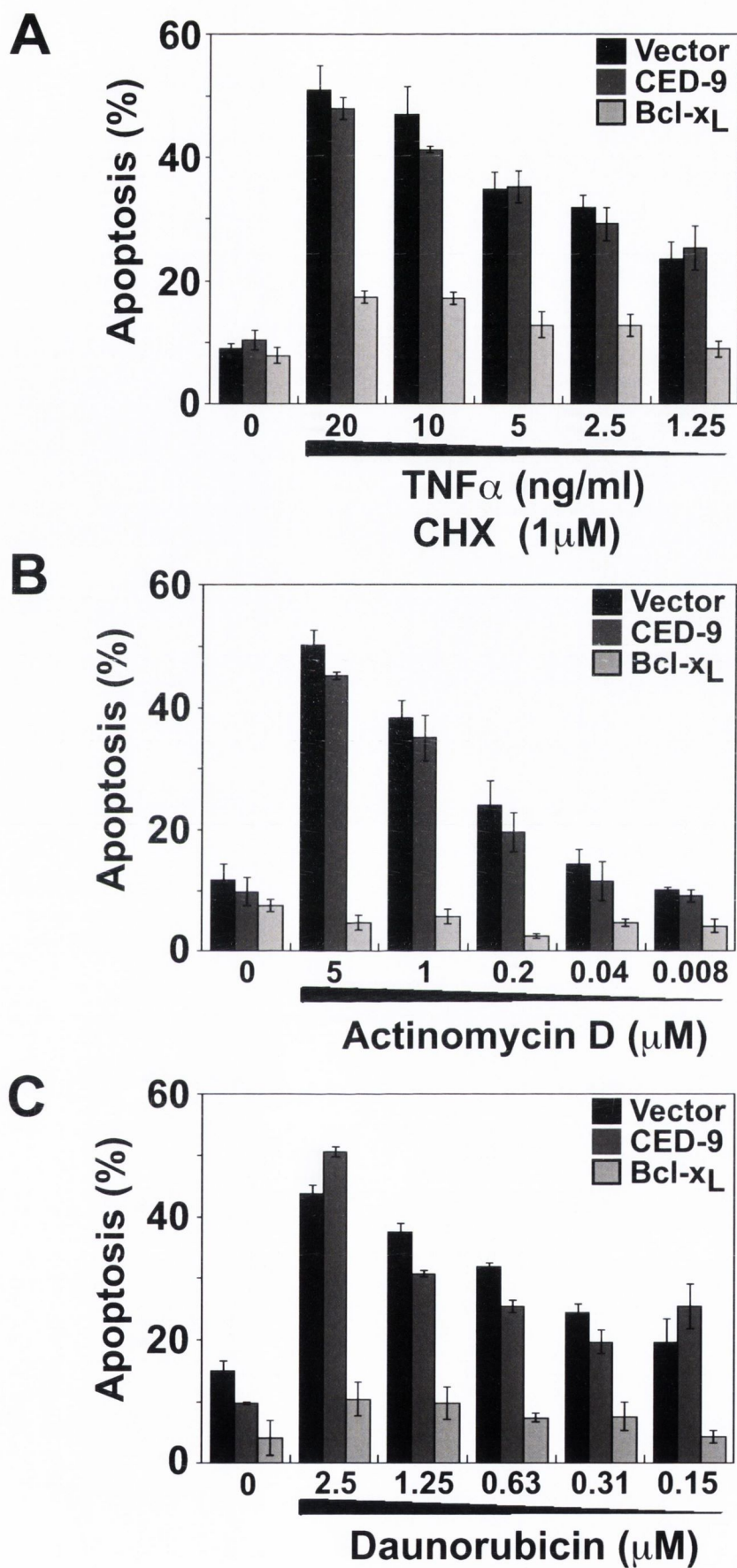
Figure 4.4: CED-9 does not block drug induced apoptosis
HeLa cells were transfected with 600 ng of either empty vector, CED-9 or Bcl-xL en-
coding plasmid for 24 hours. Following expression, cells were treated with a titration
of TNF plus CHX as indicated (A), actinomycin D (B) or daunorubicin (C). A further
6-10 hours later, apoptosis was quantitated by GFP, which was included in all experi-
ments. Results are representative for at least three independent experiments.

illustrates that CED-9 did not exhibit any inhibitory function against the applied drugs, even when they were added at very low concentrations. In contrast, Bcl-xL strongly inhibited apoptosis induced by TNF/CHX (Figure 4.4, A), Actinomycin D (Figure 4.4, B) or Daunorubicin (Figure 4.4, C).

Taken together, these experiments showed that the *C. elegans* cell death inhibitory protein CED-9 cannot substitute for Bcl-2 or Bcl-xL in human cells. It further indicates that CED-9 most probably acts in a functionally different way in the nematode and that this is not transferable into human cells.

4.3.3 Remodeling of mitochondria by CED-9

Previously our attention was attracted by the mitochondrial phenotype seen when we observed HeLa cells expressing CED-9 (see figures 3.16 and 3.17). Because CED-9 contains a transmembrane domain, and has been reported to localize to mitochondria, we speculated that the structures were mitochondria. Additionally, when we immunostained for cytochrome *c*, which is confined to the mitochondrial inter-membrane space, in cells expressing CED-9 we again detected unusual mitochondrial shapes (Figure 4.2). Thus, we decided to investigate the function of CED-9 in remodeling mitochondria. MCF-7 cells, which were transfected with plasmid encoding either Bax or CED-9, were incubated with MitoTracker dye (50 nM) at 37°C for 30 minutes. MitoTracker is a mitochondrion selective stain that can be taken up by viable cells. It is a cationic dye that is intrinsically fluorescent and has an alkylating chloromethyl moiety attached. MitoTracker can passively diffuse across the plasma membranes, but to enter mitochondria it has to be taken up actively by viable organelles. This is achieved by their membrane potential. Once the dye accumulates in mitochondria the chloromethyl group can react with accessible nucleophiles to form fixable conjugates.

In our experiments, CED-9 expressing cells displayed complete overlap of the specific protein staining with this mitochondrial dye (Figure 4.5, A, bottom panels). This showed that CED-9 is indeed localized to mitochondria. In addition, MitoTracker staining was unperturbed by CED-9 over-expression (Figure 4.5, B). Contrary to this, when Bax was expressed in cells, staining of MitoTracker was abolished despite the presence of zVADfmk, which blocks
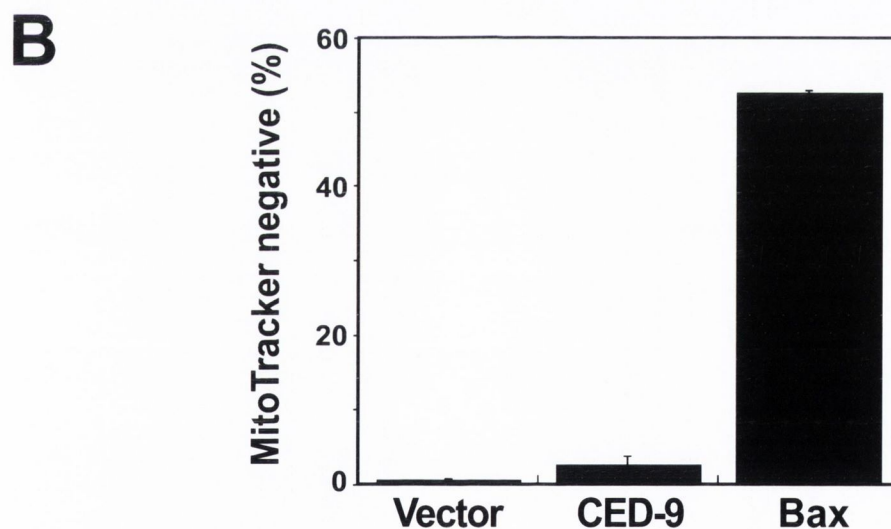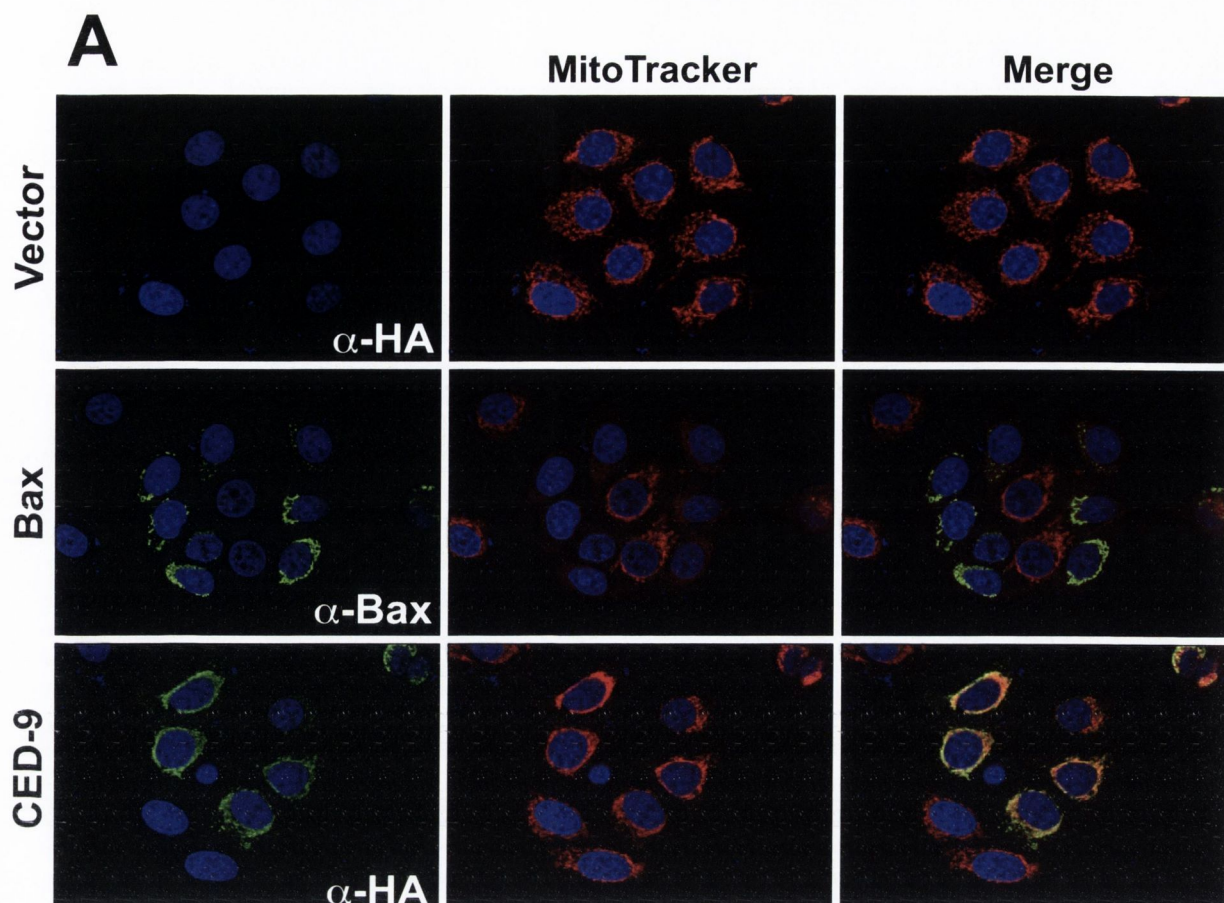
Figure 4.5: CED-9 localizes to mitochondria and changes their phenotype
A) MCF-7 cells, which were transfected with empty vector, 200 ng Bax or 600 ng CED-9 encoding plasmid, were subsequently stained with 50 nM MitoTrackerCMXRos dye. After 24 hours expression, cells were fixed and stained with α-Bax or α-HA for CED-9 detection. Note that CED-9 staining co-localizes to the mitochondrial network. B) Cells treated as in A) were quantitated for the percent of cells that had MitoTracker dye released. Note that CED-9, but not Bax positive cells had retained MitoTracker dye. To prevent cell detachment caused by Bax-induced apoptosis, experiments were carried out in the presence of 50 μM zVADfmk. Representative confocal images were taken on an Olympus laser-scanning microscope FV1000 at 60 X magnification. Pictures depict representative areas of three independent experiments.
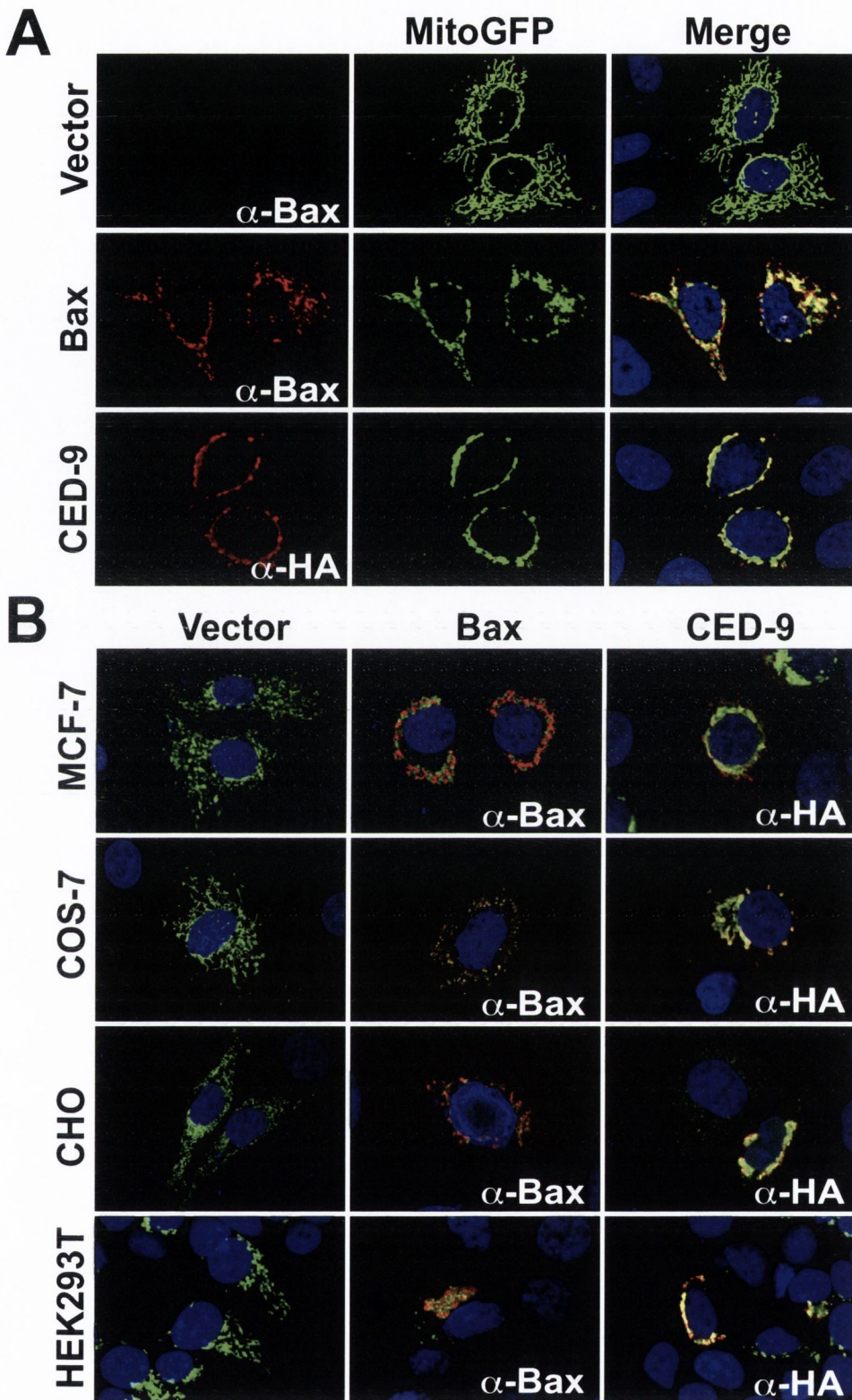
Figure 4.6: Mitochondrial changes confirmed by MitoGFP
A) The reporter MitoGFP (200 ng) was transfected into HeLa cells along with empty vector, 200 ng Bax or 600 ng CED-9 encoding plasmid. 24 hours later, cells were stained with α-Bax or α-HA. B) Different cell types, as designated on the left, were co-transfected with MitoGFP along with Bax or CED-9 as in A). Note that CED-9 co-localizes to the MitoGFP, depicting the mitochondrial network. Both CED-9 and Bax induced changes to the mitochondria. Bax expressing cells included 50 μM zVADfmk. Representative confocal images were taken on an Olympus laser-scanning microscope FV1000 at 60 X magnification. Pictures depict representative areas of three independent experiments.

apoptosis. This indicates that the affected cells lost membrane potential due to Bax expression before treatment with MitoTracker, and therefore could not retain the staining.

To further evaluate the mitochondrial localization of the investigated proteins, we used a mitochondrial marker plasmid (pEFMitoGFP, labeled in the figures as MitoGFP) that comprises a mitochondrial matrix targeting protein (Cytochrome *c* oxidase subunit VIII) fused to GFP. HeLa cells expressing MitoGFP alone displayed a well-distributed filamentous mitochondrial network throughout the cells as shown in figure 4.6, A, top right panel. When we over-expressed CED-9 along with MitoGFP, and detected CED-9 positive cells by immunostaining, we again observed a dramatic rearrangement of the mitochondrial network. The organelles were now all collapsed around the nucleus in a big cluster, seemingly as one mitochondrion (Figure 4.6, A, bottom panels). Compared to the literature, the observed CED-9 mitochondrial changes resembled a fusion-induced phenotype, which suggested that CED-9 is capable of promoting fusion of mitochondria and as a consequence they form an enormous cluster. Bax expressing cells (Figure 4.6, A, middle panels) also displayed altered mitochondrial networks with a fragmented appearance of seemingly single mitochondria that were spread throughout the cells.

Because this could be an effect specific to the cell type in use, we tested additional mammalian cell types with this approach. In figure 4.6, B we show that CED-9 and Bax also rearranged mitochondria in human MCF-7 and HEK293T cells as well as in monkey cells (COS-7) and hamster cells (CHO).

4.3.4 FRAP analysis of the CED-9 fusion activity

Because the fusion effects of CED-9 thus far were only examined by visual analysis and depended on the subjective opinion of the observer, we decided to use FRAP (Fluorescence recovery after photobleaching) as a method that is widely used to examine the fusion activity of mitochondria. To do this, mitochondria are labeled with MitoTracker dye and cells are followed in real time for a defined period. On a confocal microscope a region of interest (ROI) is chosen, which is bleached by a short but intense laser pulse and observed over time. Refilling or recovery of the bleached area by MitoTracker dye
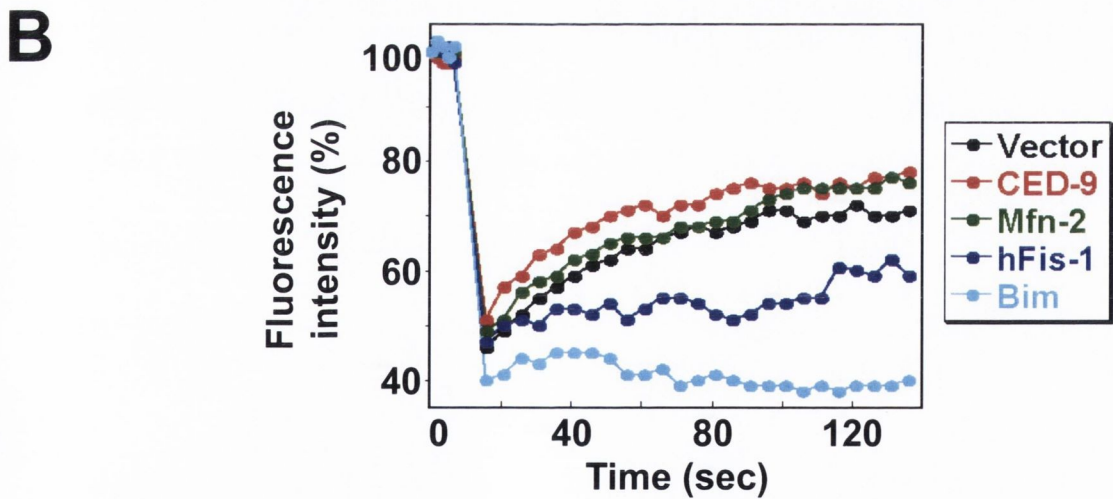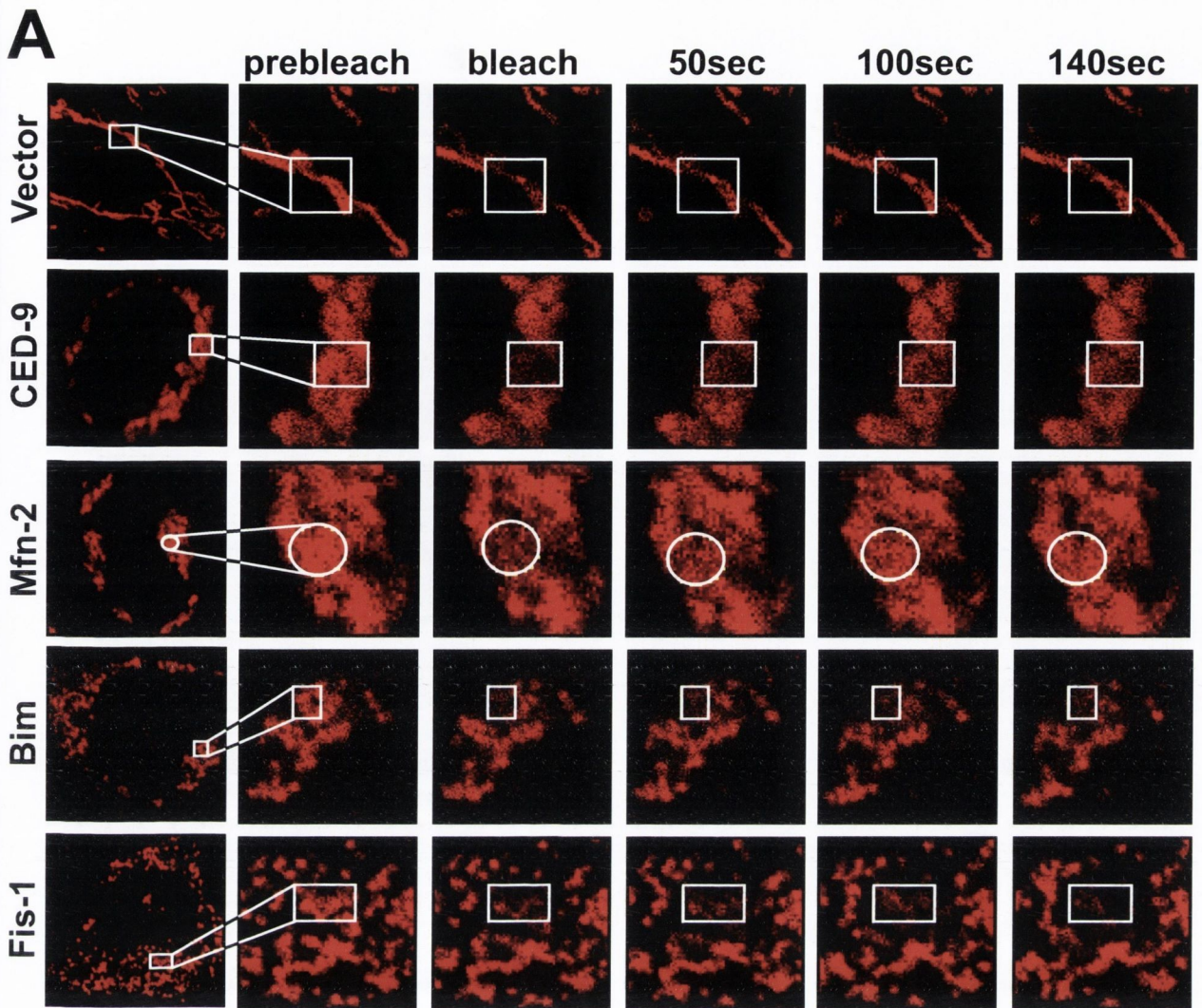
Figure 4.7: FRAP analysis of the mitochondrial fusion effects of CED-9
A) HeLa cells transfected with 600 ng of the indicated plasmids were stained with Mi-toTracker dye after 24 hours expression. The marker MitoGFP (200 ng) was utilized to identify transfected cells and those were used to perform FRAP as described in 2.2.12. The white boxes indicate the observed region of interest (ROI). B) Representative graph of cells treated as above. Bim and Fis-1 expressing cells included 50 µM zVADfmk. Experiments were carried out and representative confocal images chosen from an Olympus laser-scanning microscope FV1000 at 60 X magnification. Results are representative of at least three independent experiments.

indicates continuity and fusion activity of the organelles. Fragmentation or discontinuity is indicated if the bleached area remains clear of MitoTracker (Collins and Bootman, 2003).

We wanted to examine CED-9 expressing cells by the FRAP method to see whether fusion of mitochondria was induced by CED-9. Thus, we transfected HeLa cells with CED-9 encoding plasmid and stained the cells with MitoTracker dye after 24 hours expression. To find CED-9 expressing cells, we used the marker MitoGFP in a 3:1 ratio along with our plasmid of interest. Thereby, cells displaying the typical mitochondrial phenotype after transfection with CED-9 plasmid could be detected. When we performed FRAP on CED-9 expressing cells, we repeatedly observed that refilling of the bleached area was rapid and to a high extent (Figure 4.7, A, second row panels). Comparing CED-9 expressing cells with cells expressing Mfn-2, a protein that is part of the fusion machinery and known to promote fusion, resulted in similar FRAP profiles. This enabled us to confirm that CED-9 was indeed promoting mitochondrial fusion (Figure 4.7, A, third row panels).

We also analyzed cells that expressed proteins known to induce mitochondrial fragmentation. Fis-1 is a component of the mitochondrial fission machinery and its over-expression consistently resulted in small sphere-like mitochondria (data not shown). There was no recovery of mitochondrial staining in this scenario, showing that those organelles were totally separate from one another and could not connect to fuse over the observed time-period (Figure 4.7, A, bottom row panels). The same observations were obtained when we used the pro-apoptotic BH3-only protein Bim, which presumably induces fragmentation through Bax activation (Figure 4.7, A, fourth row panels).

4.3.5 Does CED-9 inhibit mitochondrial fragmentation?

Because we could not find an inhibitory effect of CED-9 as a substitute for its human homologues, we wondered what effect CED-9-induced fusion might have on apoptosis. During apoptosis the mitochondrial network is destroyed and becomes fragmented into small parts. To explore whether CED-9 could interfere with this effect, we transfected HeLa cells with CED-9 encoding plasmid and then induced apoptosis with chemotherapeutic drugs (Figure 4.8).
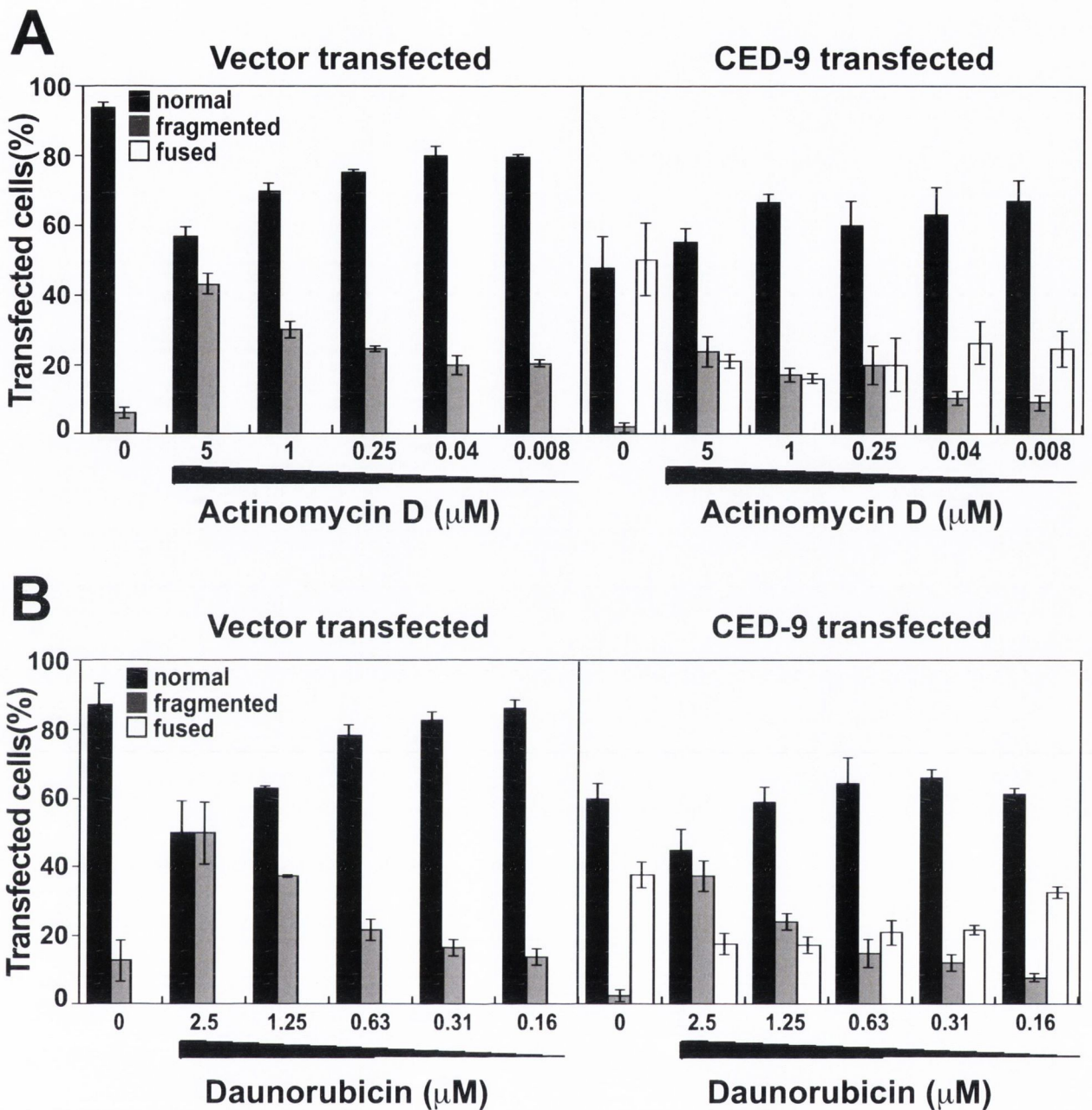
Figure 4.8: CED-9 blocks mitochondrial fragmentation induced by cytotoxic drugs

A) HeLa cells transfected with 600 ng of either empty vector or CED-9 encoding plasmid and the mitochondrial marker MitoGFP were left for 24 hours. Then the cells were treated with a decreasing concentration of actinomycin D for 10 hours. Cells were fixed and mitochondrial fusion was quantified on a fluorescence microscope. B) Cells were equally setup as in A) but subsequently treated with a titration of daunorubicin as shown. Note that CED-9 expressing cells inhibited fragmentation of mitochondrial networks after treatment with chemotherapeutic chemicals. Drug treated cells included 50 µM zVADfmk to prevent dettachment. Results are representative of at least three independent experiments.

Our transfections included the marker MitoGFP in order to be able to analyze the mitochondrial phenotype after apoptotic stimulation. We looked at the whole population of transfected cells and found that in un-treated cells, over 40% of CED-9 expressing cells displayed fused mitochondria, compared to the empty vector condition, which displayed the normal tubular mitochondrial network. After addition of actinomycin D (Figure 4.8, A) or Daunorubicin (Figure 4.8, B), the majority of vector transfected cells displayed fragmented mitochondrial networks. This effect diminished in response to decreasing amounts of the apoptosis-inducing agent. In contrast to this, when cells expressed CED-9 and were subsequently treated to induce apoptosis, the fusion phenotype of mitochondria was not completely abolished. Over the range of drug-concentrations used, the number of cells that displayed fused and clustered mitochondria almost stayed the same or even increased at low concentrations of Actinomycin D or Daunorubicin (Figure 4.8, A and B). Therefore, we concluded that CED-9 could antagonize mitochondrial fragmentation provoked during the process of cell death.

4.3.6 The CED-9 transmembrane domain is necessary for fusion-activity, but not for inhibition of CED-4/CED-3 induced cell death

To further analyze the ability of CED-9 to promote mitochondrial fusion we used our available CED-9 mutant constructs (see Figure 3.15). The gain of function (CED-9(G169E)) and loss of function (CED-9(Y149N)) mutations of CED-9 have an impact in the context of programmed cell death in the worm. We asked if those mutations had an impact on the function of CED-9 to promote fusion. We transfected the plasmids into HeLa cells along with MitoGFP and immunostained after 24 hours with α-HA to detect our target proteins. We found that irrespective of the CED-9 mutation, mitochondria displayed a fused phenotype as seen by MitoGFP (Figure 4.9, second to fourth row panels) in contrast to empty vector expressing cells (top row). This was quantified over a range of decreasing plasmid concentrations and the results confirmed. Figure 4.10, A shows that independent of the CED-9 mutations the fusion efficiency is unchanged. Although a weaker effect of the loss of function mutant was
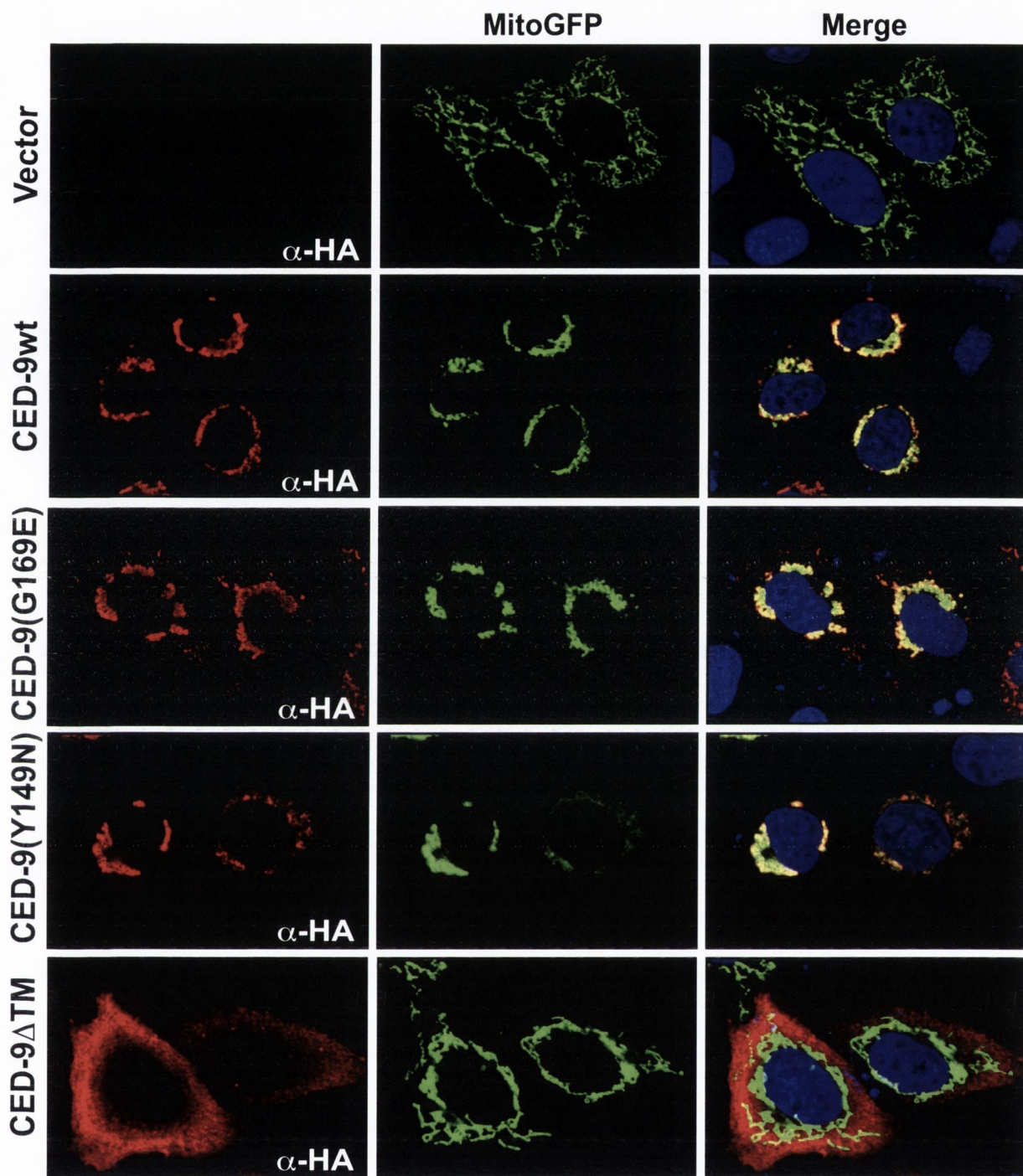
Figure 4.9: Mitochondrial phenotypes of CED-9 wild type and mutants
HeLa cells were transfected with 200 ng MitoGFP together with 600 ng plasmids encoding the indicated proteins. Following 24 hours expression, cells were immunostained with the displayed antibodies to reveal protein expression. Pictures depict representative areas of at least three independent experiments. Representative confocal images were taken on an Olympus laser-scanning microscope FV1000 at 60 X magnification.
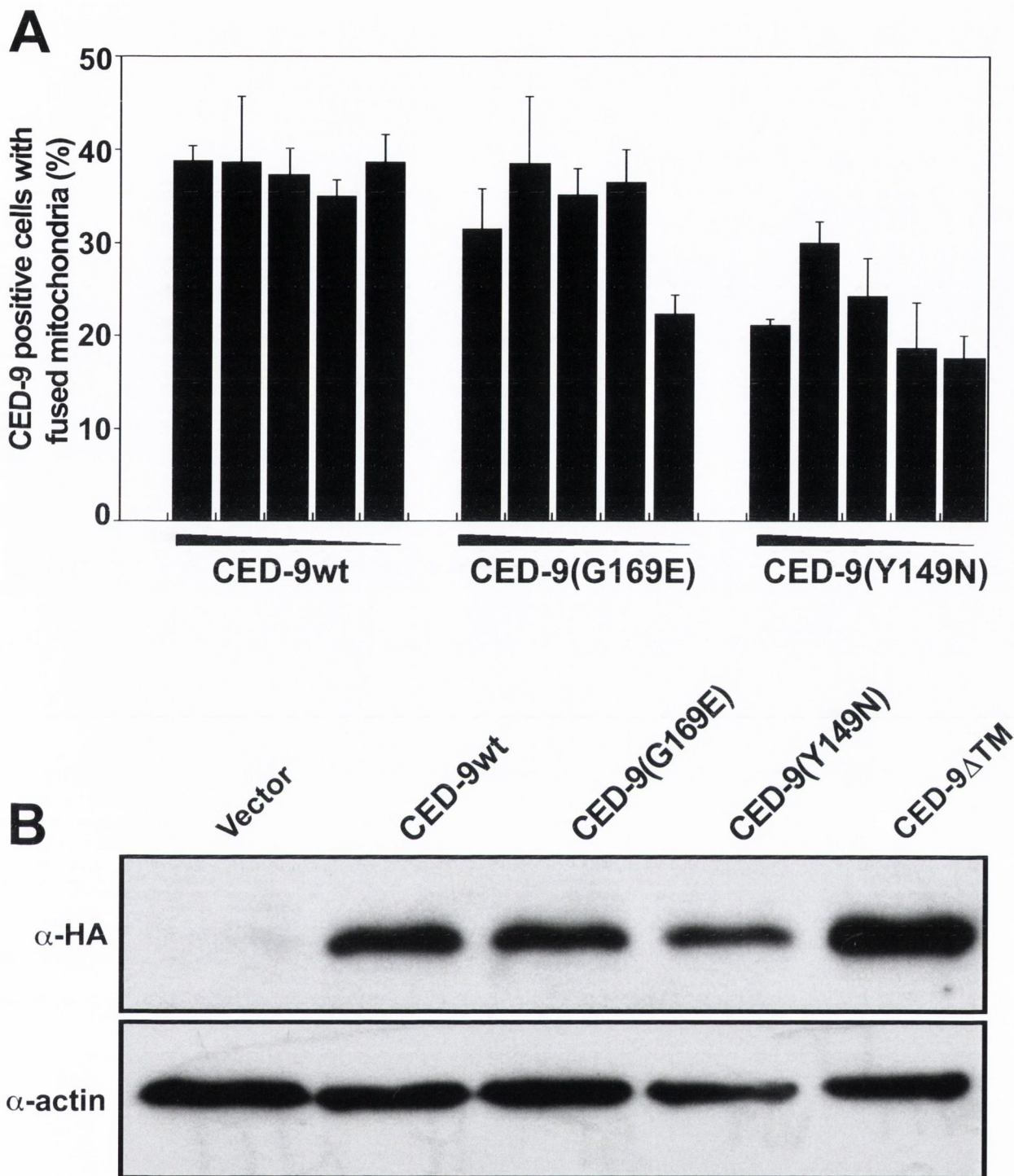
Figure 4.10: Wild type and mutant CED-9 induce mitochondrial fusion

A) Representative graph of experiment shown in 4.9. HeLa cells expressing decreasing plasmid amounts of CED-9 wild type, CED-9G169E or CED-9Y149N along with MitoGFP, were quantified for mitochondrial fusion events. Cells were immunostained and counted for CED-9 expressing cells with fused mitochondria. Result is representative for at least three independent experiments.

B) Western blot analysis for CED-9 clones. Plasmids (5 μg) encoding the above shown proteins were transfected into HEK293T cells and harvested after 24 hours. Western blot analysis of over-expressed proteins was carried out with α-HA (upper panel) antibody and α-actin as loading control (lower panel). Blots are representative for at least three independent experiments.

CED-3	-	50	-	-	50	50	50	50	50	-	-	-
CED-4	-	-	400	-	400	400	400	400	400	-	-	-
CED-9wt	-	-	-	400	-	400	-	-	-	-	-	-
ED-9(G169E)	-	-	-	-	-	-	400	-	-	400	-	-
ED-9(Y149N)	-	-	-	-	-	-	-	400	-	-	400	-
CED-9 ΔTM	-	-	-	-	-	-	-	-	400	-	-	400

Plasmids (ng)
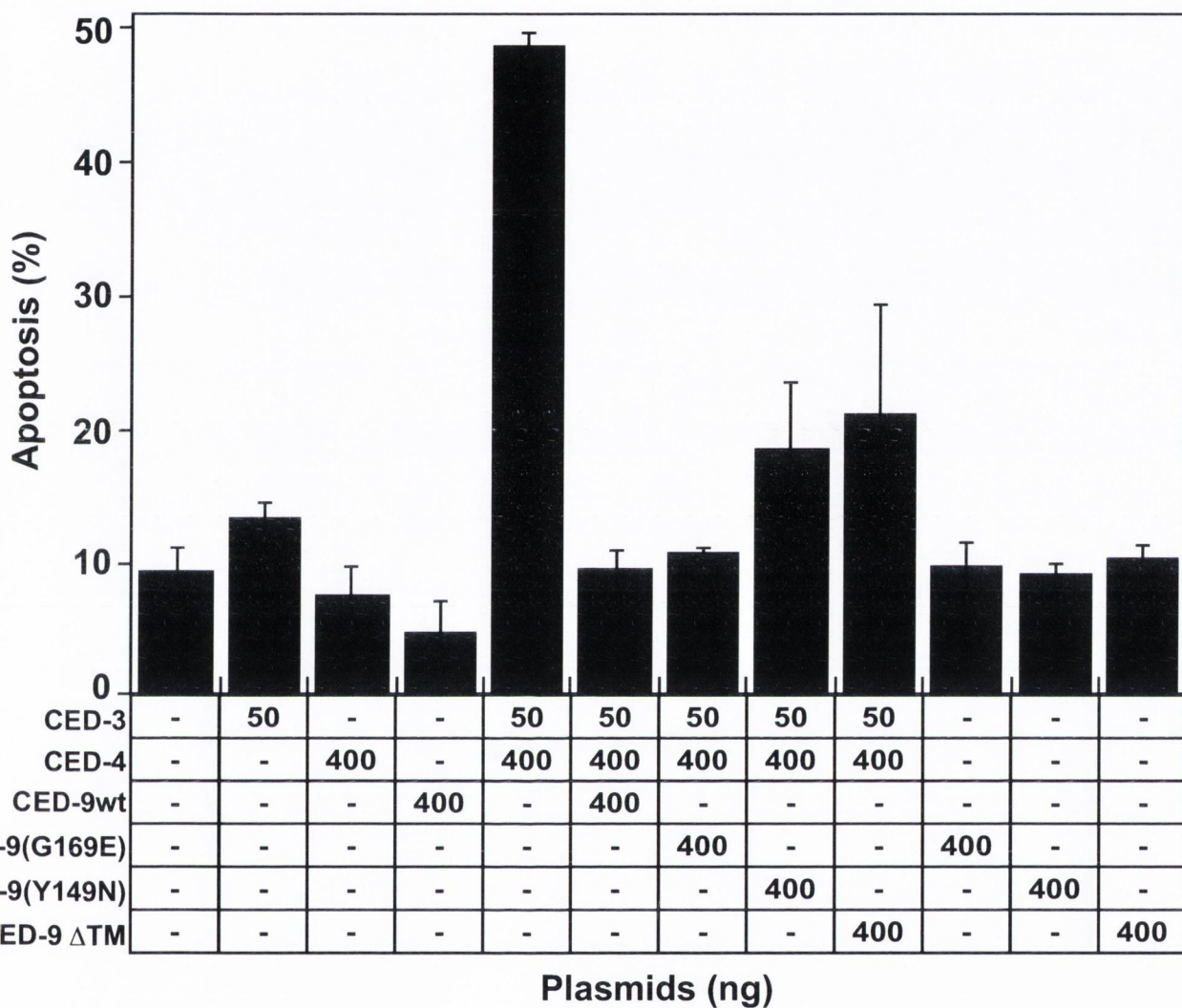
Figure 4.11: Cell death induced by CED-3/CED-4 is blocked by all CED-9 clones independent of their mitochondrial fusion activity

Analysis of cell death was carried out by transfecting CED-3 and CED-4 together with all CED-9 mutants into HeLa cells in various combinations with the amounts shown above. Co-expression of a GFP reporter plasmid assisted the quantification of dying cells. Result is representative for at least three independent experiments.

apparent this may have been due to its suboptimal expression in these cells (Figure 4.10, B).

However, when we transfected the CED-9 mutant missing the C-terminal transmembrane domain, we saw that it did not promote mitochondrial fusion. Hence, the transmembrane domain appeared to be essential for CED-9 in order to induce fusion (Figure 4.9, bottom row panels). In addition we could say that, this effect was not due to the expression efficiency of the construct as seen by the Western blot experiments in figure 4.10, B, because it was well expressed in cells.

Although we detected differences between the tested constructs concerning the mitochondrial fusion effect, when we examined these mutants in the cell death context they all appeared to function similarly. The point mutations and the truncated form of CED-9 blocked CED-4 induced CED-3 killing in HeLa cells (Figure 4.11). Even if CED-9ΔTM was a weaker inhibitor than the wild type, this mutant could still block apoptosis in this scenario. These two effects might therefore be separable functions of the cell death inhibitor CED-9.

4.3.7 EGL-1 inhibits CED-9 induced mitochondrial fusion

In the worm CED-9 is neutralized by the BH3-only protein EGL-1, which is the only known cell death inducer during embryonic development (Conradt and Horvitz, 1998). If EGL-1 becomes up-regulated it induces programmed cell death by binding to CED-9 thereby disengaging CED-4, which occurs as result of the structural rearrangement of CED-9 through binding of EGL-1 (Yan et al., 2006).

We wanted to investigate whether EGL-1 could also impact on the CED-9 mitochondrial fusion effect. Therefore, we cloned full-length egl-1 coding sequence into a mammalian expression vector and transfected it into human cells. When we expressed pcDNA3-EGL-1 in HeLa cells and looked at the mitochondrial phenotype with MitoGFP, we saw that EGL-1 alone disrupted the mitochondrial network (Figure 4.12, second row). This observation had been described in worm embryos in an earlier study with a heat shock inducible EGL-1, indicating a role of EGL-1 in mitochondrial dynamics (Jagasia et al., 2005). Expressing CED-9 on its own again resulted in fused mitochondria, but when
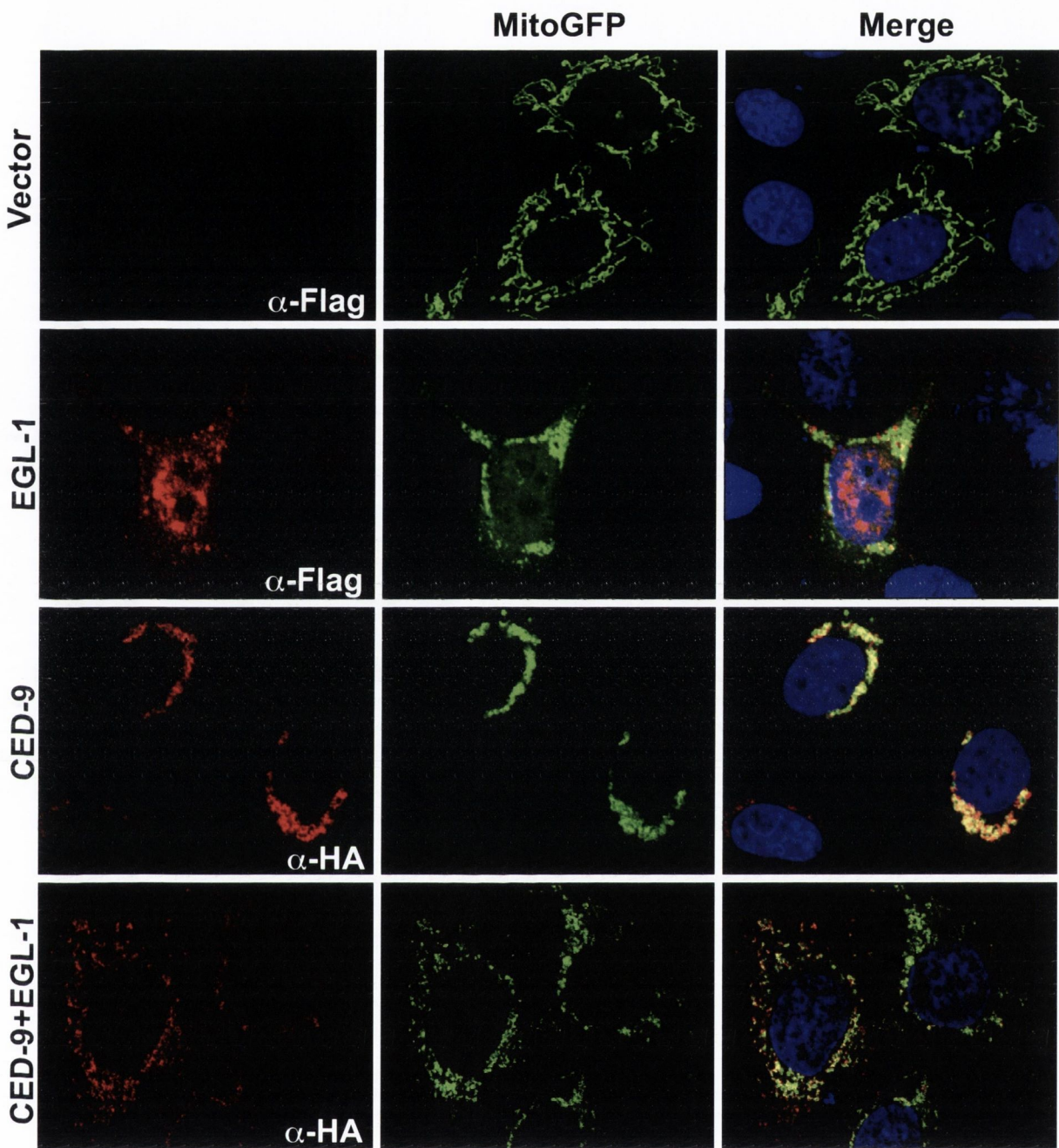
Figure 4.12: EGL-1 induces mitochondrial fragmentation, alone and in the presence of CED-9

HeLa cells, transfected with vector, CED-9 (200 ng), EGL-1 (800 ng) and MitoGFP (200ng), were immunostained after 24 hours expression. The indicated tag-antibodies were used to identify cells expressing the target protein and the mitochondrial phenotype observed. Representative confocal images were taken on an Olympus laser-scanning microscope FV1000 at 60 X magnification. Results are representative for at least three independent experiments.
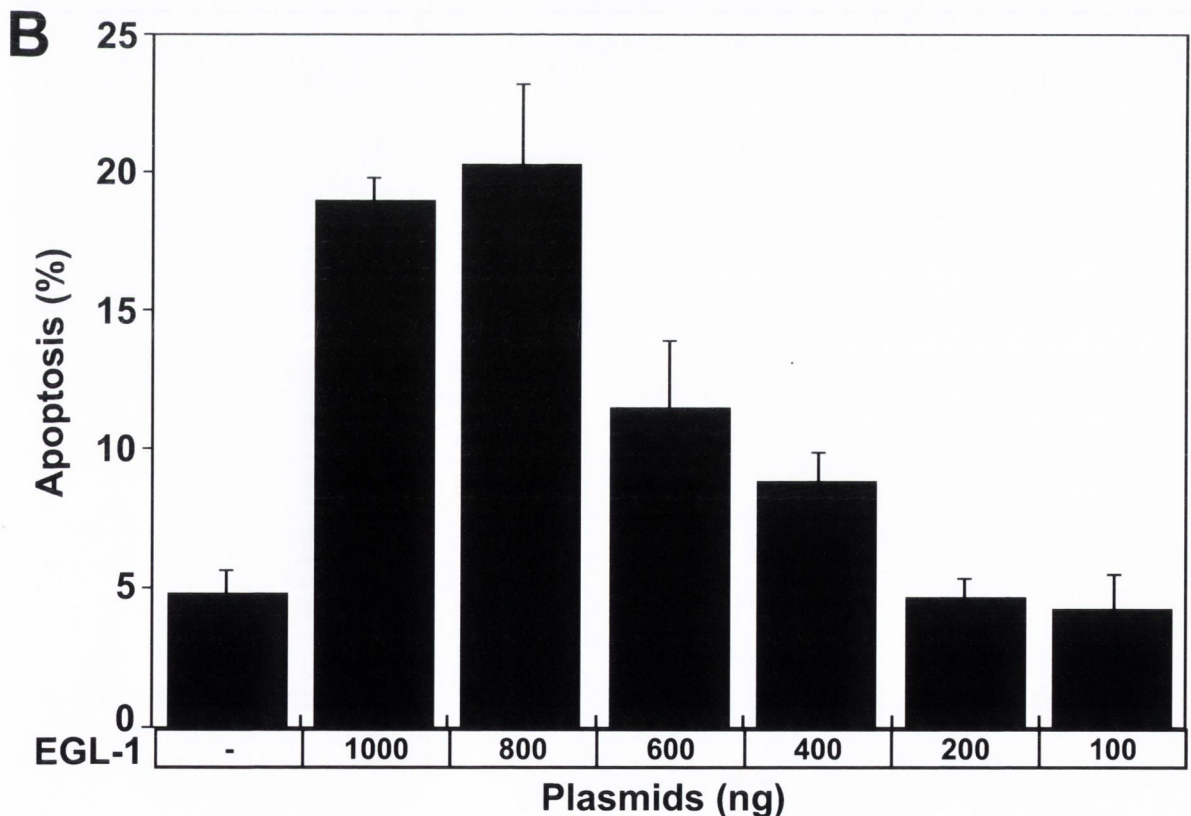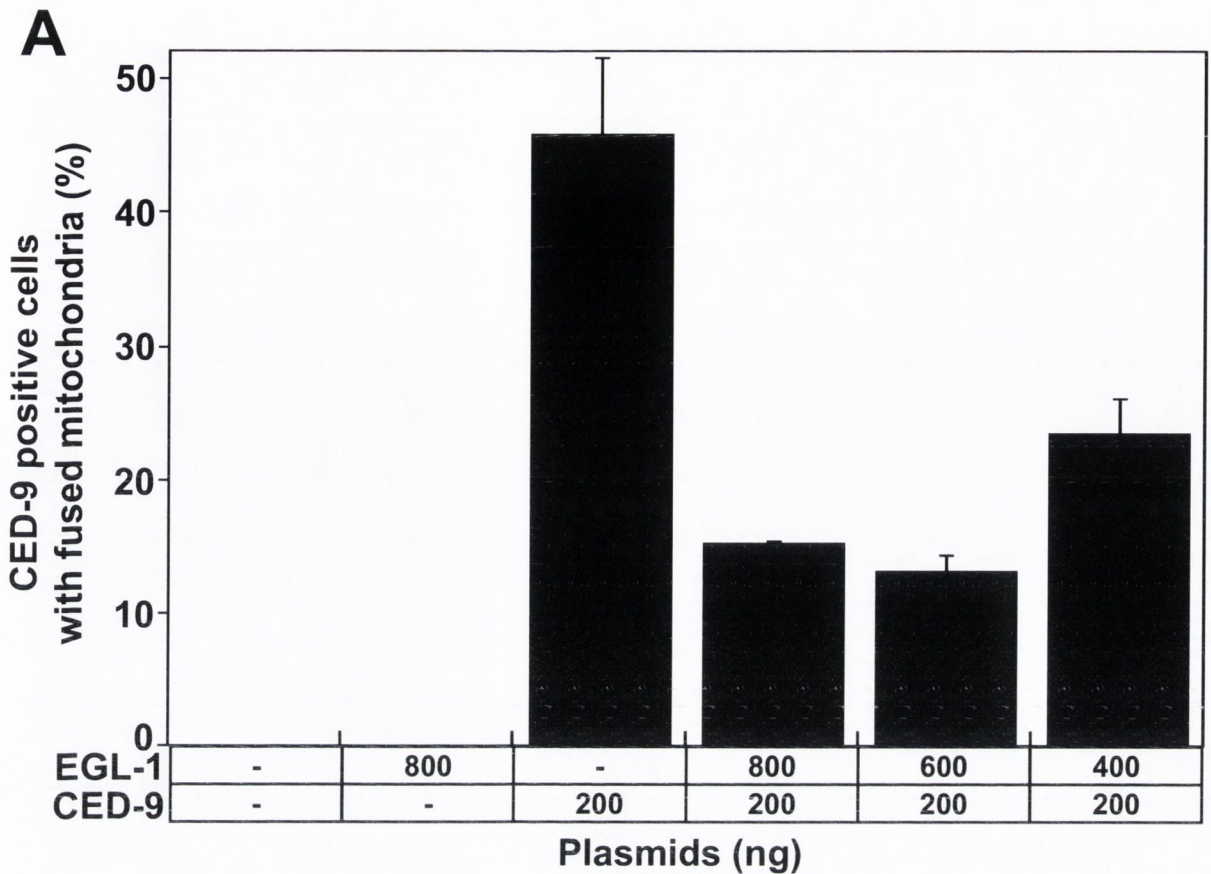
Figure 4.13: EGL-1 induces mitochondrial fragmentation and apoptosis
A) Graph represents quantitation of cells treated as in 4.13. HeLa cells, transfected with the indicated amounts of CED-9 and EGL-1, and MitoGFP (200ng), were immunostained and their mitochondrial phenotype detected. B) EGL-1 induced apoptosis was scored by co-expression of a GFP-reporter along with the shown amounts of EGL-1. Results are representative for at least three independent experiments.
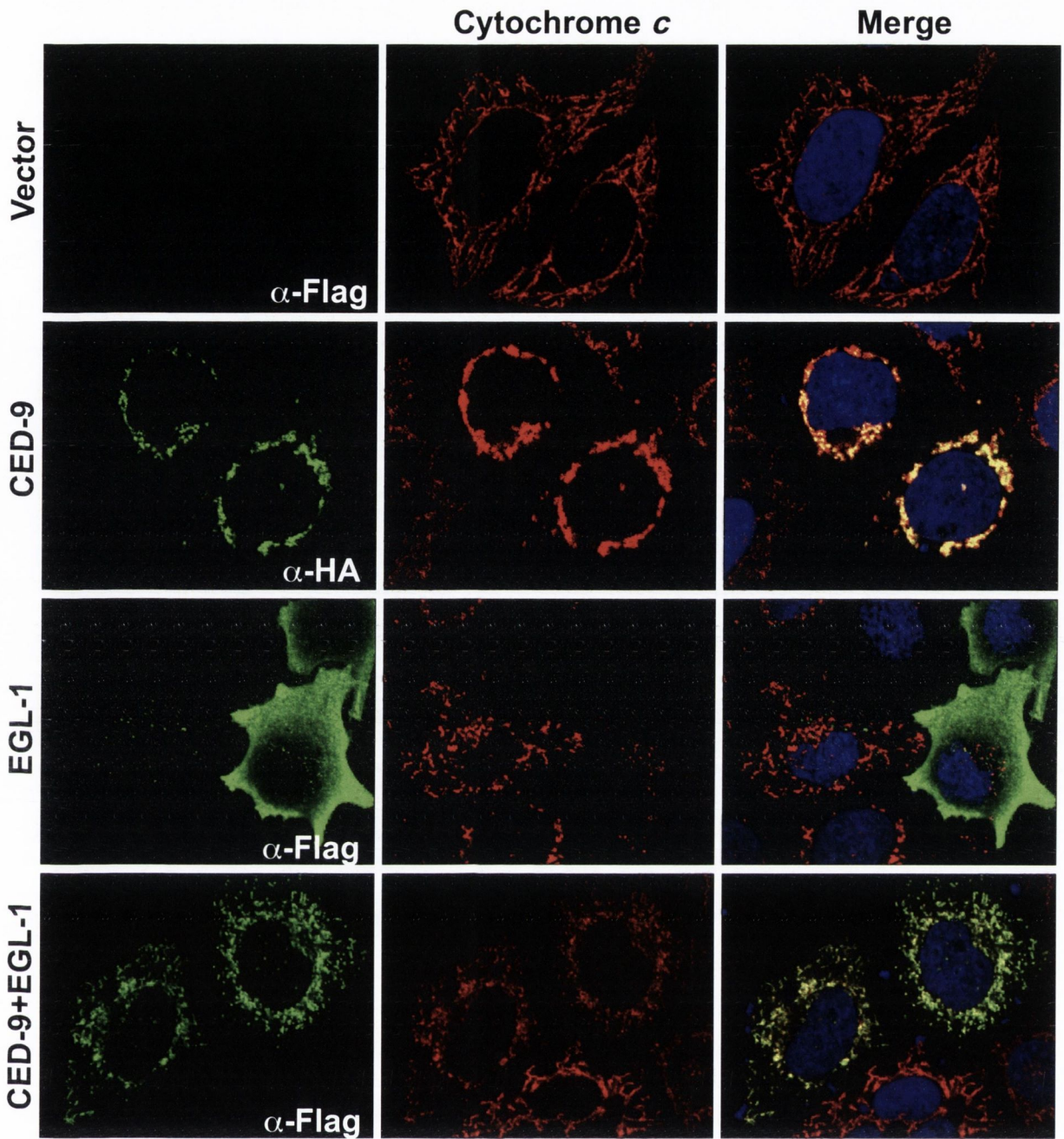
Figure 4.14: Release of cytochrome *c* by EGL-1 is abolished in the presence of CED-9

HeLa cells, transfected with vector, CED-9 (200 ng) and EGL-1 (800 ng), were fixed and immunostained after 24 hours expression. Anti-HA and anti-Flag antibodies revealed target protein expressing cells (left hand panels). Cytochrome *c* was detected by co-immunostaining for endogenous cytochrome c with a specific antibody (α-Cyt *c*, BD) (middle panels). Representative confocal images were taken on an Olympus laser-scanning microscope FV1000 at 60 X magnification. Results depict representative areas for at least three independent experiments.
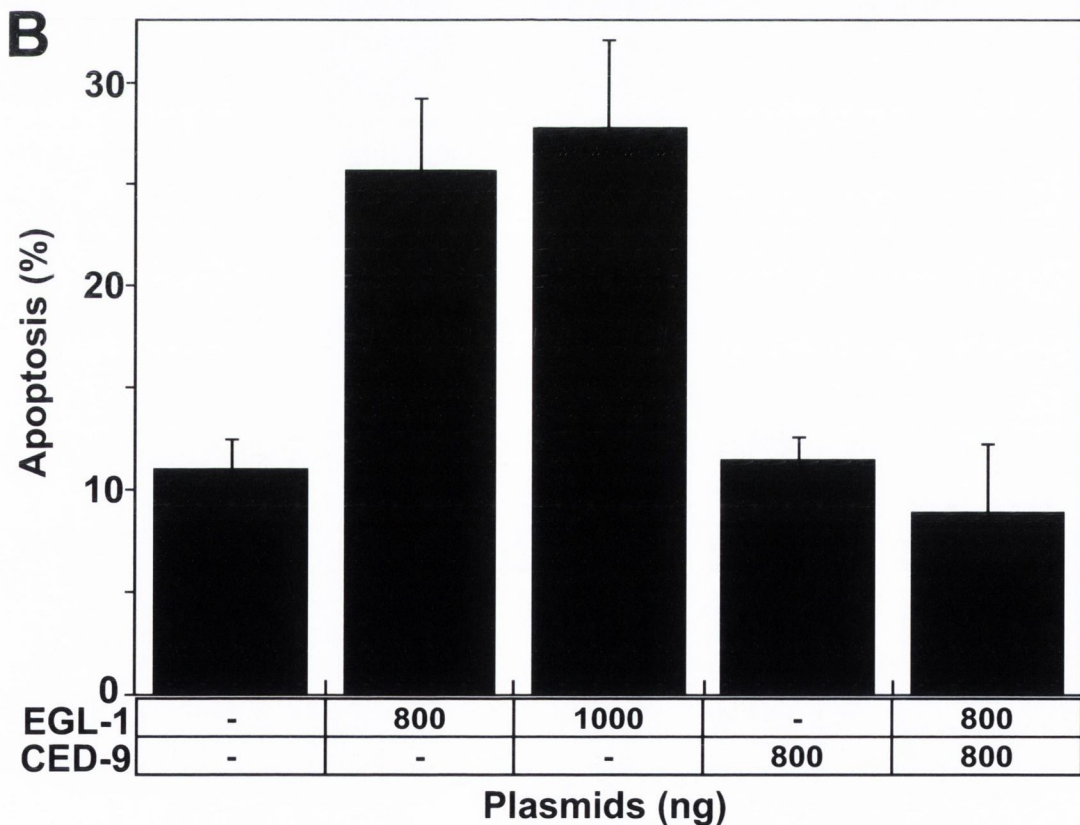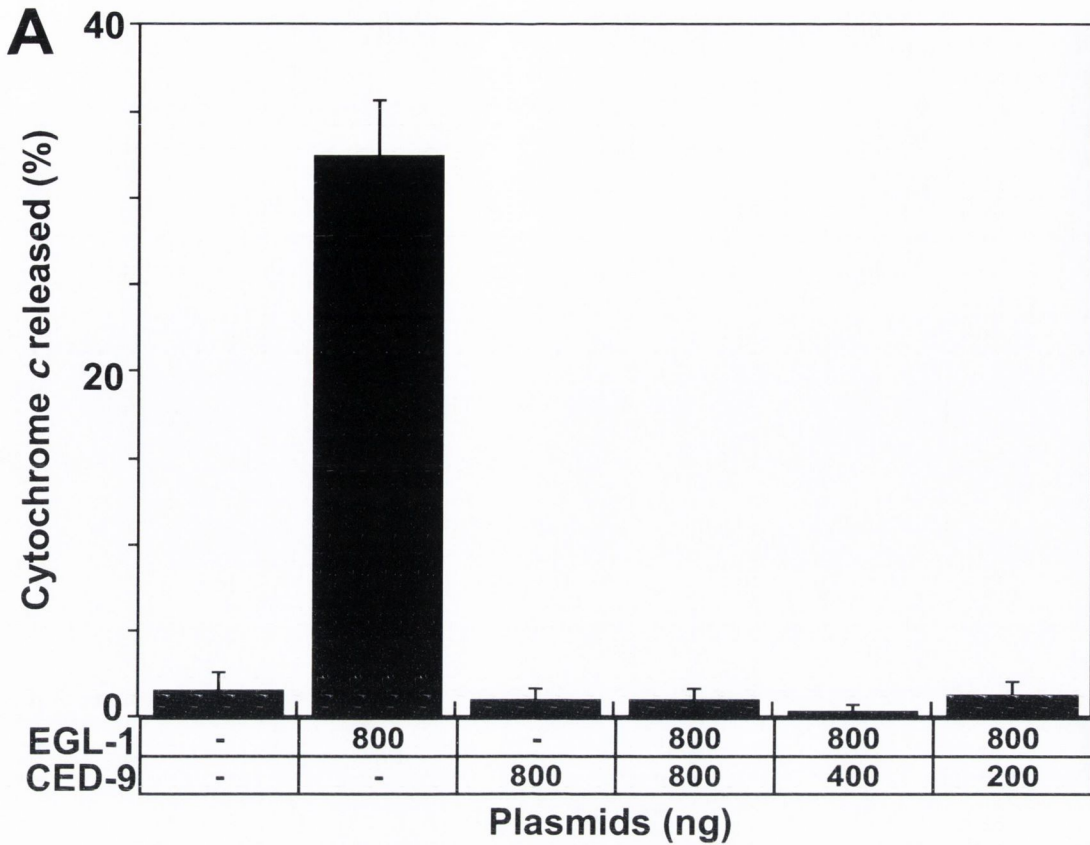
Figure 4.15: Release of cytochrome *c* by EGL-1 is abolished in the presence of CED-9

A) Representative graph of Figure 4.15. CED-9 and EGL-1 expressing HeLa cells were fixed and immunostained and Cytochrome *c* release detected by co-immunostaining for endogenous cytochrome *c*. B) EGL-1 induced apoptosis was inhibited by CED-9, this was scored by co-expression of a GFP-reporter and subsequent assessment of apoptotic cells. Results are representative for at least three independent experiments.

we co-expressed it together with EGL-1, the fused phenotype was completely disrupted. We found mitochondria that were widely distributed throughout the cell body, but in small round shapes, seemingly single organelles (Figure 4.12, third and bottom row). By quantifying CED-9/EGL-1 expressing cells, we saw that the majority of cells displayed a fragmented mitochondrial network induced by the presence of EGL-1 (Figure 4.13, A). In addition EGL-1 was able to induce apoptosis in HeLa cells to some extent, which would indicate that this BH3-only protein acts in a similar way as its human counterparts to provoke cell death in this cell type (Figure 4.13, B).

Mammalian BH3-only proteins can either directly or indirectly regulate the release of the inter-membrane space protein cytochrome *c*, via the Bax/Bak channel (Youle and Strasser, 2008). The results we obtained when we included *C. elegans* EGL-1 in our study prompted us to ask if it acted like mammalian BH3-only proteins. Since EGL-1 expression killed the cells and changed the mitochondrial phenotype dramatically as shown above, the question arose whether it also influenced the release of cytochrome *c*. As figure 4.14 shows, when we stained HeLa cells for endogenous cytochrome *c*, we found that expression of EGL-1 on its own lead to cytochrome *c* release (Figure 4.15, A). This was to a similar extent as its ability to kill cells (Figure 4.13, B). In contrast, the introduction of CED-9 completely inhibited EGL-1-induced cytochrome *c* release and apoptosis, although we repeatedly saw fragmented mitochondria that were spread out through the cell (Figure 4.14 and 4.15). From these results we conclude, that CED-9-induced fusion of the mitochondrial network could be inhibited by EGL-1, which led to a fragmentation phenotype. Despite this, mitochondrial fragmentation did not necessarily result in the release of cytochrome *c* and apoptosis.

4.3.8 Comparison of CED-9 with fusion-inducing proteins

Mitochondria divide under the control of the fission-promoting proteins Drp-1 and Fis-1. Fusion-promoting proteins Mfn-1, Mfn-2 and Opa-1, counteract this function to balance fission and maintain the mitochondrial network. A dominant negative form of Drp-1 was found (Drp-1K38A) that also promotes fusion by inhibiting its division-effect (Chen and Chan, 2005). To further explore whether
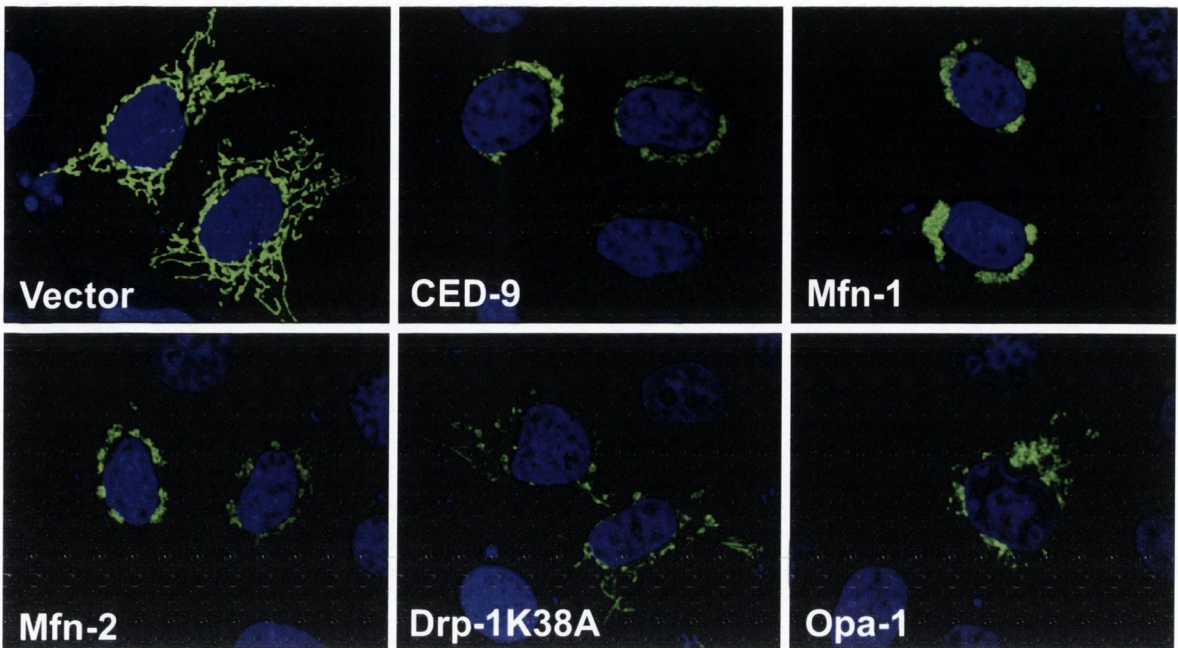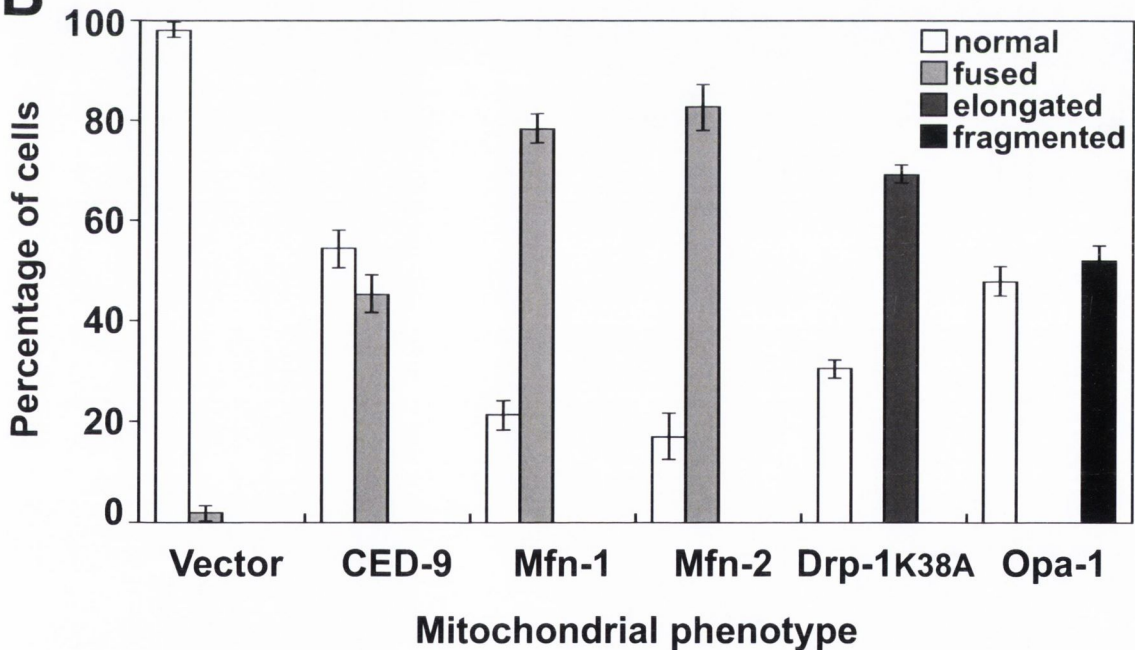
Figure 4.16: Mitochondrial fusion induced by CED-9 resembles that of fusio-genic proteins
A) Representative confocal images of HeLa cells expressing a combination of the indicated proteins (600 ng) along with the mitochondrial marker MitoGFP (200 ng). Cells were fixed and mounted to be scored for phenotypes. B) Quantification of cells treated as in A. Graph is representative for at least three independent experiments. Confocal images were taken on an Olympus laser-scanning microscope FV1000 at 60 X magnification.

CED-9 also induces mitochondrial fusion, we chose to compare it to those known regulators of mitochondrial dynamics. As a marker we again employed MitoGFP and transfected HeLa cells along with CED-9, Mfn-1, Mfn-2, Drp1K38A and Opa-1. Figure 4.16, A shows that the mitochondrial phenotype of CED-9 expressing cells resembled that of Mfn-1 and Mfn-2 expressing cells, which all induced a hyperfused cluster of mitochondria around the nucleus. This was different to Drp1K38A induced fusion, which had a distinct effect on the mitochondrial network. We, like others, observed very elongated tubules of mitochondria, but in contrast to the fusion proteins, no clusters surrounding the nucleus (Smirnova *et al.*, 2001). In contrast, when Opa-1 was expressed in HeLa cells, the mitochondrial network appeared disrupted and the organelles fragmented. This was unexpected, since Opa-1 protein is necessary for mitochondrial fusion (Cipolat *et al.*, 2004). Our observations were underlined by quantitative assessment of cells expressing above-mentioned proteins (Figure 4.16, B).

To further analyze the mechanism of the CED-9-induced phenotype, we asked whether CED-9 could interact with mitofusins. To explore this, CED-9 was co-expressed with Mfn-1 and Mfn-2 in HEK293T cells and co-immunoprecipitation was carried out (by Dr. C. Adrain). Surprisingly, we detected an interaction of CED-9 with Mfn-2 (Figure 4.17, A). This indicated a possible way by which CED-9 might promote fusion of mitochondria, which is through protein-protein interaction with mitofusin-2. No interaction of any other mitochondrial controlling proteins with CED-9 was found, but we could see CED-9/CED-4 interaction, which verified our results (Figure 4.17, A and B). In addition, interaction of CED-9 with Mfn-2 could not be disrupted by the presence of EGL-1 (Figure 4.18).

The results obtained so far lead us to suggest that CED-9 indeed induces mitochondrial fusion in a similar way as the mitofusins. This function is likely to be promoted through protein-protein interactions of CED-9 with Mfn-2 on two opposing mitochondria. Finally EGL-1 did not disrupt this function, indicating that it might bind to a different part of CED-9 than Mfn-2.

C. elegans contains a protein that is homologous to mitofusins, but had not been previously characterized. Through blast searches we found FzoRP-1
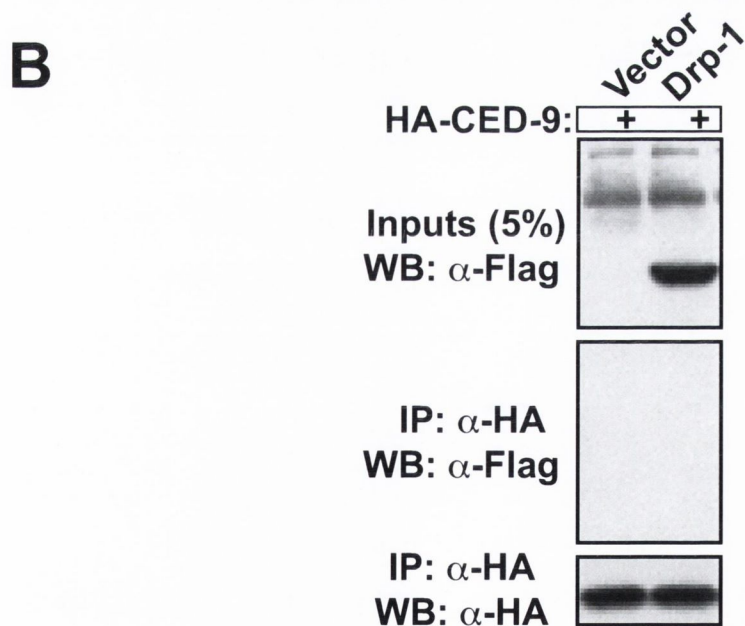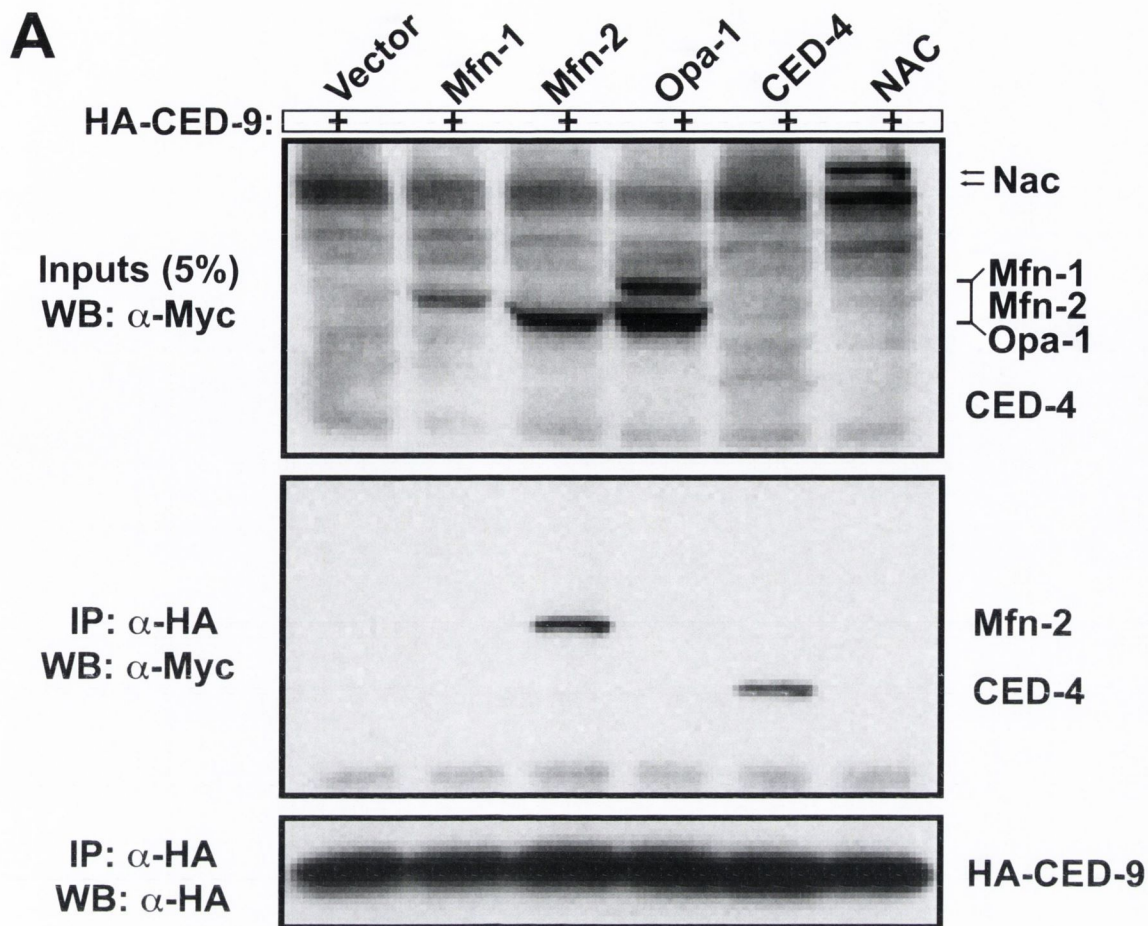
Figure 4.17: Co-immunoprecipitation for CED-9 interactions
A) HEK293T cells were transfected with plasmids encoding CED-9 (10 µg), vector (20 µg), Mfn-1 (20 µg), Mfn-2 (20 µg), Opa-1 (20 µg), CED-4 (20 µg) and Nac (20 µg) as a control. 48 hours after expression cells were harvested and lysates incubated with α-HA antibody for CED-9 capture. Co-immunoprecipitates were probed with α-Myc antibody. B) CED-9 (10 µg) was transfected with vector (20 µg) or Drp-1 (20 µg) into HEK293T cells and co-IP carried out with α-HA antibody and then probed with α-Flag. Experiments are representative for a triplicate of the same setup. These experiments were carried out by Dr. Colin Adrain.
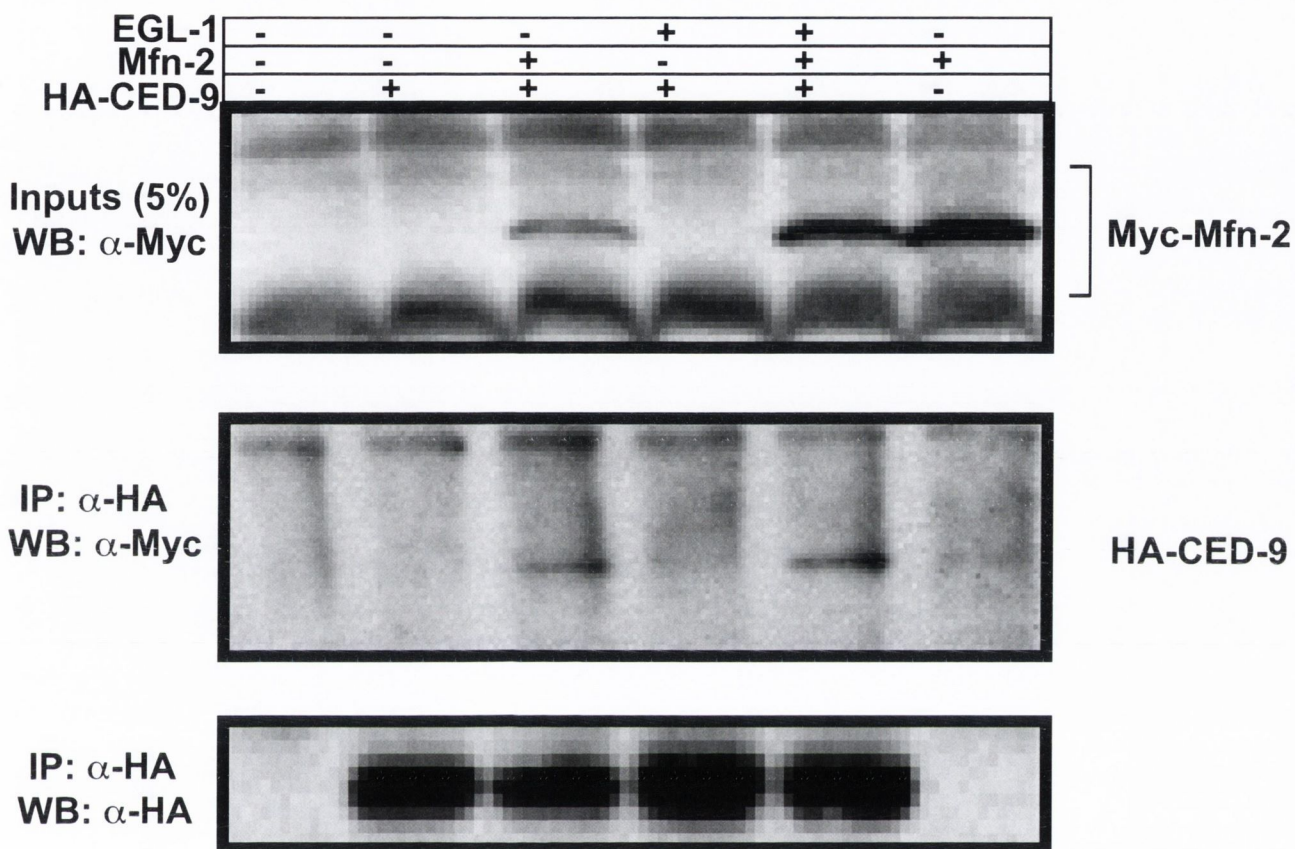
Figure 4.18: EGL-1 had no effect on CED-9 interactions with Mfn-2
HEK293T cells were transfected with plasmids encoding CED-9 (10 µg), vector (20 µg), Mfn-2 (20 µg) and EGL-1 (20 µg). 48 hours after expression cells were harvested and lysates incubated with α-HA antibody for CED-9 capture. Co-immunoprecipitates were probed with α-Myc antibody. Experiment is representative for a triplicate of the same setup. These experiments were carried out by Dr. Colin Adrain.

(fuzzy-onions-related-protein 1; accession number: AAC71095), a 774 amino acids protein, which is comprised of a GTPase domain, heptad repeats and two C-terminal transmembrane domains, like mitofusins-1 and –2 (Figure 4.19, A). To see whether we could repeat our earlier results with this worm protein, we cloned the coding sequence of FzoRP-1 into a human expression vector including a Myc-tag. HeLa cells expressing FzoRP-1 showed a fused mitochondrial phenotype similar to the mitofusins-induced clusters, as revealed by MitoGFP (Figure 4.19, B and C). We also found that FzoRP-1 shared the mitochondrial localization of CED-9 when we immunostained cells co-expressing the two proteins (Figure 4.19, D). However, despite various attempts, we were not able to extract FzoRP-1 from cell-pellets to perform co-immunoprecipitation and were therefore unable to check protein-protein interaction of CED-9 with FzoRP-1 (Figure 4.19, E).

4.3.9 Human homologues of CED-9 and their role in mitochondrial dynamics

Like CED-9, members of the human anti-apoptotic Bcl-2 protein family contain a C-terminal transmembrane domain, with which they localize to intracellular compartments such as mitochondria (Antignani and Youle, 2006). In addition, the human Bcl-2 family members act primarily on mitochondria to regulate apoptosis. Therefore, we wondered if these proteins might also play a role in regulating mitochondrial dynamics. We transfected HeLa cells with pcDNA3-BclxL together with MitoGFP and analyzed cells expressing Bcl-xL protein by staining with specific antibodies as shown in figure 4.20. We found that Bcl-xL perturbed the mitochondrial network. Bcl-xL expressing cells contained fused mitochondrial clusters (Figure 4.20, third row panels). Similarly to CED-9 around half the cells containing Bcl-xL showed fused mitochondria concentrated around the nucleus (Figure 4.21, A). In contrast to CED-9, 50% of the cells also displayed fragmented mitochondrial networks (data not shown). This was a dose dependent phenomenon where the fused phenotype of mitochondria was out-titrated at decreasing Bcl-xL levels. However, all the cells expressing Bcl-xL displayed a rearranged mitochondrial network, not a single cell had retained tubular organelles.
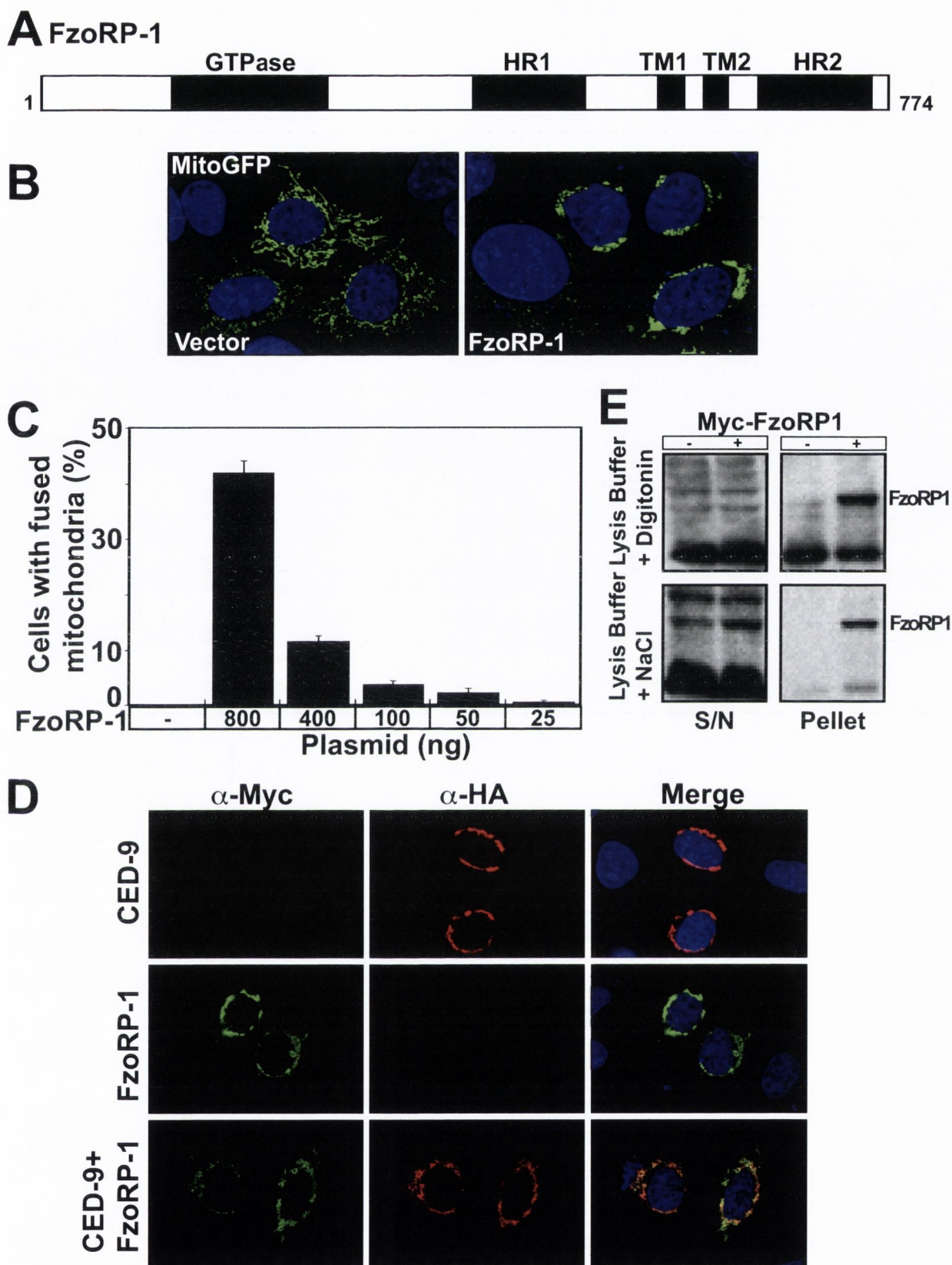
Figure 4.19: FzoRP1 is the *C. elegans* homolog of mitofusins
A) Schematic domain structure of FzoRP-1 as obtained from Pubmed (AAC71095). HR=heptad repeat, TM=transmembrane domain. B) HeLa cells were transfected with plasmids encoding vector (600 ng), FzoRP-1 (600 ng) and MitoGFP (200 ng). C) Quantification of FzoRP1 expressing cells, transfected as in B. D) HeLa cells, transfected as indicated on the left, were immunostained after 24 hours with the respective antibodies to visualize CED-9 and/or FzoRP-1. Note the overlap if they are co-expressed. E) HEK293T cells were transfected with 10 µg of vector or Myc-tagged FzoRP1 plasmid. 48 h after transfection, cells were lysed in either standard Lysis buffer with NaCl, or lysis buffer with 1% digitonin, followed by centrifugation. Samples of the supernatant (S/N), and the insoluble pellet (Pellet) were analysed by Western Blot using α-Myc antibodies. Pictures depict representative cells. Experiments are representative for a triplicate of the same setup.

On the contrary, Bax expressing cells all contained shattered mitochondria that were scattered throughout the cell, resembling the low dose of Bcl-xL expressing cells (Figure 4.20, second row panels). Despite this, the state of cytochrome *c* in cells with Bcl-xL-induced mitochondrial changes was always identical to healthy cells as seen by cytochrome c-GFP (Figures 4.21, B and 4.22). Even if mitochondria appeared fragmented, cytochrome *c* was never released. In contrast, Bax over-expression, even in the presence of the caspase inhibitor zVADfmk, always had resulted in cytochrome *c* release and fragmentation of mitochondria (Figure 4.21, B). This was almost completely inhibited by Bcl-xL co-expression (Figure 4.21, B and Figure 4.22).

Next we analyzed Bcl-xL and Bax by FRAP to establish whether they would display a fission or fusion effect. As expected, mitochondria of Bcl-xL expressing cells recovered quickly after bleaching. However, mitochondria in cells transfected with Bax, were fragmented and incapable of recovering by fusion of their mitochondria (Figure 4.23, A and B). Finally, to exclude that this was a HeLa specific mitochondrial phenotype of Bcl-xL, we repeated our experiments in MCF-7, COS-7, CHO and HEK293T cells and observed the same results as in HeLa cells, where we saw the phenotypical changes with Bcl-xL (Figure 4.24). Moreover, we subjected Bcl-xL to co-immunoprecipitation assays, asking whether it could bind any mitochondrial dynamics-regulating protein. Our data (kindly provided by Dr. C. Adrain) showed, that like CED-9, Bcl-xL interacted with mitofusin-2, but no other fusion protein (Figure 4.25, A). In addition, Bcl-2 behaved in the same way and exclusively bound Mfn-2 in our co-immunoprecipitation experiments (Figure 4.25, B).

Together these findings support a role for Bcl-2 family members in mitochondrial dynamics from worm to men.

4.3.10 Mitochondria of CED-9-mutant *C. elegans* embryos

An available *C. elegans* mutant strain is the MT3970, which contains the ced-9n1653 allele. This strain (MT3970) is characterized by a loss of CED-9 function, resulting in massive programmed cell death of developing worm embryos (Hengartner *et al.*, 1992). The CED-9 allele of this strain is temperature-sensitive (*ced-9*^{ts}), which loses its function by incubation at 25°C.
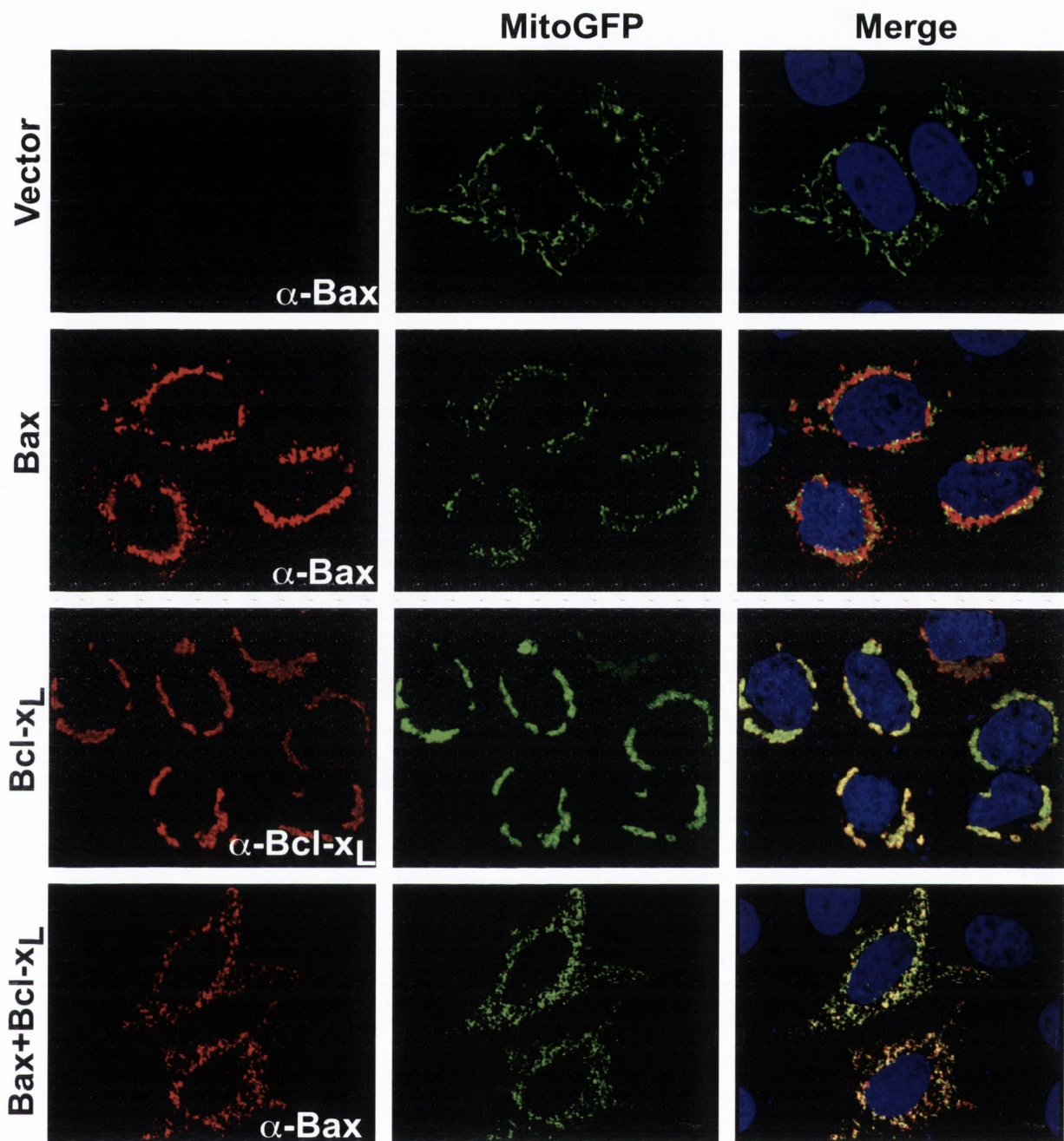
Figure 4.20: Mitochondrial networks are remodeled by Bcl-xL
HeLa cells, transfected with vector, Bax (200 ng), Bcl-xL (800 ng) or a combination of both,were fixed and immunostained after 24 hours expression. Specific antibodies revealed target protein expressing cells (left hand panels). The mitochondrial marker MitoGFP was co-transfected (middle panels), merges, including HOECHST staining, are on the right. Representative confocal images were taken on an Olympus laser-scanning microscope FV1000 at 60 X magnification. Results depict representative areas for at least three independent experiments.
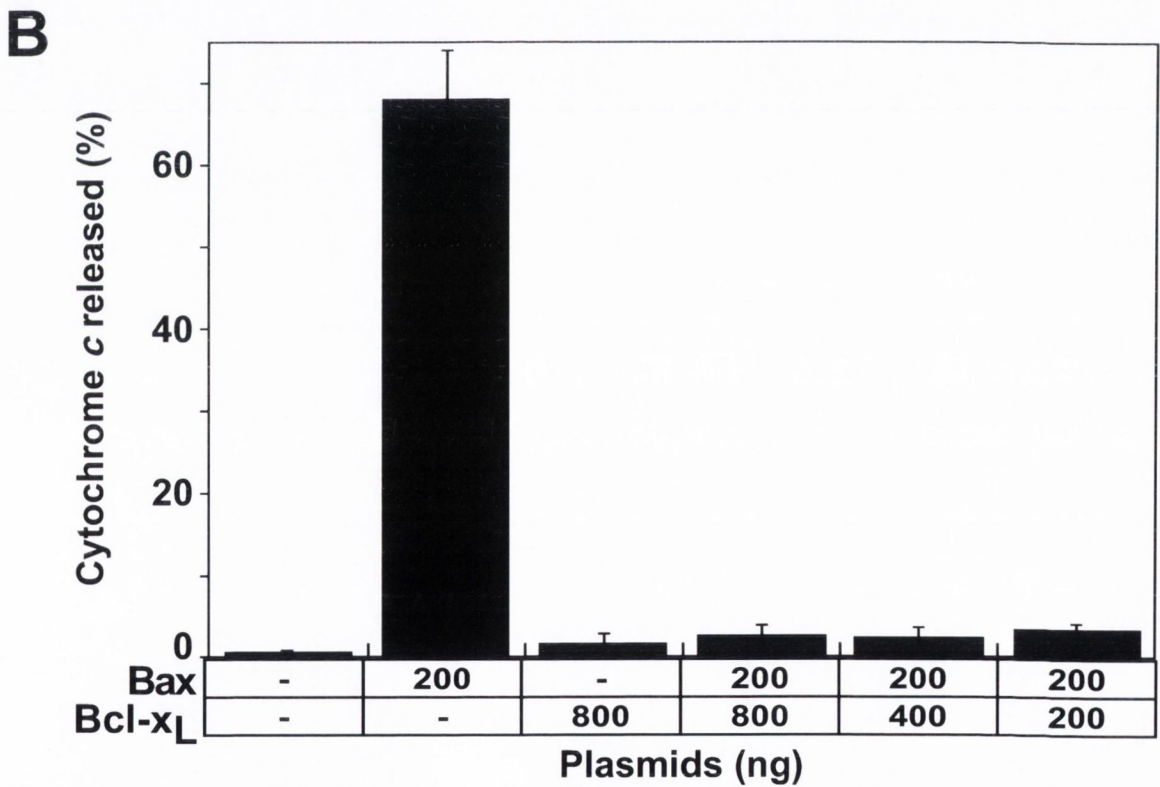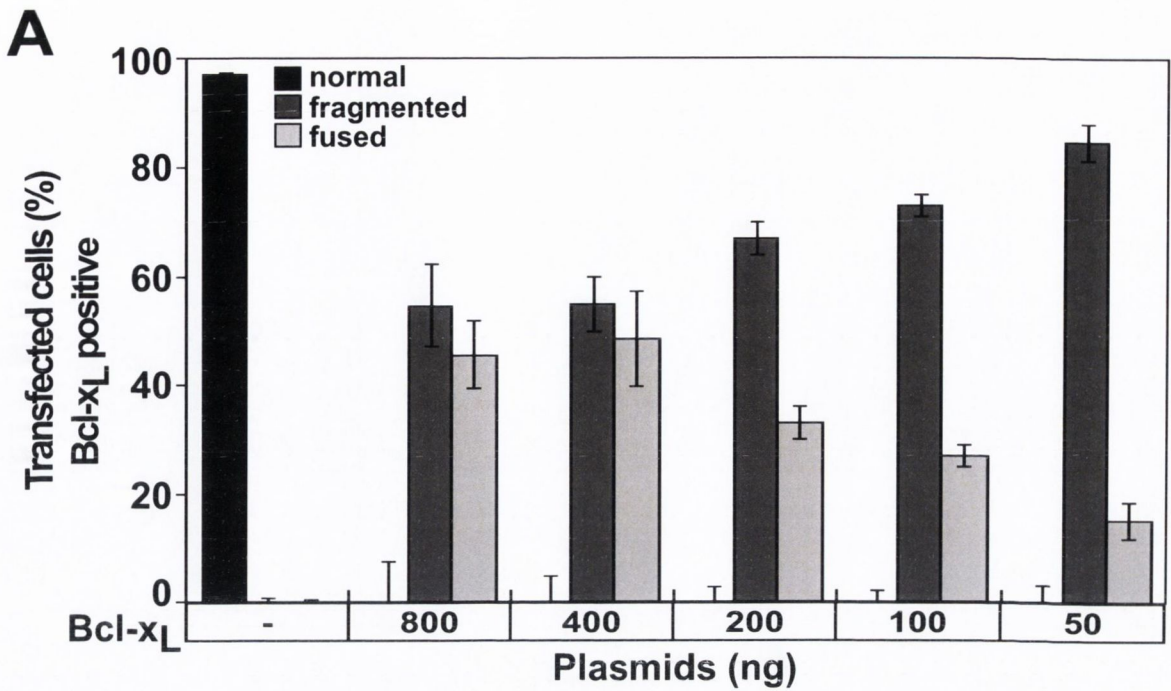
Figure 4.21: Bcl-xL remodels the mitochondrial network and blocks cytochrome *c* release

A) HeLa cells, transfected with the shown amounts of Bcl-xL and the mitochondrial marker MitoGFP, were fixed and immunostained after 24 hours expression (as in Figure 4.21). Specific antibody revealed Bcl-xL expressing cells, which were scored for their mitochondrial phenotype. B) HeLa cells, stably expressing cytochrome *c*-GFP, were transfected with combinations of Bax and Bcl-xL as indicated. Cytochrome *c* release was scored in cells, which were positively stained with α-Bax or α-Bcl-xL. Results are representative for at least three independent experiments.
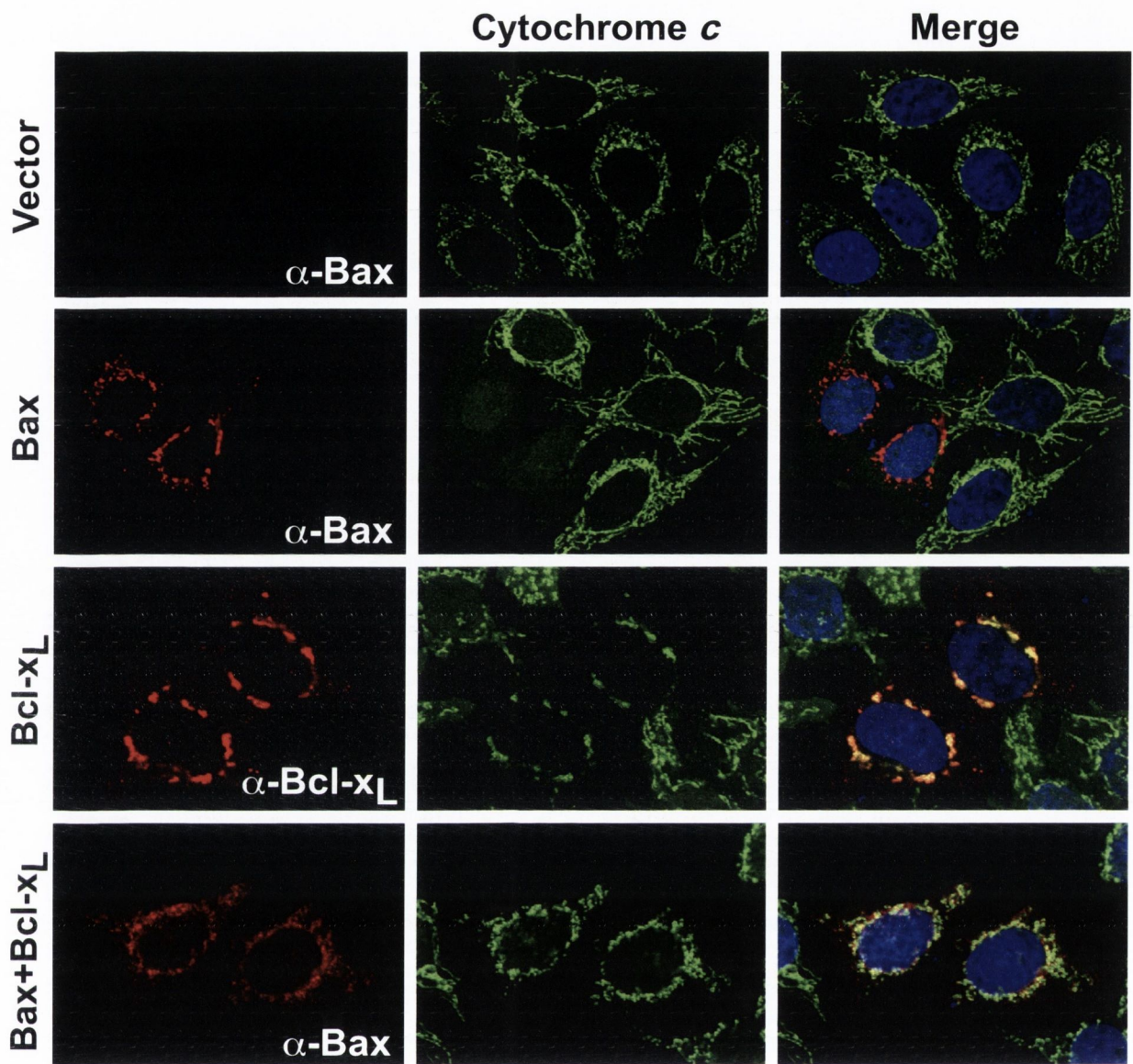
Figure 4.22: Bcl-xL blocks Bax induced cytochrome *c* release
HeLa cells, stably expressing cytochrome *c*-GFP, were transfected with vector, Bax (200 ng), Bcl-xL (800 ng) or a combination of both as indicated. After 24 hours, cells were fixed and immunostained. Specific antibodies revealed target protein expressing cells (left hand panels). Retention or release of cytochrome *c* was evident the GFP fusion (middle panels). Merges, including HOECHST staining, are on the right. Representative confocal images were taken on an Olympus laser-scanning microscope FV1000 at 60 X magnification. Results depict representative areas for at least three independent experiments.

In order to study mitochondria in nematode embryos, we decided to use this strain and compare it to the wild type N2.

First we examined embryos that were isolated from worms, by the Sodium-hypochlorite treatment, that were growing at the permissive temperature of 20°C on NGM plates. We observed that already at this temperature, the CED-9-mutant strain embryos did not hatch at the same rate as the wild type embryos (Figure 4.26, A). The effect was even stronger at the restrictive temperature of 25°C for four hours. While it had little influence on the wild type, hatching of mutant embryos was noticeably reduced. We also checked the phenotype of the embryos by light-microscopy and could see remarkable differences in morphology. The wild type embryos displayed a normal appearance at the permissive and restrictive temperature, whereas the mutant embryos had an abnormal morphology, were reduced in size and contained a high number of dying cells (Figure 4.26, B). These first insights of the CED-9 mutant strain confirmed earlier observations, which described that losing CED-9 function resulted in embryonic lethality by presumably a higher rate of cell death (Hengartner et al., 1992).

To analyze the influence of CED-9 on mitochondria phenotype in the worm, we compared the two strains for their mitochondrial phenotype. For this, wild type and mutant embryos were isolated from worms grown on NGM plates soaked with MitoTracker dye (0,4 µg/ml) (Chen et al., 2000). The embryos were then incubated at 20°C or 25°C for two to four hours before they were examined on the microscope. The enlargements in figure 4.27 show quite intriguingly that mitochondria of wild type embryos are well distributed around the nucleus and were MitoTracker positive at both tested temperatures. However, mitochondria of ced-9^{ts} embryos looked disrupted and fragmented. This effect even increased at 25°C and the staining with MitoTracker was greatly reduced in those cells (Figure 4.27 and 4.28, A). Mitochondrial staining was detectable as spots distributed throughout the cell. We already could see disturbed mitochondria in the mutant embryos at 20°C, but the number of the affected embryos was even greater at 25°C (Figure 4.28, A). Finally we also analyzed a gain of function CED-9 strain (ced-9^{gf}) looking for changes of the mitochondrial phenotype. However, this mutant behaved largely like wild type and had
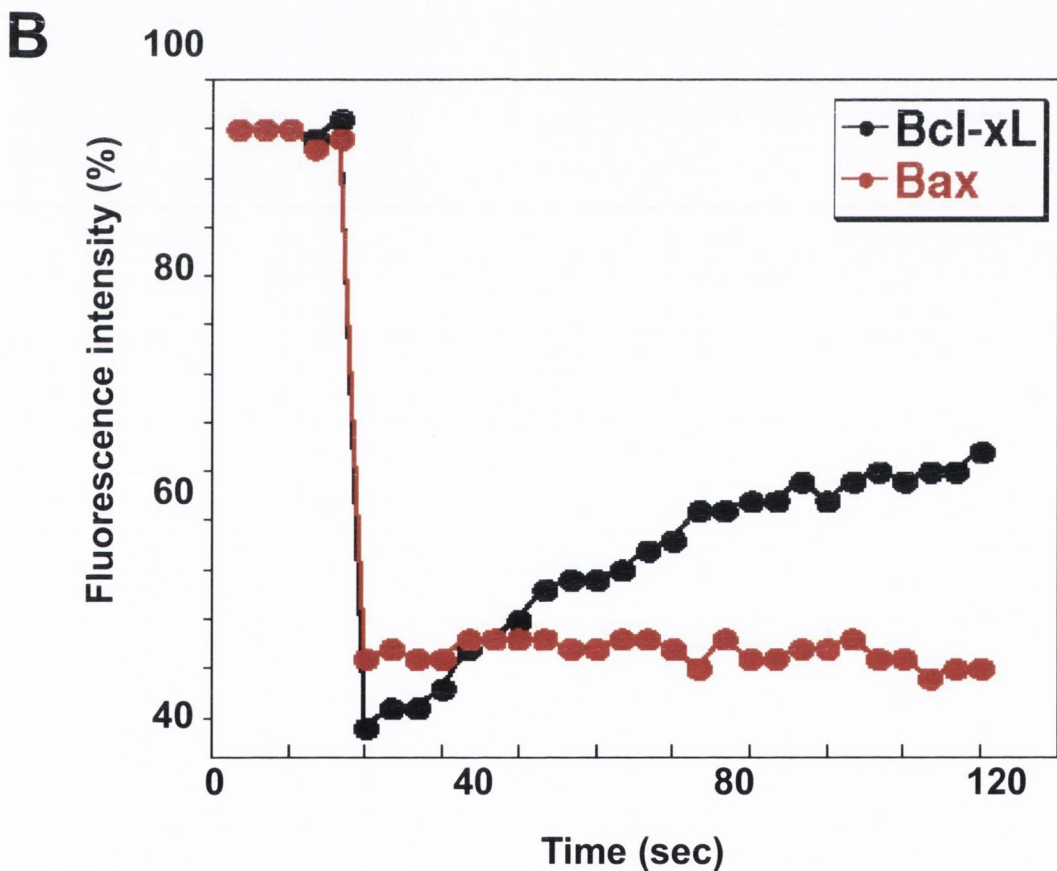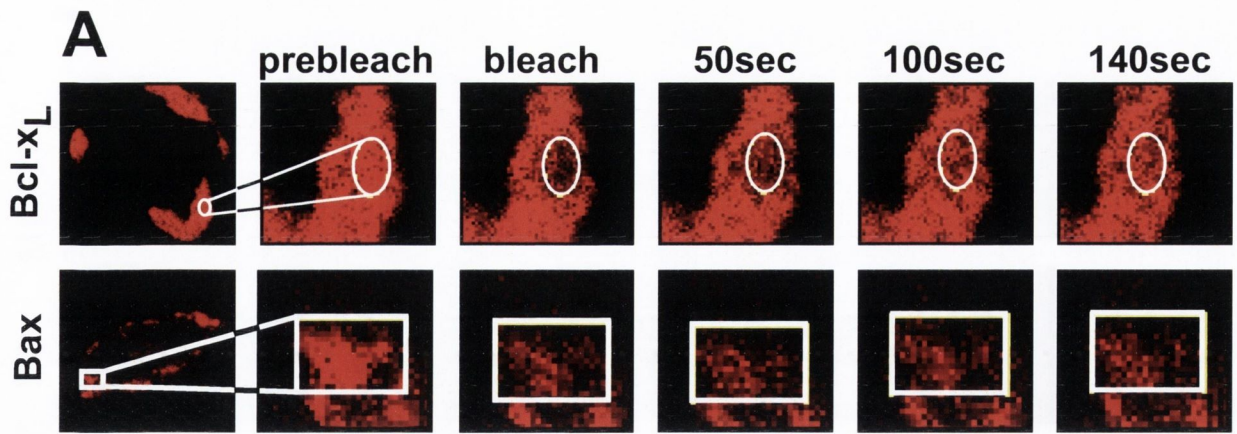
Figure 4.23: FRAP analysis of mitochondrial fusion dynamics by Bcl-xL and Bax

A) HeLa cells transfected with 200 ng of the indicated plasmids were stained with Mi-toTracker dye after 24 hours expression. The marker MitoGFP (200 ng) was utilezed to identify transfected cells and those were used to perform FRAP as described in 2.2.12. B) Representative graph of above experiment. Bax expressing cells included 50 µM zVADfmk. Experiments were carried out and representative confocal images chosen from an Olympus laser-scanning microscope FV1000 at 60 X magnification. Results are representative of at least three independent experiments.
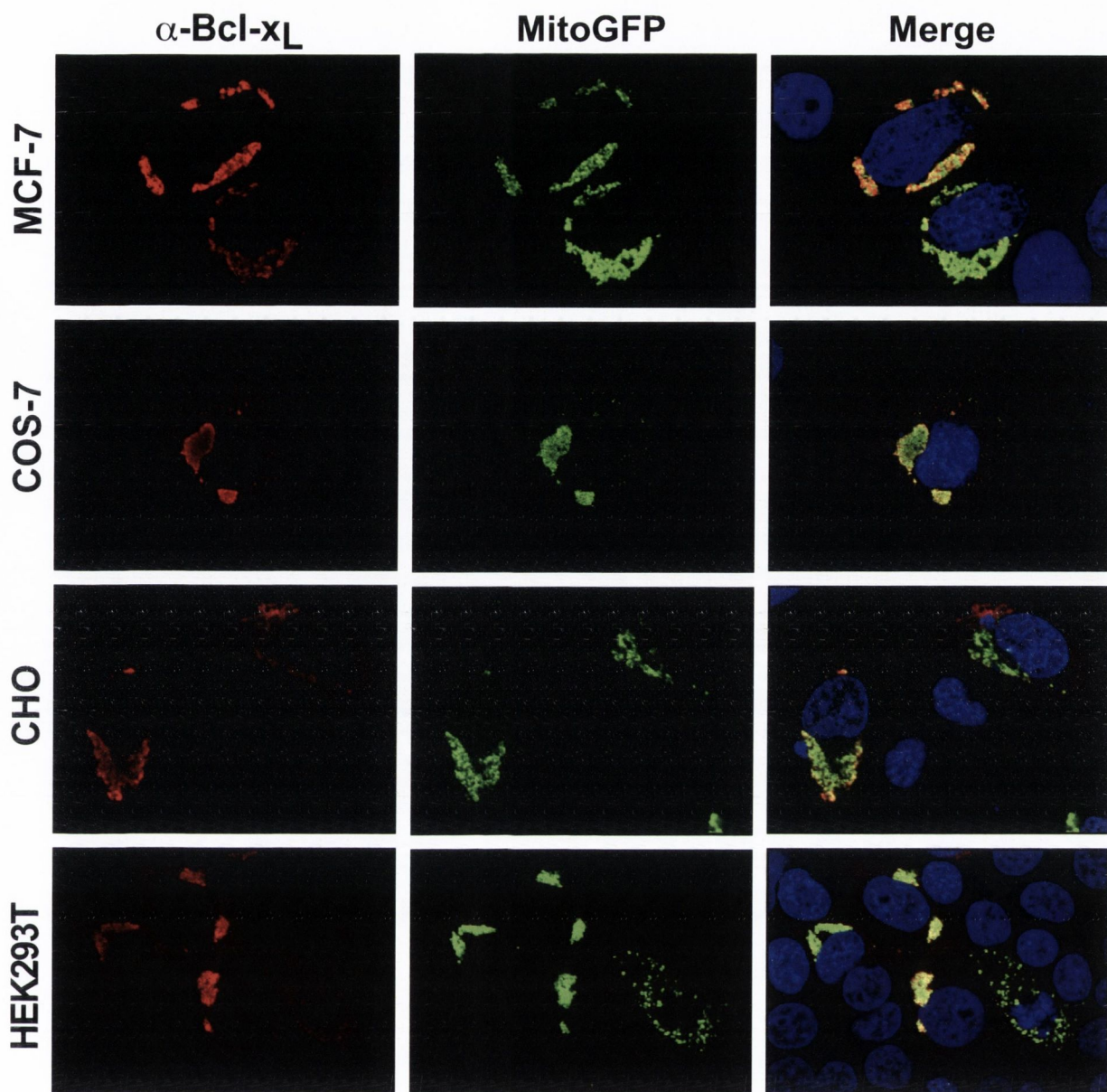
**Figure 4.24: Effects of Bcl-xL on mitochondrial dynamics in different cell lines**

Four further cell lines, as specified on the left, were transfected with 600 ng Bcl-xL and immunostained with α-Bcl-xL antibody after 24 hours expression. Mitochondrial morphology was detected by co-transfection of 200 ng MitoGFP (middle panels). Merges including HOECHST staining are on the right. Images were taken on an Olympus laser-scanning microscope FV1000 at 60 X magnification. Pictures depict representative areas of at least three independent experiments.
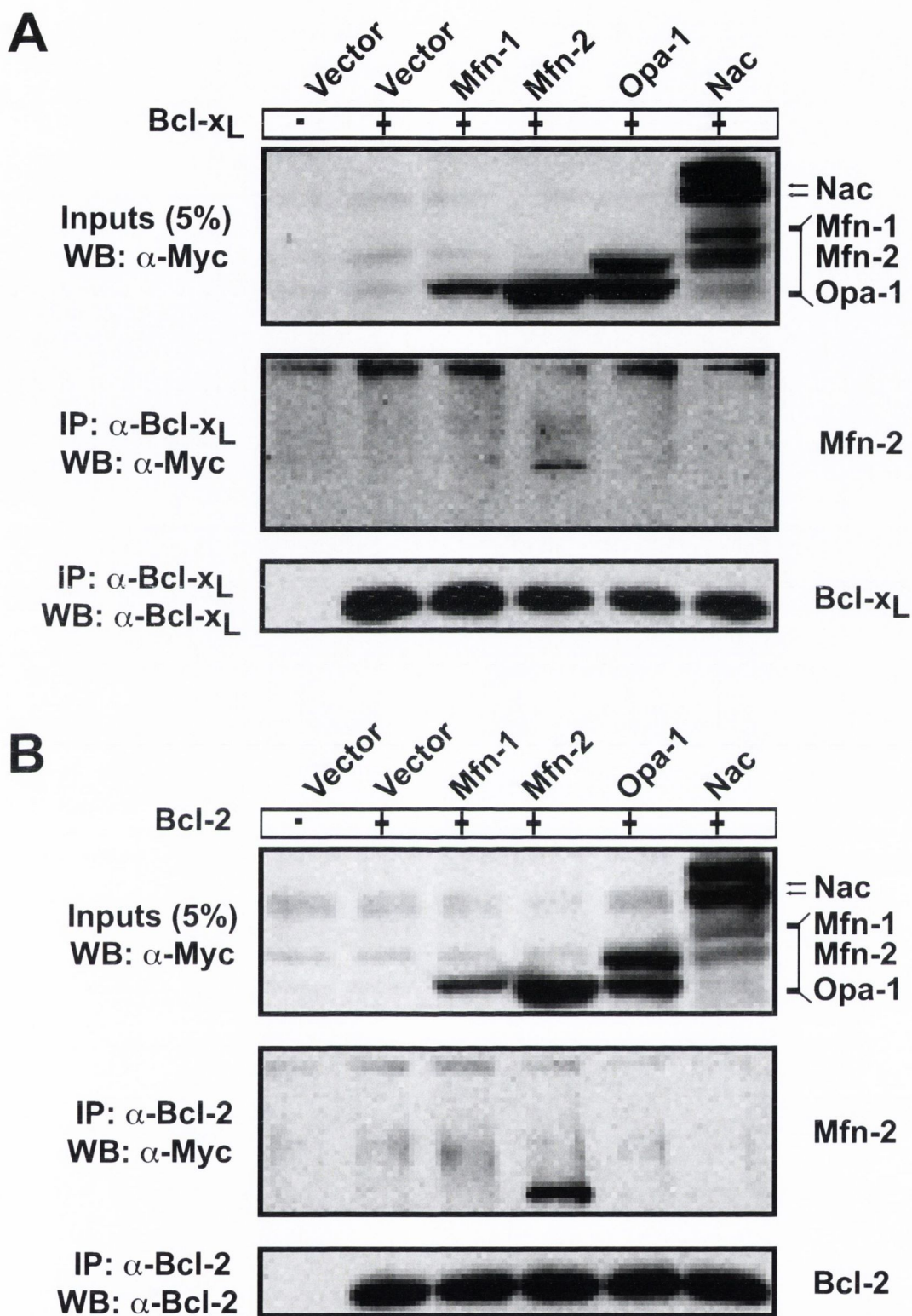
Figure 4.25: Co-immunoprecipitation for Bcl-xL and Bcl-2 interactions
A) HEK293T cells were transfected with plasmids encoding Bcl-xL (10 μg), vector (20 μg), Mfn-1 (20 μg), Mfn-2 (20 μg), Opa-1 (20 μg) and Nac (20 μg). 48 hours after expression cells were harvested and lysates incubated with α-Bcl-xL antibody. Co-immunoprecipitates were probed with α-Myc antibody to reveal interactions. B) Bcl-2 (10 μg) was transfected along with vector (20 μg), Mfn-1 (20 μg), Mfn-2 (20 μg), Opa-1 (20 μg) and Nac (20 μg) into HEK293T cells and co-IP carried out as above. Experiments are representative for a triplicate of the same setup. Data was generated by Dr. Colin Adrain.

normal mitochondrial appearance and MitoTracker staining (Figure 4.27 and 4.28,B).

These results illustrated that a loss of CED-9 function not only influences the number of cells that die in worm embryos, but it is also important for mitochondrial maintenance. Of note is that in CED-9 loss of function embryos almost all cells seemed to contain disrupted mitochondria, while in fact not all cells were showing the characteristics of dying cells by Nomarski optics. This might underline a role for CED-9 in keeping mitochondria healthy, before cells are triggered to undergo apoptosis.
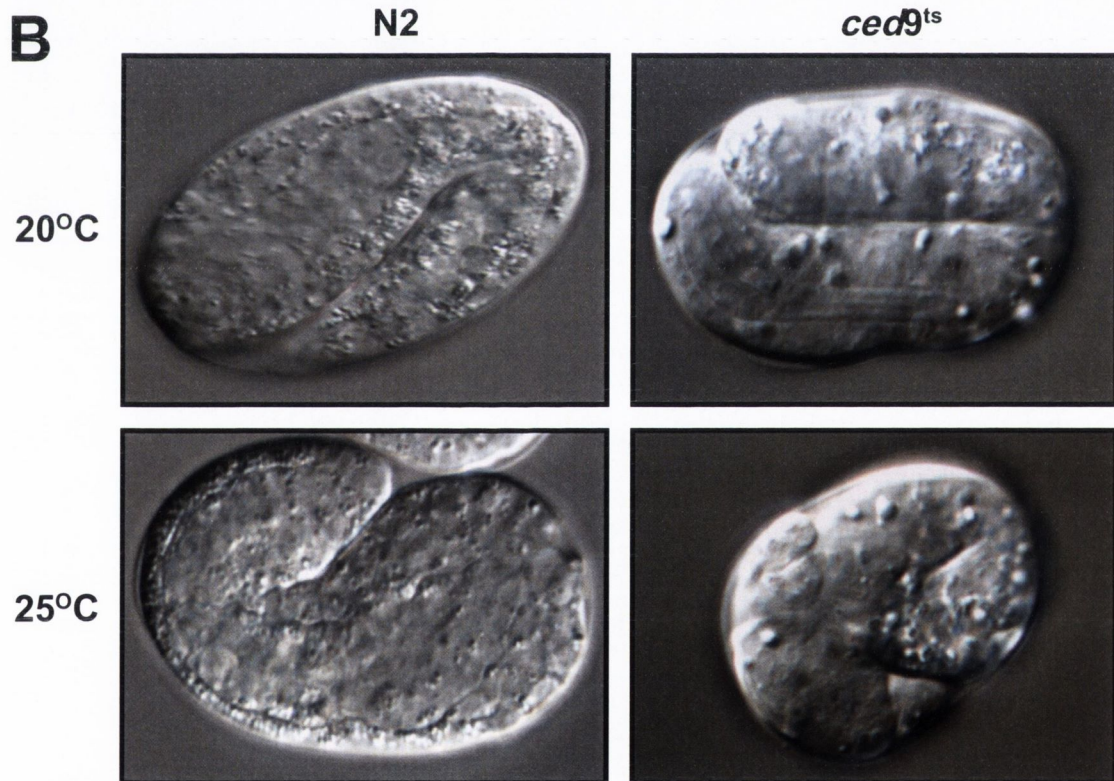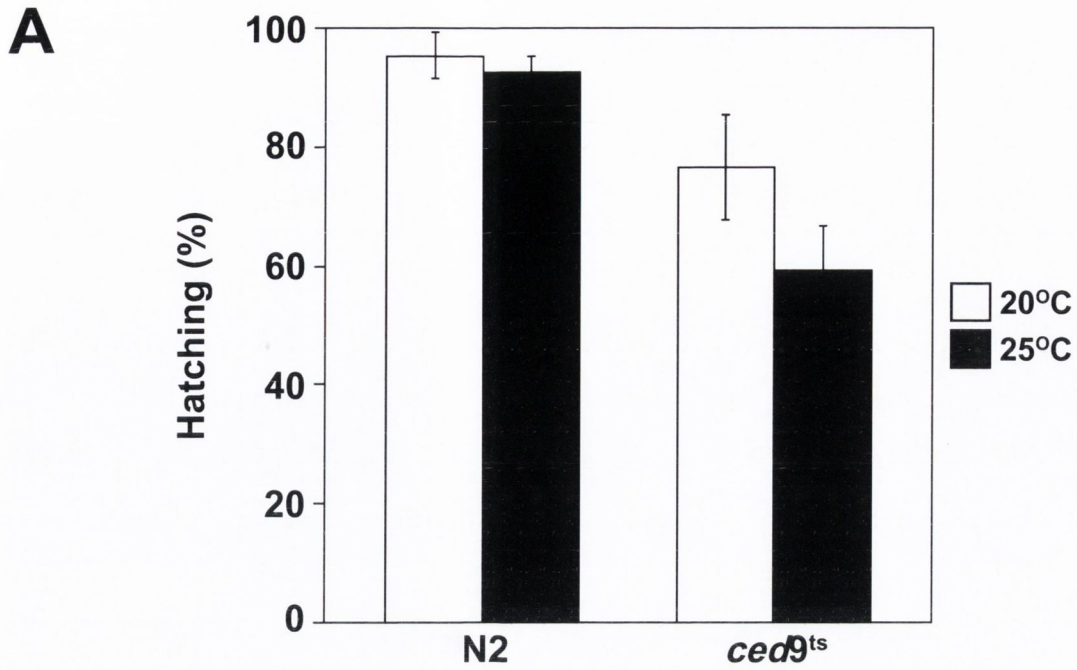
Figure 4.26: CED-9 mutant worms display somatic differencs and lower hatching rates compared to wild type worms

A) *C. elegans* embryos isolated from either N2 or *ced*9ts worms, were incubated at the permissive (20°C) and the restrictive temperature (25°C) for 4 hours. Embryos were observed over time and the percentage of worms that hatched to L4 stage scored. B) Representative images of wild type and mutant embryos at permissive and restrictive temperature as shown. Pictures were taken on an Olympus microscope with Hoffman optics at 60 X magnification. Pictures depict representative embryos of at least three independent experiments. These experiments were carried out by Dr. Rebecca C. Taylor.
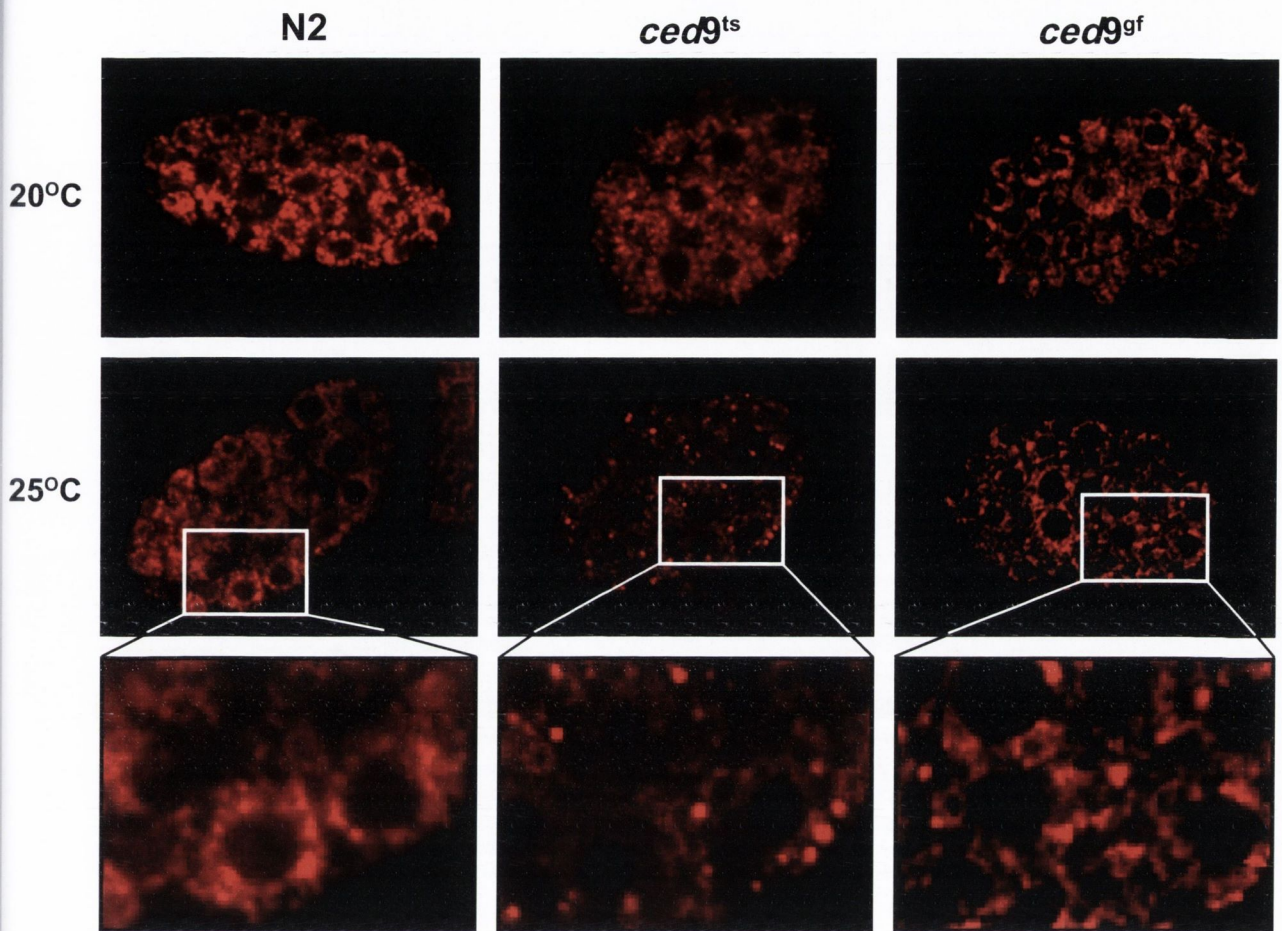
Figure 4.27: Mitochondria of mutant _C. elegans_ embryos display fragmentation

Wild type, ced9ts and ced9gf _C. elegans_ embryos were isolated from worms that were grown on MitoTracker soaked NGM plates for 3 days at either 20°C or 25°C as shown. Mitochondrial morphology was observed on an Olympus laser-scanning confocal microscope and pictures taken at 60 X magnification. Note the disrupted MitoTracker staining of ced9lf mutant embryos (middle, bottom panel) Pictures depict representative embryos of at least three independent experiments. Data were generated by Dr. Rebecca C. Taylor.
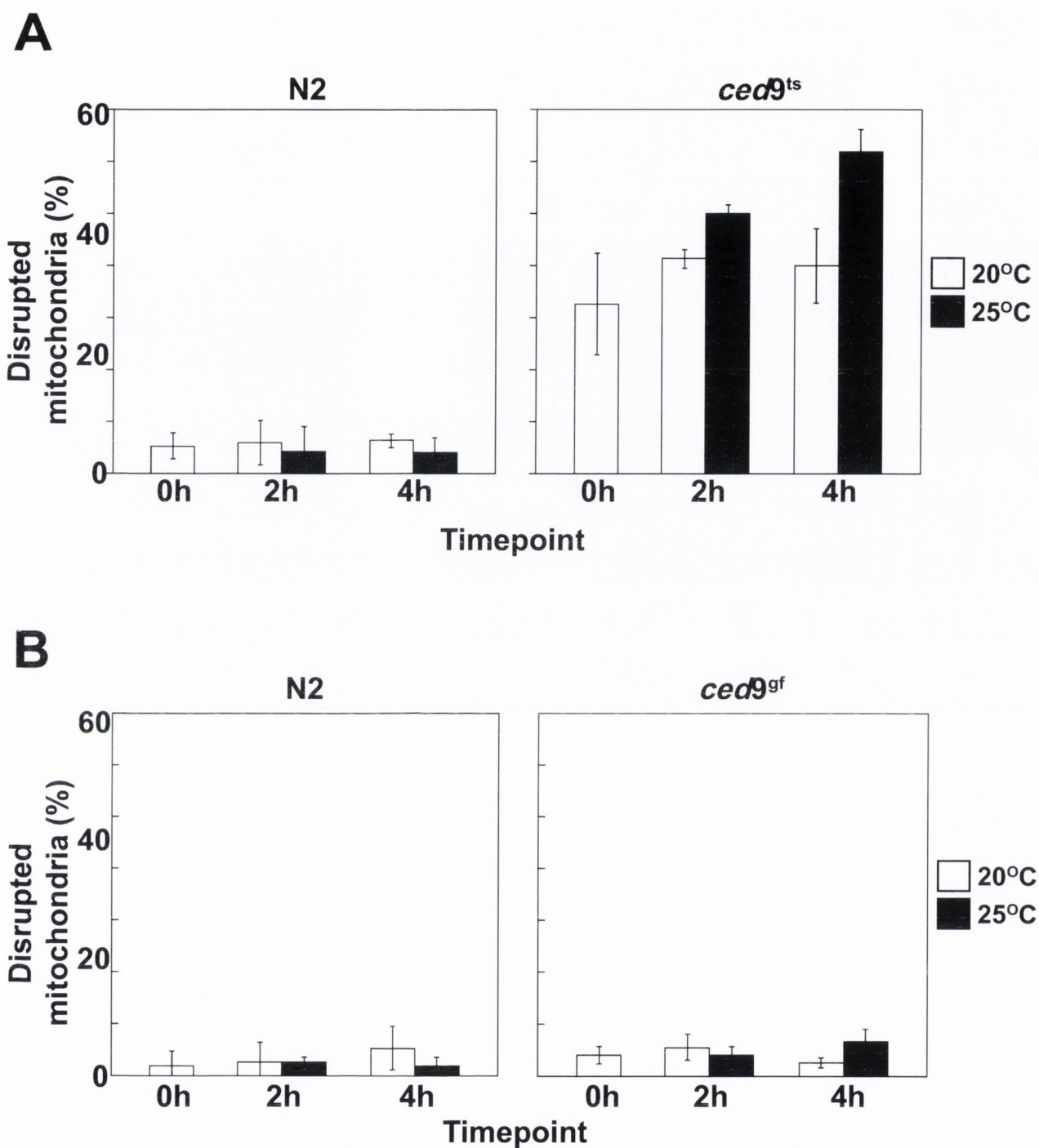
Figure 4.28: Quantitation of *C. elegans* embryos with damaged mitochondria
A) Wild type and ced9ts *C. elegans* embryos were prepared as in Figure 4.28. Sub-
sequently worms were scored for disrupted mitochondria at the permissive and re-
strictive temperature. Graphs display percentage of embryos that showed disrupted
MitoTracker staining. B) Wild type and ced9gf embryos were treated as in A) and
quantified. Results are representative of at least three independent experiments.
These experiments were carried out by Dr. Rebecca C. Taylor.

4.4 Discussion

4.4.1 Summary

To summarize this chapter, we can say that first, the inhibitor of cell death protein of the nematode *C. elegans* CED-9 acts in a different way than its human homologues Bcl-2 and Bcl-xL. This study showed that CED-9 failed to block cytochrome *c* release and induction of apoptosis in human cells induced by diverse stimuli. This had not been reported previously in such detail.

Second, we found that the CED-9 and Bcl-2 family proteins induced mitochondrial fusion and furthermore could interact with the fusion protein Mfn-2, but not with Mfn-1 or Opa-1, suggesting a possible mechanism for the observed phenotype.

Third, we observed an inhibition of CED-9 induced mitochondrial fusion by the worm BH3-only molecule EGL-1, which resulted in mitochondrial fragmentation. EGL-1 is known to directly bind to CED-9 and change its confirmation, leading to a functional change. In our study we showed that EGL-1 influences multiple functions of CED-9.

Finally, from these results, we suggest that proteins of the Bcl-2 family harbor an additional function separate to their role in programmed cell death or apoptosis, which is to modulate mitochondrial dynamics. This function is conserved between species, and may represent an ancestral role for this protein family.

4.4.2 CED-9, the inhibitor of PCD in *C. elegans*, but not in man

In the initial part of this chapter we investigated whether the *C. elegans* protein CED-9 inhibits apoptosis in mammalian cells. While human Bcl-2 can substitute for CED-9 in the worm and inhibit programmed cell death in this context (Vaux *et al.*, 1992), it was not clear whether the worm equivalent could function similar to human Bcl-2.

Here we found that CED-9 failed to block apoptosis in human cells. Although, when we expressed the triad of the worm programmed cell death machinery, CED-9 blocked CED-4/CED-3 induced apoptosis in mammalian cells, which was in accordance with earlier studies (Chinnayian *et al.*, 1997a; Yang *et al.*, 1998). In response to diverse pro-apoptotic stimuli however, CED-9

failed to block apoptosis. These results suggested that although CED-9 and Bcl-2 share structural and functional homology they block apoptosis in a mechanistically distinct way. It also underlined the model pathway of death inhibition in *C. elegans*, and the divergent pathway of apoptosis regulation that has emerged through evolution from worm to man by the Bcl-2 family proteins.

4.4.3 Cytochrome *c* release: regulation by the CED-9/Bcl-2 family

An early hallmark of apoptosis in mammals is the release of cytochrome *c* from the mitochondrial intermembrane space into the cytoplasm where it activates the cell death machinery. In *C. elegans*, cytochrome *c* has not been found to play a role during programmed cell death to date, thus it remains unclear if CED-9 could regulate cytochrome *c* release in that system.

In Drosophila melanogaster a role for cytochrome *c* and mitochondria during cell death has been under debate. Two different cytochrome *c* variants exist in the fly, cyt c-p and cyt c-d, which are expressed in the soma or the testis, respectively (Dorstyn *et al.*, 2002; Arama *et al.*, 2003). From readings of cyt c-d mutant male flies (which were sterile), expression of this cytochrome *c* variant appeared necessary for proper sperm development and Drosophila caspase (DRICE) activation (Arama *et al.*, 2003). However, biochemical analysis of cytochrome *c*-d and –p by RNA interference treated invertebrate cells, still displayed DRONC and DRICE processing after apoptosis induction (Dorstyn *et al.*, 2004). Interestingly, despite the contradictory results of the two groups, concerning the importance of cytochrome *c* for fly apoptosis, they both found the downstream effectors DRICE and DRONC associated to mitochondrial structures (Dorstyn *et al.*, 2002; Arama *et al.*, 2003; Dorstyn *et al.*, 2004). These observations suggested a role for mitochondria in the activation phase of cell death in the fly, although the release of cytochrome *c* is uncertain and may not be necessary.

In our study, we explored whether CED-9 could act like human Bcl-2 family members to regulate cytochrome *c* release in mammalian cells. The elucidation of this could lead to further clues of a possible role for cytochrome *c* in the worm. Here we showed that Bax-induced cytochrome *c* release was not inhibited by CED-9 expression. In addition, CED-9 was not able to block drug

induced apoptosis, unlike for example Bcl-xL, which completely protected cells from death and cytochrome *c* release either by Bax over-expression or by the addition of apoptotic drugs. Therefore, our results suggest that CED-9 does not interact with Bax. Unlike Bcl-xL, CED-9 could not block Bax pore formation activity that leads to mitochondrial outer membrane permeabilization. Although the exact mechanism of inhibition of Bax-induced MOMP is still unresolved and under investigation (Youle and Strasser, 2008), it is clear that anti-apoptotic Bcl-2 family proteins are required for cell death inhibition (Veis *et al.*, 1993). Based on this, it is most likely that CED-9 cannot interact with Bax or Bak, as has been shown for Bcl-2 and Bcl-xL, and which is necessary for blocking Bax/Bak-oligomer assembly (Oltvai *et al.*, 1993; Ottilie *et al.*, 1997; Kuwana *et al.*, 2002). However, direct interaction experiments between Bax and CED-9 would clarify this question.

CED-9 interacts with the BH3-only molecule EGL-1, which might in fact be an ancestor of Bax. EGL-1 binds with a high affinity to CED-9 and was found localized to the mitochondrial outer membrane when the two proteins were co-expressed (Figure 4.14). CED-9 and EGL-1 interact via binding of the BH3-domain of EGL-1 to a hydrophobic cleft in the CED-9 molecule, which is formed by its BH domains (Yan *et al.*, 2004). Therefore, it is surprising that CED-9 cannot sequester Bax, which like EGL-1 contains a pro-apoptotic BH3-domain. Maybe the affinity of those two proteins is not strong enough, which might result from conformational constrictions. For example the structure of Bax has been shown to be a rather closed globular one, where the C-terminal end is hidden in a hydrophobic cleft and only released after Bax activation (Nechushtan *et al.*, 1999, Suzuki *et al.*, 2000). However, the BH3-domain of Bax, necessary for interaction with anti-apoptotic proteins, might not be accessible for CED-9. In contrast interaction of human Bcl-2 family members with Bax have been shown to be through the binding of the BH3-domain of Bax into the hydrophobic pocket of anti-apoptotic proteins (Sedlak *et al.*, 1995; Borner, 2003). How exactly exposure of the Bax-BH3-domain is stimulated after activation, and how then the anti-apoptotic proteins bind to them, remains elusive. In this context it might be more likely that CED-9 has a higher binding affinity to mammalian BH3-only proteins, which resemble EGL-1, than to the multi-BH-domain protein Bax,. Therefore, it would be of interest to analyze

interactions between for example Bid and Bim with CED-9, or the indirect Bax and Bak activating molecules like Hrk, Noxa and Bik.

Despite conservation of the localization of the CED-9/Bcl-2 family on mitochondrial membranes, their precise function of cell death inhibition is not conserved. While mammalian Bcl-2 family proteins regulate apoptosis by blocking the formation of a Bax/Bak-channel and thereby cytochrome *c* release, CED-9 sequesters CED-4 onto the mitochondrial membrane. The reason for this is still unclear. It might be that the primordial role of CED-9 was on mitochondrial dynamics, which localized the protein to the organelle. Regulation of cell death then could have been additionally acquired later in evolution. Vice versa, studies that have analyzed whether the human CED-4 homologous protein Apaf-1 interacts and is sequestered to mitochondria by Bcl-2 family proteins, although firstly thought to be the case (Hu *et al.*, 1998; Pan *et al.*, 1998), was found not to be reproducible when examining endogenous protein interactions (Moriishi *et al.*, 1999; Hausmann *et al.*, 2000; Hill *et al.*, 2004). This reflects again the differential function between CED-9 and the human Bcl-2 family.

Surprisingly, during the course of the above-discussed experiments we observed dramatic rearrangements of mitochondrial networks in cells over-expressing CED-9. Specifically, CED-9 promoted extensive mitochondrial fusion in several different mammalian cell lines, such as HeLa, HEK293T, MCF-7, CHO and COS-7 cells. Furthermore, while CED-9 failed to block drug-induced cytochrome *c* release it was able to prevent mitochondrial fragmentation under the same conditions. This also suggested that the CED-9/Bcl-2 family may play a previously unrecognized role in the process of mitochondrial fission or fusion, and that this might be an evolutionary ancient function preceding their role in the regulation of programmed cell death. These observations are discussed in the next paragraph.

4.4.4 Mitochondrial fission and fusion and its role in apoptosis

During apoptosis, the mitochondrial tubular network collapses, connections between organelles are disrupted and fragmented mitochondria are dispersed

throughout the cell (Karbowski and Youle, 2003). Changes in mitochondrial shape in healthy cells are driven by the fission proteins (Drp-1 and Fis-1) and counteracted by fusion proteins (Mfn-1, Mfn-2 and Opa-1). We, like others, observed that Bax expression resulted in fragmented mitochondria, resembling the action of fission proteins (Desagher and Martinou, 2000). Foci of mitochondrial fragmentation sites have been found to harbor Mfn-2, Drp-1 and Bax, implicating the family of Bcl-2 proteins to mitochondrial dynamics during cell death (Nechushtan *et al.*, 2001). However, it is still unclear if this is only a coincidence of co-localization, or if it is due to interactions of those proteins. In addition there have not been any studies addressing the co-localization of anti-apoptotic proteins with fission and fusion proteins. Recently a study by Karbowski and co-workers described the necessity of Bax and Bak for mitochondrial fusion, because cells lacking both proteins displayed fragmented mitochondria in healthy cells (Karbowski *et al.*, 2006). We rather believe that pro-apoptotic proteins cooperate to promote fission during apoptosis, according to our results and going along with their role of opposing anti-apoptotic Bcl-2 proteins.

Sugioka *et al.* (2004) and Frezza *et al.* (2006) observed that fusion proteins Mfn-1, Mfn-2 and Opa-1 could inhibit apoptosis when over-expressed (Sugioka *et al.*, 2004; and Frezza *et al.*, 2006). We however, could not confirm this when we induced fusion through over-expression of CED-9. It might have been that the apoptotic stimuli we used were too strong to achieve inhibition of cell death by mere fusion. However, there is no convincing proposed mechanism for the inhibition of apoptosis by the fusion family proteins. In contrast to this, Bcl-2 and Bcl-xL also displayed fused mitochondria and could potently block cytochrome *c* release, which suggests an inhibitory effect of apoptosis through fusion. This finding requires further investigations.

How exactly cytochrome *c* is released from mitochondria is still a subject of much debate. Fragmentation of mitochondria could be one mechanism that leads to the leakage and loss of cytochrome *c* from these organelles. Therefore, over-expression of the fission inducing protein Drp-1 should induce mitochondrial fragmentation followed by cytochrome *c* release and apoptosis.

Studying the worm Drp-1 homolog Dlp-1, Labrousse and colleagues found that over-expression induced a phenotype of unconnected, single, fragmented mitochondria in worm muscle cells (Labrousse *et al.*, 1999). But no cell death was reported in those experiments, in contrast, RNA interference of Dlp-1 in the worm lead to embryonic lethality, indicating an important role for mitochondrial division during development. In mammalian cells there is no convincing description of Drp-1 over-expression leading to mitochondrial fragmentation, much less so the induction of cytochrome *c* release and apoptosis. However, one component of the fission machinery might be interesting in this context. The receptor for Drp-1 on mitochondria, Fis-1, is more potent than Drp-1. When Fis-1 was over-expressed, it induced mitochondrial fission and activated cell death in human cells (James *et al.*, 2003; Lee *et al.*, 2004). In our experiments however, we observed that, at low doses of apoptotic-inducing agents, CED-9 could overcome mitochondrial fission and a significant number of cells retained fused organelles. This suggested that mitochondrial fragmentation per se is not needed or sufficient for apoptosis.

In addition we found that over-expression of Bcl-xL in HeLa cells caused a phenotype of fragmented mitochondria in about fifty percent of the Bcl-xL positive population, and resembled the phenotype of Bax (or Fis-1) over-expression. In stark contrast to Bax-expressing cells, cytochrome *c* was still retained in mitochondria in Bcl-xL expressing cells. Those cells were viable with no signs of apoptosis or cytochrome *c* release. These observations suggested that fragmentation of mitochondria can also occur within healthy cells and does not necessarily result in cytochrome *c* release and cell death. The fragmented phenotype of Bcl-xL over-expressing cells could be through the imbalance of the fusion and fission machinery by impared fusion. This could result in a block of membrane fusion and the appearance of small round mitochondria. In light of this we suggest that mitochondrial scission per se is not sufficient or required for the release of cytochrome *c* and apoptosis.

Our observations were confirmed by a recent study by Alirol and colleagues, where Fis-1 was carefully examined (Alirol *et al.*, 2006). The group expressed Fis-1, which induced apoptosis, as previously reported (James *et al.*, 2003; Lee *et al.*, 2004). However, when a Fis-1 mutant construct was used, lacking the transmembrane-domain, it lost the ability to target to mitochondria.

Still, mitochondria became fragmented by Fis-1, but apoptosis was abolished. In addition, Alirol *et al.* showed that Fis-1 induced cell death was dependent on Bax and Bak, since no death was observed when Bax/Bak double knockout cells were used (Alirol *et al.*, 2006). This is in accordance with the results in this study, which separates fission processes from apoptotic events.

4.4.5 Mechanism of fusion induced by Bcl-2-like molecules

For the first time we describe here that CED-9 and other Bcl-2 family molecules lead to mitochondrial fusion. Their phenotype of over-expression resembled the phenotypes shown with Mfn-1 and Mfn-2 proteins (Santel and Fuller, 2001; Rojo *et al.*, 2002; Eura *et al.*, 2003). This suggests that these proteins might share a common function. Because the above was merely based on observational assays, we employed an additional technique (FRAP) to follow mitochondrial fusion dynamics of CED-9 and Bcl-2 (Szabadaki *et al.*, 2004). Using the FRAP-technique, we found positive recovery of the Bcl-2 family proteins, which were similar to the behavior of mitofusins on fusing mitochondria. However, further experiments would be useful to evaluate the fusion function of the Bcl-2 family proteins. A simple experiment would be the 'PEG (polyethylenglycol) – fusion assay', in which cells are transfected with a mitochondrial marker plasmid either expressing green- or red- fluorescence (GFP or RFP) protein. Subsequently cells are treated with PEG and observed on a microscope. PEG induces the fusion of the plasma-membrane of two adjacent cells. If one cell with GFP fuses with a RFP expressing cell and their mitochondria mix, the result should be yellow stained mitochondria. Using this assay, it could be analyzed if for example in Bcl-2 knockout cells the mitochondria do still fuse and this would indicate its importance in mitochondrial fusion (Legros *et al.*, 2002; Chen *et al.*, 2003).

Another technique to evaluate fusion events is to use photo-activateable GFP protein targeted to mitochondria. This mitochondrial marker that is initially invisible, can be activated by a short laser impulse. By this, ongoing fusion events can be observed on a microscope where mitochondria start to light up shortly after the laser treatment. In cells that are incapable of mitochondrial fusion, i.e. Mfn-2 knockout cells, the photo-activated GFP is not transferred

throughout the cell. Thereby, it could be analyzed whether Bcl-2 family proteins recover fusion events after their expression (Karbowski *et al.*, 2004).

Although structurally the Bcl-2 family and the fission and fusion proteins are very different, they might share some common roles. The only apparent common feature of the two protein families though is their association to mitochondria. The Bcl-2 family proteins are rather small molecules of around 20-30 kDa and the fission and fusion proteins are mainly around 70 kDa or more, and in addition are mostly dependent on GTP to function. There are no similarities in domain-composition or structure. Despite these differences, these protein families might share common functions. For example, it could be that fission and fusion proteins are purely responsible for mitochondrial dynamics in healthy cells, and their functions are taken over by the Bcl-2 family during apoptosis. This could be based on the dependency of the fusion event on mitochondrial membrane potential (Legros *et al.*, 2002; Mattenberger *et al.*, 2003). Therefore, during apoptosis, as mitochondria lose their membrane potential, the Bcl-2 family might promote rescue by fusing mitochondria. The process by which two membranes fuse is very complex and even more when it comes to mitochondria, because there are four membranes that have to fuse on two opposing organelles. Tethering, docking and fusion of the membranes have to occur, but how exactly the mitofusins promote this remains hypothetical (Modzy and Shaw, 2003). How the Bcl-2 family proteins promote mitochondrial fusion requires further investigation. One way to analyze their function in more detail is to undertake truncation studies. For example dissecting CED-9 and its human homologues into their sub-sequential domains followed by fusion to a GFP-reporter protein. This could help identifying which part of CED-9 is necessary and sufficient for promoting mitochondrial fusion. Additionally it would contribute to exclude whether such domains induce the mentioned function on their own in a way that would account for an artefact.

To explain fusion promotion by the Bcl-2 family proteins, it appears logical to think of a mechanism that is based on fusion induced by two interacting proteins. To examine this, we undertook interaction experiments of fission and fusion proteins with the family of CED-9 and Bcl-2 proteins. In Addition to the

microscopic observations we also detected interaction between CED-9, Bcl-2, Bcl-xL with the fusion protein Mfn-2 by co-immunoprecipitation. This result suggests a mechanism of fusion through physical contact of the two different molecules. It was shown by Koshiba *et al.* (2004), that mitofusins require interaction between their C-terminal coiled-coil domains in order to fuse mitochondrial membranes (Koshiba *et al.*, 2004). CED-9, Bcl-2 and Bcl-xL may be capable of tethering mitofusin proteins on adjacent mitochondria to fuse their membranes in the same way as mitofusins communicate with each other. Furthermore, two CED-9 (Bcl-2 or Bcl-xL) molecules could connect to each other on opposing mitochondrial membranes and bring them together for a fusion reaction. However, the exact mechanism of mitochondrial fusion by Bcl-2 family proteins remains elusive at this point.

A protein that was not investigated to date is the fusion protein FzoRP-1, the Mfn-1/2 homolog of the worm *C. elegans*. By homology searches we identified FzoRP-1 using the BLAST search tool, cloned this gene, and investigated its potency in terms of mitochondrial fusion. Along with its sequence similarity to the mitofusins, FzoRP-1 induced fusion of mitochondria in human cells. We also observed colocalization with mitochondrial markers and CED-9 in these cells. The insolubility of FzoRP-1 did not allow us to explore its ability to interact with Bcl-2 family proteins and CED-9. It would be of great interest to explore whether CED-9 can interact physically with the *C. elegans* homologous of Mfn-2, FzoRP-1. In addition knockout experiments of FzoRP-1 in worms, as has been done for fly Fzo-1 (Hales and Fuller, 1997) and mammalian Mfn-1 and Mfn-2 (Chen *et al.*, 2003) could enhance knowledge of those proteins and their impact on cell viability.

4.4.6 EGL-1 and CED-9

During worm cell death, the BH3-only molecule EGL-1 is transcriptionally up-regulated to inactivate CED-9 (Conradt and Horvitz, 1998). By binding of EGL-1 to CED-9 the conformation of CED-9 is changed and it can no longer sequester CED-4, which in turn activates the caspase CED-3 (Yan *et al.*, 2004).

In our study, expression of EGL-1 alone led to fragmentation of mitochondria in mammalian cells, release of cytochrome *c* and apoptosis. This

was reminiscent of the findings in the worm embryo, and suggested that EGL-1 is able to substitute for the function of mammalian BH3-only proteins (Willis *et al.*, 2005; Jagasia *et al.*, 2005). Presumably, in human cells, EGL-1 mediated activation of Bax or Bak and led to MOMP, which resulted in cytochrome *c* release. In our experiments, when we co-expressed CED-9 with EGL-1, the function of EGL-1 was suppressed by sequestration so it could no longer activate Bax or Bak. This observation allows the conclusion, that the mechanism of apoptosis activation by BH3-only proteins, and the inhibition of it by CED-9 or other anti-apoptotic proteins, is partially conserved throughout different species.

Recently it was suggested that EGL-1 promotes mitochondrial fragmentation in worm embryos, which is blocked by CED-9 (Jagasia *et al.*, 2005). Surprisingly co-expression of CED-9 and EGL-1 abolished the mitochondrial fusogenic phenotype of CED-9. No more collapsed mitochondrial structures were observed when those proteins were co-transfected into mammalian cells. In contrast mitochondria displayed a dramatic fragmented phenotype throughout the cell. However, this dramatic rearrangement again did not lead to cytochrome *c* release or apoptosis, in a similar way as we saw for Bcl-xL expression. EGL-1 causes a conformational change of the CED-9 molecule by binding to it. This change could be responsible for preventing the interaction of CED-9 with other molecules on neighboring mitochondria, possibly with the mitofusins or other Bcl-2 family members, which would explain the resulting phenotype of a fragmented mitochondrial network. The high affinity of EGL-1 to CED-9 could be responsible for this, for the competition for binding sites on CED-9 with other interaction partners.

4.4.7 CED-9 in the development of the worm embryo

Identification of the core programmed cell death machinery in the nematode *C. elegans* has shed light on the mechanism of apoptosis for many organisms. CED-3, CED-4 and CED-9 act together as the platform required for death in the worm. Investigating the CED-9 function in the worm has helped to deepen our understanding of how programmed cell death occurs even in higher organisms. Over-expression of CED-9 in the nematode showed complete inhibition of cell

death, whereas loss of function mutants displayed embryonic lethality during development of worms (Hengartner *et al.*, 1992; Hengartner *et al.* 1994).

We confirmed that loss-of-function mutant embryos were less viable than wild type and gain-of-function embryos by obtaining a lower number of hatching animals. The precise mechanism by which CED-9 blocks apoptosis in the worm is still under investigation. By analysis of the structure of the gain-of-function mutant one study by Yan *et al.* (2004) found that this mutant is so potent because EGL-1 cannot bind to it anymore and displace CED-4 (Yan *et al.*, 2004). Such detailed explanation has not been found for the loss-of-function mutant of CED-9. The loss of the ability to block apoptosis might be explained by its instability and rapid degradation (Yan *et al.*, 2004). When we looked at loss-of-function mutant embryos stained with MitoTracker red to reveal mitochondria within the embryo, we found that they displayed disrupted mitochondria. The organelles had a much weaker staining compared to wild type and gain-of-function animals. These findings could reflect an important function of the CED-9 protein in mitochondrial maintenance in *C. elegans* and explain the death caused by CED-9 loss of function. In addition, interaction of CED-9 molecules with each other or interaction with FzoRP-1 could be required for dynamics in worm mitochondria.

The fission protein Drp-1 was described to induce fragmentation of worm mitochondria when over-expressed in muscle cells and in embryos (Labrousse *et al.*, 1999; Jagasia *et al.*, 2005). In the study by Jagasia *et al.* (2005) it is speculated that CED-9 acts to activate Drp-1 or to function in parallel to it. Our results in mutant CED-9 embryos instead suggested that during development, CED-9 might be necessary to counteract Drp-1 and its fragmentation function.

CHAPTER V

Bax or Bak-induced Mitochondrial Fission can be Uncoupled from Cytochrome *c* release

5.1 Introduction

Mitochondria form the crucial platform for the intrinsic apoptosis pathway. Cytochrome *c* is released together with several other proteins (Smac/DIABLO, Omi/HtrA2) at an early time-point during apoptosis (Goldstein *et al.*, 2000; Munoz-Pinedo *et al.*, 2006). Once released into the cytosol, cytochrome *c* leads to the activation of the apoptosome, which in turn activates a caspase cascade (Slee *et al.*, 1999). The liberation of IMS proteins depends on permeability of the mitochondrial outer membrane, which is controlled by the Bcl-2 family, and referred to as mitochondrial outer membrane permeabilization (Goldstein *et al.*, 2000; Martinou and Green, 2001). Activation of the pro-apoptotic molecules Bax and Bak is required for MOMP and occurs via BH3-only proteins. These molecules can either directly bind Bax or Bak, like Bid or Bim, or indirectly lead to their activation by suppressing anti-apoptotic Bcl-2 family proteins (Chen *et al.*, 2005; Kuwana *et al.*, 2005; Youle and Strasser, 2008). The most important and most studied apoptosis-inhibiting family members are Bcl-2, Bcl-xL, Mcl-1 and A1, which block the release of cytochrome *c* from the intermembrane space (Finucane *et al.*, 1999; Youle and Strasser, 2008, Zhai *et al.*, 2008).

During apoptosis, there is a change of the typical mitochondrial filamentous network, which turns into a fragmented, sphere-like phenotype (Desagher and Martinou, 2000; Frank *et al.*, 2001; Karbowski *et al.*, 2002; Karbowski and Youle, 2003). These dramatic changes during apoptosis are probably caused through either increased fission rates or reduced fusion rates of mitochondria. Appearance of more numerous and fragmented mitochondria has been linked with Bax activation and cytochrome *c* release (Karbowski *et al.*, 2004). The exact mechanism of this phenotypical network rearrangement remains unclear to date, but it might indicate a cooperative effect of the mechanisms that induce apoptosis and mitochondrial fission.

Proteins driving mitochondrial fission or fusion in healthy cells have been suggested to play a role in mitochondrial destruction during cell death. In mammalian cells, Drp-1 controls fission together with its outer membrane adaptor Fis-1 (Smirnova *et al.*, 2001; James *et al.*, 2003; Yoon *et al.*, 2003).

Fusion is mediated and dependent on two proteins of the outer mitochondrial membrane, Mfn-1, and -2, and the inner mitochondrial membrane associated protein Opa-1 (Chen *et al.*, 2003; Olichon *et al.*, 2002; Arnoult *et al.*, 2005). While the inhibition of mitochondrial division is blocked by a dominant negative form of Drp-1 or knockdown of Drp-1 by siRNA, it is still unclear if this affects apoptosis, as was suggested (Neuspiel *et al.*, 2005; Arnoult *et al.*, 2005a; Brooks *et al.*, 2007). On the other hand, enforced expression of the fusion-promoting proteins Mfn-1, Mfn-2 and Opa-1 have been suggested to influence apoptosis by blocking cytochrome *c* release (Lee *et al.*, 2004; Jahani-Asl *et al.*, 2007; Cipolat *et al.*, 2006; Frezza *et al.*, 2006). Cells lacking Bax/Bak, or over-expressing Bcl-2 clearly affect the regulation of apoptosis by inhibiting the release of cytochrome *c* from mitochondria (Wei *et al.*, 2001; Tsujimoto *et al.*, 1984). In addition, a recent study found that Bax/Bak knockout cells contained fragmented mitochondria (Karbowski *et al.*, 2006). Instead of mitochondrial regulatory proteins having an impact during apoptosis these findings favor a role of Bcl-2 family proteins in the control of mitochondrial dynamics in healthy and dying cells.

5.2 Aims and Summary

Mitochondria are dynamic organelles that form an interconnected network, which is balanced by interactions of members of the fission and fusion super-family and which are crucial for the phenotypical appearance of healthy mitochondria. During apoptosis this balance is disturbed and mitochondria undergo dramatic morphological rearrangements.

In the previous chapter we obtained results that prompted us to attribute fission and fusion events to the family of Bcl-2 proteins. In this last chapter, we now wanted to explore whether components of the mitochondrial fission and fusion machinery can affect apoptosis. By over-expression experiments we aimed to find indications of their impact on apoptosis-associated mitochondrial fragmentation and cytochrome *c* release. This might enable us to clearly separate the function of mitochondrial fission events from cytochrome *c* release. We indeed found evidence to suggest that mitochondrial fragmentation is not a required step in apoptosis and that Bax and/or Bak-induced mitochondrial

fragmentation can be uncoupled from cytochrome *c* release through co-expression of Bcl-xL and other members of the Bcl-2 subfamily.

5.3 Results

5.3.1 Mitochondrial changes of fission and fusion proteins analyzed in mammalian cells

To explore the impact of proteins of the fission and fusion machinery on apoptosis, we first verified that the proteins were well expressed from our expression plasmids. HEK293T cells were transfected by the calcium chloride precipitation method as described in chapter II with plasmids encoding Drp-1, Drp-1K38A, Mfn-1, Mfn-2, Opa-1 and Fis-1. After 24 hours incubation, cells were harvested with lysis-buffer and the lysates ran on 8-12% SDS-PAGE gels (see figure 1.11). In figure 5.1 it is shown, that all constructs used were well expressed.

Next, we analyzed the effect of the fission and fusion proteins on mitochondria. HeLa cells were transfected with the expression plasmids mentioned above and before fixation of cells for immunostaining, they were incubated in MitoTracker dye to reveal their mitochondria. Anti-epitope-tag antibodies were used to detect those cells that expressed the target proteins (Figure 5.2). As shown in figure 5.2 on the left hand panels, fission and fusion protein expression was evident by the green immunostaining. In those positive cells we scrutinized the mitochondrial phenotype by MitoTracker staining. We could not find any changes of the mitochondrial network when Drp-1 was over-expressed in contrast to what had been previously reported (Szabadkai et al., 2004). Although our construct was sequenced and contained proper Drp-1 coding sequence, we did not find mitochondrial fragmentation even when we varied the plasmid concentration (data not shown). Quite the opposite effect was obtained by expressing a dominant negative form of Drp-1. Strong mitochondrial changes were found in cells positive for Drp-1K38A, which showed very elongated organelles (Figure 5.2). We also saw rearrangements with Mfn-1 and Mfn-2, which, when expressed, displayed the typical perinuclear mitochondrial cluster of fused organelles, as previously seen by others (Santel and Fuller, 2001; Legros et al., 2002; Santel et al., 2003). However, despite reports by Cipolat and colleagues, Opa-1 expressing cells contained fragmented
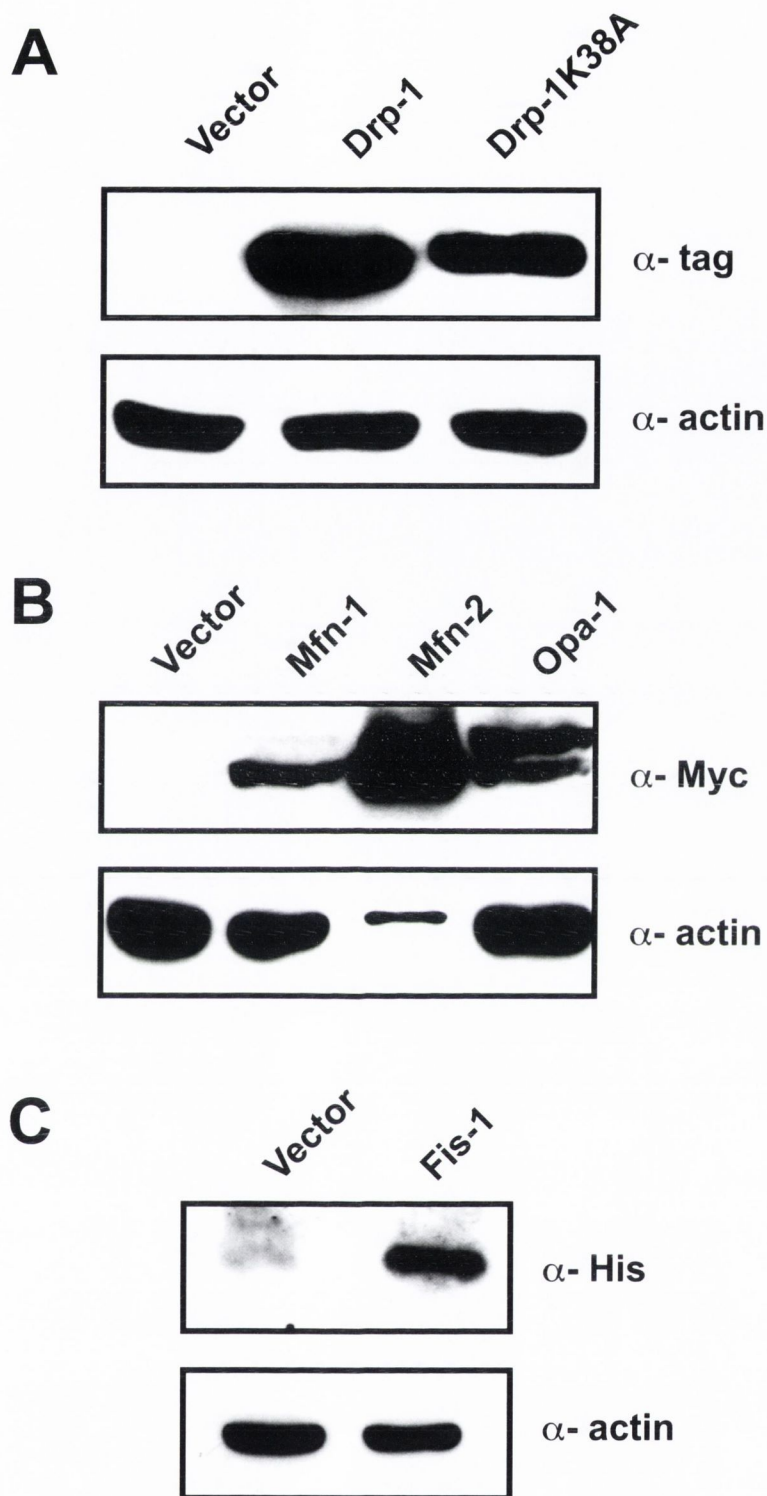
Figure 5.1: Expression profile of fission and fusion proteins by Western blot
HEK293T cells were transfected with 5 µg of the indicated expression plasmids and
Lysates were prepared 24 hours later. Lysates were run on a 8-12% SDS-PAGE
and proteins transferred onto Nitrocellulose membranes. To probe for the target
proteins, the indicated anti epitope-tag specific antibodies were used for A) α-HA to
detect Drp-1 and Drp-1K38A, for B) α-Myc to detect Mfn-1, Mfn-2 and Opa-1 and in
C) α-His to detect Fis-1. At least three rounds of experiments were undertaken and
representative blots chosen.

mitochondria in our experiments (Cipolat *et al.*, 2006). As we expected, Fis-1 expression led to fragmented mitochondrial structures.

A quantitative illustration of the above results is shown in figure 5.3. Cells, treated as described in the paragraph above, were used for quantification of the mitochondrial phenotype. Mitochondria of empty vector transfected cells were of normal filamentous networks in all cases. Of note is that the Drp-1 wild type showed some elongated mitochondria in our hands, but no fragmentation phenotype. This might be due to a similar effect that is induced by the dominant negative Drp-1K38A, merely by blocking fission through excessive expression of Drp-1. However, transfection of the Drp-1K38A resulted in more than fifty percent elongated mitochondria. Mfn-1 and Mfn-2 expressing cells displayed fused mitochondria from thirty up to fifty percent. And finally Opa-1 and Fis-1 fragmented the mitochondrial networks, which was in over fifty percent of all cases.

In order to exclude that our findings were unique to the HeLa cell line, we examined other mammalian cell types for their mitochondria. A Human breast cancer cell line (MCF-7) and a monkey kidney cell line (COS-7) displayed filamentous networks of tubular mitochondria when we transfected only empty vector along with MitoGFP (data not shown). In line with what was seen in HeLa cells, dramatic rearrangement of mitochondria occurred by expressing Drp-1K38A, Mfn-1 and Mfn-2, which presented either elongated or fused mitochondrial structures. In addition, Opa-1 and Fis-1 expression in these cells led to fragmentation of the mitochondrial network. Again, we could not find changes when wild type Drp-1 was expressed. We also enumerated the observed changes by scoring MitoGFP-positive cells for their mitochondrial appearance and found that mitochondria of MCF-7 and COS-7 possessed alteration to a similar degree as in HeLa cells (data not shown).

5.3.2 Effect of mitochondrial network regulating proteins on apoptosis

Fission and fusion controlling proteins have been recently implicated to play a role in the regulation of apoptosis. It has been suggested that by over-expression of either Drp-1K38A or Opa-1 mitochondria were not only induced to
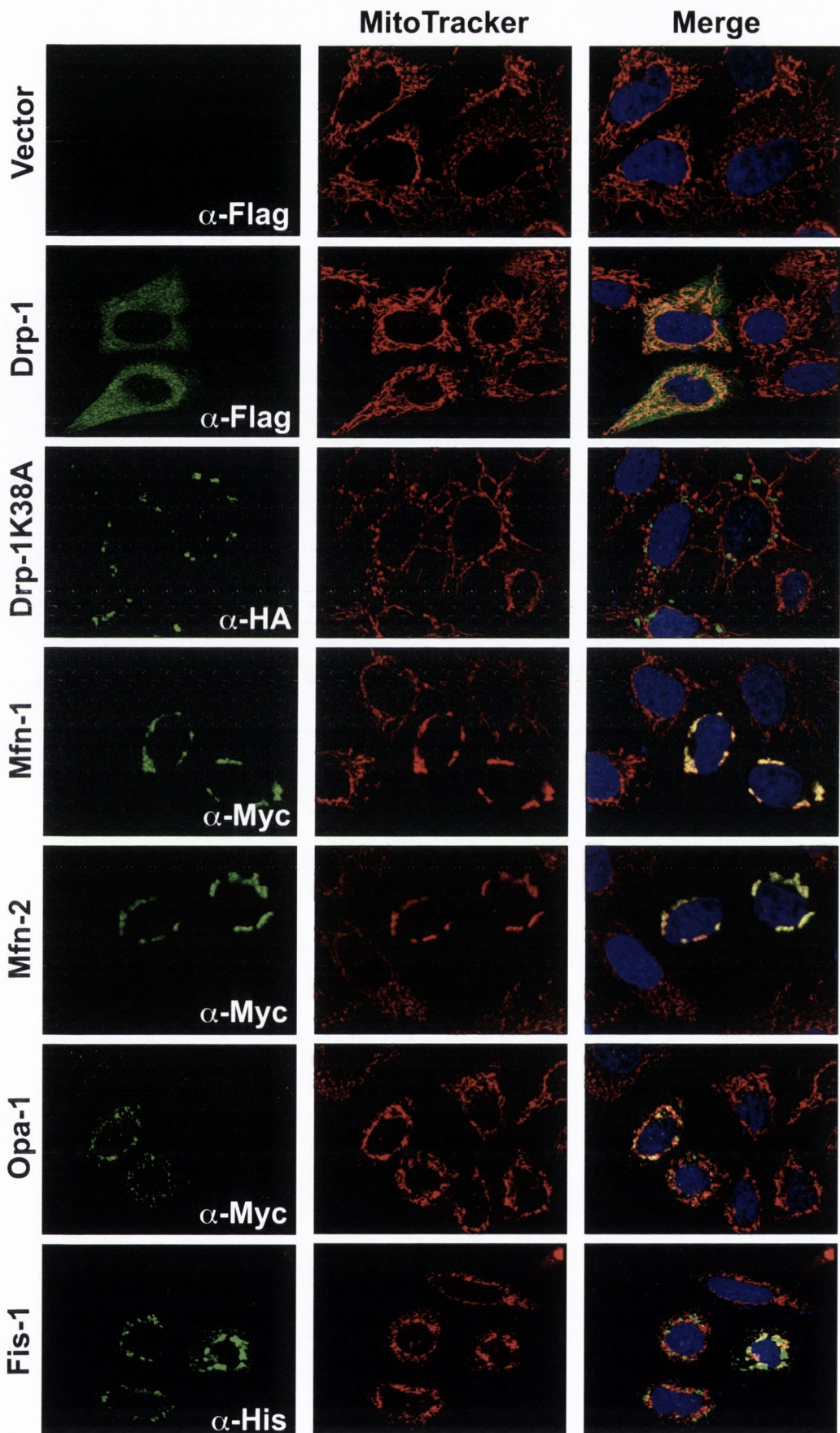
Figure 5.2: Fission and fusion proteins expressed in HeLa cells, change mito-chondria

HeLa cells were transfected with 1 μg of either pCDNA3 vector, or expression plasmids encoding the indicated components of the mitochondrial fission/fusion machinery. 24 hours later, cells were stained with mitotracker dye (50 nM, 30 min, 37°C) followed by immunostaining for overexpressed genes using anti epitope-tag antibodies, as indicated in the left hand panels. Pictures depict representative areas. Confocal images were taken on an Olympus laser-scanning microscope FV1000 at 60 X magnification.
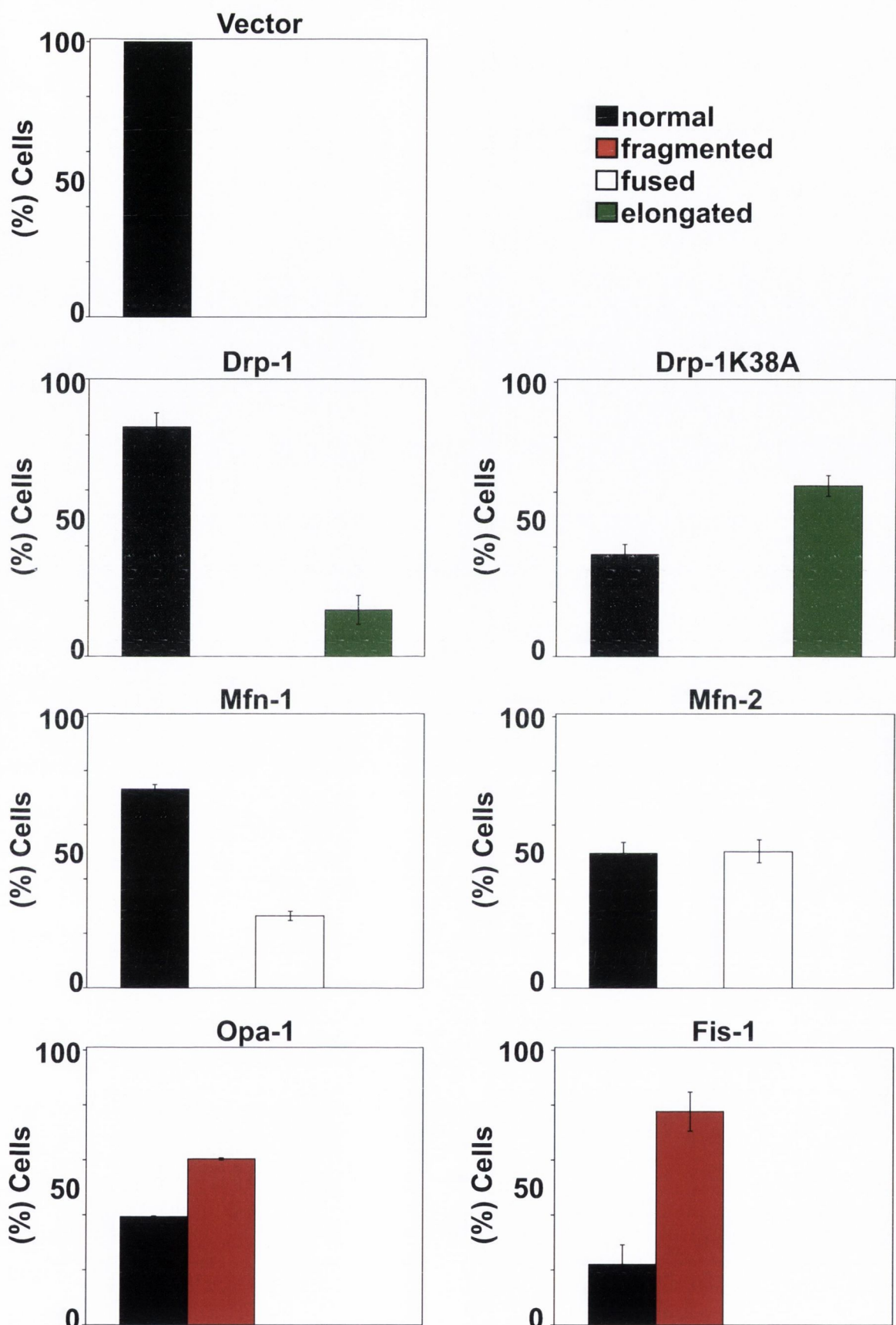
Figure 5.3: Quantification of mitochondrial phenotypes in HeLa cells
Mitochondrial phenotypes of cells transfected with the indicated protein expressing plasmids (1 µg for Drp-1, Drp-1K38A, Mfn-1 and Mfn-2; 0.5 µg for Opa-1 and 0.2 µg for Fis-1) were scored after 24 hours. First cells were stained with MitoTracker dye before performing immunostaining with anti-epitope-tag antibodies. In stained cells, mitochondrial networks were scored as normal (black), fragmented (red), fused (white) or elongated (green) by comparison to the empty vector transfected control. Data are triplicate counts of 100 cells from a representative experiment.

fuse, but also that apoptosis and the release of cytochrome *c* from the mitochondrial intermembrane space was inhibited (Frank *et al.*, 2001; Arnoult *et al.*, 2005b; Cipolat *et al.*, 2006). We wondered if we could reproduce these findings and observe enhancement or inhibition of apoptosis in the presence of fission and fusion proteins. Therefore, we transfected HeLa cells with the fission and fusion proteins along with a GFP-reporter and induced apoptosis with chemotherapeutic drugs. After evaluation of the right drug dose for death induction (Figure 5.4), we added this concentration on transfected HeLa cells. GFP-positive cells were used to score the percentage of dying cells with apoptotic morphology (Figure 5.4, A). We used 5 µM actinomycin D on cells transfected as shown in figure 5.5, A, and incubated cells for 12 hours. After this period, we observed cell death occurring indistinguishable from vector-transfected cells in those cells expressing Drp-1, Drp-1K38A, Mfn-1 and Mfn-2. This indicated that expression of Drp-1 containing plasmid did not enhance apoptosis, expression of the fusion promoting proteins Drp-1K38A, Mfn-1 and Mfn-2 alone also had no effect on death of HeLa cells, and the same was true when actinomycin D was added. We could not find inhibition of apoptosis by expression of fusion proteins under our experimental conditions. In contrast, expressing Opa-1 or Fis-1 in HeLa cells, which were left untreated led to an increased number of dead cells to a total of 30 percent. As a control for cell death inhibition, transfection of cells with the potent inhibitor of apoptosis Bcl-xL was included in our experiments. This showed that compared to the fission and fusion proteins, Bcl-xL blocked apoptosis very efficiently.

To further examine the influence of fission and fusion proteins on apoptosis and to exclude that the effects seen were due to the drug used, we included another range of drugs. The protease inhibitor TPCK and DCI were used at 50 µM and induced apoptosis to about 40-50 percent in vector-transfected cells (Figure 5.5, B and C). Again, cells expressing Bcl-xL completely opposed the death-inducing stimuli. Neither inhibition, nor enhancement of apoptosis could be observed with fusion and fission proteins, respectively. Similar results, as shown in figure 5.5, A, were seen for Opa-1, Fis-1 and Bax transfected cells.

Finally, we wondered if fission and fusion proteins could modulate the outcome of other proteins that induce apoptosis in HeLa cells. The BH3-only
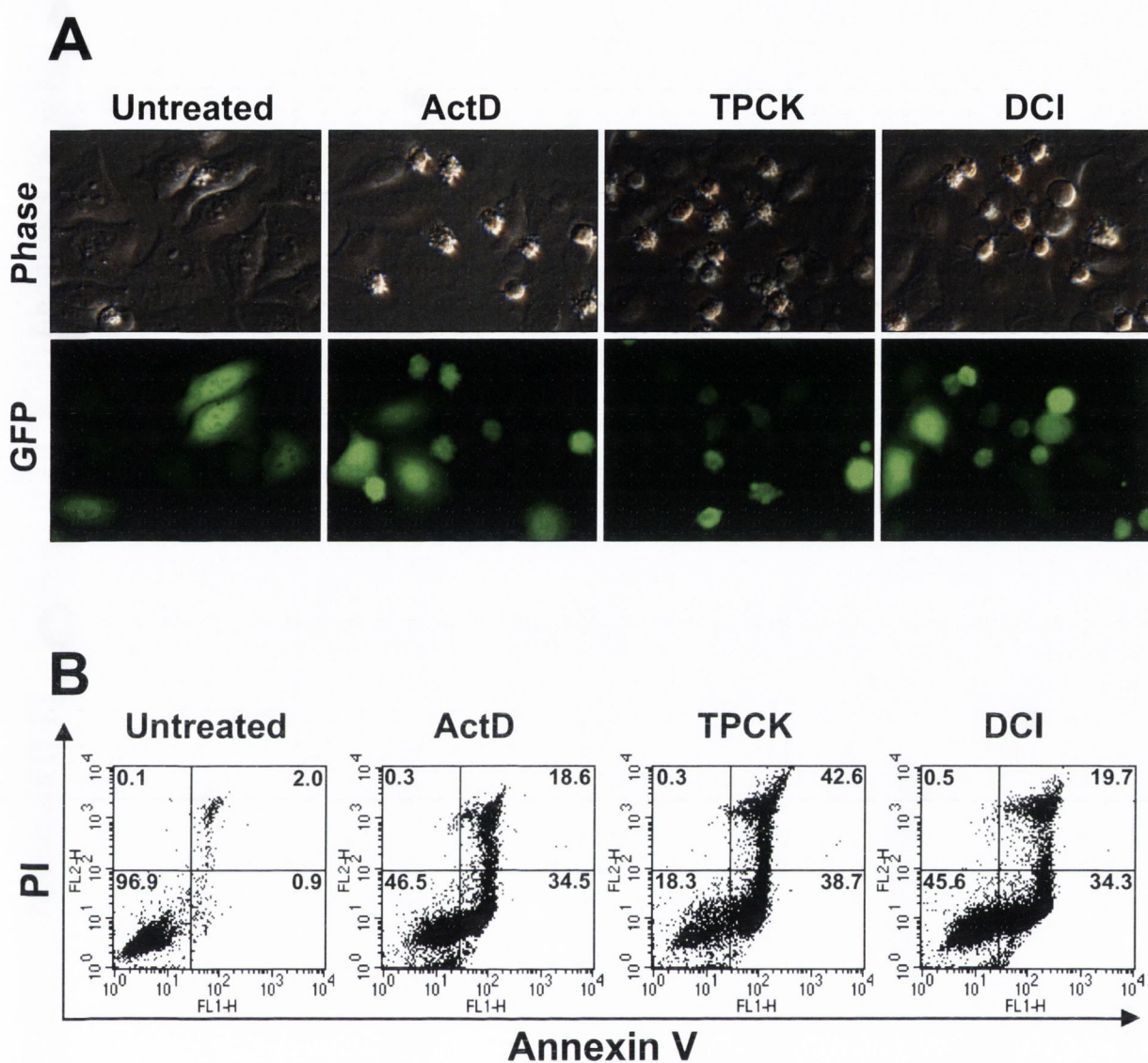
Figure 5.4: Demonstration of typical apoptosis detection methods
A) HeLa cells, transfected with 1 µg empty vector along with a GFP-reporter plasmid (50 ng) were treated with actinomycin D (5 µM), TPCK (50 µM) or DCI (50 µM) for 10-12 hours. Representative images of cells with typical features of apoptosis are shown. In each treatment rounding of the cell, plasma membrane blebbing and cell detachment from the tissue culture dish were observed. B) Cells treated as in (A) were analyzed by flow cytometry for annexin V-binding and PI uptake, as described in experimental procedures. Numbers represent the % of cells in each quadrant out of a total of 10,000 cells analysed per condition. Dotplots are representative of at least three independent experiments.
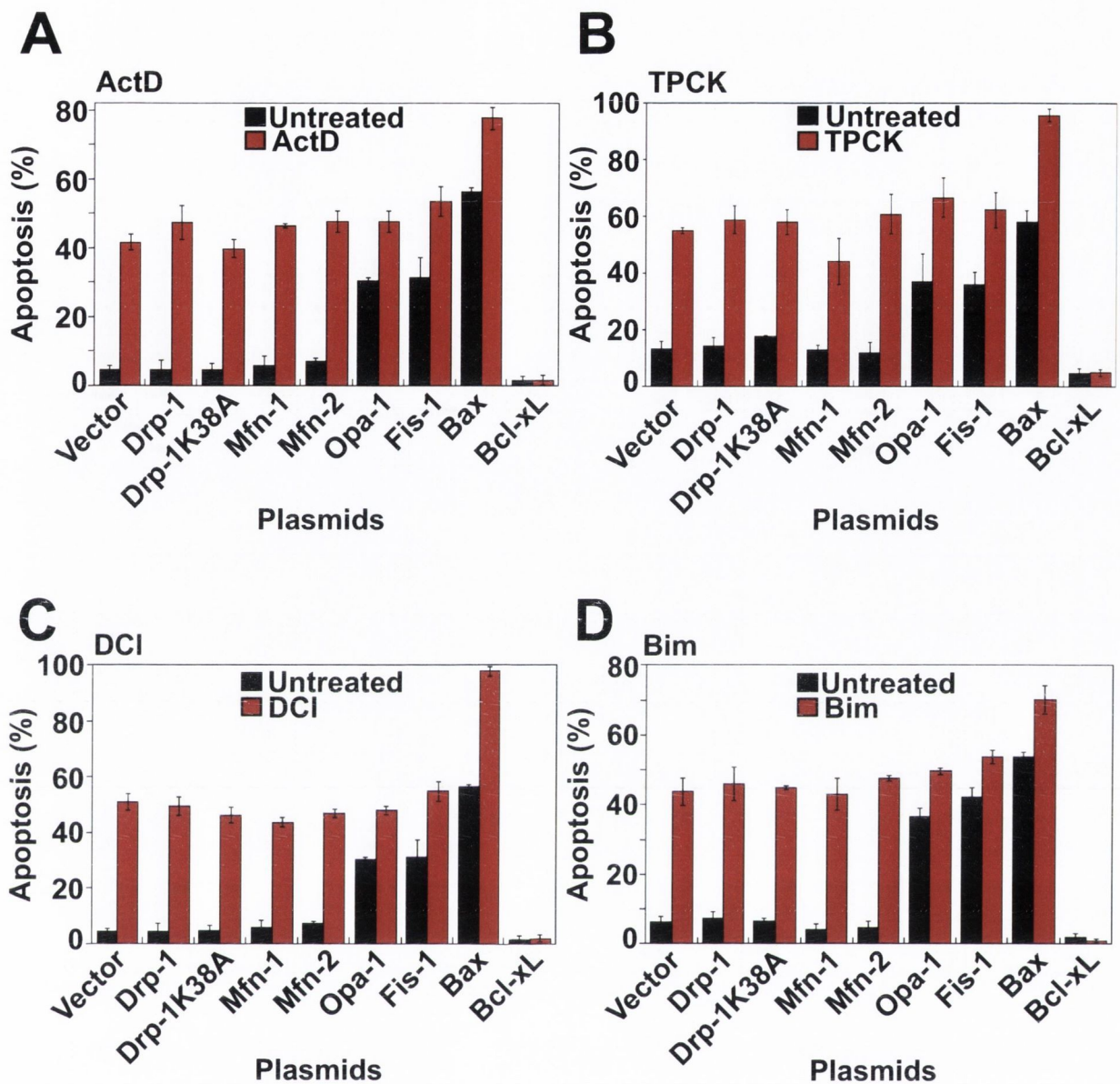
Figure 5.5: Proteins that regulate mitochondrial fission and fusion are not important for apoptosis in HeLa cells

HeLa cells transfected with either 1 µg of plasmids encoding Drp-1, Drp-1K38A, Mfn-1, Mfn-2 and Opa-1, 0.5 µg of Fis-1, 0.2 µg of Bax or Bcl-xL plasmids, along with 50 ng of a GFP-reporter plasmid were treated after 24 hours after transfection for apoptosis induction with (A) ActD (5 µM), (B) TPCK (50 µM), or (C) DCI (50 µM). Cell death was scored in GFP-positive cells 10-12 h later. Where cell death was induced by overexpression of Bim (D), cells were transfected with 50 ng of Bim encoding plasmid at the same time as the other plasmids indicated and cell death was quantitated 18 hours later. Results are representative of three independent experiments with counts of 100 cells per treatment.
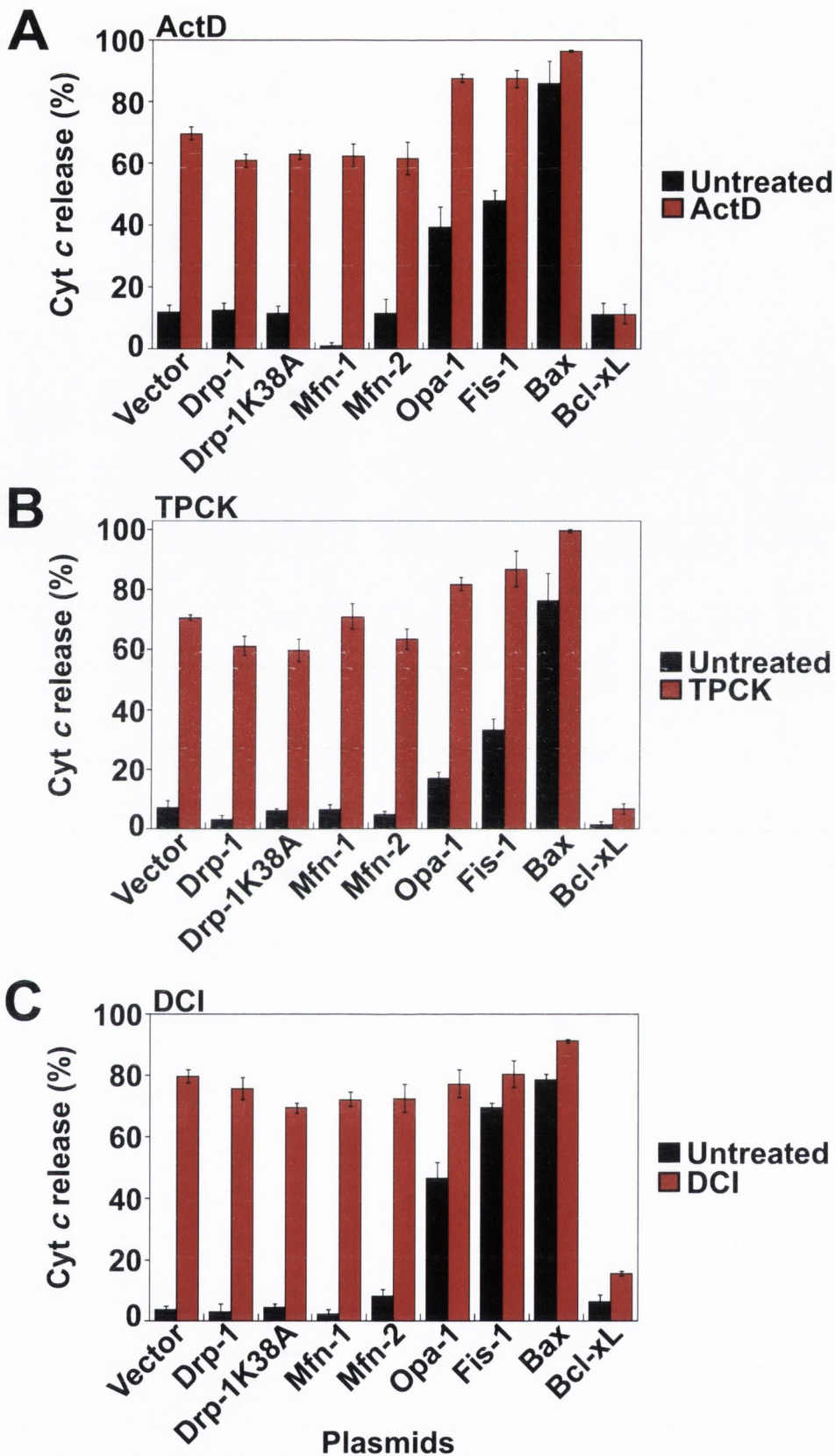
Figure 5.6: Proteins that regulate mitochondrial fission and fusion cannot block apoptosis-associated cytochrome *c* release

HeLa cells were transfected with 150 ng of MitoGFP reporter plasmid along with 1 µg of plasmids encoding Drp-1, Drp-1K38A, Mfn-1, Mfn-2 and Opa-1, 0.5 µg of Fis-1, 0.2 µg of Bax or Bcl-xL encoding plasmids. After 24 hours, cells were treated with (A) ActD (5 µM), (B) TPCK (50 µM), or (C) DCI (50 µM), in the presence of 50 µM zVADfmk to block cell detachment. 10-12 hours later cells were fixed and stained with an antibody specific for cytochrome *c*, followed by assessing cytochrome *c* release in MitoGFP-positive cells. Results are representative of three independent experiments with counts of 100 cells per treatment.
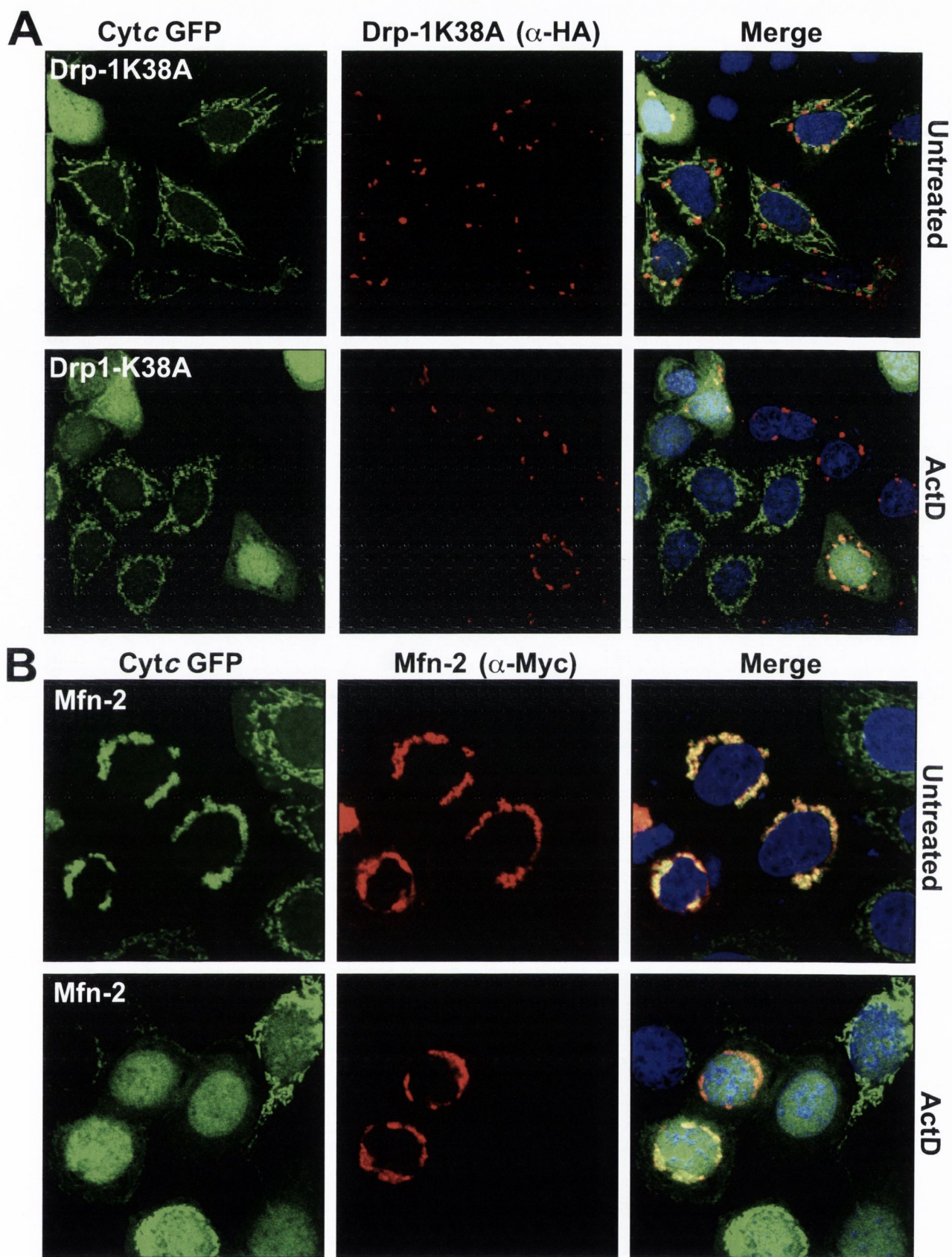
Figure 5.7: Drp-1K38A and Mfn-2 cannot block ActD-induced cytochrome *c* release

HeLa cells expressing GFP-tagged cytochrome *c* were transfected with 1 µg of Drp-1K38A (A) or Mfn-2 (B) expression plasmids and were then either left untreated or treated with ActD (5 µM). The pan-caspase inhibitor zVADfmk (50 µM) was included to block cell detachment. After 12 hours drug-incubation cells were stained for Drp-1K38A with α-HA or for Mfn-2 with α-Myc. Representative confocal images were taken on an Olympus laser-scanning microscope FV1000 at 60 X magnification.

protein Bim is a direct activator of apoptosis by stimulating Bax translocation to mitochondria and thereby cytochrome *c* release. In this experiment we combined expression of fission and fusion proteins, transfected as above, with 50 ng Bim encoding plasmid, a concentration that was sufficient to kill cells. Again, while Bcl-xL very potently inhibited apoptosis, no effect was observed for fission and fusion proteins (Figure 5.5, D). Bim augmented Bax-induced death as it was with all the drugs we used above.

Since all the results we obtained could have been due to the used cell type, we repeated our apoptosis experiments in MCF-7 and COS-7 cells, as we did for examination of the mitochondrial phenotype in the section above. In those two cell types, we obtained almost equal results as in HeLa cells, which indicated that the cell type did not play a role (data not shown). Taken together, these results indicated that modulation of mitochondria by fission and fusion proteins did not change the outcome of apoptosis induction. This was in contrast to the expression of Bcl-xL, which potently blocked cell death in these experiments in all cell types tested.

5.3.3 Regulation of cytochrome *c* release by the fission/fusion-super-family

As shown above, we found no evidence for a role of the fission and fusion proteins in apoptosis regulation. However, we wondered if they could possibly modulate the release of cytochrome *c* to some extent. HeLa cells were transfected with the mitochondrial marker MitoGFP along with varying amounts of fission or fusion proteins as described in figure 5.6. After sufficient time for protein expression, cells were either left untreated, or treated with different chemotherapeutic drugs. They were then fixed and stained for endogenous cytochrome *c* and we scored MitoGFP-positive cells for the percentage of cells that had released cytochrome *c*. Cells expressing Fis-1 and Opa-1 displayed cytochrome *c* release even before treatment with apoptosis-inducing drugs. This effect was increased by the addition of ActD, TPCK or DCI (Figure 5.6, A-C). Mitochondrial fusion or elongation induced by the expression of Drp-1K38A, Mfn-1 or Mfn-2 failed to block the release of cytochrome *c* after treating cells
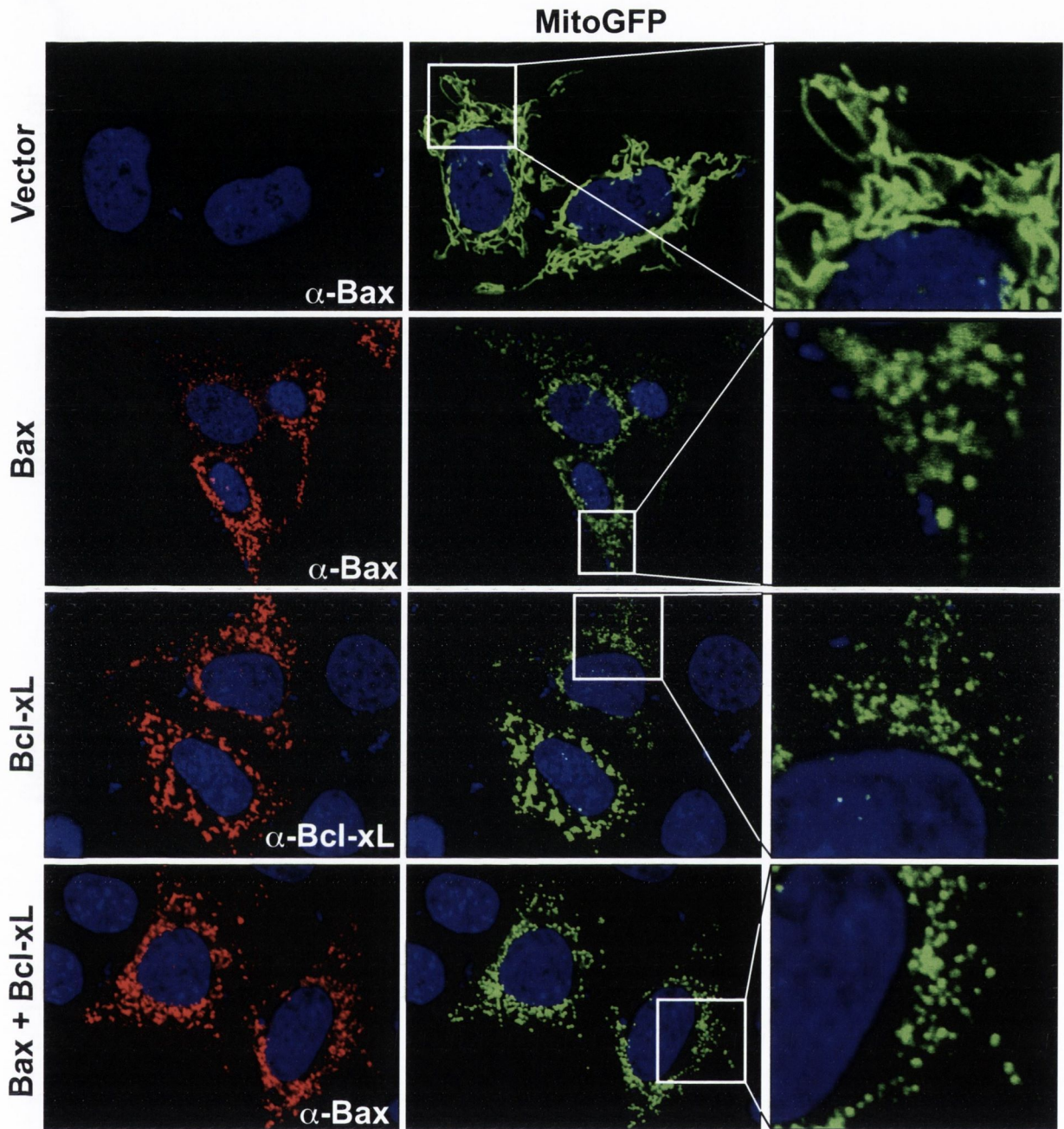
Figure 5.8: Bcl-xL failed to block Bax-induced mitochondrial fragmentation
HeLa cells were transfected with 150 ng MitoGFP along with 200 ng of empty vector, or plasmids encoding Bax, Bcl-xL, or a combination of both. All treatments were carried out in the presence of 50 µM zVADfmk to block cell detachment. After overnight expression, cells were fixed and stained for Bax or Bcl-xL as indicated, and analysed by confocal microscopy. The right hand panels represent enlargements of the boxed regions within the middle panels. Representative confocal images were taken on an Olympus laser-scanning microscope FV1000 at 60 X magnification.

Figure 5.9: Bcl-xL can block Bax induced apoptosis and cytochrome *c* release

A) HeLa cells stably expressing cytochrome *c*-GFP were transfected with plasmids encoding Bax (200 ng), Bcl-xL (800 ng), or a combination of both. Cells were then fixed and stained for Bax or Bcl-xL, as indicated. Note the complete retention of cytochrome *c* in mitochondria when Bax is co-expressed with Bcl-xL. B) HeLa cells were transfected with the indicated amounts of Bax and Bcl-xL expression plasmids, along with 50 ng of a GFP reporter plasmid and apoptosis
was quantitated in transfected cells after 18 hours. C) HeLa cells were transfected with 150 ng MitoGFP-reporter plasmid along with the indicated amounts of Bax and Bcl-xL plasmids. 18 hours later, cells were fixed and immunostained for cytochrome *c*, followed by quantitation of the % of MitoGFP-positive cells that had released cytochrome *c*. Immunostaining experiments were done in the presence of 50 μM zVADfmk to block cell detachment. Representative confocal images were taken on an Olympus laser-scanning microscope FV1000 at 60 X magnification. Results are representative of three independent experiments with counts of 100 cells per treatment.

with ActD, TPCK or DCI (Figure 5.6, A-C). In contrast, Bcl-xL expression did very efficiently inhibit the release of cytochrome *c* in all treatments.

We further looked at a cell type stably expressing cytochrome *c* tagged to GFP. In these cells, the kinetics of cytochrome *c* release are the same as the endogenous protein after induction of apoptosis (Goldstein *et al.*, 2000). When we transfected these cells with Drp-1K38A and stained them with anti-HA to reveal Drp-1K38A expressing cells, we saw mitochondrial elongation in untreated ones. Nevertheless, these cells failed to display any retention of cytochrome *c* in mitochondria after treatment with ActD (Figure 5.7, A). In addition, cells expressing Mfn-2 also failed to inhibit cytochrome *c* release although exhibiting fused mitochondrial structures, which were apparent by Mfn-2 immunostaining (Figure 5.7, B).

These findings were in agreement with the results obtained looking at the influence of fission and fusion proteins on apoptosis.

5.3.4 Uncoupling cytochrome *c* release from fragmentation of mitochondrial networks

After the onset of apoptosis, the network of mitochondria fragments into sphere-like small organelles that are dispersed throughout the cell or gathered around the nucleus. Expression of Bax in mammalian cells induced such a mitochondrial phenotype (Desagher and Martinou, 2000), as did the treatment of cells with apoptosis-inducing drugs (Frank *et al.*, 2001). We confirmed this observation by expressing Bax in HeLa cells (in the presence of zVADfmk to block apoptosis) and analyzed mitochondria with MitoGFP. Bax-positive cells, detected by specific immunostaining, revealed a fragmented mitochondrial network compared to empty-vector transfected cells (Figure 5.8, first and second row panels). Since Bcl-xL was a very strong inhibitor of apoptosis (Figure 5.9, B) we wondered if it could also block Bax-induced mitochondrial fragmentation. To our surprise, Bax and Bcl-xL co-expression also displayed a seemingly fragmented phenotype of mitochondria (Figure 5.8, bottom panels and Figure 5.11). Despite this, when we examined cells co-expressing Bax and Bcl-xL for their cytochrome *c* state, we found it retained in mitochondria. Figure 5.9, A shows that although the mitochondrial network was vastly fragmented,
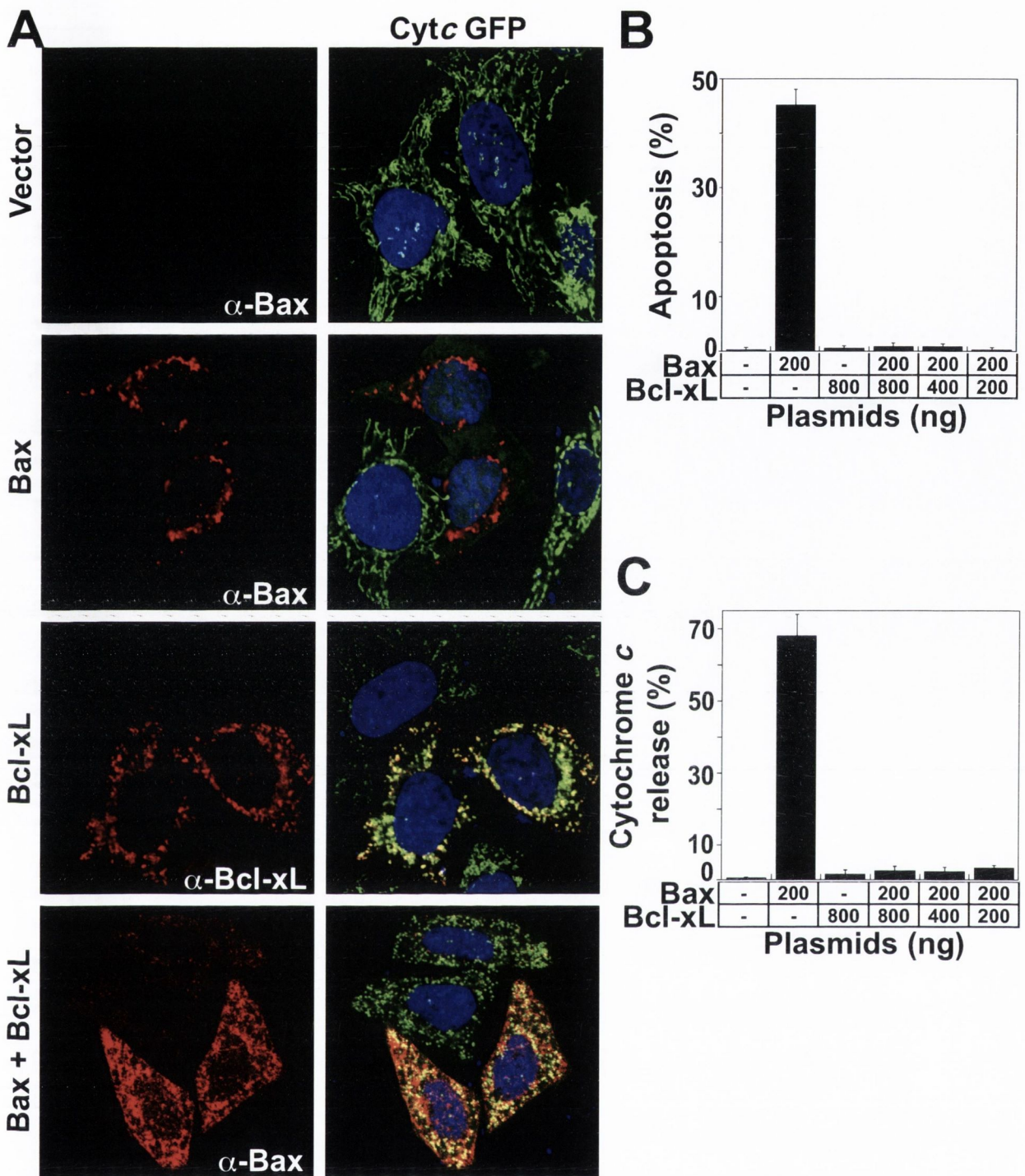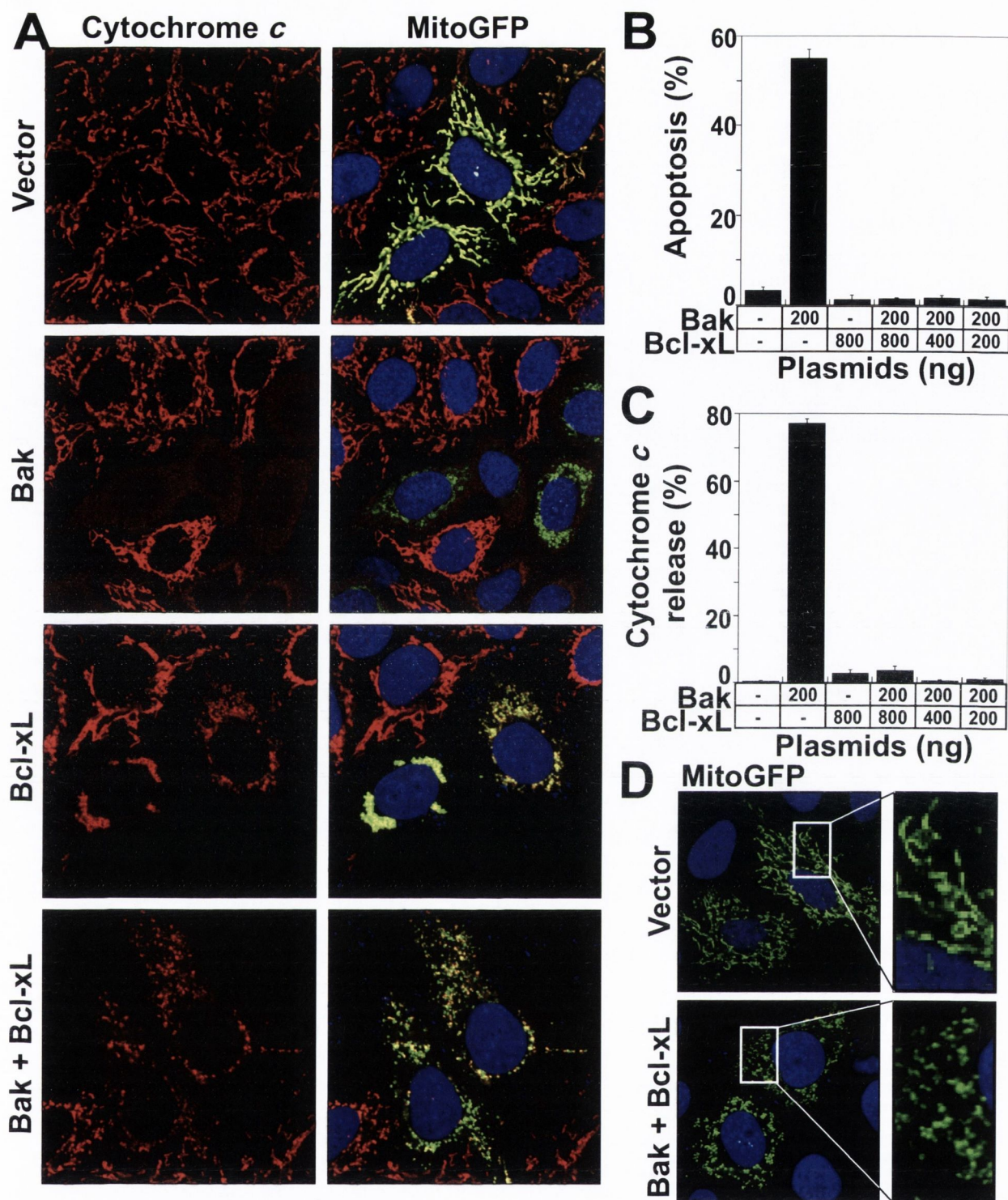
Figure 5.10: Bcl-xL can block Bak induced apoptosis and cytochrome *c* release

A) HeLa cells were transfected with 150 ng MitoGFP and plasmids encoding Bak (200 ng), Bcl-xL (800 ng), or a combination of both. Cells were fixed and stained for endogenous cytochrome *c*. Note the complete retention of cytochrome *c* in mitochondria by Bcl-xL when Bak is co-expressed. B) HeLa cells were transfected with the indicated amounts of Bak and Bcl-xL expression plasmids, along with 50 ng of a GFP-reporter plasmid and apoptosis was quantitated in transfected cells after 18 hours. C) HeLa cells were transfected with 150 ng of MitoGFP-reporter plasmid along with the indicated amounts of Bak and Bcl-xL plasmids. 18 hours later, cells were fixed and immunostained for cytochrome *c*, followed by quantitation of the % of MitoGFP-positive cells that had released cytochrome *c*. D) Cells transfected as in A). Immunostaining experiments were done in the presence of 50 µM zVADfmk to block cell detachment. Representative confocal images were taken on an Olympus laser-scanning microscope FV1000 at 60 X magnification. Results are representative of three independent experiments with counts of 100 cells per treatment.
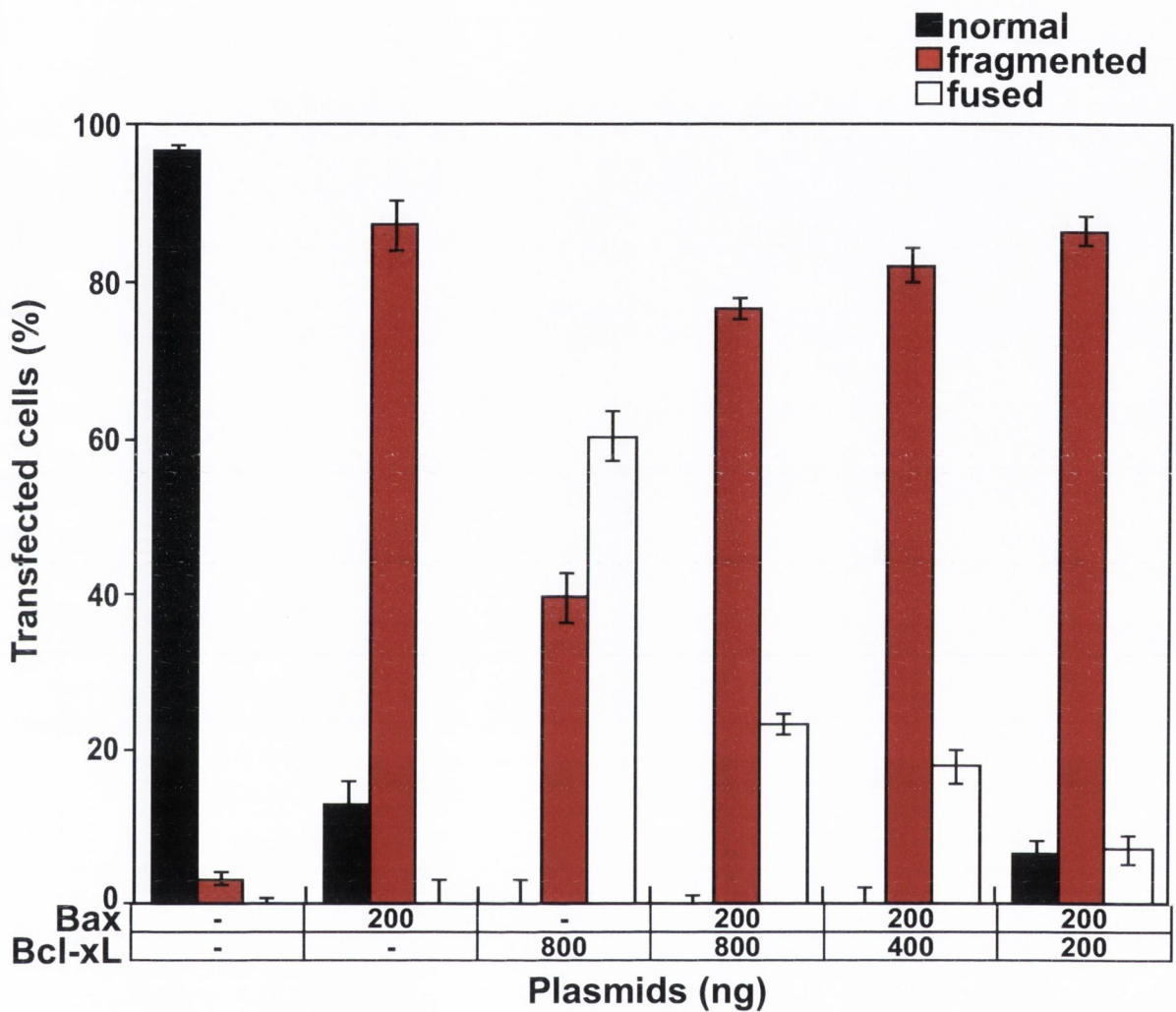
Figure 5.11: Quantitation of Bax-induced mitochondrial fragmentation
HeLa cells were transfected with 150 ng MitoGFP along with the indicated amounts of either empty vector, or plasmids encoding Bax, Bcl-xL, or a combination of both. All treatments were carried out in the presence of 50 μM zVADfmk to block cell detachment. After overnight expression, cells were fixed and stained for Bax or Bcl-xL as indicated, and scored for the % of MitoGFP-positive cells with a rearranged mitochondrial phenoytpe. Result is representative of three independent experiments with counts of 100 cells per treatment.

this had no effect on the state of cytochrome *c*. Bcl-xL, although completely blocking cytochrome *c* release in Bax-expressing cells, could not block the fragmentation of the mitochondrial network (Figure 5.9, C). This might be due to Bcl-xL itself, which on its own fragmented mitochondria in about 40 % of the cells (Figure 5.8, third row panels and Figure 5.11). In addition to the above, we included Bak in our experiments (Figure 5.10). We obtained almost identical results for Bak and Bcl-xL co-expression in HeLa cells as seen with Bax. Albeit Bcl-xL blocked Bak-induced cytochrome *c* release and apoptosis (Figure 5.10, B and C), it could not block Bak-induced mitochondrial fragmentation (Figure 5.10, D).

Because Bcl-xL caused a fragmented mitochondrial phenotype when it was expressed alone, it was difficult to assign the fragmentation phenotype of Bax plus Bcl-xL to one of the two proteins. Therefore, we decided to examine another member of the anti-apoptotic protein family, Mcl-1, which seemingly had no effect on mitochondrial dynamics. We transfected HeLa cells with the mitochondrial marker MitoGFP along with Mcl-1 encoding plasmid. Mcl-1, which was mainly localized to the cytoplasm as seen by specific immunostaining, had no effect on the mitochondrial network in contrast to Bax (Figure 5.12). In addition, Mcl-1 could not block Bax-induced mitochondrial fragmentation (Figure 5.12). However, examining cytochrome *c* release induced by Bax or Bak, we found that in a dose-dependent manner, Mcl-1 could block apoptosis and cytochrome *c* release (Figure 5.13 and 5.14).

These results gave strong evidence, that fragmentation of mitochondria can occur in the absence of MOMP, seen by retention of cytochrome *c* and inhibition of apoptosis. Therefore, fragmentation might be an accompanying element occurring during apoptosis, but is not sufficient to cause it by the mere breakdown of the mitochondrial network. In order to induce apoptosis, cytochrome *c* must be released and this is dependent on MOMP.

5.3.5 Mitochondrial fragmentation induced by BH3-only proteins

The Bcl-2-family subgroup of BH3-only proteins activates Bax and/or Bak to induce apoptosis either directly by binding to them, or indirectly by sequestering anti-apoptotic family members. We wondered if the expression of direct Bax
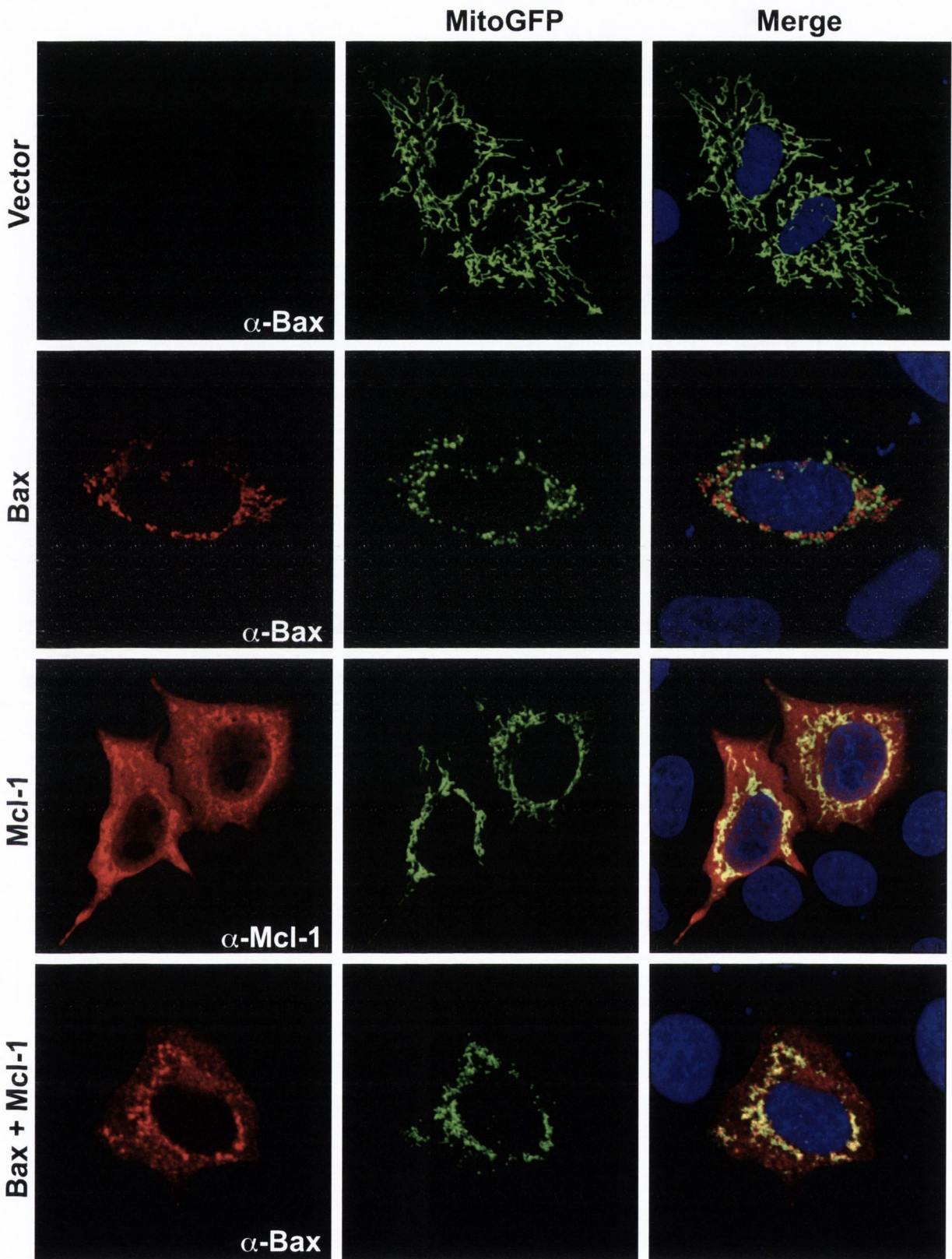
Figure 5.12: Bax induced mitochondrial fragmentation is not blocked by Mcl-1
HeLa cells were transfected with 150 ng of MitoGFP along with either 200 ng Bax,
800 ng Mcl-1, or a combination of both. After 24 hours cells were stained for Bax or
Mcl-1 with specific antibodies, as indicated and analyzed on the microscope. Note
that Mcl-1 alone did not change the mitochondrial network and also failed to block
Bax-induced mitochondrial fragmentation. Pictures depict representative areas. Con-
focal images were taken on an Olympus laser-scanning microscope FV1000 at 60 X
magnification.
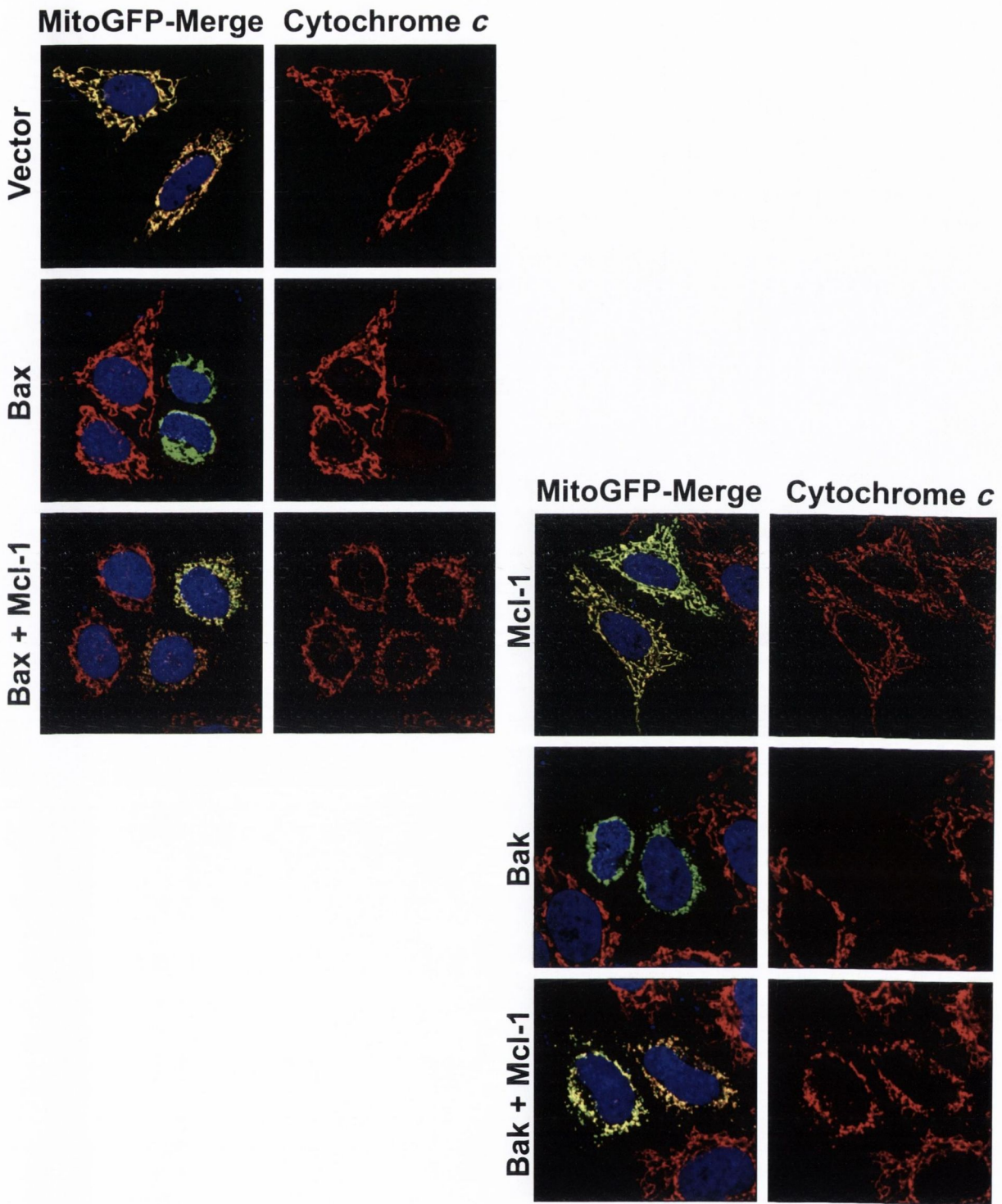
Figure 5.13: Mcl-1 blocks Bax- or Bak-induced cytochrome *c* release
HeLa cells, transfected with 150 ng MitoGFP along with 200 ng of expression plasmids encoding Bax or Bak and 800 ng Mcl-1, or combinations of Bax/Mcl-1 and Bak/Mcl-1 as indicated, were stained after 24 hours for endogenous cytochrome *c*. Of note is that expression of Mcl-1 alone failed to perturb the mitochondrial network, but it was able to block cytochrome c release induced by Bax or Bak. Pictures depict representative areas of target-gene expressing cells, detected by MitoGFP expression. Confocal images were taken on an Olympus laser-scanning microscope FV1000 at 60 X magnification.
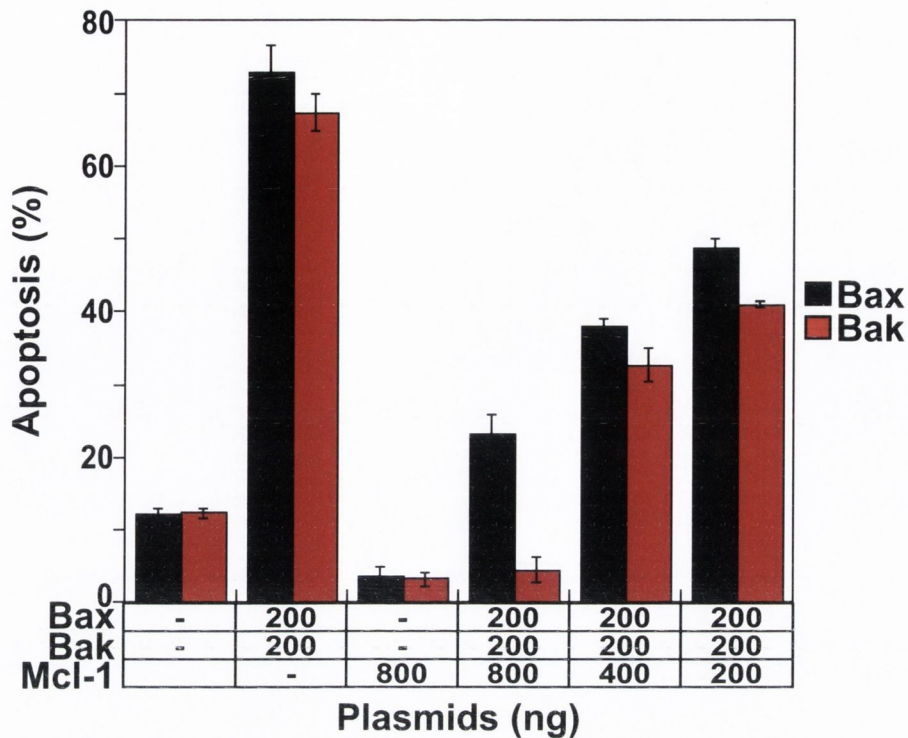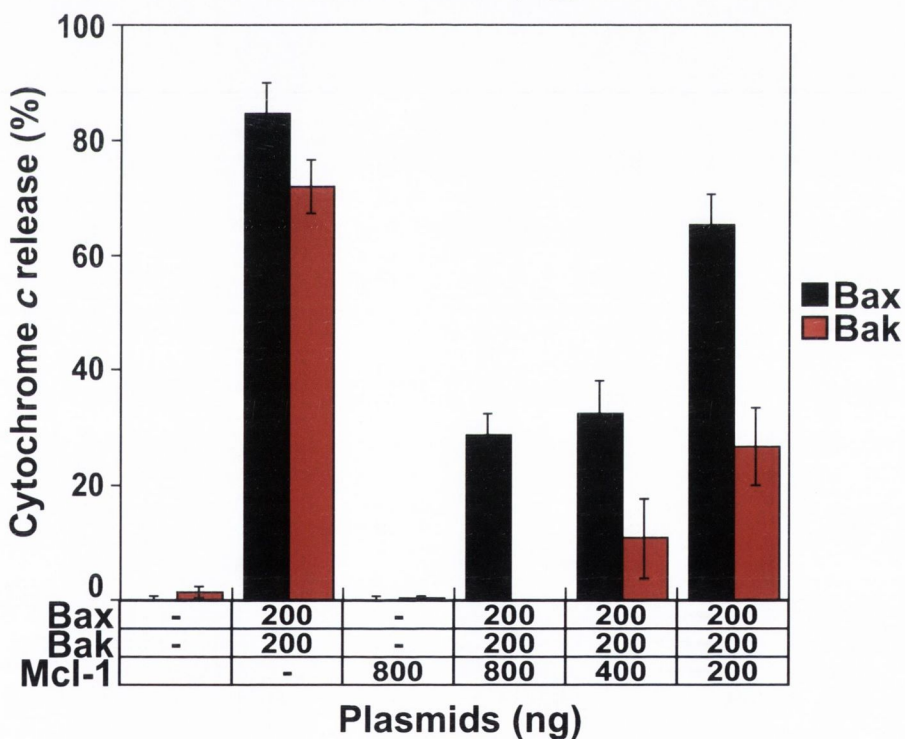
Figure 5.14: Quantification of Mcl-1 blocking apoptosis and cytochrome *c* release induced by Bax or Bak

A) HeLa cells were transfected with the indicated amounts and combinations of Bax, Bak and/or Mcl-1 encoding plasmids along with a GFP-reporter. After overnight expression, cells were scored for % cells with apoptotic morphology of GFP-expressing cells. B) HeLa cells were transfected with the indicated amounts and combinations of Bax, Bak and/or Mcl-1 encoding plasmids along with a MitoGFP-reporter. After 24 hours, cells were fixed and stained for cytochrome *c*, followed by quantitation of the % of GFP-positive cells that had released cytochrome *c*. Results are representative of three independent experiments with counts of 100 cells per treatment.

activators would also have an effect on mitochondria, and if this could be uncoupled from cytochrome *c* release by anti-apoptotic Bcl-xL and Mcl-1. Plus, we wanted to rule out that over-expression of the Bax-plasmid itself was responsible for what we saw in the above experiments. Therefore, we chose this indirect way of Bax activation.

HeLa cells were transfected with MitoGFP along with plasmids encoding Bcl-xL, Mcl-1 and/or Bid (Figure 5.15), and as well with Bim and Puma (data not shown). Mitochondrial fragmentation was the dominant phenotype we observed when BH3-only proteins were transfected either alone or in the mentioned combinations (Figure 5.16, A). Despite this, we found a strong blockade of cytochrome *c* release by Bcl-xL and Mcl-1, which suppressed Bid, Bim and Puma potently (Figure 5.16, B and C). In order to enumerate this effect, we transfected HeLa cells stably expressing cytochrome *c*-GFP with Bid plus Bcl-xL or Mcl-1 as shown in figure 5.17, and Bim and Puma plus or minus Bcl-xL or Mcl-1 (data not shown). We detected expression of the transfected plasmids after immunostaining with specific antibodies. While Bid on its own resulted in cytochrome *c* release of the target cells, in the combination with Bcl-xL and Mcl-1, this was abrogated (Figure 5.17). Once again, using cytochrome *c* as a read-out, the mitochondrial network appeared fragmented in both Bid/Bcl-xL and Bid/Mcl-1 expressing cells, indicating that Bid activated Bax or Bak and lead to mitochondrial fragmentation.

These results further underlined that mitochondrial fragmentation is only accompanying apoptosis, but not causing it per se, as fragmented organelles were present in perfectly healthy cells.
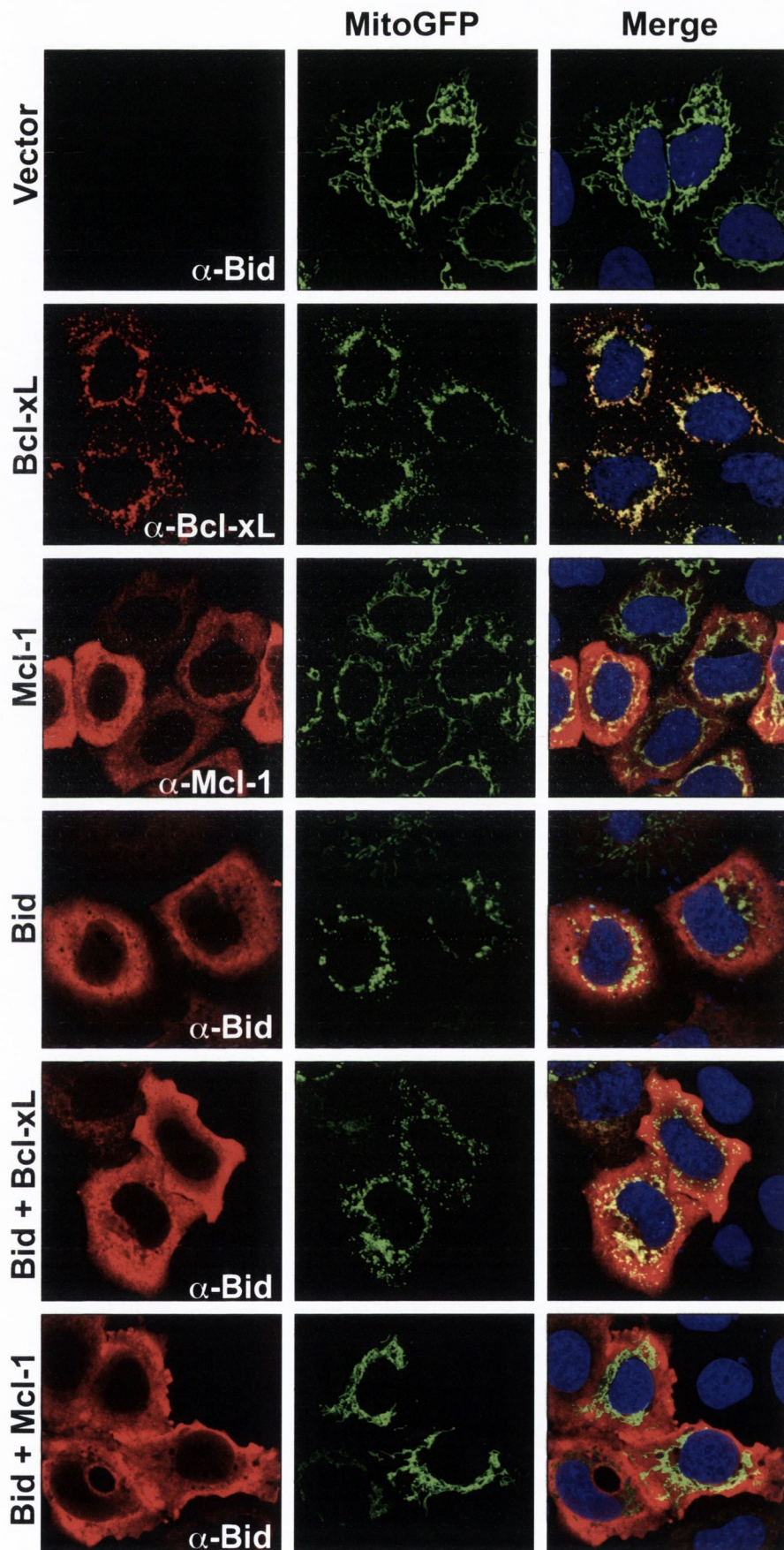
Figure 5.15: Bid induces mitochondrial alterations
HeLa cells were transfected with 150 ng of MitoGFP reporter plasmid along with 200 ng of empty vector or Bid alone or in combination with 400 ng of Bcl-xL and 800 ng of Mcl-1. After overnight incubation in the presence of 50 μM zVADfmk, cells were fixed and immunostained as indicated. Representative confocal images were taken on an Olympus laser-scanning microscope FV1000 at 60 X magnification and represent three independent epxeriments.
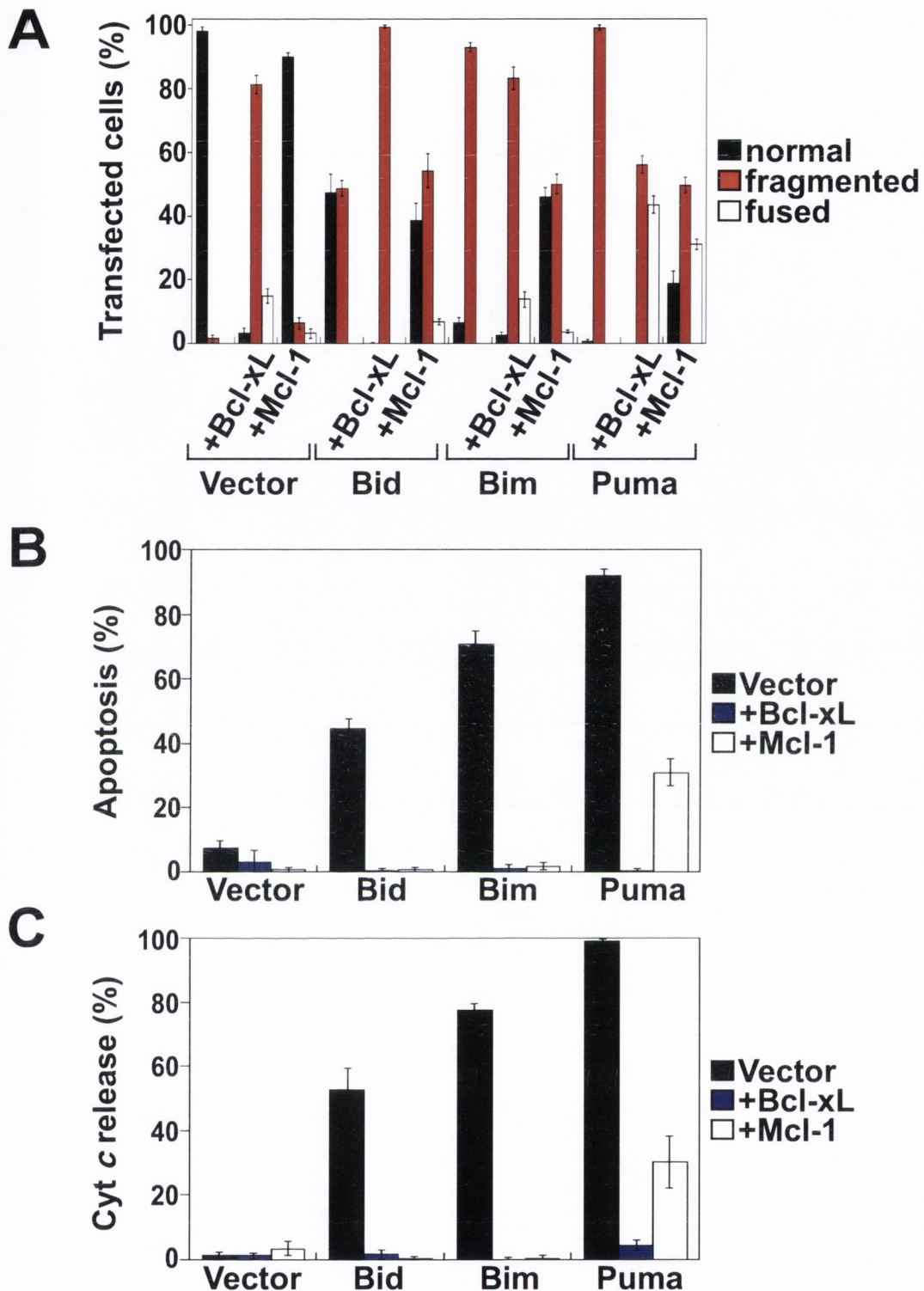
Figure 5.16: BH3-only proteins are blocked by Bcl-xL and Mcl-1 for apoptosis, cytochrome c release and mitochondrial changes

A) HeLa cells were transfected with 150 ng of MitoGPF reporter plasmid along with 200 ng of plasmids encoding Bid, Bim or Puma, plus or minus 400 ng of Bcl-xL or 800 ng Mcl-1 plasmids. After overnight incubation, mitochondrial networks in transfected cells were scored as normal, fragmented or fused. B) HeLa cells were transfected with 100 ng of a GPF-reporter plasmid along with 200 ng of plasmids encoding Bid, Bim or Puma, plus or minus 400 ng of Bcl-xL or 800 ng Mcl-1. After overnight incubation, apoptosis was scored in GFP-positive cells. C) HeLa cells were transfected with 200 ng plasmids encoding Bid, Bim or Puma, plus or minus 400 ng of Bcl-xL or 800 ng Mcl-1. After overnight incubation in the presence of 50 µM zVADfmk, cells were fixed and stained for Bid, Bim or Puma and endogenous cytochrome *c*. Release was scored in BH3-only-positive cells. All data represent triplicate counts of 100 cells per treatment.
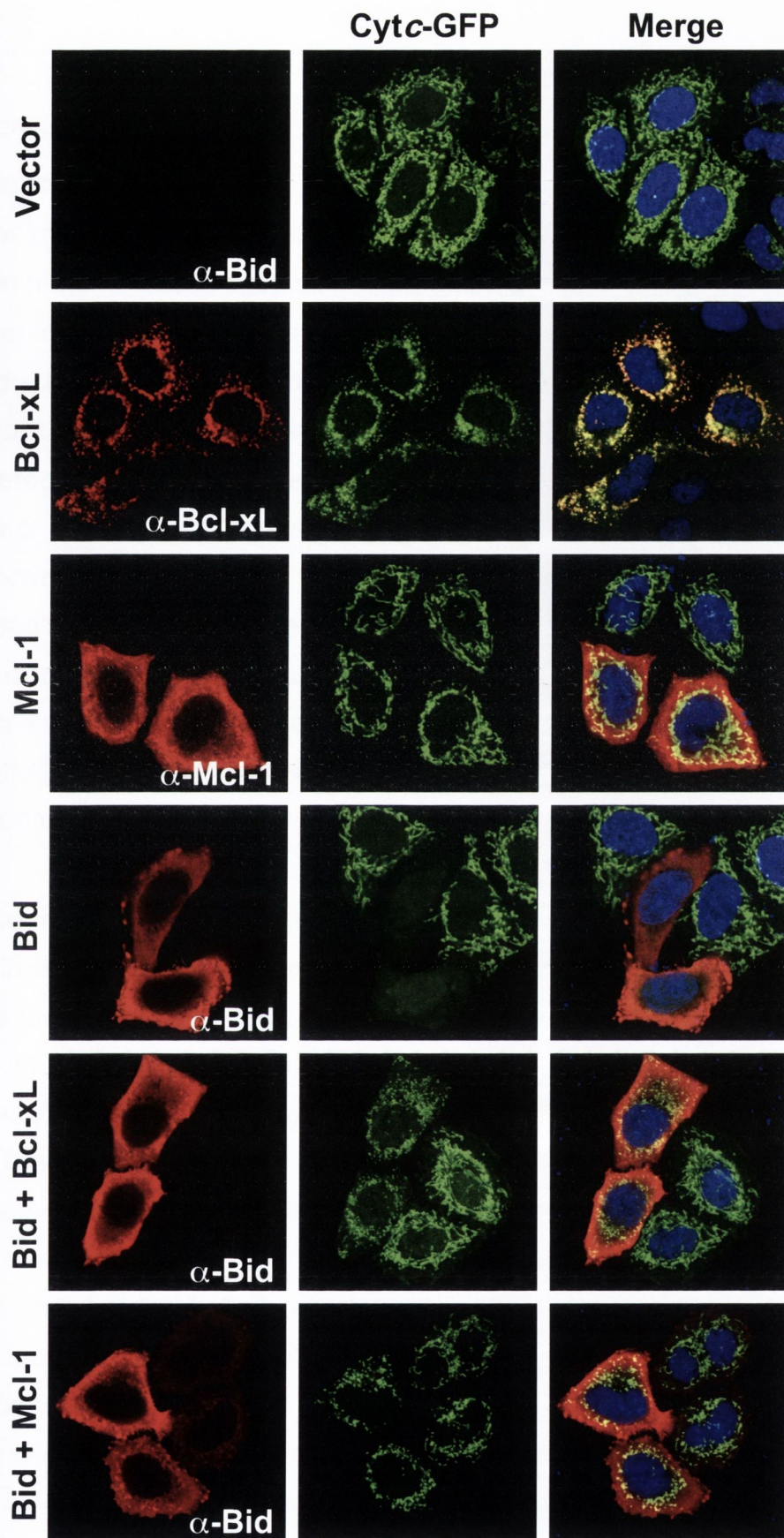
Figure 5.17: Bid-induced release of cytochrome *c* is blocked by Bcl-xL and Mcl-1

HeLa cells stably expressing cytochrome *c*-GFP were transfected with expression plasmids encoding Bid (200 ng), Bcl-xL (400 ng), Mcl-1 (800 ng) or the indicated combinations of these plasmids. After overnight incubation in the presence of 50 µM zVADfmk, cells were fixed and immunostained for Bid, Bcl-xL or Mcl-1 as indicated. Note the complete retention of cytochrome *c* in fragmented mitochondria when Bid was co-expressed with either Bcl-xL or Mcl-1. Representative confocal images were taken on an Olympus laser-scanning microscope FV1000 at 60 X magnification.

5.4 Discussion

5.4.1 Summary

In this last chapter we presented a detailed examination of the effect of fission and fusion proteins during apoptosis. Approaches commonly used to induce or inhibit apoptosis and observe its effect were employed here to see if apoptosis is modulated when mitochondria are perturbed. We used different cell types, which were expressing fusion or fission proteins, and added various chemotherapeutic drugs. However, we found no evidence to suggest that apoptosis or cytochrome *c* release was somehow influenced by their presence. Furthermore, perturbations of mitochondria indeed accompany apoptosis without leading to a life threatening effect in cells. These perturbations in fact were induced by Bcl-2 family molecules. Our findings suggest that as long as cytochrome *c* release is inhibited, no cell death can occur, regardless whether or not mitochondrial organelles are in a tubular network. This means that mitochondrial fragmentation by itself is not sufficient to induce apoptosis.

5.4.2 Mitochondrial dynamics during apoptosis

Observations of the disintegration of the mitochondrial network in cells during apoptosis led to the hypothesis that this was a crucial step for this process. Drp-1, a protein involved in the regulation of mitochondrial fission, was suggested to sensitize cells towards apoptosis by enhancing mitochondrial fission (Frank *et al.*, 2001; Szabadkai *et al.*, 2004). Unfortunately, fragmentation of the mitochondrial network by Drp-1 was never convincingly presented in those studies, as it was for example in *C. elegans* (Labrousse *et al.*, 1999). In the present study, we also did not find compelling changes for this potential function of Drp-1, confirming data from James *et al.* (James *et al.*, 2003). Expression of Drp-1 did not induce mitochondrial fission or apoptosis. Moreover we could not reproduce observations for a sensitization of cells to cell death by various drugs. Thus, it seems speculative to suggest that Drp-1 induces fission of mitochondria. In contrast, when Drp-1 was knocked down by RNA interference, or when a dominant negative mutant of Drp-1 (Drp-1K38A) was over-expressed, mitochondrial division appeared vastly blocked. This was easily detectable by mitochondrial markers, finally allowing the conclusion that

Drp-1 in fact is responsible for fission of the mitochondrial tubules. In addition, both knock down of Drp-1 and expression of Drp-1K38A, was described to render cells resistant to apoptotic stimuli (Frank *et al.*, 2001; Lee *et al.*, 2004). However, when we over-expressed Drp-1K38A in different cell lines, no inhibition of apoptosis was observed. Importantly, we compared inhibition of apoptosis by Drp-1K38A with the inhibition of Bcl-xL, a well-known inhibitor of apoptosis. Already a fifth of the amount of Bcl-xL was sufficient to block drug induced cell death very potently. Compared to our study, other groups induced apoptosis with other components and evaluated different endpoints (Frank *et al.*, 2001; Lee *et al.*, 2004; Szabadkai *et al.*, 2004). Thus, the discrepancies of the results obtained are most likely due to the different approaches.

A better candidate for sensitizing cells to apoptosis is Fis-1. We, like others found that merely its expression induced cytochrome *c* release and apoptosis (James *et al.*, 2003; Alirol *et al.*, 2006). Not only did Fis-1 induce apoptosis, it also enhanced it when cells were treated with drugs, displaying a similar behavior to Bax. Fis-1 induced apoptosis though depended on its C-terminal membrane-targeting domain and was not through activation of the Bax/Bak channel (James *et al.*, 2003). Alirol and co-workers confirmed this by examining Fis-1 in Bax/Bak double knockout cells, and suggested that Fis-1 induced apoptosis was by calcium-dependent mitochondrial dysfunction through the ER-gateway, which was not examined in our study (Alirol *et al.*, 2006). Furthermore, two groups observed that depletion of Drp-1 or Fis-1 from cells by RNA interference, might have delayed the release of cytochrome *c*, but could not prevent apoptosis, when conditions were used that activated Bax and Bak (Parone *et al.*, 2006; Estaquier and Arnoult, 2007). In those studies, it was additionally examined how Smac behaves, another inter-mitochondrial membrane space protein that is released during apoptosis. Smac release was not blocked by the absence of mitochondrial fission, indicating that the Bax/Bak channel was activated and it was only a matter of time for cytochrome *c* to exit mitochondria (Parone *et al.*, 2006; Estaquier and Arnoult, 2007). Because most of cytochrome *c* is sequestered in mitochondrial cristae structures (Scorrano *et al.*, 2002), and is associated with proteins of the electron transport chain, its release is hampered (Newmeyer and Fergusion-Miller, 2003). Compared to

this, Smac is a freely diffusing intermembrane space protein, which can quickly flux out of a pore formed in the mitochondrial outer membrane (Uren *et al.*, 2005). The analyses in this study by Uren *et al.* were undertaken on isolated and fractionated cells, showing that release of cytochrome *c in vitro* is much dependent on the buffers used, which change the milieu, thereby allowing dissociation of cytochrome *c* from bound proteins. Although it was observed that different mitochondrial intermembrane space proteins like Smac, cytochrome *c* and Omi are released simultaneously in live cells and therefore, most probably use the same channel (Munoz-Pinedo *et al.*, 2006), it remains unclear if it takes more action to lure out cytochrome *c* from the intermembrane space. In light of this, mitochondrial fragmentation per se can be uncoupled from cytochrome *c* release and the induction of apoptosis.

To our surprise over-expression of Opa-1 induced fragmentation of mitochondria. This was to a lesser extend compared to Fis-1 or Bax, but in company with cytochrome *c* release and apoptosis. Although another group had made similar observations (Griparic *et al.*, 2004), this was unexpected because Opa-1 was reported to be responsible for mitochondrial fusion, which we expected to become visually apparent through over-expression of it. Indeed, the phenotype we observed was similar to the effect of silencing Opa-1 with RNA interference, where the loss of Opa-1 led to mitochondrial fragmentation and release of cytochrome *c* (Lee *et al.*, 2004; Arnoult *et al.*, 2005a). Thus, two different ways of interfering with Opa-1 resulted in the same outcome, which was perturbation of mitochondrial fusion and subsequent break down of the network. While we undertook our experiments, Olichon and colleagues published a study, where they thoroughly dissected the Opa-1 protein (Olichon *et al.*, 2007). They described eight splice-variants of Opa-1 that are differentially expressed in various organs and may have diverging roles. Most importantly, the group reported that independent of the splice variant, Opa-1 over-expression always resulted in fragmented mitochondrial networks, most probably by interfering with the endogenous fusion machinery and causing an imbalance. However, the coinciding release of cytochrome *c* and induction of apoptosis either by knockdown of Opa-1 or by its over-expression, should

depend on the Bax/Bak channel activation. This could be examined in Bax/Bak double knockout cells for example.

Since the destruction of the mitochondrial network might lead to loss of intermembrane space proteins, resulting in the demise of cells, it is tempting to speculate that the opposite effect is achieved by processes inhibiting mitochondrial fission. In fact, proteins regulating mitochondrial fusion have been described as cell protectors. Specifically, in HeLa cells when transfected with rat Fzo1, cells were protected against apoptotic stimuli (Sugioka *et al.*, 2004). However, the level of protection in that study was rather low. Another study also claimed to protect cells with Mfn-2 over-experssion using an activated Mfn-2$_{Ras}$ construct. In this study however, only one apoptotic stimulus was tested and this was not compared to protection of common inhibitors of apoptosis (Neuspiel *et al.*, 2005). In addition, it was not discernible how much Mfn-2 is expressed. We repeated similar experiments with human Mfn-1 and Mfn-2 in HeLa cells, but could not find protection from apoptosis induced by various stimuli, especially compared to the protection seen with Bcl-xL. Although presence of Mfn-1 and Mfn-2 appear largely significant for cell protection and viability as seen in MEFs of knockout animals, a correlation to their function on apoptosis remains unclear (Chen *et al.*, 2003; 2005; 2007). In fact, it has been suggested that over-expression of Mfn-2 causes cell death by inhibiting mitochondrial fusion thereby inducing fragmented clusters, similar to Opa-1 over-expression (Huang *et al.*, 2007).

Taken together, these findings question the role of proteins of the fission and fusion machinery in apoptosis. Although, maintaining proper mitochondrial physiology appears important as mutations in Opa-1 or Mfn-2 have caused human diseases (Alexander *et al.*, 2000; Zuchner *et al.*, 2004). Because Bax and Bak are absolutely required for the onset of apoptosis, above experiments would have to be considered again under this view.

5.4.3 Bcl-2 family regulate MOMP and mitochondrial dynamics

In a recent study, we suggested that proteins of the cell death inhibition machinery of *C. elegans* and mammals play a role in the dynamics of mitochondria (Delivani *et al.*, 2006). As described in chapter IV, we found that

CED-9 could induce fusion, but failed to block cytochrome *c* release in human cells. Since then, several other groups have reported about the action of the Bcl-2 family proteins on the mitochondrial permeability and regulation of mitochondrial dynamics (Karbowski *et al.*, 2007; Brooks *et al.*, 2007).

In this last chapter we wanted to scrutinize this relationship. We looked at Bax and Bak expressing cells, and found that the mitochondrial network was destroyed. Although Bcl-xL co-expression with Bax or Bak potently blocked MOMP, it did not inhibit the fragmented mitochondrial distribution. The same was true for Mcl-1, which could block Bax- or Bak-induced cytochrome *c* release, but was not able to convert the mitochondrial phenotype to a normal tubular network. This showed two things, first, mitochondrial fragmentation was indeed induced by the pro-apoptotic molecules and second, apoptosis was blocked despite the presence of a disrupted mitochondrial network. Therefore, we claimed that fragmentation of mitochondria is not important during apoptosis and this can be uncoupled from cytochrome *c* release. As the group around Youle described in an early paper, Bax coalesced into foci of mitochondrial scission sites with Drp-1 and Mfn-2 (Karbowski *et al.*, 2002). It was suggested that Bax contributed to the scission of mitochondria. However, the exact mechanism did not become clear. So the question remained if this was through activation of Drp-1 and its induction of fission, or through inhibiting Mfn-2, thereby blocking fusion. Last year Karbowski and colleagues presented data to suggest that Bax is necessary for mitochondrial elongation, because when it was inhibited by a viral protein, Bax was sequestered and the mitochondrial network became fragmented (Karbowski *et al.*, 2007). The fragmented mitochondrial network we observed by expression of Bcl-xL, could be from sequestration of Bax by Bcl-xL. However, it remains unknown if Mfn-2 is also possibly sequestered and thereby inhibited to form fusing mitochondria, resulting in the fission phenotype. In contrast to Bcl-xL, Mcl-1 does only bind to Bak but not to Bax to block apoptosis (Willis *et al.*, 2005). As apparent in our results, Mcl-1 expression did not induce mitochondrial changes. Therefore, it would be interesting to examine Bax-knockout cells, which are transfected with Mcl-1 to see if this would induce mitochondrial fragmentation by sequestration of Bak. A positive result would support the idea that Bax and Bak are essential for mitochondrial fusion. However, we favor the hypothesis that anti-apoptotic

Bcl-2 family members regulate mitochondrial fusion. Nevertheless, modulation of the mitochondrial network could be a function that all multi-BH-domain Bcl-2 molecules share. During apoptosis, this secondary task could be inhibited therefore the network fragments after cytochrome c is released. In this context BH3-only molecules might act as tools for switching anti- and pro-apoptotic proteins from one role to the other, which is outlined by their differential affinity to them (Chen *et al.*, 2005; Kuwana *et al.*, 2005).

CHAPTER VI

Discussion

6. Discussion

Regulation of the pathway of programmed cell death appears to be a complex scenario of protein activation, sequestration, interaction and break down. Such processes are evolutionary conserved from unicellular organisms to humans. Adopting elucidated pathways from lower organisms we can reconstruct mechanistic cascades for apoptosis in man. The worm *C. elegans* has been instrumental for such explorations. Its caspase CED-3 was the first gene product found to be necessary for cell death (Yuan and Horvitz, 1990). While much is already known about initiation of programmed cell death pathways, precise mechanisms are often still unresolved and additional functions of proteins involved in apoptosis, are discovered. In the present study we aimed to illuminate the subcellular localization of the proteins involved in the control of cell death in the worm and transfer such proteins into human cells. By doing this, we made some exciting observations, which designated the following approaches undertaken in this study.

C. elegans caspase CED-3 is essential for the execution of all cell death in this organism. Its absence resulted in the survival of cells that were normally destined to die during development of the nematode embryo. However, its presence in cells of worm embryos has not been shown to date. Initially we had aimed to identify the subcellular localization of this caspase in *C. elegans* embryos.

In order to do this we employed immunostaining procedures, but failed to find cells with positive CED-3 staining. All together, the reasons for this seems that there are yet unknown fundamental difficulties in generating antibodies that specifically recognize native CED-3 protein. Although twelve antibodies were used, none of them detected the protein in our approaches. Those twelve antibodies were generated with three different methods, which usually should be regarded as a quite sufficient number to find some that are specific and applicable for immunostaining. In addition, most of the antibodies tested, worked in Western blot analysis. Although this is not a direct hint towards the applicability of them for immunostaining, it still verifies the proper immunization of the host animals, i.e., that antibodies were produced that recognize some

form of CED-3. However, simply the antibody titer might have been too low for proper detection of CED-3.

While CED-4 and CED-9 *in vivo* expression patterns have now been published some time ago (Chen *et al.*, 2000), CED-3 expression has not been shown yet, which is of the same, if not more, importance. This is despite the fact that commercially available antibodies exist on the market. Such discrepancy probably reflects, that other groups have encountered similar difficulties as is described here. Alternative routes to acquire information on *in vivo* CED-3 protein expression that do not require antibodies should be explored in the future. Examples could be in situ hybridization on worm embryos. This could give ideas on the time-course of CED-3 expression throughout embryonic development, but not on the subcellular localization. Another approach could be the generation of transgenic worms with an insertion of a reporter gene (GFP) fused to the end of the CED-3 protein sequence. If such a fusion protein would be properly expressed under control of the endogenous promoter, it would allow investigation of temporal and spatial CED-3 expression *in vivo*.

Specific immunostaining could only be seen in HeLa cells expressing recombinant *C. elegans* proteins. Staining in those experiments were done with anti-tag antibodies, revealing proper expression of the proteins. Also in this context, CED-3 antibodies were not useful. However, during the course of this experiments we discovered unusual rearrangements of subcellular structures when CED-9 was expressed in cells.

In the second part of this study we chose to investigate this observation in more detail. It appeared interesting to ask whether and how CED-9 and its human homologous proteins were responsible for the seen changes. Therefore, we investigated expression of CED-9 and other Bcl-2 family members in mammalian cells. By comparison with proteins regulating fission and fusion dynamics, and by using established fusion-detecting techniques, we concluded that CED-9 and its human homologues could promote fusion. However, the precise mechanism of these events was initially not apparent. Therefore, we performed interaction studies, which displayed contacts between the Bcl-2 family members and members of the fusion machinery. This allowed

us to conclude that the mechanism of mitochondrial fusion by the Bcl-2 family proteins is through sequestration of Mfn-2 on an opposing mitochondrion. Despite this, the exact fusion events throughout the four membranes of two mitochondria cannot be simply explained by this and remains elusive to date. In addition, we did not examine endogenous protein levels and their ability to interact. In order to evaluate new protein functions in our in vitro experiments we consistently analyzed over-expressed proteins. This is a very potent tool to accelerate hidden roles of proteins and reveal their function. However, in this study the relative protein levels of over-expressed proteins were not compared to the endogenous levels of the investigated proteins. Doing this would add to the importance of our findings. In many cases though useful antibodies are lacking, which are required to determine endogenous proteins. In addition, future experiments investigating the role of Bcl-2 family proteins in mitochondrial fission and fusion should preferably occur on endogenous proteins. Using siRNA or knockout cells of all Bcl-2 family proteins, would also be of great value to observe their function on mitochondria, although one would have to consider the redundancy between these proteins.

For the past decade it has been accepted that the worm protein CED-9 and its human homologous share the same function of inhibiting apoptosis. Despite the fact that the mechanism of their inhibition is very different, the same evolutionary roots have been suggested for these proteins. In the worm, CED-9 sequesters the Apaf-1 homolog CED-4 and seizes it to mitochondria thereby preventing it from activating the caspase CED-3. In contrast, Bcl-2 and other inhibitory proteins in mammals control the release of cytochrome c from mitochondria. These two different cell death-inhibiting pathways rise the question to the functional homology between the organisms. We suggest here that an ancient evolutionary role of the CED-9/Bcl-2 family lies in another function. Their ability to regulate mitochondrial morphology is the primordial function of this family, which would explain the localization to mitochondria. Further down the evolution pathway, those proteins might have then co-opted the function to regulate cell death, and different mechanisms that have evolved from worm to mammals.

117

In the last chapter we have further analyzed the second role of the Bcl-2 family proteins in regulating mitochondrial fission and fusion. Our results point towards an independence of cytochrome *c* release and apoptosis from the morphological status of mitochondria. This conclusion is derived from the observations in chapter V, that mitochondrial fragmentation could be uncoupled from the release of the inter-membrane space protein cytochrome *c*.

In addition we examined proteins that orchestrate the day-to-day processes of fission and fusion for cell homeostasis. Since those proteins had been implicated in the regulation of apoptosis, we asked if they would display positive or negative regulation of it. Neither did we find changes of cytochrome *c* release in the presence of fission and fusion proteins alone, nor did those molecules influence the regulation of apoptosis. In contrast, we saw that Bcl-2 family proteins not only regulate cytochrome *c* retention or release but also manipulated mitochondrial structures, further underlining their dual role.

Relatives of the proteins modulating a cell death apparatus have been found in worm, fly and man. In fact, knowledge of such proteins in lower organisms has been instrumental to discover human homologues. As for the cell death machinery, lately more and more proteins emerge that seem to be implicated in the regulation of mitochondrial dynamics, and that are conserved throughout evolution. Although mitochondria are crucial for apoptosis in man, their role in lower organisms has only recently come to light. For example, the only role mitochondria seemed to play in *C. elegans* was to offer a base for CED-9, which is bound to the organelle through its transmembrane domain. However, a study from Jagasia and colleagues implicated mitochondrial maintenance in life and death decisions (Jagasia *et al.*, 2005). Expressing heat-shock inducible EGL-1 the group observed fragmented mitochondria, which was blocked by CED-9, indicating that the Bcl-2 family member might be able to influence mitochondrial dynamics. In addition, Drp-1 expression in the worm resulted in fragmentation of mitochondrial networks, which in the case of worm embryos, was lethal (Labrousse *et al.*, 1999; Jagasia *et al.*, 2005).

Cell death in the worm however, is dependent on CED-3 activation. The basic caspase activation pathway through apoptosome assembly in *C. elegans* is different from that in mammalian cells and cytochrome *c* seems not to take

part in it. Therefore, a role for mitochondria during worm developmental cell death remains speculative. However, in our study loss of CED-9 function resulted in disruption of mitochondria and in this context might be the reason for death in those mutant embryos. In any case, all these findings support the idea that Bcl-2 family proteins have more than one role. Besides inhibiting cell death they seem to regulate mitochondrial fission and fusion dynamics by either directly fusing or dividing them or by activating the fission and fusion machinery.

In the fly *D. melanogaster*, the picture looks quite similar to the one described here for the worm. Assembly of the fly apoptosome for caspase activation is independent of cytochrome *c* and cytochrome *c* release from mitochondria does not occur during fly apoptosis (Dorstyn *et al.*, 2004). Thus, the importance for mitochondria during fly apoptosis is unclear. Regulation of the apoptotic pathway in the fly is overlooked by DIAP-1, which inhibits the constitutively expressed caspase DRONC. In order to activate caspases DIAP-1 is antagonized by pro-apoptotic fly proteins, known as the RHG group (R=reaper, H=hid, G=grim), which are equivalent to Smac. RHG proteins are transcriptionally up-regulated after stimulation by cell stress components, and subsequently inhibit DIAP-1 (Hay *et al.*, 2004). But this all happens in the cytoplasm of cells and the mitochondrion is not involved.

Proteins that belong to the Bcl-2 family were also discovered in *D. melanogaster*. Debcl and Buffy were both identified as pro-apoptotic proteins, containing BH1-BH4 domains and a transmembrane domain. Mitochondrial anchorage was found to be necessary for Debcl to ectopically induce apoptosis in human cells. Despite these findings, the precise mechanism of their action is still unclear and both proteins have also been suggested to act as cell death inhibitors in certain contexts (Igaki and Miura 2004). However, their role in mitochondrial dynamics has not been tackled yet.

Two recent studies demonstrated data that suggest that mitochondria in the fly undergo phenotypical changes and fragment during cell death (Abdelwahid *et al.*, 2007; Goyal *et al.*, 2007). This fragmentation depended on the presence of Drp-1, although its regulation did not become clear. The role for the fly Bcl-2 family members in this context remains to be elucidated.

For future aspects, it would be of interest to observe further mitochondrial inter-membrane space proteins, like Smac or Omi, in this context, since their release seems to be different to cytochrome *c*. Furthermore, the precise mechanism of how Bcl-2 family molecules interfere with mitochondrial morphology was not shown here therefore, more experiments would be helpful to elucidate such interesting questions. For example, co-immunoprecipitation experiments for endogenous proteins would help to define those details. In addition, analysis of action of the single domains of all Bcl-2 families, by truncations for example, could help to verify interaction profiles.

References

7. References

Abdelwahid, E., Yokokura, T., Krieser, R. J., Balasundaram, S., Fowle, W. H., and White, K. (2007). Mitochondrial disruption in Drosophila apoptosis. Dev Cell 12, 793-806.

Acehan, D., Jiang, X., Morgan, D. G., Heuser, J. E., Wang, X., and Akey, C. W. (2002). Three-dimensional structure of the apoptosome: implications for assembly, procaspase-9 binding, and activation. Mol Cell 9, 423-432.

Adrain, C., Slee, E. A., Harte, M. T., and Martin, S. J. (1999). Regulation of apoptotic protease activating factor-1 oligomerization and apoptosis by the WD-40 repeat region. J Biol Chem 274, 20855-20860.

Adrain, C., Brumatti, G., and Martin, S. J. (2006). Apoptosomes: protease activation platforms to die from. Trends Biochem Sci 31, 243-247.

Alexander, C., Votruba, M., Pesch, U. E., Thiselton, D. L., Mayer, S., Moore, A., Rodriguez, M., Kellner, U., Leo-Kottler, B., Auburger, G., et al. (2000). OPA1, encoding a dynamin-related GTPase, is mutated in autosomal dominant optic atrophy linked to chromosome 3q28. Nat Genet 26, 211-215.

Alirol, E., James, D., Huber, D., Marchetto, A., Vergani, L., Martinou, J. C., and Scorrano, L. (2006). The Mitochondrial Fission Protein hFis1 Requires the Endoplasmic Reticulum Gateway to Induce Apoptosis. Mol Biol Cell 17, 4593-4605.

Antignani, A., and Youle, R. J. (2006). How do Bax and Bak lead to permeabilization of the outer mitochondrial membrane? Curr Opin Cell Biol 18, 685-689.

Antonsson B., Conti F., Ciavatta A., Montessuit S., Lewis S., Martinou I., Bernasconi L., Bernard A., Mermod J.J., Mazzei G., Maundrell K., Gambale F., Sadoul R., Martinou J.C. (1997). Inhibition of Bax channel-forming activity by Bcl-2. Science 277, 370-372.

Antonsson, B., Montessuit, S., Lauper, S., Eskes, R., and Martinou, J. C. (2000). Bax oligomerization is required for channel-forming activity in liposomes and to trigger cytochrome *c* release from mitochondria. Biochem J 345 Pt 2, 271-278.

Antonsson, B., Montessuit, S., Sanchez, B., and Martinou, J. C. (2001). Bax is present as a high molecular weight oligomer/complex in the mitochondrial membrane of apoptotic cells. J Biol Chem 276, 11615-11623.

Arama, E., Agapite, J., and Steller, H. (2003). Caspase activity and a specific cytochrome *c* are required for sperm differentiation in Drosophila. Dev Cell 4, 687-697.

Arnoult, D., Grodet, A., Lee, Y. J., Estaquier, J., and Blackstone, C. (2005a). Release of OPA1 during apoptosis participates in the rapid and complete release of cytochrome *c* and subsequent mitochondrial fragmentation. J Biol Chem 280, 35742-35750.

Arnoult, D., Rismanchi, N., Grodet, A., Roberts, R. G., Seeburg, D. P., Estaquier, J., Sheng, M., and Blackstone, C. (2005b). Bax/Bak-dependent release of DDP/TIMM8a promotes Drp1-mediated mitochondrial fission and mitoptosis during programmed cell death. Curr Biol 15, 2112-2118.

Ashkenazi, A., and Dixit, V. M. (1998). Death receptors: signaling and modulation. Science 281, 1305-1308.

Baines, C. P., Kaiser, R. A., Purcell, N. H., Blair, N. S., Osinska, H., Hambleton, M. A., Brunskill, E. W., Sayen, M. R., Gottlieb, R. A., Dorn, G. W., et al. (2005). Loss of cyclophilin D reveals a critical role for mitochondrial permeability transition in cell death. Nature 434, 658-662.

Bauer, M. F., Hofmann, S., Neupert, W., and Brunner, M. (2000). Protein translocation into mitochondria: the role of TIM complexes. Trends Cell Biol 10, 25-31.

Borner, C. (2003). The Bcl-2 protein family: sensors and checkpoints for life-or-death decisions. Mol Immunol 39, 615-647.

Brooks, C., Wei, Q., Feng, L., Dong, G., Tao, Y., Mei, L., Xie, Z. J., and Dong, Z. (2007). Bak regulates mitochondrial morphology and pathology during apoptosis by interacting with mitofusins. Proc Natl Acad Sci U S A 104, 11649-11654.

Chen, F., Hersh, B. M., Conradt, B., Zhou, Z., Riemer, D., Gruenbaum, Y., and Horvitz, H. R. (2000). Translocation of C. elegans CED-4 to nuclear membranes during programmed cell death. Science 287, 1485-1489.

Chen, H., Detmer, S. A., Ewald, A. J., Griffin, E. E., Fraser, S. E., and Chan, D. C. (2003). Mitofusins Mfn1 and Mfn2 coordinately regulate mitochondrial fusion and are essential for embryonic development. J Cell Biol 160, 189-200.

Chen, L., Willis, S. N., Wei, A., Smith, B. J., Fletcher, J. I., Hinds, M. G., Colman, P. M., Day, C. L., Adams, J. M., and Huang, D. C. (2005). Differential targeting of prosurvival Bcl-2 proteins by their BH3-only ligands allows complementary apoptotic function. Mol Cell 17, 393-403.

Chen, H., and Chan, D. C. (2005). Emerging functions of mammalian mitochondrial fusion and fission. Hum Mol Genet 14 Spec No. 2, R283-289.

Chen, H., McCaffery, J. M., and Chan, D. C. (2007). Mitochondrial fusion protects against neurodegeneration in the cerebellum. Cell 130, 548-562.

Chinnaiyan, A. M., O'Rourke, K., Lane, B. R., and Dixit, V. M. (1997a). Interaction of CED-4 with CED-3 and CED-9: a molecular framework for cell death. Science 275, 1122-1126.

Chinnaiyan, A. M., Chaudhary, D., O'Rourke, K., Koonin, E. V., and Dixit, V. M. (1997b). Role of CED-4 in the activation of CED-3. Nature 388, 728-729.

Chipuk, J. E., Kuwana, T., Bouchier-Hayes, L., Droin, N. M., Newmeyer, D. D., Schuler, M., and Green, D. R. (2004). Direct activation of Bax by p53 mediates mitochondrial membrane permeabilization and apoptosis. Science 303, 1010-1014.

Cipolat, S., Martins de Brito, O., Dal Zilio, B., and Scorrano, L. (2004). OPA1 requires mitofusin 1 to promote mitochondrial fusion. Proc Natl Acad Sci U S A 101, 15927-15932.

Cipolat, S., Rudka, T., Hartmann, D., Costa, V., Serneels, L., Craessaerts, K., Metzger, K., Frezza, C., Annaert, W., D'Adamio, L., et al. (2006). Mitochondrial rhomboid PARL regulates cytochrome *c* release during apoptosis via OPA1-dependent cristae remodeling. Cell 126, 163-175.

Cohen, G. M. (1997). Caspases: the executioners of apoptosis. Biochem J 326 (Pt 1), 1-16.

Collins, T. J., and Bootman, M. D. (2003). Mitochondria are morphologically heterogeneous within cells. J Exp Biol 206, 1993-2000.

Colussi P.A., Harvey N.L., Kumar S. (1998). Prodomain-dependent nuclear localization of the caspase-2 (Nedd2) precursor. A novel function for a caspase prodomain. J Biol Chem 273, 24535-24542.

Conradt, B., and Horvitz, H. R. (1998). The C. elegans protein EGL-1 is required for programmed cell death and interacts with the Bcl-2-like protein CED-9. Cell 93, 519-529.

Creagh, E. M., and Martin, S. J. (2003a). Cell stress-associated caspase activation: intrinsically complex? Sci STKE 2003, pe11.

Creagh, E. M., Conroy, H., and Martin, S. J. (2003b). Caspase-activation pathways in apoptosis and immunity. Immunol Rev 193, 10-21.

Danial, N. N., and Korsmeyer, S. J. (2004). Cell death: critical control points. Cell 116, 205-219.

De Vos, K., Goossens, V., Boone, E., Vercammen, D., Vancompernolle, K., Vandenabeele, P., Haegeman, G., Fiers, W., and Grooten, J. (1998). The 55-kDa tumor necrosis factor receptor induces clustering of mitochondria through its membrane-proximal region. J Biol Chem 273, 9673-9680.

del Peso, L., Gonzalez, V. M., and Nunez, G. (1998). Caenorhabditis elegans EGL-1 disrupts the interaction of CED-9 with CED-4 and promotes CED-3 activation. J Biol Chem 273, 33495-33500.

Delettre, C., Lenaers, G., Griffoin, J. M., Gigarel, N., Lorenzo, C., Belenguer, P., Pelloquin, L., Grosgeorge, J., Turc-Carel, C., Perret, E., et al. (2000). Nuclear gene OPA1, encoding a mitochondrial dynamin-related protein, is mutated in dominant optic atrophy. Nat Genet 26, 207-210.

Delivani, P., Adrain, C., Taylor, R. C., Duriez, P. J., and Martin, S. J. (2006). Role for CED-9 and Egl-1 as regulators of mitochondrial fission and fusion dynamics. Mol Cell 21, 761-773.

Desagher, S., Osen-Sand, A., Nichols, A., Eskes, R., Montessuit, S., Lauper, S., Maundrell, K., Antonsson, B., and Martinou, J. C. (1999). Bid-induced conformational change of Bax is responsible for mitochondrial cytochrome *c* release during apoptosis. J Cell Biol 144, 891-901.

Desagher, S., and Martinou, J. C. (2000). Mitochondria as the central control point of apoptosis. Trends Cell Biol 10, 369-377.
Donald L. Riddle, Thomas Blumenthal, Barbara J. Meyer, James R. Priess, *C. elegans* II : Monograph 33. Cold Spring Harbor Laboratory Press; 1. edition (1998) ISBN-10: 0879695323

Dorstyn, L., Read, S., Cakouros, D., Huh, J. R., Hay, B. A., and Kumar, S. (2002). The role of cytochrome *c* in caspase activation in Drosophila melanogaster cells. J Cell Biol 156, 1089-1098.

Dorstyn, L., Mills, K., Lazebnik, Y., and Kumar, S. (2004). The two cytochrome *c* species, DC3 and DC4, are not required for caspase activation and apoptosis in Drosophila cells. J Cell Biol 167, 405-410.

Earnshaw, W. C., Martins, L. M., and Kaufmann, S. H. (1999). Mammalian caspases: structure, activation, substrates, and functions during apoptosis. Annu Rev Biochem 68, 383-424.

Ellis, H. M., and Horvitz, H. R. (1986). Genetic control of programmed cell death in the nematode C. elegans. Cell 44, 817-829.

Epand, R. F., Martinou, J. C., Montessuit, S., Epand, R. M., and Yip, C. M. (2002). Direct evidence for membrane pore formation by the apoptotic protein Bax. Biochem Biophys Res Commun 298, 744-749.

Eskes, R., Antonsson, B., Osen-Sand, A., Montessuit, S., Richter, C., Sadoul, R., Mazzei, G., Nichols, A., and Martinou, J. C. (1998). Bax-induced cytochrome *c* release from mitochondria is independent of the permeability transition pore but highly dependent on Mg2+ ions. J Cell Biol 143, 217-224.

Estaquier, J., and Arnoult, D. (2007). Inhibiting Drp1-mediated mitochondrial fission selectively prevents the release of cytochrome c during apoptosis. Cell Death Differ 14, 1086-1094.

Eura, Y., Ishihara, N., Yokota, S., and Mihara, K. (2003). Two mitofusin proteins, mammalian homologues of FZO, with distinct functions are both required for mitochondrial fusion. J Biochem 134, 333-344.

Finucane, D. M., Bossy-Wetzel, E., Waterhouse, N. J., Cotter, T. G., and Green, D. R. (1999). Bax-induced caspase activation and apoptosis via cytochrome c release from mitochondria is inhibitable by Bcl-xL. J Biol Chem 274, 2225-2233.

Fischer, U., Janicke, R. U., and Schulze-Osthoff, K. (2003). Many cuts to ruin: a comprehensive update of caspase substrates. Cell Death Differ 10, 76-100.

Frank, S., Gaume, B., Bergmann-Leitner, E. S., Leitner, W. W., Robert, E. G., Catez, F., Smith, C. L., and Youle, R. J. (2001). The role of dynamin-related protein 1, a mediator of mitochondrial fission, in apoptosis. Dev Cell 1, 515-525.

Frezza, C., Cipolat, S., Martins de Brito, O., Micaroni, M., Beznoussenko, G. V., Rudka, T., Bartoli, D., Polishuck, R. S., Danial, N. N., De Strooper, B., and Scorrano, L. (2006). OPA1 controls apoptotic cristae remodeling independently from mitochondrial fusion. Cell 126, 177-189.

Goldstein, J. C., Waterhouse, N. J., Juin, P., Evan, G. I., and Green, D. R. (2000). The coordinate release of cytochrome c during apoptosis is rapid, complete and kinetically invariant. Nat Cell Biol 2, 156-162.

Goyal, G., Fell, B., Sarin, A., Youle, R. J., and Sriram, V. (2007). Role of mitochondrial remodeling in programmed cell death in Drosophila melanogaster. Dev Cell 12, 807-816.

Green, D. R., and Kroemer, G. (2004). The pathophysiology of mitochondrial cell death. Science 305, 626-629.

Green, D. R. (2006). At the gates of death. Cancer Cell 9, 328-330.

Griparic, L., van der Wel, N. N., Orozco, I. J., Peters, P. J., and van der Bliek, A. M. (2004). Loss of the intermembrane space protein Mgm1/OPA1 induces swelling and localized constrictions along the lengths of mitochondria. J Biol Chem 279, 18792-18798.

Hales, K. G., and Fuller, M. T. (1997). Developmentally regulated mitochondrial fusion mediated by a conserved, novel, predicted GTPase. Cell 90, 121-129.

Hausmann, G., O'Reilly, L. A., van Driel, R., Beaumont, J. G., Strasser, A., Adams, J. M., and Huang, D. C. (2000). Pro-apoptotic apoptosis protease-activating factor 1 (Apaf-1) has a cytoplasmic localization distinct from Bcl-2 or Bcl-x(L). J Cell Biol 149, 623-634.

Hay, B. A., Huh, J. R., and Guo, M. (2004). The genetics of cell death: approaches, insights and opportunities in Drosophila. Nat Rev Genet 5, 911-922.

Hengartner, M. O., Ellis, R. E., and Horvitz, H. R. (1992). Caenorhabditis elegans gene ced-9 protects cells from programmed cell death. Nature 356, 494-499.

Hengartner, M. O., and Horvitz, H. R. (1994). C. elegans cell survival gene ced-9 encodes a functional homolog of the mammalian proto-oncogene bcl-2. Cell 76, 665-676.

Hetz, C., Vitte, P. A., Bombrun, A., Rostovtseva, T. K., Montessuit, S., Hiver, A., Schwarz, M. K., Church, D. J., Korsmeyer, S. J., Martinou, J. C., and Antonsson, B. (2005). Bax channel inhibitors prevent mitochondrion-mediated apoptosis and protect neurons in a model of global brain ischemia. J Biol Chem 280, 42960-42970.

Hill, M. M., Adrain, C., Duriez, P. J., Creagh, E. M., and Martin, S. J. (2004). Analysis of the composition, assembly kinetics and activity of native Apaf-1 apoptosomes. Embo J 23, 2134-2145.

Hisahara, S., Kanuka, H., Shoji, S., Yoshikawa, S., Okano, H., and Miura, M. (1998). Caenorhabditis elegans anti-apoptotic gene ced-9 prevents ced-3-induced cell death in Drosophila cells. J Cell Sci 111 (Pt 6), 667-673.

Hockenbery, D., Nunez, G., Milliman, C., Schreiber, R. D., and Korsmeyer, S. J. (1990). Bcl-2 is an inner mitochondrial membrane protein that blocks programmed cell death. Nature 348, 334-336.

Hope I. A., C. elegans: A Practical Approach. Oxford University Press, USA; 1. edition (2000) ISBN-10: 0199637393

Hu, Y., Benedict, M. A., Wu, D., Inohara, N., and Nunez, G. (1998). Bcl-XL interacts with Apaf-1 and inhibits Apaf-1-dependent caspase-9 activation. Proc Natl Acad Sci U S A 95, 4386-4391.

Huang, P., Yu, T., and Yoon, Y. (2007). Mitochondrial clustering induced by overexpression of the mitochondrial fusion protein Mfn2 causes mitochondrial dysfunction and cell death. Eur J Cell Biol 86, 289-302.

Igaki, T., and Miura, M. (2004). Role of Bcl-2 family members in invertebrates. Biochim Biophys Acta 1644, 73-81.

Inoue, H., Nojima, H., and Okayama, H. (1990). High efficiency transformation of Escherichia coli with plasmids. Gene 96, 23-28.

Irmler, M., Hofmann, K., Vaux, D., and Tschopp, J. (1997). Direct physical interaction between the Caenorhabditis elegans 'death proteins' CED-3 and CED-4. FEBS Lett 406, 189-190.

Jacobson, M. D., Weil, M., and Raff, M. C. (1997). Programmed cell death in animal development. Cell 88, 347-354.

Jagasia, R., Grote, P., Westermann, B., and Conradt, B. (2005). DRP-1-mediated mitochondrial fragmentation during EGL-1-induced cell death in C. elegans. Nature 433, 754-760.

Jahani-Asl, A., Cheung, E. C., Neuspiel, M., MacLaurin, J. G., Fortin, A., Park, D. S., McBride, H. M., and Slack, R. S. (2007). Mitofusin 2 protects cerebellar granule neurons against injury-induced cell death. J Biol Chem 282, 23788-23798.

James, C., Gschmeissner, S., Fraser, A., and Evan, G. I. (1997). CED-4 induces chromatin condensation in Schizosaccharomyces pombe and is inhibited by direct physical association with CED-9. Curr Biol 7, 246-252.

James, D. I., Parone, P. A., Mattenberger, Y., and Martinou, J. C. (2003). hFis1, a novel component of the mammalian mitochondrial fission machinery. J Biol Chem 278, 36373-36379.

Karbowski, M., Lee, Y. J., Gaume, B., Jeong, S. Y., Frank, S., Nechushtan, A., Santel, A., Fuller, M., Smith, C. L., and Youle, R. J. (2002). Spatial and temporal association of Bax with mitochondrial fission sites, Drp1, and Mfn2 during apoptosis. J Cell Biol 159, 931-938.

Karbowski, M., and Youle, R. J. (2003). Dynamics of mitochondrial morphology in healthy cells and during apoptosis. Cell Death Differ 10, 870-880.

Karbowski, M., Arnoult, D., Chen, H., Chan, D. C., Smith, C. L., and Youle, R. J. (2004). Quantitation of mitochondrial dynamics by photolabeling of individual organelles shows that mitochondrial fusion is blocked during the Bax activation phase of apoptosis. J Cell Biol 164, 493-499.

Karbowski, M., Norris, K. L., Cleland, M. M., Jeong, S. Y., and Youle, R. J. (2006). Role of Bax and Bak in mitochondrial morphogenesis. Nature 443, 658-662.

Kerr, J. F., Wyllie, A. H., and Currie, A. R. (1972). Apoptosis: a basic biological phenomenon with wide-ranging implications in tissue kinetics. Br J Cancer 26, 239-257.

Kischkel, F. C., Hellbardt, S., Behrmann, I., Germer, M., Pawlita, M., Krammer, P. H., and Peter, M. E. (1995). Cytotoxicity-dependent APO-1 (Fas/CD95)-associated proteins form a death-inducing signaling complex (DISC) with the receptor. Embo J 14, 5579-5588.

Kluck, R. M., Bossy-Wetzel, E., Green, D. R., and Newmeyer, D. D. (1997). The release of cytochrome c from mitochondria: a primary site for Bcl-2 regulation of apoptosis. Science 275, 1132-1136.

Kluck, R. M., Esposti, M. D., Perkins, G., Renken, C., Kuwana, T., Bossy-Wetzel, E., Goldberg, M., Allen, T., Barber, M. J., Green, D. R., and Newmeyer, D. D. (1999). The pro-apoptotic proteins, Bid and Bax, cause a limited permeabilization of the mitochondrial outer membrane that is enhanced by cytosol. J Cell Biol 147, 809-822.

Kokoszka, J. E., Waymire, K. G., Levy, S. E., Sligh, J. E., Cai, J., Jones, D. P., MacGregor, G. R., and Wallace, D. C. (2004). The ADP/ATP translocator is not essential for the mitochondrial permeability transition pore. Nature 427, 461-465.

Koshiba, T., Detmer, S. A., Kaiser, J. T., Chen, H., McCaffery, J. M., and Chan, D. C. (2004). Structural basis of mitochondrial tethering by mitofusin complexes. Science 305, 858-862.

Kuwana, T., Mackey, M. R., Perkins, G., Ellisman, M. H., Latterich, M., Schneiter, R., Green, D. R., and Newmeyer, D. D. (2002). Bid, Bax, and lipids cooperate to form supramolecular openings in the outer mitochondrial membrane. Cell 111, 331-342.

Kuwana, T., Bouchier-Hayes, L., Chipuk, J. E., Bonzon, C., Sullivan, B. A., Green, D. R., and Newmeyer, D. D. (2005). BH3 domains of BH3-only proteins differentially regulate Bax-mediated mitochondrial membrane permeabilization both directly and indirectly. Mol Cell 17, 525-535.

Kyte, J., and Doolittle, R. F. (1982). A simple method for displaying the hydropathic character of a protein. J Mol Biol 157, 105-132.

Labrousse, A. M., Zappaterra, M. D., Rube, D. A., and van der Bliek, A. M. (1999). C. elegans dynamin-related protein DRP-1 controls severing of the mitochondrial outer membrane. Mol Cell 4, 815-826.

Lee, Y. J., Jeong, S. Y., Karbowski, M., Smith, C. L., and Youle, R. J. (2004). Roles of the mammalian mitochondrial fission and fusion mediators Fis1, Drp1, and Opa1 in apoptosis. Mol Biol Cell 15, 5001-5011.

Legros, F., Lombes, A., Frachon, P., and Rojo, M. (2002). Mitochondrial fusion in human cells is efficient, requires the inner membrane potential, and is mediated by mitofusins. Mol Biol Cell 13, 4343-4354.

Lindsten, T., Ross, A. J., King, A., Zong, W. X., Rathmell, J. C., Shiels, H. A., Ulrich, E., Waymire, K. G., Mahar, P., Frauwirth, K., et al. (2000). The combined functions of proapoptotic Bcl-2 family members bak and bax are essential for normal development of multiple tissues. Mol Cell 6, 1389-1399.

Martin, S. J., and Green, D. R. (1995). Protease activation during apoptosis: death by a thousand cuts? Cell 82, 349-352.

Martinou, J. C., and Green, D. R. (2001). Breaking the mitochondrial barrier. Nat Rev Mol Cell Biol 2, 63-67.

Marzo, I., Brenner, C., Zamzami, N., Jurgensmeier, J. M., Susin, S. A., Vieira, H. L., Prevost, M. C., Xie, Z., Matsuyama, S., Reed, J. C., and Kroemer, G. (1998). Bax and adenine nucleotide translocator cooperate in the mitochondrial control of apoptosis. Science 281, 2027-2031.

Mattenberger, Y., James, D. I., and Martinou, J. C. (2003). Fusion of mitochondria in mammalian cells is dependent on the mitochondrial inner membrane potential and independent of microtubules or actin. FEBS Lett 538, 53-59.

Maurer, C. W., Chiorazzi, M., and Shaham, S. (2007). Timing of the onset of a developmental cell death is controlled by transcriptional induction of the C. elegans ced-3 caspase-encoding gene. Development 134, 1357-1368.

Medema, J. P., Scaffidi, C., Kischkel, F. C., Shevchenko, A., Mann, M., Krammer, P. H., and Peter, M. E. (1997). FLICE is activated by association with the CD95 death-inducing signaling complex (DISC). Embo J 16, 2794-2804.

Miura, M., Zhu, H., Rotello, R., Hartwieg, E. A., and Yuan, J. (1993). Induction of apoptosis in fibroblasts by IL-1 beta-converting enzyme, a mammalian homolog of the C. elegans cell death gene ced-3. Cell 75, 653-660.

Moriishi, K., Huang, D. C., Cory, S., and Adams, J. M. (1999). Bcl-2 family members do not inhibit apoptosis by binding the caspase activator Apaf-1. Proc Natl Acad Sci U S A 96, 9683-9688.

Mozdy, A. D., McCaffery, J. M., and Shaw, J. M. (2000). Dnm1p GTPase-mediated mitochondrial fission is a multi-step process requiring the novel integral membrane component Fis1p. J Cell Biol 151, 367-380.

Mozdy, A. D., and Shaw, J. M. (2003). A fuzzy mitochondrial fusion apparatus comes into focus. Nat Rev Mol Cell Biol 4, 468-478.

Muchmore, S. W., Sattler, M., Liang, H., Meadows, R. P., Harlan, J. E., Yoon, H. S., Nettesheim, D., Chang, B. S., Thompson, C. B., Wong, S. L., et al. (1996). X-ray and NMR structure of human Bcl-xL, an inhibitor of programmed cell death. Nature 381, 335-341.

Munoz-Pinedo, C., Guio-Carrion, A., Goldstein, J. C., Fitzgerald, P., Newmeyer, D. D., and Green, D. R. (2006). Different mitochondrial intermembrane space proteins are released during apoptosis in a manner that is coordinately initiated but can vary in duration. Proc Natl Acad Sci U S A 103, 11573-11578.

Muzio, M., Chinnaiyan, A. M., Kischkel, F. C., O'Rourke, K., Shevchenko, A., Ni, J., Scaffidi, C., Bretz, J. D., Zhang, M., Gentz, R., et al. (1996). FLICE, a novel FADD-homologous ICE/CED-3-like protease, is recruited to the CD95 (Fas/APO-1) death--inducing signaling complex. Cell 85, 817-827.

Nakagawa, T., Shimizu, S., Watanabe, T., Yamaguchi, O., Otsu, K., Yamagata, H., Inohara, H., Kubo, T., and Tsujimoto, Y. (2005). Cyclophilin D-dependent mitochondrial permeability transition regulates some necrotic but not apoptotic cell death. Nature 434, 652-658.

Nakano, K., and Vousden, K. H. (2001). PUMA, a novel proapoptotic gene, is induced by p53. Mol Cell 7, 683-694.

Nechushtan, A., Smith, C. L., Hsu, Y. T., and Youle, R. J. (1999). Conformation of the Bax C-terminus regulates subcellular location and cell death. Embo J 18, 2330-2341.

Nechushtan, A., Smith, C. L., Lamensdorf, I., Yoon, S. H., and Youle, R. J. (2001). Bax and Bak coalesce into novel mitochondria-associated clusters during apoptosis. J Cell Biol 153, 1265-1276.

Neuspiel, M., Zunino, R., Gangaraju, S., Rippstein, P., and McBride, H. (2005). Activated mitofusin 2 signals mitochondrial fusion, interferes with Bax activation, and reduces susceptibility to radical induced depolarization. J Biol Chem 280, 25060-25070.

Newmeyer, D. D., and Ferguson-Miller, S. (2003). Mitochondria: releasing power for life and unleashing the machineries of death. Cell 112, 481-490.

Nicholson, D. W. (1999). Caspase structure, proteolytic substrates, and function during apoptotic cell death. Cell Death Differ 6, 1028-1042.

Oda, E., Ohki, R., Murasawa, H., Nemoto, J., Shibue, T., Yamashita, T., Tokino, T., Taniguchi, T., and Tanaka, N. (2000). Noxa, a BH3-only member of the Bcl-2 family and candidate mediator of p53-induced apoptosis. Science 288, 1053-1058.

Olichon, A., Emorine, L. J., Descoins, E., Pelloquin, L., Brichese, L., Gas, N., Guillou, E., Delettre, C., Valette, A., Hamel, C. P., et al. (2002). The human dynamin-related protein OPA1 is anchored to the mitochondrial inner membrane facing the inter-membrane space. FEBS Lett 523, 171-176.

Olichon, A., Baricault, L., Gas, N., Guillou, E., Valette, A., Belenguer, P., and Lenaers, G. (2003). Loss of OPA1 perturbates the mitochondrial inner membrane structure and integrity, leading to cytochrome c release and apoptosis. J Biol Chem 278, 7743-7746.

Olichon, A., Elachouri, G., Baricault, L., Delettre, C., Belenguer, P., and Lenaers, G. (2007). OPA1 alternate splicing uncouples an evolutionary conserved function in mitochondrial fusion from a vertebrate restricted function in apoptosis. Cell Death Differ 14, 682-692.

Oltvai, Z. N., Milliman, C. L., and Korsmeyer, S. J. (1993). Bcl-2 heterodimerizes in vivo with a conserved homolog, Bax, that accelerates programmed cell death. Cell 74, 609-619.

Ottilie, S., Diaz, J. L., Chang, J., Wilson, G., Tuffo, K. M., Weeks, S., McConnell, M., Wang, Y., Oltersdorf, T., and Fritz, L. C. (1997). Structural and functional complementation of an inactive Bcl-2 mutant by Bax truncation. J Biol Chem 272, 16955-16961.

Pan, G., O'Rourke, K., and Dixit, V. M. (1998). Caspase-9, Bcl-XL, and Apaf-1 form a ternary complex. J Biol Chem 273, 5841-5845.

Parone, P. A., James, D. I., Da Cruz, S., Mattenberger, Y., Donze, O., Barja, F., and Martinou, J. C. (2006). Inhibiting the mitochondrial fission machinery does not prevent Bax/Bak-dependent apoptosis. Mol Cell Biol 26, 7397-7408.

Paroni G., Henderson C., Schneider C., Brancolini C. (2002). Caspase-2 can trigger cytochrome C release and apoptosis from the nucleus. J Biol Chem. 277, 15147-15161.

Peter, M. E., and Krammer, P. H. (2003). The CD95(APO-1/Fas) DISC and beyond. Cell Death Differ 10, 26-35.

Praefcke, G. J., and McMahon, H. T. (2004). The dynamin superfamily: universal membrane tubulation and fission molecules? Nat Rev Mol Cell Biol 5, 133-147.

Puthalakath, H., Huang, D. C., O'Reilly, L. A., King, S. M., and Strasser, A. (1999). The proapoptotic activity of the Bcl-2 family member Bim is regulated by interaction with the dynein motor complex. Mol Cell 3, 287-296.

Puthalakath, H., and Strasser, A. (2002). Keeping killers on a tight leash: transcriptional and post-translational control of the pro-apoptotic activity of BH3-only proteins. Cell Death Differ 9, 505-512.

Raff, M. (1998). Cell suicide for beginners. Nature 396, 119-122.

Ricci, J. E., Gottlieb, R. A., and Green, D. R. (2003). Caspase-mediated loss of mitochondrial function and generation of reactive oxygen species during apoptosis. J Cell Biol 160, 65-75.

Rojo, M., Legros, F., Chateau, D., and Lombes, A. (2002). Membrane topology and mitochondrial targeting of mitofusins, ubiquitous mammalian homologs of the transmembrane GTPase Fzo. J Cell Sci 115, 1663-1674.

Saito, M., Korsmeyer, S. J., and Schlesinger, P. H. (2000). BAX-dependent transport of cytochrome c reconstituted in pure liposomes. Nat Cell Biol 2, 553-555.

Salvesen, G. S., and Dixit, V. M. (1999). Caspase activation: the induced-proximity model. Proc Natl Acad Sci U S A 96, 10964-10967.

Santel, A., and Fuller, M. T. (2001). Control of mitochondrial morphology by a human mitofusin. J Cell Sci 114, 867-874.

Santel, A., Frank, S., Gaume, B., Herrler, M., Youle, R. J., and Fuller, M. T. (2003). Mitofusin-1 protein is a generally expressed mediator of mitochondrial fusion in mammalian cells. J Cell Sci 116, 2763-2774.

Schlesinger P.H., Gross A., Yin X.M., Yamamoto K., Saito M., Waksman G., Korsmeyer S.J (1997). Comparison of the ion channel characteristics of proapoptotic BAX and antiapoptotic BCL-2. Proc Natl Acad Sci U S A 94, 11357-11362.

Schmitz, I., Kirchhoff, S., and Krammer, P. H. (2000). Regulation of death receptor-mediated apoptosis pathways. Int J Biochem Cell Biol 32, 1123-1136.

Schumacher, B., Schertel, C., Wittenburg, N., Tuck, S., Mitani, S., Gartner, A., Conradt, B., and Shaham, S. (2005). C. elegans ced-13 can promote apoptosis and is induced in response to DNA damage. Cell Death Differ 12, 153-161.

Scorrano, L., Ashiya, M., Buttle, K., Weiler, S., Oakes, S. A., Mannella, C. A., and Korsmeyer, S. J. (2002). A distinct pathway remodels mitochondrial cristae and mobilizes cytochrome c during apoptosis. Dev Cell 2, 55-67.

Sedlak, T. W., Oltvai, Z. N., Yang, E., Wang, K., Boise, L. H., Thompson, C. B., and Korsmeyer, S. J. (1995). Multiple Bcl-2 family members demonstrate selective dimerizations with Bax. Proc Natl Acad Sci U S A 92, 7834-7838.

Seshagiri, S., and Miller, L. K. (1997). Caenorhabditis elegans CED-4 stimulates CED-3 processing and CED-3-induced apoptosis. Curr Biol 7, 455-460.

Shaham, S., and Horvitz, H. R. (1996). Developing Caenorhabditis elegans neurons may contain both cell-death protective and killer activities. Genes Dev 10, 578-591.

Shaham, S., Reddien, P. W., Davies, B., and Horvitz, H. R. (1999). Mutational analysis of the Caenorhabditis elegans cell-death gene ced-3. Genetics 153, 1655-1671.

Shi, Y. (2002). Mechanisms of caspase activation and inhibition during apoptosis. Mol Cell 9, 459-470.

Shimizu, S., Narita, M., and Tsujimoto, Y. (1999). Bcl-2 family proteins regulate the release of apoptogenic cytochrome c by the mitochondrial channel VDAC. Nature 399, 483-487.

Slee, E. A., Harte, M. T., Kluck, R. M., Wolf, B. B., Casiano, C. A., Newmeyer, D. D., Wang, H. G., Reed, J. C., Nicholson, D. W., Alnemri, E. S., et al. (1999). Ordering the cytochrome c-initiated caspase cascade: hierarchical activation of caspases-2, -3, -6, -7, -8, and -10 in a caspase-9-dependent manner. J Cell Biol 144, 281-292.

Smirnova, E., Shurland, D. L., Ryazantsev, S. N., and van der Bliek, A. M. (1998). A human dynamin-related protein controls the distribution of mitochondria. J Cell Biol 143, 351-358.

Smirnova, E., Griparic, L., Shurland, D. L., and van der Bliek, A. M. (2001). Dynamin-related protein Drp1 is required for mitochondrial division in mammalian cells. Mol Biol Cell 12, 2245-2256.

Spector, M. S., Desnoyers, S., Hoeppner, D. J., and Hengartner, M. O. (1997). Interaction between the C. elegans cell-death regulators CED-9 and CED-4. Nature 385, 653-656.

Sugioka, R., Shimizu, S., and Tsujimoto, Y. (2004). Fzo1, a protein involved in mitochondrial fusion, inhibits apoptosis. J Biol Chem 279, 52726-52734.

Sulston, J. E., and Horvitz, H. R. (1977). Post-embryonic cell lineages of the nematode, Caenorhabditis elegans. Dev Biol 56, 110-156.

Suzuki, M., Youle, R. J., and Tjandra, N. (2000). Structure of Bax: coregulation of dimer formation and intracellular localization. Cell 103, 645-654.

Szabadkai, G., Simoni, A. M., Chami, M., Wieckowski, M. R., Youle, R. J., and Rizzuto, R. (2004). Drp-1-dependent division of the mitochondrial network blocks intraorganellar Ca2+ waves and protects against Ca2+-mediated apoptosis. Mol Cell 16, 59-68.

Taylor, R. C., Brumatti, G., Ito, S., Hengartner, M. O., Derry, W. B., and Martin, S. J. (2007). Establishing a blueprint for CED-3-dependent killing through identification of multiple substrates for this protease. J Biol Chem 282, 15011-15021.

Thornberry, N. A., Rano, T. A., Peterson, E. P., Rasper, D. M., Timkey, T., Garcia-Calvo, M., Houtzager, V. M., Nordstrom, P. A., Roy, S., Vaillancourt, J. P., et al. (1997). A combinatorial approach defines specificities of members of the caspase family and granzyme B. Functional relationships established for key mediators of apoptosis. J Biol Chem 272, 17907-17911.

Tsujimoto, Y., Yunis, J., Onorato-Showe, L., Erikson, J., Nowell, P. C., and Croce, C. M. (1984). Molecular cloning of the chromosomal breakpoint of B-cell lymphomas and leukemias with the t(11;14) chromosome translocation. Science 224, 1403-1406.

Tzur, Y. B., Hersh, B. M., Horvitz, H. R., and Gruenbaum, Y. (2002). Fate of the nuclear lamina during Caenorhabditis elegans apoptosis. J Struct Biol 137, 146-153.

Tzur, Y. B., Margalit, A., Melamed-Book, N., and Gruenbaum, Y. (2006). Matefin/SUN-1 is a nuclear envelope receptor for CED-4 during Caenorhabditis elegans apoptosis. Proc Natl Acad Sci U S A 103, 13397-13402.

Uren, R. T., Dewson, G., Bonzon, C., Lithgow, T., Newmeyer, D. D., and Kluck, R. M. (2005). Mitochondrial release of pro-apoptotic proteins: electrostatic interactions can hold cytochrome c but not Smac/DIABLO to mitochondrial membranes. J Biol Chem 280, 2266-2274.

Vaux, D. L., Weissman, I. L., and Kim, S. K. (1992). Prevention of programmed cell death in Caenorhabditis elegans by human bcl-2. Science 258, 1955-1957.

Veis, D. J., Sorenson, C. M., Shutter, J. R., and Korsmeyer, S. J. (1993). Bcl-2-deficient mice demonstrate fulminant lymphoid apoptosis, polycystic kidneys, and hypopigmented hair. Cell 75, 229-240.

Wei, M. C., Lindsten, T., Mootha, V. K., Weiler, S., Gross, A., Ashiya, M., Thompson, C. B., and Korsmeyer, S. J. (2000). tBID, a membrane-targeted death ligand, oligomerizes BAK to release cytochrome c. Genes Dev 14, 2060-2071.

Wei, M. C., Zong, W. X., Cheng, E. H., Lindsten, T., Panoutsakopoulou, V., Ross, A. J., Roth, K. A., MacGregor, G. R., Thompson, C. B., and Korsmeyer, S. J. (2001). Proapoptotic BAX and BAK: a requisite gateway to mitochondrial dysfunction and death. Science 292, 727-730.

Willis, S. N., Chen, L., Dewson, G., Wei, A., Naik, E., Fletcher, J. I., Adams, J. M., and Huang, D. C. (2005). Proapoptotic Bak is sequestered by Mcl-1 and Bcl-xL, but not Bcl-2, until displaced by BH3-only proteins. Genes Dev 19, 1294-1305.

Wu, D., Wallen, H. D., and Nunez, G. (1997a). Interaction and regulation of subcellular localization of CED-4 by CED-9. Science 275, 1126-1129.

Wu, D., Wallen, H. D., Inohara, N., and Nunez, G. (1997b). Interaction and regulation of the Caenorhabditis elegans death protease CED-3 by CED-4 and CED-9. J Biol Chem 272, 21449-21454.

Xue, D., and Horvitz, H. R. (1995). Inhibition of the Caenorhabditis elegans cell-death protease CED-3 by a CED-3 cleavage site in baculovirus p35 protein. Nature 377, 248-251.

Yaffe, M. P. (1999). The machinery of mitochondrial inheritance and behavior. Science 283, 1493-1497.

Yan, N., Gu, L., Kokel, D., Chai, J., Li, W., Han, A., Chen, L., Xue, D., and Shi, Y. (2004). Structural, biochemical, and functional analyses of CED-9 recognition by the proapoptotic proteins EGL-1 and CED-4. Mol Cell 15, 999-1006.

Yan, N., Chai, J., Lee, E. S., Gu, L., Liu, Q., He, J., Wu, J. W., Kokel, D., Li, H., Hao, Q., et al. (2005). Structure of the CED-4-CED-9 complex provides insights into programmed cell death in Caenorhabditis elegans. Nature 437, 831-837.

Yan, N., Xu, Y., and Shi, Y. (2006). 2:1 Stoichiometry of the CED-4-CED-9 complex and the tetrameric CED-4: insights into the regulation of CED-3 activation. Cell Cycle 5, 31-34.

Yang, X., Chang, H. Y., and Baltimore, D. (1998). Essential role of CED-4 oligomerization in CED-3 activation and apoptosis. Science 281, 1355-1357.

Yoon, Y., Krueger, E. W., Oswald, B. J., and McNiven, M. A. (2003). The mitochondrial protein hFis1 regulates mitochondrial fission in mammalian cells through an interaction with the dynamin-like protein DLP1. Mol Cell Biol 23, 5409-5420.

Yoshida, H., Kong, Y. Y., Yoshida, R., Elia, A. J., Hakem, A., Hakem, R., Penninger, J. M., and Mak, T. W. (1998). Apaf1 is required for mitochondrial pathways of apoptosis and brain development. Cell 94, 739-750.

Youle, R. J., and Strasser, A. (2008). The BCL-2 protein family: opposing activities that mediate cell death. Nat Rev Mol Cell Biol 9, 47-59.

Yu, T., Robotham, J. L., and Yoon, Y. (2006). Increased production of reactive oxygen species in hyperglycemic conditions requires dynamic change of mitochondrial morphology. Proc Natl Acad Sci U S A 103, 2653-2658.

Yuan, J., and Horvitz, H. R. (1992). The Caenorhabditis elegans cell death gene ced-4 encodes a novel protein and is expressed during the period of extensive programmed cell death. Development 116, 309-320.

Yuan, J., Shaham, S., Ledoux, S., Ellis, H. M., and Horvitz, H. R. (1993). The C. elegans cell death gene ced-3 encodes a protein similar to mammalian interleukin-1 beta-converting enzyme. Cell 75, 641-652.

Yuan, J. Y., and Horvitz, H. R. (1990). The Caenorhabditis elegans genes ced-3 and ced-4 act cell autonomously to cause programmed cell death. Dev Biol 138, 33-41.

Zamzami, N., and Kroemer, G. (2001). The mitochondrion in apoptosis: how Pandora's box opens. Nat Rev Mol Cell Biol 2, 67-71.

Zamzami, N., Marchetti, P., Castedo, M., Decaudin, D., Macho, A., Hirsch, T., Susin, S. A., Petit, P. X., Mignotte, B., and Kroemer, G. (1995). Sequential reduction of mitochondrial transmembrane potential and generation of reactive oxygen species in early programmed cell death. J Exp Med 182, 367-377.

Zha, H., Aime-Sempe, C., Sato, T., and Reed, J. C. (1996). Proapoptotic protein Bax heterodimerizes with Bcl-2 and homodimerizes with Bax via a novel domain (BH3) distinct from BH1 and BH2. J Biol Chem 271, 7440-7444.

Zhai, D., Jin, C., Huang, Z., Satterthwait, A. C., and Reed, J. C. (2008). Differential regulation of Bax and Bak by anti-apoptotic Bcl-2-family proteins, Bcl-B and Mcl-1. J Biol Chem.

Zuchner, S., Mersiyanova, I. V., Muglia, M., Bissar-Tadmouri, N., Rochelle, J., Dadali, E. L., Zappia, M., Nelis, E., Patitucci, A., Senderek, J., et al. (2004). Mutations in the mitochondrial GTPase mitofusin 2 cause Charcot-Marie-Tooth neuropathy type 2A. Nat Genet 36, 449-451.